JOINT EUROPEAN TORUS JET

JET JOINT UNDERTAKING

PROGRESS REPORT 1988

Volume I

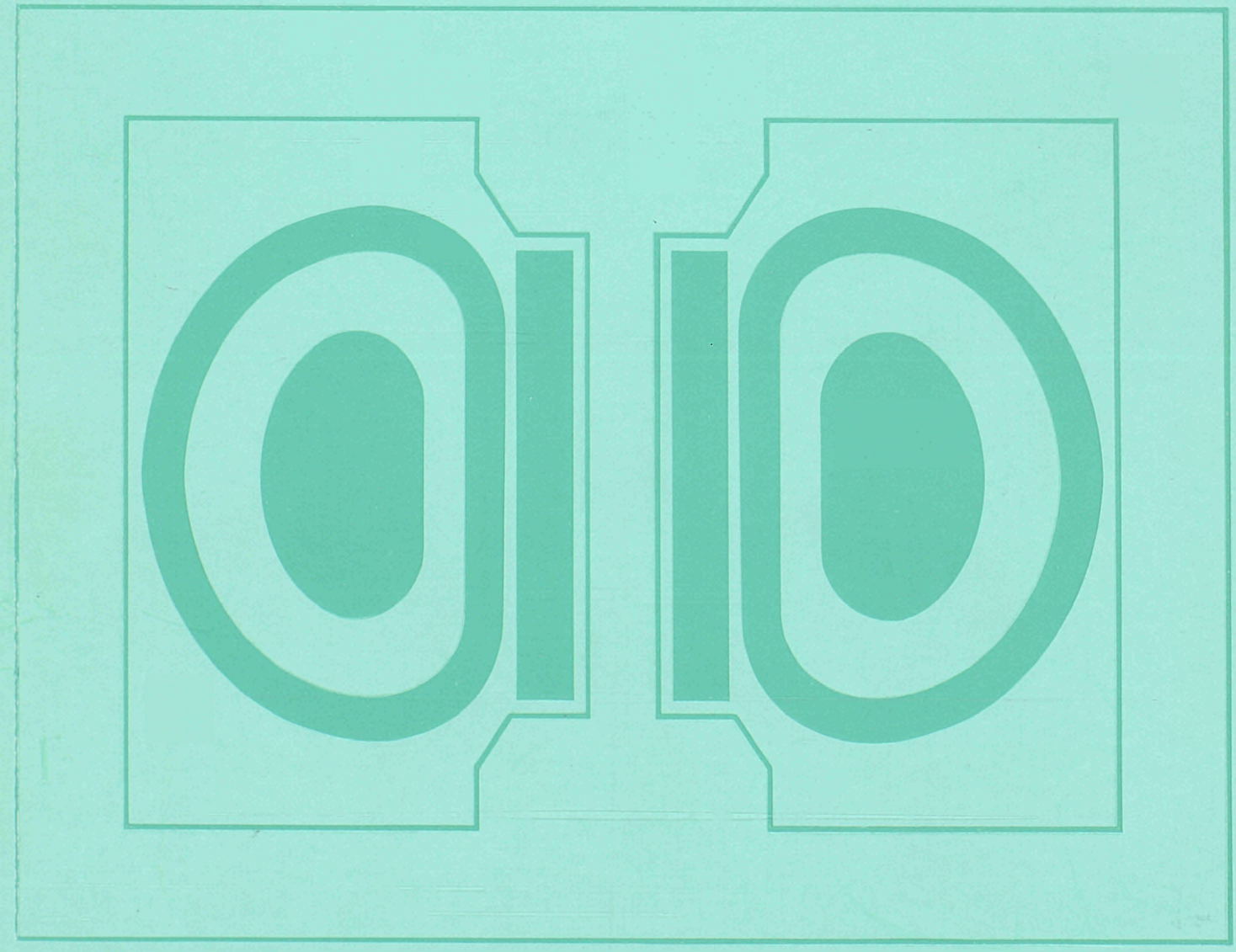

EUR 12323 EN
EUR-JET-PR6

JET JOINT UNDERTAKING

PROGRESS REPORT 1988

Volume I

JUNE 1989

This document is intended for information only
and should not be used as a technical reference.

EUR 12323 EN (EUR-JET-PR6) June 1989.
Editorial work on this report was carried out by B.E.Keen
The preparation for publication was undertaken by
the Documentation Service Unit, Culham Laboratory. UK.

Catalogue number: **CD-NA-12323-EN-C** *for the report* **EUR 12323-EN**

Printed in England

Contents

Volume I

Volume II

Foreword

This is the sixth of the JET Progress Reports, which covers the fifth full year of JET's operation. It provides an overview summary and puts into context the scientific and technical advances made on JET during the year. In addition, the document is supplemented by appendices of contributions (in preprint form) of the more important JET articles published during the year, which set out the details of JET activities. The report provides a more detailed account of JET's scientific and technical progress than that contained in the JET Annual Reports.

The document is still aimed not only at specialists and experts engaged in nuclear fusion and plasma physics, but also at a more general scientific community. To assist in meeting these general aims, the Report contains a brief summary of the background to the Project, describes the basic objectives of JET and the principal design aspects of the machine. In addition, the Project Team structure is included as it is within this structure that the activities and responsibilities for machine operation are carried out and the scientific programme is executed.

There is no doubt that 1988 proved to be another successful year for JET both from the technical and scientific viewpoints. The Project reached the midway point in its overall programme by completing Phase II devoted to exploring the most promising regimes for energy confinement and high fusion yield and to optimising conditions with full additional heating power in the plasma. The ultimate objective was to achieve full performance with all systems operating simultaneously.

Most of 1988 was devoted to machine operations with a previously planned major shutdown starting in October. Nine months were devoted to tokamak operations during 1988, which was one of the longest continuous operating periods on JET. The number of pulses during 1988 was 4673, bringing the total cummulative number of JET pulses to 18786. In spite of the complexity of introducing new systems, there was a further clear shift to the use of higher plasma currents with the number exceeding 3 MA in 1988 rising to 2398, which doubled the total number obtained up to that time.

An important aspect of the JET programme during the year was the introduction, commissioning and operation of the second neutral beam injector. The level of operation reached with two injectors was up to 21.6 MW of power injected into the torus with 80 keV deuterium beams, which should be compared with the design value of 20 MW. Towards the end of the operating period, a high degree of availability and reliability were achieved. With this power available ion temperatures exceeding 23 keV were reached in JET.

The radio-frequency heating system is gradually being upgraded so that each of the eight units will provide 4 MW source power instead of the original 3 MW. Ultimately, this should permit up to 24 MW RF power into JET plasmas. During 1988, partial modifications have permitted up to 18 MW in the plasma for 2 seconds duration. In combination, with neutral beam injection and RF heating, up to 35 MW of total power was applied to JET plasmas and in excess of 10 MJ of stored energy was obtained in the plasma.

During the year, the plasma current was raised to 7 MA for 2 second flat-top duration and has routinely operated with currents above 5 MA. This should be compared with the original design rating of 4.8 MA. A current of 6 MA was maintained for 7 seconds. In addition, a plasma current of 3 MA has been maintained for 30 seconds, and this was heated for over 20 seconds with 5 MW of RF power; both ion and electron temperatures exceeding 5 keV were sustained for this period.

JET operation above original design rated values was carried out with a number of technical restrictions imposed to operate the machine within conservative limits. The forces acting on the vessel during disruptions or vertical instabilities could pose risks to the mechanical integrity of the vessel and were limited by restricting operation at large plasma currents to smaller plasma elongations. The power deposited by the plasma on the water cooled RF antennae or the inboard wall was also limited to avoid damage to antennae and wall protections. These technical limitations were being addressed and design modifications were being planned to allow further progress in 1989.

The use of small pellets of solid deuterium is one of the possible methods of fuelling a fusion reactor. Experiments have been carried out with a multi-pellet injector which JET and the US Department of Energy (USDoE) have jointly installed and are jointly operating under the umbrella of the Bilateral Agreement on Fusion Research. Using 2.7 and 4 mm deuterium pellets, peaked density

profiles with central densities up to $2\times10^{20}m^{-3}$ have been achieved in material limiter and magnetic limiter configurations with decay times in the several seconds range. Centrally heating these plasmas with ICRF power has resulted in ion and electron temperatures together exceeding 10keV.

During the year, the current capability of single-null magnetic limiter (X-point) discharges and H-mode operation has been extended to currents of 5MA, full toroidal fields of 3.4T and neutral beam powers of 20MW. With the global energy confinement time, increasing roughly linearly with current, confinement times in the range 0.8-1s and stored plasma energies of more than 10MJ have been achieved with ~10MW of additional neutral beam heating. H-modes have also been obtained in the double-null X-point configuration with currents up to 3MA. Present JET H-mode plasmas are restricted to neutral beam heating of deuterium plasmas in a single-null X-point configuration, but further experiments will be carried out with ICRF heating, particularly using beryllium walls to reduce impurity levels in the plasma.

A record value of the fusion product ($n_i\ \tau_E\ T_i$) of $2.5\times10^{20}m^{-3}$.s.keV was achieved during 1988 in the H-mode of magnetic limiter operation (X-point) with ~15MW of neutral beam input into a 4MA plasma, following optimization of the various plasma parameters. In addition, a significant improvement was made in the fusion product with RF heating of a pellet seeded plasma. A value of $2.0\times10^{20}m^{-3}$.s.keV ($n_i=5.4\times10^{19}m^{-3}$, $T_i=7.2$keV, and $\tau_E=0.5$s) was reached using 12MW RF heating in a 3MA deuterium plasma. In addition, fusion reactivity studies were undertaken in which minority ^{3}He ions were accelerated to energies in the MeV range using ICRF heating. The fusion reactivity at the highest power levels (>15MW) was $2\times10^{16}s^{-1}$, which is equivalent to 60kW of fusion power in the charged particle products. Although this is small compared with the input, it is the highest that has been achieved in a fusion device so far. The reactivity was close to theoretical predictions. The maximum neutron yield obtained so far was $1.2\times10^{16}s^{-1}$ produced with neutral beam heating. This resulted mainly from D-D reactions occurring between the deuterium particles in the heating beams and the plasma. The best ratio of fusion power to input power obtained was $Q_{DD}=5\times10^{-4}$ which is equivalent to $Q_{DT}\sim0.3$, if tritium was introduced into the machine under these conditions. This would correspond to a fusion power production of above 5MW. This enhanced reaction rate is due to interactions between the plasma and neutral heating beams.

During 1988, operation concentrated on bringing the two neutral beam boxes and the RF heating system into full operation. During the first half of 1989, one of the neutral beam boxes should be ready for operation at increased energy (~140keV) allowing greater penetration into the plasma at higher density. In addition, all eight generators of the ICRF heating system should be upgraded to a total power of 32MW which should provide about 24MW into the plasma. This should make available a total additional heating power of 44MW. Reinforcements will have been introduced to strengthen the vacuum vessel and allow higher powers into the plasma for longer duration at the highest currents. This should make operations possible with 7MA plasma currents in the material limiter configuration and over 5MA in the magnetic limiter mode at the highest power levels. In addition, the belt limiter and the RF antennae carbon protection tiles will be replaced by beryllium to improve the plasma purity and assist in controlling the plasma density. A prototype lower hybrid current-drive (LHCD) system and a prototype high speed pellet injector will be installed later in 1989. These should allow checks on the confinement properties as the current and density profiles are tailored. However, emphasis will be given to controlling plasma density and improving plasma purity. These enhancements should enable improved plasma parameters to be obtained as well as higher fusion products.

To date, the scientific results obtained in JET have been most encouraging. Plasma temperatures, plasmas densities and confinement times have now reached individually those needed in a reactor, but not simultaneously. JET is the only machine in the world to have reached this stage. Both ion and electron temperatures over 10keV have been achieved at the same time, albeit at a lower density than required in a reactor. In some experiments, ion temperatures up to 23keV were reached. Energy confinement times greater than 1s have been obtained in JET – the only machine to do so. Plasma densities have also reached values suitable for a reactor. Therefore, JET has successfully achieved and contained plasmas of thermonuclear grade.

Although JET is presently about a factor 20 below the simultaneous values of density, temperatures and confinement time required in a reactor, knowledge gained within the JET Programme enables us to define confidently the parameters of a fusion reactor. It is known that a reactor will be about two and a half times the linear dimensions of JET, have a plasma current capability of about 25-30MA and an output of several GW. In addition, the plasma must be maintained for very long times, such as 1 hour, rather than the 20-30s bursts in JET.

Sufficient knowledge exists to design such a device, but there are still a number of so-called plasma engineering problems that remain to be solved. These relate mainly to the interaction of the plasma with the vessel walls, including control of impurities, fuelling and exhaust. JET has the capability of studying these problems and will be doing so in the second half of its programme. Ultimately, JET will operate with deuterium-tritium plasmas, rather than pure deuterium ones, so that we can study the production of alpha-particles in a true thermonuclear plasma. This will require a tritium fuelling system and, since JET will become active, remote handling equipment will be used. JET is already devoting considerable effort to design-

ing, procuring and commissioning this equipment for later installation.

JET is the largest and most powerful fusion experiment, it has the capability for studying these reactor relevant problems and providing decisive information required in designing and planning the Next Step devices, such as the Next European Torus (NET) and the International Thermonuclear Experimental Reactor (ITER). It is important that JET provides these results. The future of Fusion relies on the success of JET: it is a necessary condition to proceed to the Next Step.

The most encouraging results obtained to date are a tribute to the dedication and skill of all who work on the Project. They also reflect the continuous co-operation and assistance received from the Associated Laboratories and from the Commission of the European Communities. I am confident that with such dedication of the staff and the support and guidance of the JET Council, JET Scientific Council and the JET Executive Committee, the Project will be able to meet these challenges to be encountered in future years and contribute substantially to crucial information for Next Step devices.

Dr. P.H. Rebut
Director
May 1989

Introduction, Background and Report Summary

Introduction

JET Progress Reports are aimed both at specialists engaged in plasma physics and nuclear fusion research and at the more general scientific community. This is in contrast to the JET Annual Reports, which are intended to provide overview descriptions of the scientific, technical and administrative status of the JET programme, and which is directed to the average member of the public. To meet these general aims, the Progress Report contains a brief summary of the background to the Project, it describes the basic objectives of JET and the principal design aspects of the machine. In addition, the Project Team structure is detailed, as it is within this framework that the activities and responsibilities for machine organization are performed and the scientific programme is executed.

The main part of the 1988 Report provides overview summaries of scientific and technical advances made during the year, supplemented by appendices of detailed contributions (in preprint form) of the most important JET technical articles produced during the year. The final part of the Report briefly sets out developments underway to further improve JET's performance and plans for future experiments through to its foreseen completion in 1992.

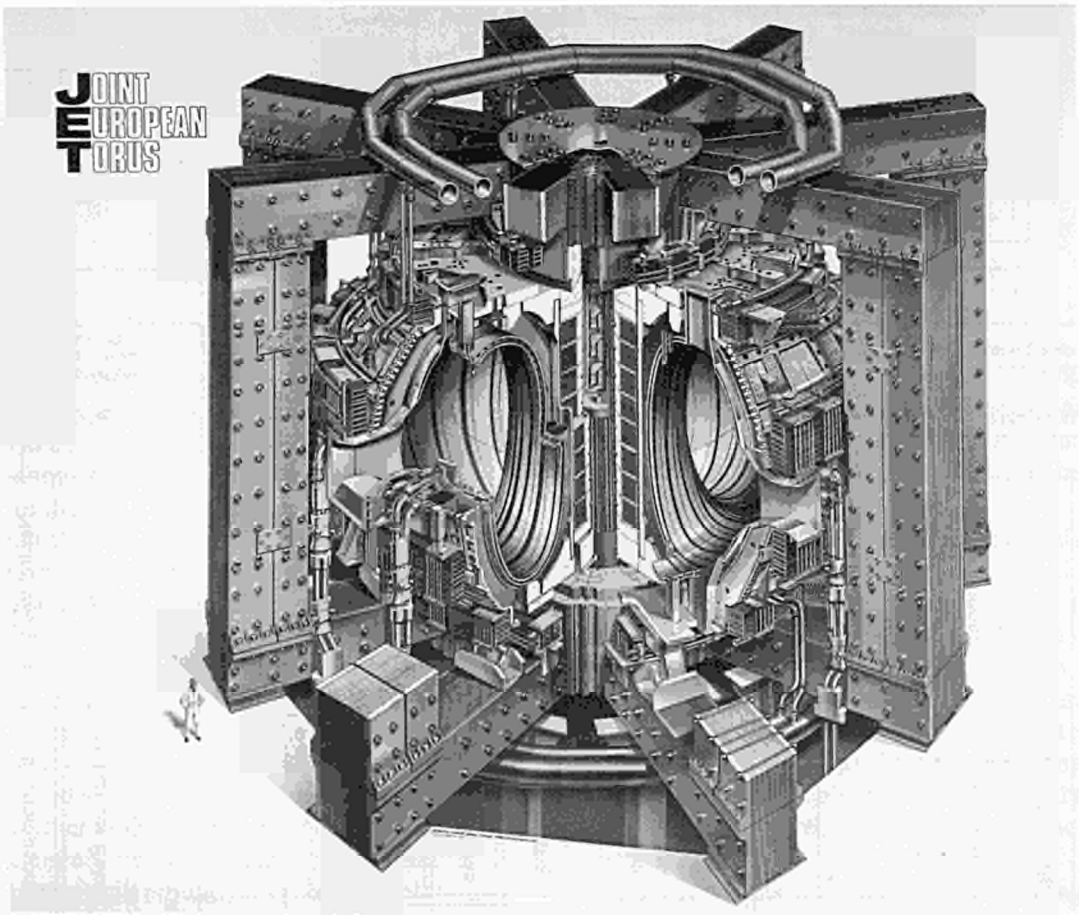

Fig. 1 Diagram of the JET Tokamak

Background

Objectives of JET

The Joint European Torus (JET) is the largest single project of the nuclear fusion research programme of the European Atomic Energy Community (EURATOM). The project was designed with the essential objectives of obtaining and studying plasma in conditions and with dimensions approaching those needed in a fusion reactor.

The studies are aimed at:

(a) investigating plasma processes and scaling laws, as plasma dimensions and parameters approach those necessary for a fusion reactor;

(b) examining and controlling plasma-wall interactions and impurity influxes in near-reactor conditions;

(c) demonstrating effective heating techniques (particularly, RF and Neutral Beam Heating), capable of approaching reactor temperatures in JET, in the presence of the prevailing loss processes;

(d) studying alpha-particle production, confinement and subsequent plasma interaction and heating produced as a result of fusion between deuterium and tritium.

Two of the key technological issues in the subsequent development of a fusion reactor are faced for the first time in JET. These are the use of tritium and the application of remote maintenance and repair techniques. The physics basis of the post-JET programme will be greatly strengthened if other fusion experiments currently in progress are successful. The way should then be clear to concentrate on the engineering and technical problems involved in progressing from an advanced experimental device like JET to a prototype power reactor.

TABLE I
Principal Parameters

Parameter	*Value*
Plasma minor radius (horizontally), a	1.25m
Plasma minor radius (vertically), b	2.10m
Plasma major radius, R_0	2.96m
Plasma aspect ratio, R_0/a	2.37
Plasma elongation ratio, e=b/a	1.68
Flat top pulse length	25s
Toroidal magnetic field (plasma centre)	3.45T
Plasma current, D shaped plasma	7.0MA
Volt-seconds available	42Vs
Toroidal field peak power	380MW
Poloidal field peak power	300MW
Additional heating power (into torus)	~50MW
Weight of vacuum vessel	108t
Weight of toroidal field coils	364t
Weight of iron core	2800t

Table II

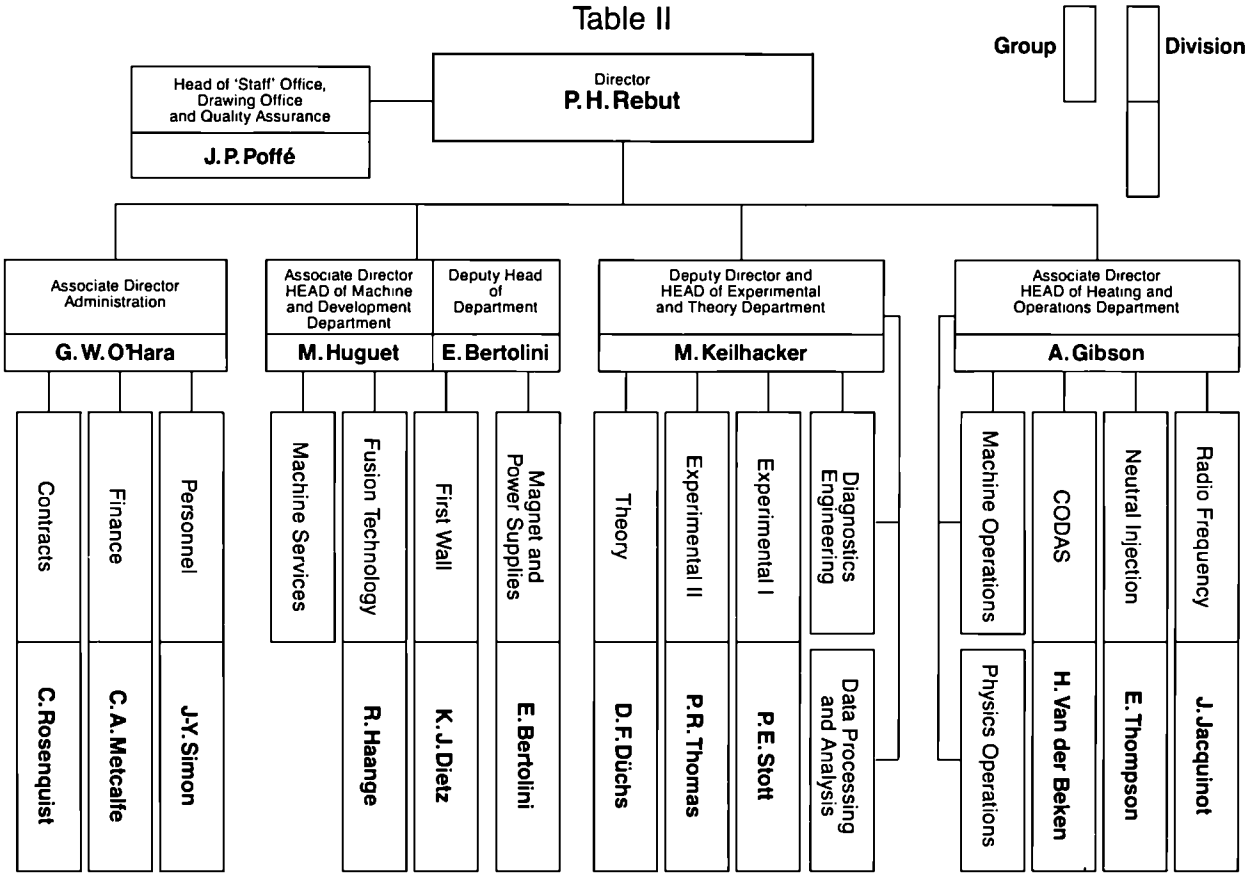

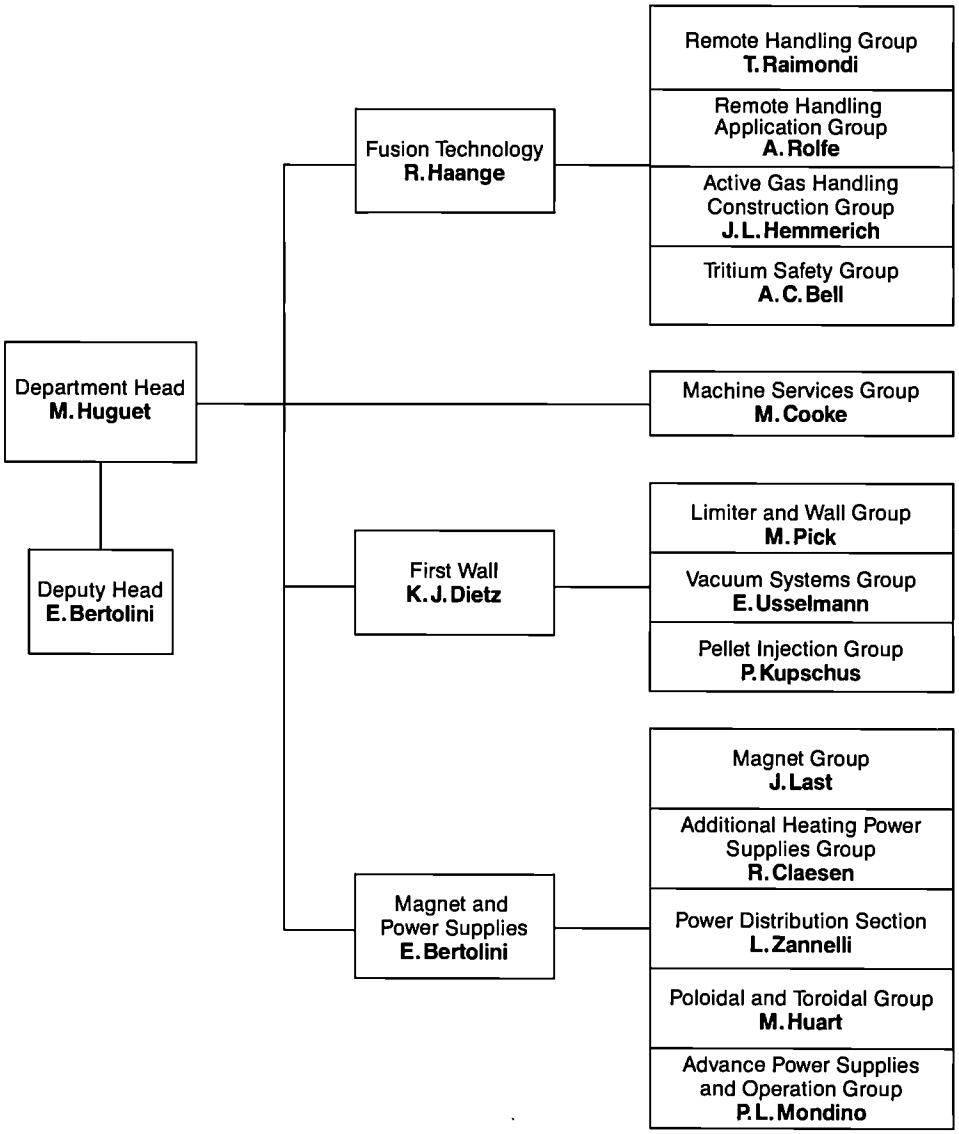

Fig. 2 Machine and Development Department, Group Structure (December 1988)

Basic JET Design

To meet these overall aims, the basic JET apparatus was designed as a large tokamak device with overall dimensions of about 15 m in diameter and 12 m in height. A diagram of the apparatus is shown in Fig. 1 and its principal parameters are given in Table I. At the heart of the machine, there is a toroidal vacuum vessel of major radius 2.96 m having a D-shaped cross-section 2.5 m wide by 4.2 m high. During operation of the machine, a small quantity of gas (hydrogen, deuterium or tritium) is introduced into the vacuum chamber and is heated by passing a large current through the gas. Originally, the machine was designed to carry 4.8 MA, but has already been modified to achieve 7 MA. This current is produced by transformer action using the massive eight-limbed magnetic circuit, which dominates the apparatus (see Fig. 1). A set of coils around the centre limb of the magnetic circuit forms the primary winding of the transformer with the plasma acting as the single turn secondary. Additional heating of the plasma is provided by propagating and absorbing high power radio frequency waves in the plasma and by injecting beams of energetic neutral atoms into the torus.

The plasma is confined away from the walls of the vacuum vessel by a complex system of magnetic fields, in which the main component, the toroidal field, is provided by 32 D-shaped coils surrounding the vacuum vessel. This field, coupled with that produced by the current flowing through the plasma, forms the basic magnetic field for the tokamak confinement system, which provides a full design field at the plasma centre of 3.45 T. The poloidal coils, positioned around the outside of the vacuum vessel, shape and position the plasma in operation.

Initial experiments have been undertaken using hydrogen and deuterium plasmas, but in the later stages of the

MACHINE AND DEVELOPMENT DEPARTMENT

Head of Department: M. Huguet
Deputy Head of Department: E. Bertolini

D Carre	S McLaughlin	M Walravens
Mrs H Marriott	L Sonnerup	

MAGNET AND POWER SUPPLIES DIVISION
Head: E Bertolini

Mrs C Allen	D Halliwell	P Presle
P Bertoldi	M Huart	C Raymond
T Bonicelli	F Jensen	A Santagiustina
I Borch	J R Last	S Shaw
O Buc	J McKivett	S Turley
J Carwardine	V Marchese	J van Veen
C Christodoulopoulos	G Marcon	N Walker
R Claesen	L Mears	Mrs L T Wall
E Daly	P Mondino	C R Wilson
P Doyle	G Murphy	G C Wilson
H T Fielding	Mrs J Nolan	L Zannelli
J Goff	P Noll	

FUSION TECHNOLOGY DIVISION
Head: R Haange

A C Bell	J Gowman	P Milverton
S J Booth	J L Hemmerich	G Newbert
P Brown	Mrs M E Jones	A Nowak
C Caldwell-Nichols	L P D F Jones	Miss S Perrissin-Fabert
P Chuilon	A Konstantellos	T Raimondi
R Cusack	E Küssel	J Removille
L Galbiati	R Lässer	A Tesini
A Galetsas	J Mart	M Wykes

FIRST WALL DIVISION
Head: K J Dietz

W P Bailey	M Gadeberg	J Orchard
H Buttgereit	D Holland	A Peacock
C Celentano	Mrs I Hyde	M Pick
Mrs D Cranmer	G Israel	L Rossi
W Daser	H Jensen	K Sonnenberg
E Deksnis	T Johnson	R Thomas
D Flory	P Kupschus	E Usselmann
C Froger	P McCarthy	T Winkel

Fig. 3 Project Team Staff in Machine and Development Department (December 1988)

operation, it is planned to operate with deuterium-tritium plasmas, so that fusion reactions can occur to produce significant α-particle heating in the plasma.

In order to reach conditions close to those relevant to a fusion reactor, a plasma density of $\sim 10^{20} m^{-3}$ at a temperature of 10-20 keV would be needed. Even with a current of up to 7 MA in JET, this would be inadequate to provide the temperature rquired using ohmic heating alone. Consequently, additional heating is required and two main systems are being used at JET, as follows:

- Injection into the plasma of highly energetic neutral atoms (Neutral Injection Heating);
- Coupling of high power electromagnetic radiation to the plasma (Radio Frequency (RF) Heating).

The total power into the torus will increase in discrete steps up to ~50 MW.

Project Team Structure

The Project structure adopted, for management purposes, is divided into four Departments (see Table II):

- Machine and Development Department;
- Experimental and Theory Department;
- Heating and Operations Department;
- Administration Department.

In addition, some scientific and technical duties are carried out within the Directorate and in the Coordinating Staff Unit.

The main duties of the Administration Department have been described in previous JET Annual Reports. This Report concentrates on progress made in the scientific and technical areas during 1988. To aid this description, the functions of these Departments are described below.

Machine and Development Department

The Machine and Development Department is responsible for the performance capacity of the machine as well as equipment for the active phase, together with enhancements directly related to it (excluding heating) and the integration of any new elements on to the

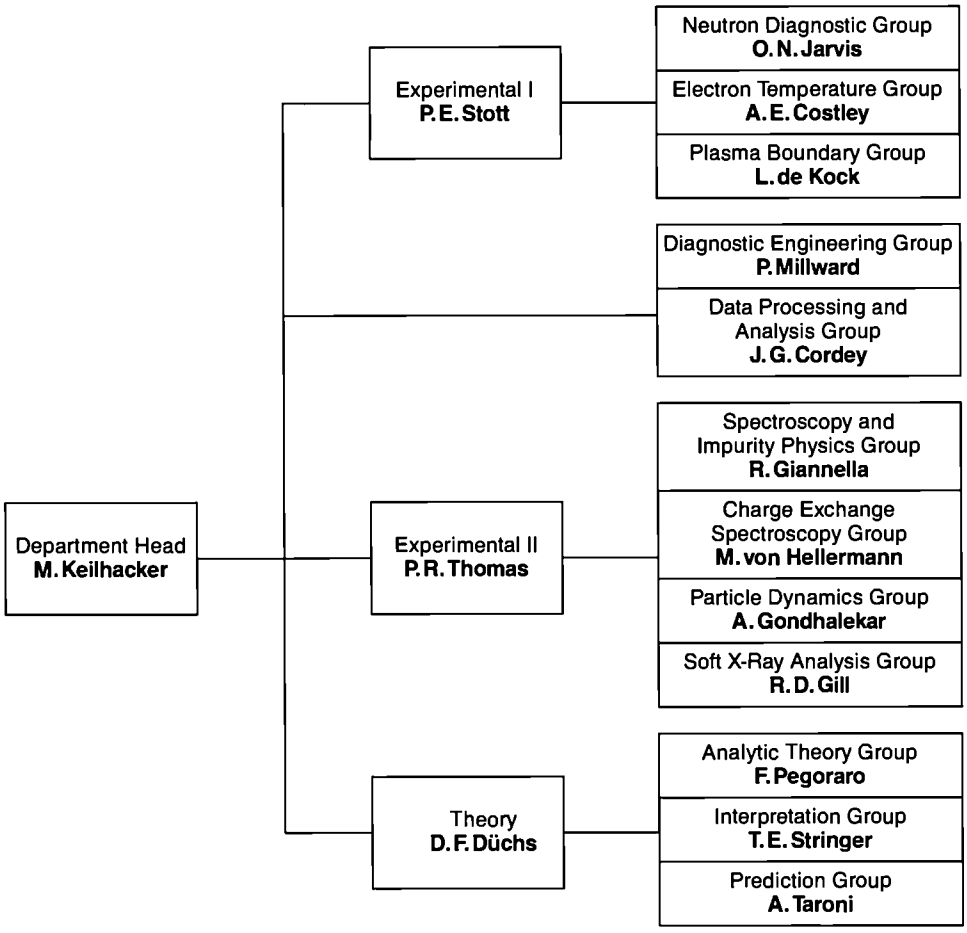

Fig. 4 Experimental and Theory Department, Group Structure (December 1988)

machine. In addition, the Department is responsible for machine services. The Department contains three Divisions:

(a) Magnet and Power Supplies Division, which is responsible for the design, installation, operation, maintenance and modification of all power supply equipment needed by the Project. In addition, the Division is responsible for maintenance and operation of the coil systems, structural components and machine instrumentation;

(b) First Wall Division, which is responsible for the vital area of plasma wall interactions. Its main tasks include the provision and maintenance inside the vacuum vessel of conditions leading to high quality plasma discharges. The Division develops, designs, procures and installs first wall systems and components, such as limiters, wall protections and internal pumping devices. The area of responsibility encompasses the vacuum vessel as a whole, together with its associated systems, such as pumping, bakeout and gas introduction;

(c) Fusion Technology Division, which is responsible for the design and development of remote handling methods and tools to cope with the requirements of the JET device, and for maintenance, inspection and repairs. Tasks also include the design and construction of facilities for handling tritium.

The Structure of the Machine and Development Department to Group Leader level is shown in Fig.2 and the list of staff within the Department is shown in Fig.3.

Experimental and Theory Department

The main functions of the Department relate to the measurement and validation of plasma parameters and to the theory of tokamak physics. The main tasks are:

- to conceive and define a set of coherent measurements;
- to be responsible for the construction of necessary diagnostics;
- to be responsible for the operation of the diagnostics and the quality of measurements and the definition of the plasma parameters;
- to follow the theory of tokamak physics;
- to play a major role in interpretation of data.

The Department contains two Groups (Diagnostics Engineering Group and Data Processing and Analysis Group) and three Divisions:

(a) Experimental Division 1 (ED1), which is responsible for specification, procurement and operation of approximately half the JET diagnostic systems. ED1

EXPERIMENTAL AND THEORY DEPARTMENT

Head of Department: M. Keilhacker

B Balet
M Barnes
J Christiansen
J G Cordey
C J Hancock
J Hoekzema
Miss J Kedward
P Millward
D O'Brien
R Oord
Miss A Reichenau
J Reid
P J Roberts
Miss K Slavin
Mrs P Stubberfield
A R Talbot
K Thomsen
A Tiscornia
E van der Goot
M L Watkins
J Wesson
C H Wilson
D Wilson

EXPERIMENTAL DIVISION I

Head: P E Stott

Miss N Avery
D Bartlett
B W Brown
D Campbell
J Coad
A E Costley
J Ehrenberg
L de Kock
J Fessey
C Gowers
P J Harbour
M Hone
I Hurdle
O N Jarvis
G Neill
C Nicholson
P Neilsen
R Prentice
Mrs D Pryor
P Roach
G Sadler
A Stevens
D Summers
P van Belle
J Vince
D J Ward

EXPERIMENTAL DIVISION II

Head: P R Thomas

G Braithwaite
J L Bonnerue
A D Cheetham
S Corti
Miss G B Denne
A Edwards
Mrs A Flowers
R Giannella
R Gill
A Gondhalekar
N Gottardi
J Holm
Mrs S Humphreys
L Lamb
G Magyar
J L Martin
F Mompean
P Morgan
H Morsi
J O'Rourke
J Ryan
D Pasini
M Stamp
M von Hellerman
B Viaccoz

THEORY DIVISION

Head: D F Düchs

W Core
Mrs S Costar
A Galway
T Hellsten
Mrs S Hutchinson
B Keegan
E Lazzaro
F Pegoraro
H C Sack
R Simonini
P Smeulders
E Springmann
T E Stringer
A Taroni
F Tibone

Fig. 5 Project Team Staff in the Experimental and Theory Department (December 1988)

undertakes electrical measurements, electron temperature measurements, surface and limiter physics and neutron diagnostics;

(b) Experimental Division 2 (ED2), which is responsible for specification, procurement and operation of the other half of the JET diagnostic systems. ED2 undertakes all spectroscopic diagnostics, bolometry, interferometry, the soft X-ray array and neutral particle analysis;

(c) Theory Division, which is responsible for prediction by computer simulation of JET performance, interpretation of JET data and the application of analytic plasma theory to gain an understanding of JET physics.

The structure of the Experimental and Theory Department to Group Leader level is shown in Fig.4 and the list of staff in the Department is shown in Fig.5.

Heating and Operations Department

Heating and Operations Department is responsible for heating the plasma, the organisation of experimental data, and the day-to-day operation of the machine. the main functions of the Department are:

- heating the plasma and analysis of its effects;
- centralising the interpretation of experimental results and investigating their coherence;
- organising data acquisition and computers;
- preparing and co-ordinating operation of the machine across the different Departments.

The Department is composed of three groups (Machine Operations Group, Physics Operation Group and Data Management Group) and three Divisions:

(a) Control and Data Acquisition System Division (CODAS), which is responsible for the implementation, upgrading and operation of computer-based

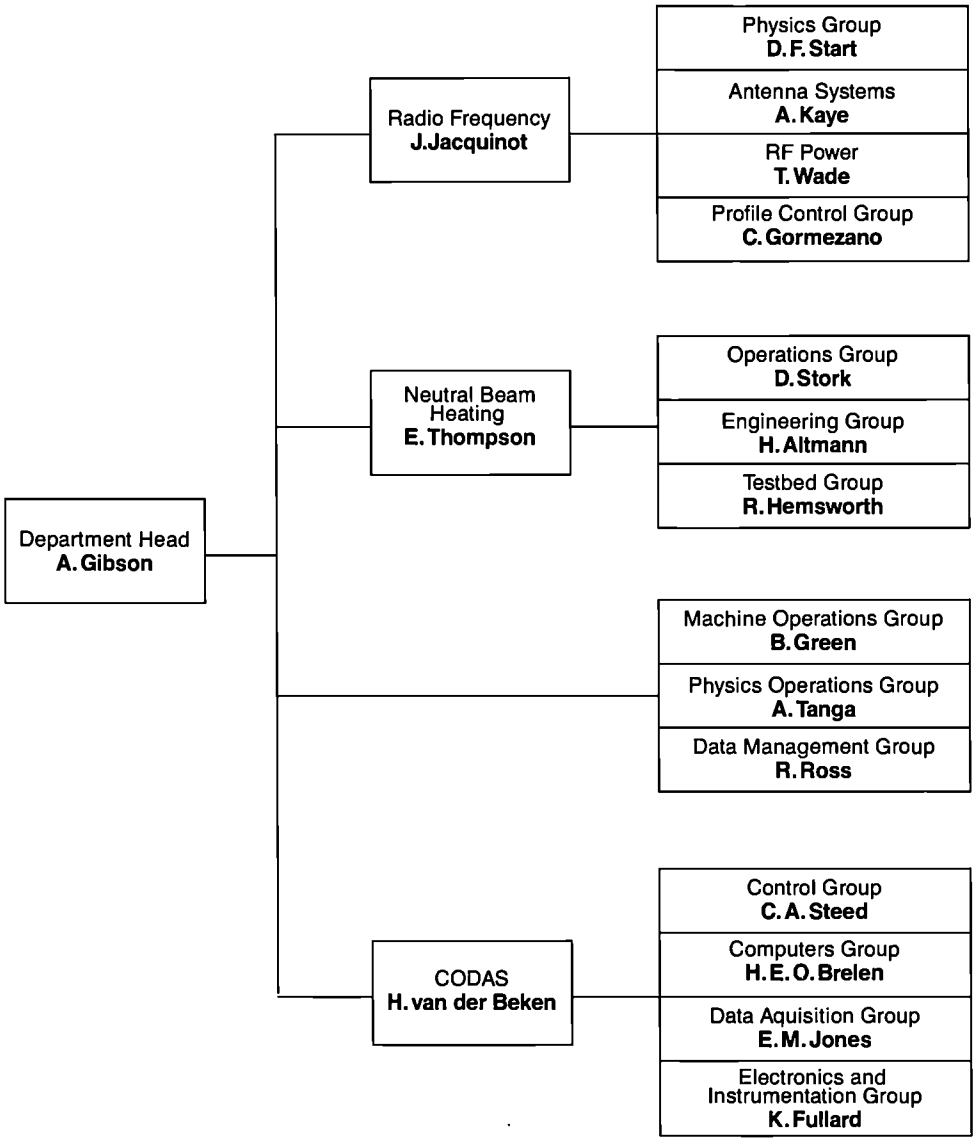

Fig. 6 Plasma Heating and Operation Department, Group Structure (December 1988)

control and data acquisition systems for JET;

(b) Neutral Beam Heating Division, which is responsible for the construction, installation, commissioning and operation of the neutral injection system, including development towards full power operation of the device. The Division also participates in studies of the physics of neutral beam heating;

(c) Radio Frequency Heating Division, which is responsible for the design, construction, commissioning and operating the RF heating system during the different stages of its development to full power. The Division also participates in studies of the physics of RF heating.

The structure of the Heating and Theory Department to Group Leader level is shown in Fig. 6, and the list of staff in the Department is shown in Fig. 7.

In addition, all Divisions are involved in:

- execution of the experimental programme;
- interpretation of results in collaboration with other appropriate Divisions and Departments;
- making proposals for future experiments.

Directorate

Within the Directorate are one scientific and one technical group, (Scientific Assistants to the Director and Technical Assistant to the Director (including Publications Office)), whose main tasks are as follows:

- Scientific Assistants to the Director, who assist and advise the Director on scientific aspects of JET operation and future development;
- Technical Assistant to the Director, who assists and advises the Director on organizational and technical matters related to JET operation and also acts as JET Publications Officer.

PLASMA HEATING AND OPERATION DEPARTMENT

Head of Department: A. Gibson

K Adams	M Hughes	J Roberts
A Conway	P Lomas	R T Ross
D Cook	P Longworth	P Rutter
S Cooper	C Lowry	W Smith
T Dale	M Macrae	A Tanga
B Green	M Malacarne	B Tubbing
N Green	Mrs M Pacco-Düchs	M Walker
Miss R Hausherr	D Pratt	B Workman
C Hookham	R Rigley	

NEUTRAL BEAM HEATING DIVISION

Head: E Thompson

H Altmann	Mrs S Gerring	D Martin
A Bickley	R Hemsworth	P Massmann
A Browne	F Hurd	C Mayaux
C D Challis	D Hurford	W Obert
D Cooper	J Z Jensen	S Papastergiou
J F Davies	A Jones	A J Parfitt
G Deschamps	T T C Jones	D Raisbeck
A Dines	D Kausch	R Romain
H P L de Esch	F Long	Mrs M Sinclair
D Ewers	J Lundqvist	D Stork
H Falter		

RADIO FREQUENCY HEATING DIVISION

Head: J Jacquinot

V Bhatnagar	A Franklin	P Murray
S C Booth	M Gammelin	M Pain
G Bosia	B Glossop	J Plancoulaine
M Brandon	C Gormezano	M Schmid
H Brinkschulte	E Hanley	Miss V Shaw
M Brusati	R Horn	A Sibley
M Bures	G Jessop	D Start
G Cottrell	A Kaye	T Wade
T Dobbing	M Lenholm	C Walker
D T Edwards	Miss J Maymond	

CONTROL AND DATA ACQUISITION SYSTEMS DIVISION

Head: H van der Beken

Mrs A M Bellido	J J Davis	G J Kelly
Mrs L Brookes	S Dmitrenko	N G Kidd
M J M Botman	S E Dorling	J G Krom
H E O Brelen	K Fullard	D S Nassi
W J Brewerton	R F Herzog	C A Steed
T Budd	Mrs F Herzog	I D Young
P J Card	E M Jones	

Fig. 7 Project Team Staff in the Plasma Heating and Operation Department (December 1988)

Coordinating Staff Unit

The Coordinating Staff Unit is responsible for the provision of engineering services to the whole Project and for the implementation of specific coordinating tasks at the Project level.

It comprises four Groups:

- Technical Services Group;
- Planning Group;
- Drawing Office;
- Quality Assurance Group.

The structure of the Directorate and Coordinating Staff Unit to Group Leader level is shown in Fig. 8 and the list of staff in these areas is shown in Fig. 9.

Report Summary

The first section of this Report provides a brief introduction and background information relevant to the Report. The second and third sections set out an overview of progress on JET during 1988 and with a survey of scientific and technical achievements during 1988 sets these advances in their general context. This summary is specifically cross-referenced to reports and articles prepared and presented by JET staff during 1988. The more important of these articles, which are of general interest, are reproduced as appendices to this Report.

The fourth section is devoted to future plans and cer-

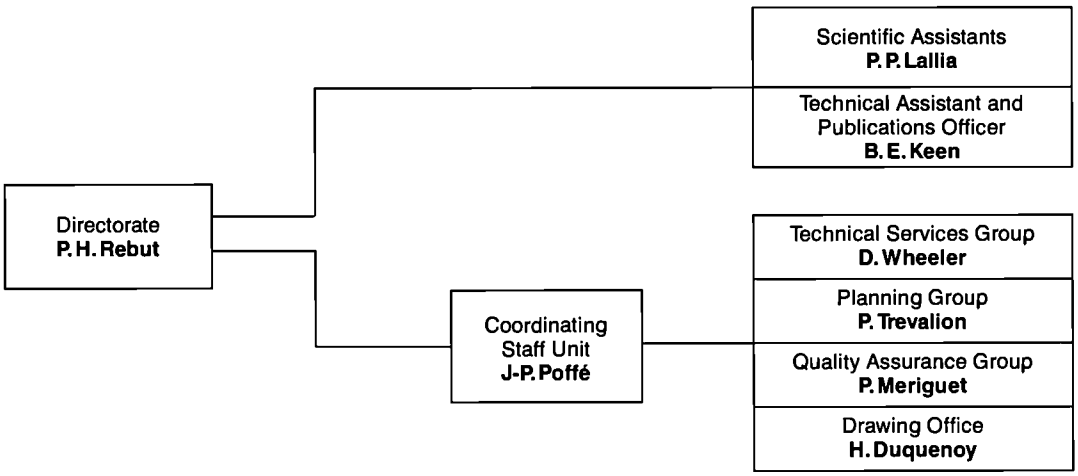

Fig.8: Directorate and Coordinating Staff Unit, Group Structure (December 1988)

DIRECTORATE AND COORDINATING STAFF UNIT

Director: Dr P H Rebut

DIRECTORATE

Mrs S-J Ashwood
M Drew
Miss C Hampson
Mrs M Harper
M Hugon
B E Keen
P P Lallia
J McMahon
P Mendonca
T O'Hanlon
Mrs C Simmons
Ms M Straub
Mrs J Talbot

COORDINATING STAFF UNIT

Head: J-P Poffé

Ms L Ashby
P Barker
G Dalle-Carbonare
Mrs D Dalziel
N Davies
H Duquenoy
G Edgar
L French
M Guillet
Mrs E Harries
H Jones
Mrs N McCullough
P Meriguet
H Panissie
P Trevalion
C Woodward

Fig.9 Project Team Staff in the Directorate and Coordinating Staff Unit (December 1988)

tain developments which might enable enhancements of the machine to further improve its overall performance. These improvements might overcome certain limitations encountered generally on Tokamaks, particularly concerned with density limits, with plasma MHD behaviour, with impurities and with plasma transport. Some attention has been devoted to methods of surmounting these limitations and these are detailed in this section.

The Appendices contain a list of work topics carried out under Task Agreements with various Association Laboratories, and selected articles prepared by JET authors are reproduced in detail, providing some details of the activities and achievements made on JET during 1988. In addition, a full list is included of all Articles, Reports and Conference papers published by JET authors in 1988.

Technical Achievements during 1988

Torus Systems

The main effort during the year was divided between: contributions to JET operation; preparation for the 1988/89 shut-down (including the procurement of in-vessel components); setting-up a test-bed for the development of a high-speed pellet injector; and preparation for the installation of a high-speed multiple pellet injector in the torus during 1989.

The contribution to JET operation is mainly services for the vacuum system and operation of the pellet injection as a part of the JET experimental programme during 1988.

Vacuum Systems

1988 was a major year of operation for JET, and this provided the opportunity to gain experience on the reliability of installed equipment. Experience gained with the vacuum equipment showed that the vacuum components (pumps, gauges, valves, flanges, etc.) performed satisfactorily, but interruptions in operation of the machine due to vacuum leaks at various locations were quite frequent. One reason was due to operation of the tokamak in excess of the design values (high plasma current, X-point operation, etc.) which in cases of plasma disruption put larger loads on the vessel and also on attached components. Some cracks were encountered in welds due to inertial forces on components. The problems were analysed and remedial action was taken during maintenance periods and during the shutdown to strengthen the weak points. Furthermore, the reliability of some components was improved by changing operation mode (e.g. the dosing valves, where fatigue failure on the bellows was observed, due to unnecessary application of power to the valves which initiated vibration in the bellows). It was found that the vessel supports needed improved locking devices which could be operated and released remotely without entering the Torus Hall. Therefore, a new thermal locking device for the supports was developed and will be installed during the 1988/89 shutdown.

Experience with other auxiliary systems, such as the new gas baking plant and the electrical baking system installed last year, was satisfactory when operated in the present mode. Nevertheless, some modifications in control systems were necessary to bring the system to its full performance. These modifications were prepared during the year and will be incorporated during the next shutdown.

There was also some progress in the development of new systems. The new piezo-driven gas[1] inlet-valve was tested on the machine and improvements were incorporated. The tests will continue by using it as an additional gas inlet system for the torus to gain further experience. Progress was also achieved in the development of the leak-test telescope. A test set-up was installed and prototype tests were continuing. In addition, a contract was placed for a prototype radiation resistant residual gas analyser following proving of the working principle.

In-vessel Components

With JET approaching full power operation, the in-vessel components were exposed to their most extreme loads yet. This included not only high power loads but also high mechanical loads during disruptions. Some weak points came to light and were remedied, but overall the in-vessel components achieved their expected performance and proved the chosen concept. The components requiring some remedial work were the bellows protection tiles, of which several were shaken loose, and of which three, each carrying three tiles, were dislodged. The attachment of these plates has been successfully modified with no further problems. Alterations were made to the X-point tiles on the top of the machine which were highly loaded during X-point operation. It was found necessary, in two mini shutdowns, to design new larger tiles for this region in order to accommodate the strongly varying position of the X-point and to align the tiles to a precision of $\sim \pm 1$ mm. This is the precision previously achieved during installation of the belt limiter. It is the aim in JET to achieve this precision for all new components in the X-point and inner wall regions.

The belt limiter, installed during the previous major shutdown, operated throughout the year with no significant damage to either the tiles or the structure. This was in spite of the fact that the belt limiter was run without water cooling for most of the time due to restrictions imposed by the interconnected antennae. New tiles were

designed and manufactured for the area adjacent to the gaps in the belt limiter which are located at both the top and bottom at Octant Nos: 3 and 6. These gaps were included to allow certain diagnostic systems unobstructed view of the plasma.
The alterations were necessary because the gaps allowed field lines which are otherwise intercepted by the belts to continue further and to cause a localized but unnacceptable power deposition onto the adjacent antennae. The alterations involved a change in the shape and size of twenty tiles on each side of the gaps. The new geometry, a result of a careful analysis, was aimed at intercepting more field lines which otherwise pass through the gap whilst ensuring that (a) the power deposition per unit area onto the new tiles remains within the limits set for the original ones and, (b) the ability of the belt limiter system to accept plasmas of varying shapes remains unimpeded. The subsequent operation with the new tiles has shown that these objectives have been achieved.

To reduce the deformation of the vessel during disruptions at high current, internal restraint rings[2,3] were designed, procured and installed during 1988. An assessment of forces showed
that during a typical disruption at 7MA, additional radial loads of 20,000kN and deflections of 15 to 20mm at the inboard wall of the vessel should be expected. To remedy this, two inconel strengthening rings, above and below the mid-plane of the torus, were welded onto the inboard wall (see Fig.10). These should resist the local radial forces by their hoop strength and stiffness, and reduce the displacements of the vessel wall and ports by an order of magnitude, down to less than 2mm. These should also eliminate the risk of overloading the existing ring reinforcements along the outside of the vessel, which at present carry all the radial loads by their hoop strength. The new rings on the inboard wall will carry approximately 30% of the radial load in a radial disruption, i.e. up to 8000kN.

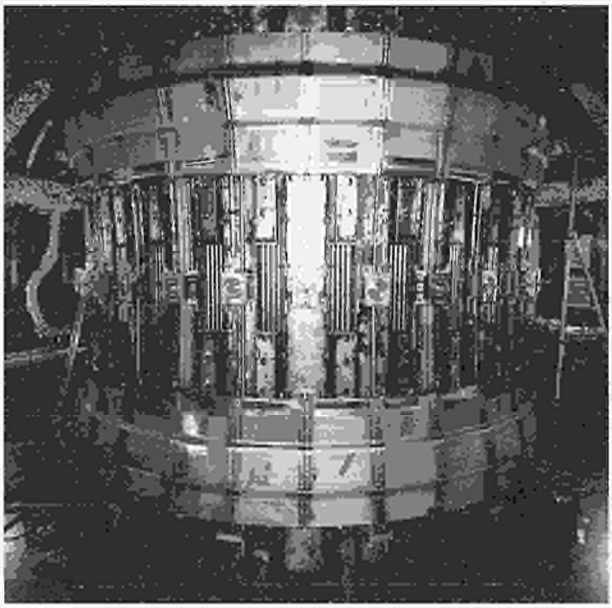

Fig.10: Reinforced ring installed inside the JET vessel;

The study and design of the pumped limiter[4] was completed successfully in collaboration with the U.S. Department of Energy. Material tests showed that loads of up to $4\,W/m^2$ could be sustained for one to two seconds at the leading edge, with surface temperatures rising up to 2200°C.

In the light of the recent results on temperature limitations in graphite to a maximum of 1100°C (to avoid avalanche impurity generation), the scheme of the pumped limiter for JET could not be validated and is not being followed in the future.

JET has now reached the stage at which there is maximum coverage of the walls with graphite[5]. An alternative was prepared (beryllium) in case operation with graphite would show major problems. Mainly due to dilution effects (up to 80% of the particles in the plasma may result from impurities, mainly graphite) and the temperature limitations due to self sputtering of graphite, it is now proposed to introduce beryllium into JET at the start of the next operational period, in order to enhance its performance and to enable it to reach the desired goal. Preparations for the required installation of beryllium components into the machine as well as the components themselves are in their final stages. The components to be installed include: four beryllium evaporators, a complete set of beryllium tiles for the belt limiter as well as for the RF-antennae protection and, in addition, eight new beryllium antennae screens.

Pellet Injection

The JET multi-pellet injector has been built and is operated under a bilateral agreement between JET and the U.S. Department of Energy (USDoE). It performed satisfactorily in 88 experimental campaigns. Singly or bunched in sequences with repetition rates up to $5\,s^{-1}$, $\sim 1000\times 2.7$mm and 250×4mm pellets were delivered into 337 plasma discharges. The major fraction of these experiments were performed within periods allocated to the 'Pellet Fuelling and Density Profile Effects' Task Force. An enhanced confinement regime was found for central pellet deposition in conjunction with central ICRF heating of limiter discharges[6-12]. There were also significant contributions to subjects of the other Task Forces, mainly preliminary experiments to probe other scenarios (e.g. Injection into X-point and H-mode discharges; Fuelling experiments in which in one case 32×2.7mm pellets were injected at $4\,s^{-1}$; Injection into neutral beam heated High-T_i shots starting at low density in which pellets were used in the density build-up and fuelled the shot with the highest neutron rate so far).

The flawless functioning of the injector and the participation of the US team in the complementary strength required by the Agreement contributed a great deal to this success. From March through to the end of the experimental period in September, the pellet injector worked particularly reliably with little maintenance, hav-

ing undergone a thorough overhaul and recommissioning prior to start-up.

Consequently, a few minor modifications and enhancements were identified; most will be implemented in the 1988/89 shutdown, as follows:

- Insertion of a flexible image guide into the existing periscope (for the observation of the D_α-plume of the pellet entering the plasma) in order to withstand plasma disruptions;
- Full commissioning of the injector-plasma interlock system (PLPS) and the development of a software package to enable the main console team (rather than the injector operator) to programme and arm the injector remotely;
- Construction of a revised pellet in-flight photography station further downstream on the pellet path than present, to avoid interference of the high-pressure driver gas with the pellet image;
- Design and construction of a regulated and voltage-programmable power supply (6 units) for improved characteristics at high-repetition pulsing of fast gas valves and puncher magnets of the ORNL Launcher;
- Installation of an upgraded hydrogen exhaust system (vacuum pumps, pipework and flame arrestors explosion-proof for any gas mixture) in order to provide inherent safety rather than relying on the rinsing/dilution with a stream of nitrogen.

Development of a high-speed pellet injector

The present multiple pellet injector is only capable of delivering pellets with speeds of up to 1500 m s^{-1}. For deeper penetration into JET plasmas, higher speeds up to 10 km s^{-1} are required. JET is presently developing a high-speed injector capable of producing pellets with 5 mm diameter and velocities of 3-5 km s^{-1}.

To identify and solve the technical problems, a test-stand[13] was set-up during 1988. The main components are shown schematically in Fig.11. The driving system is based on a two-stage gun in which the projectile is driven by hot hydrogen gas, which is heated in the first stage through adiabatic compression when driving the piston into the hydrogen filled pump tube. The piston is propelled by helium gas from a high pressure reservoir. The deuterium pellets are produced in a cryostat, which is an integratal part of the barrel. For measuring the position, velocity and acceleration of the pellet, pressure sensors are positioned along the barrel. These also allow measurement of the driving pressure of the pellet. The size and shape of the pellet is determined by flash photography. From the imprint that the pellet leaves on the target plate at the rear flange of the expansion tank, the reproducibility of the flight path of the pellet can be inferred.

Two such gun systems have been set up in parallel, as shown in Fig.12, to simultaneously attack different experimental issues. In the foreground, the highest stressed parts of the gun can be covered by movable mantles of rope netting. The testbed is equipped with an explosion-proof Roots forevacuum pump set for evacuation of the expansion tanks, with flame arrestors at the exhaust in compliance with safety requirements.

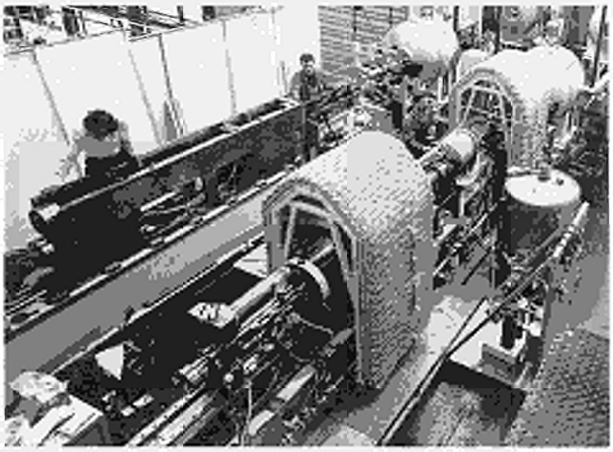

Fig.12: Layout of the test stand.

An adjacent control room houses most of the electronics and provides shelter for personnel during gun operation. At present, controls and data acquisition are facilitated by using custom-built hardware and oscilloscopes but they are being converted to employ data acquisition and control hardware as used in JET multi-pellet injector.

The following problems have been identified on the prototype launcher and the majority have been solved successfully:

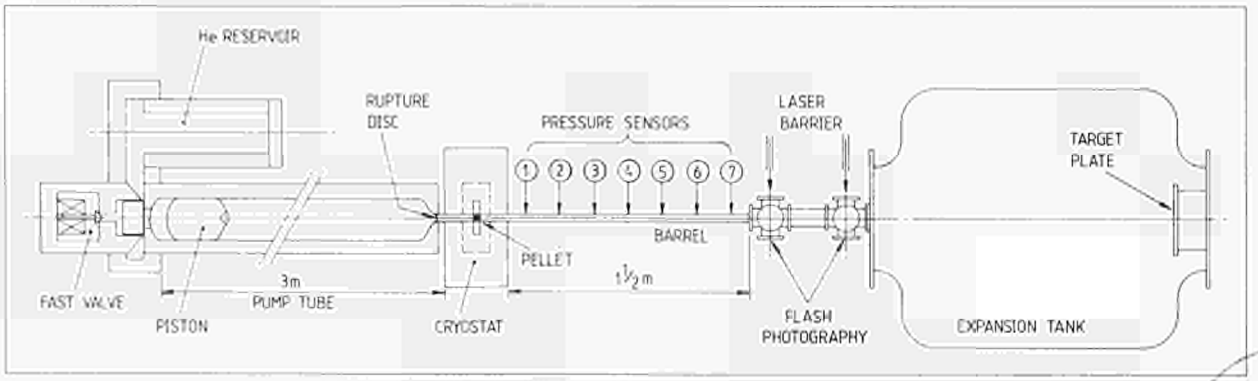

Fig.11: High-speed pellet gun system.

- in conventional two-stage guns, several components such as rupture discs and pistons must be replaced after each shot. To substitute the rupture disc which usually separates the helium reservoir from the pump tube, a fast (1 ms) high pressure (300 bar) high conductance (about 5 cm^2 aperture) valve has been developed and successfully operated. Such valves were not available commercially;
- Damage on the heavy fast moving piston ($E_{kin} \approx 50$ kJ; $v \approx 250\,ms^{-1}$) upon its impact onto the front face of the pump tube is avoided by reflecting it softly on a gas cushion and by using high strength materials (e.g. Ti alloys). Damage to the piston due to friction with the pump tube wall is prevented by employing centering forces generated by the gas flow using a properly shaped piston and an optimised gap between the piston and the wall. Also low friction coatings of the piston and glide rings are used to increase the lifetime of the piston. Pistons have survived more than 50 shots which is considered a sufficient number for a prototype gun;
- It has been found that the deuterium ice pellet must be supported by a 'sabot' to increase its shock and erosion resistance and to achieve higher acceleration. However, the sabot must be separated from the pellet and prevented from injection into the plasma. A technique has been successfully tested for plastic pellets by using split sabots and hollowing the rear end of the sabot. The propellant gas effectively splits the two halves of the sabot sideways when it leaves the barrel. In this way, the sabot can be caught by a target plate in front of the torus while the pellet is injected through a hole in the plate. Further development on the sabot technique is still necessary; particularly, to allow for higher acceleration values;
- A new cryostat, developed in cooperation with CEN Grenoble, France, to be employed for the sabot technique, has been used successfully. It allows replacement of the sabot by remote control and different production techniques for the pellet. It can be formed by condensing deuterium inside a sabot, or outside with subsequent transfer into the sabot or it can be injection moulded into sabots.

The testbed has been operational since mid-1988 and investigations have been performed using plastic as well as deuterium pellets formed and accelerated in sabots. Maximum pellet speeds achieved so far were 3800 m s^{-1}. This is mainly limited by insufficient strength of the sabot and the ice and this problem as well as the sabot separation and removal will be further investigated. Processes and components will be further optimised to permit installation of a high-speed prototype launcher by late 1989.

Preparation for installation of a high speed injector

The main engineering work has been devoted to preparation for the implementation of the high-speed prototype launcher, the final advanced, remote handling and tritium compatible, injector system for the JET Tritium Phase[14]:

- Design, construction and installation of a support system is now being completed for the two-stage guns (the type to be employed for the prototype as well as for the gun) featuring a large (~8 m long) beam for mounting the guns and for taking their considerable impact momentum of several 100 t to a suspension frame anchored to the Torus Hall concrete wall. The beam can be tilted around the axles of trunnion bearings on this frame (in the manner of a drawbridge) to make way for the transport of large equipment around the machine;
- Pulling and termination of the main cabling into its junction box is being completed for the final system;
- Conversion of the pellet injector box (PIB) from a vacuum vessel to a pressure vessel for 2.5 bar gauge to increase its hydrogen accumulation capacity to 2500 barℓ compatible with advanced gun requirements is in an advanced state;
- Finite element calculations and redesign have been completed; the lid is being secured by installing 35 lid clamps. Taking account of past experience, the cryogenic distribution valve box and the LHe dewar for the launcher have been redesigned for the Tritium Phase and new components have been ordered;
- Changes to the internal pellet diagnostics have been redesigned in view of the higher pellet speeds and are being incorporated. An adequate micro-wave interferometer for the prototype pellet mass and speed monitoring has been ordered and a new non-destructive in-flight target has been proven to work as a breadboard model and is now in design[15].

References

[1] E. Usselmann et al., 15th Symposium on Fusion Technology (SOFT), Utrecht, Netherlands (1988)

[2] M.A. Pick et al., 15th Symposium on Fusion Technology (SOFT), Utrecht, Netherlands (1988)

[3] M.A. Pick et al., 15th Symposium on Fusion Technology (SOFT), Utrecht, Netherlands (1988)

[4] K. Sonnenberg et al., 15th Symposium on Fusion Technology (SOFT), Utrecht, Netherlands (1988)

[5] K.J. Dietz, Vacuum, 38, (1988), 591

[6] P. Kupschus et al., 15th European Conf. on Controlled Fusion and Plasma Physics, Dubrovnik 1988, Europhys. Conf. Abstr. Vol 12b. 1, p147-150

[7] S. Milora et al., 15th European Coinf. on Controlled Fusion and Plasma Physics, Dubrovnik 1988. Europhys. Conf. Abstr. Vol.12b. 1, p147-150

[8] A. Gibson, 15th European Conference on Controlled Fusion and Plasma Physics, Dubrovnik, Yugoslavia, 1988, Plasma Phys. and Contr. Fusion, 30, 11, 1375-1390, 1988

[9] J. Jacquinot, 15th European Conference on Controlled Fusion and Plasma Physics, Dubrovnik, Yugoslavia, 1988, Plasma Phys. and Contr. Fusion, 30, (11), 1467-1478, 1988

[10] G.L. Schmidt et al., 12th IAEA Conf. on Plasma Physics and Controlled Nuclear Fusion Research, Nice, France, 1988, (Paper IAEA-CN-50/A-4-1)

[11] P. Kupschus et al., 'JET Multi-Pellet Injection Experiments', IAEA Technical Committee Meeting on Pellet Injection and Toroidal Confinement, Gut Ising FRG, Oct 24-26, 1988, to be published

[12] P. Kupschus, Invited paper 5-I-2, 'JET Multi-Pellet Injection Experiments', 30th Annual APS Meeting, Div of Plasma Physics, Hollywood Fla, USA, (1988)

[13] K. Sonnenberg et al, Proc. 15th Symposium on Fusion Technology (SOFT), Utrecht, Netherlands, (1988)

[14] P. Kupschus et al., 'The JET Multi-Pellet Injector and its Future Upgrades', IAEA Technical Committee Meeting on Pellet Injection and Toroidal Confinement, Gut Ising FRG, Oct 24-26, 1988, to be published

[15] W. Bailey et al., Proc. 15th Symposium on Fusion Technology (SOFT), Utrecht, Netherlands, (1988)

Power Supplies and Magnet Systems

The JET electromagnetic system is made up of the toroidal and poloidal coils, the purpose of which is to establish, maintain and control the tokamak magnetic configuration (see Fig.13). It includes the toroidal coils, the poloidal coil P1, acting as primary winding of the tokamak transformer and the coils P2, P3 and P4, to control plasma radial position, vertical position and shape. To perform these functions, the coils must be energised by suitable DC power supplies, whose voltages and currents are controlled in real-time by the plasma position and current control system (PPCC).

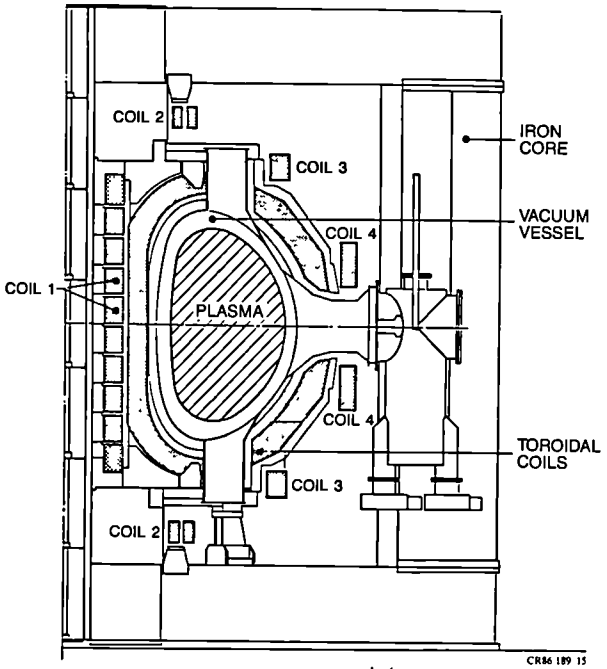

Fig.13: Cross-section of JET showing toroidal and poloidal coils.

Additional DC power supplies energize the neutral beam (NB) and radio frequency (RF) heating systems. The total installed DC power required by JET is well in excess of 1500MVA with a peak above 1000MW and an energy content per pulse up to 10,000MJ. More than half of the power and of the energy is taken directly from the National Grid at 400kV and the rest is provided by two vertical shaft flywheel generators. Consequently, a major feature of the JET power supply scheme is the 400kV-33kV distribution system. Auxiliary power is supplied by the 20MVA, 11kV-3.3kV-415V distribution system.

The development programme to bring JET, first to its full design performance and subsequently well above, calls for continuous modification and upgrading of the electromagnetic system. The key objective of 1988 was to extend the JET operating regime to plasma currents approaching 7MA in material limiter configurations and to ~5MA in magnetic limiter ('X-Point') configurations. In addition, considerable effort has been devoted to detailed studies to investigate the feasibility of longer pulse operations at 7MA and setting up X-Point configurations approaching 7MA, (in the so-called 7MA Study).

Study of New Extended Operating Conditions: The 7MA Study

Operation at currents up to 7MA in the material limiter configuration and in excess of 4MA in the magnetic limiter configuration required a complete engineering reappraisal in order to determine the safe operating limits for major machine components and identify any changes that might be needed.

The objectives of the study were ambitious since they called for a considerable extension of the machine design parameters both in terms of current level and energy dissipation. These objectives are highlighted in Table III.

Table III
Objectives of the 7MA Study

Parameter	*Original Design values*	*Objectives of the 7MA Study*
Plasma current (limiter configuration) (MA)	4.8	7
Plasma current (X-point configuration) (MA)	Not foreseen	6
Plasma current flat top at4.8MA (s)	10	–
at 7MA (s)	Not foreseen	10
Plasma elongation b/a	1.67	≈2
Toroidal field (Tesla)	3.45	3.45
Toroidal field flat top duration (s)	12	17
Primary winding current (kA)	40	60*
Primary winding flux swing (Wb)	34	42

(Note* 60kA in the 6 central coils only)

Three problem areas were identified during the course of the study:

- The containment of forces acting on the vacuum vessel during disruptions and vertical instabilities.
- The safe limits for the lateral forces acting on the toroidal field coils and due to the poloidal magnetic field crossing these coils.
- The thermomechanical problems in the ohmic heating coil due to the much increased energy dissipation.

1. Containment of forces acting on the Vacuum Vessel

The forces acting on the vacuum vessel during a radial disruption are due to eddy currents flowing in the toroidal and poloidal direction. The eddy currents flowing in the poloidal direction were found to be the most critical since these induce large displacements (~10mm at 6MA) of the inboard vessel wall and large amplitude radial oscillations (~6mm at 6MA) of the vertical ports. Extensive finite element calculations revealed that under such conditions the yield limit of the material is exceeded over a significant area at the base of the ports and structural failure could occur after only a few thousand disruptions.

Although the pattern of eddy currents during vertical instabilities is still not well understood, a number of theoretical and experimental studies indicate that the vertical force acting on the vacuum vessel would reach an amplitude of 6,000-10,000kN at plasma currents of 6-7MA.

The containment of these forces requires a number of modifications to the vacuum vessel and its supports:

a) The inboard wall of the vessel should be reinforced by toroidal inconel rings welded inside the vessel. These rings should virtually eliminate the radial deflection of the vessel wall and the radial oscillations of the ports during radial instabilities. This work was undertaken during the shutdown in October-1988 and is due for completion in early 1989.
b) The vacuum vessel supports which were installed in 1987, should be complemented by inertial brakes linking the vertical ports to the mechanical structure. These brakes should slow down radial displacements due to the rocking motion of the vessel. Installation has been planned for a short shutdown in September 1989.

These modifications should allow safe operation up to 7MA in the limiter configuration and 6MA in the X-point configuration.

2. Forces acting on the Toroidal Field Coils

The prototype toroidal field coil was subjected to a run of mechanically applied cycled loads simulating the lateral loads due to the poloidal field. The coil survived 10,000 cycles without detectable damage many including a run at a stress level 1.75 times higher than the most severe stress expected during operation at 7MA. It was concluded that lateral forces acting on toroidal field coils should not limit the machine performance.

3. Thermomechanical behaviour of the Ohmic Heating Coil

Refined finite element calculations were completed in 1988 and confirmed a thermal stress problem due to the temperature gradient produced by the cold incoming cooling water. To circumvent this problem, a new cooling loop was designed and commissioned in 1988. The water is now circulated in a closed loop and the temperature brought down in a controlled way so that temperature gradients are minimised. With this modification, the ohmic heating coil has now the current and flux capability shown in Table III.

Conclusion of the 7MA Study

The main conclusion of the 7MA Study is that the electromagnetic system, ie. coils and power supplies, should allow operation at plasma currents in excess of 7MA in both limiter and X-point configurations. The main limitation seems to come from the mechanical problems associated with the forces acting in the vacuum vessel during vertical instabilities. This should set a limit to the plasma current in the X-point configuration of ~6MA.

Magnet System

Investigations within the 7MA Study concentrated in two main areas of the magnet system:

- increased flux swing from the P1 magnetising winding;
- effects of out of plane forces on toroidal field (TF) coils and structure.

Increased Flux Swing

The six central inner poloidal coils (P1) support the inward force of the TF coils and are also pressed outwards by their own poloidal field. In the original JET design, the inward pressure was greater than that outwards. Therefore, it appeared to be feasible to increase the outward pressure by increasing the current in the P1 coil until the two balanced. An increase in P1 centre coil current from 40 to 60kA, with flux swing increased from 34 to 42Wb, was investigated.

To assist in the study several new finite element models were constructed ranging from simple 2D to detailed 3D models of large coil sections. These showed that increased current, was feasible but that problems of thermal stresses arose because of the increased energy dissipated in the coil. The problem of thermal stresses was overcome by a new cooling scheme, which reduced the temperature gradients across the coils during cool down. The coil protection system also had to be modified to ensure that the TF coil pressure was present when operating at high current. With these modifications, the coils were run at the new high current enabling 7MA plasma current to be reached.

Effects on Toroidal Field (TF) Coils

The present toroidal field is sufficient for plasma stability at 7MA. Higher plasma currents and poloidal fields increase the out of plane forces on the TF coils.

The overall effect of this is to increase the torque acting on the coil set, which is supported by the mechanical structure. Examination of the effect of increased torque showed that the structure had adequate margins of safety and also that the coils were well supported in their outer regions. Stresses in the coils were found to be highest where the curved part of the coils joined the straight section, known as the collar tooth region. The collar tooth is a narrow support between the coils, attached to the structure, which supports the coils in this region.

Problems in the collar tooth region were addressed by:

- reducing transverse shaping fields in the region by the use of a new poloidal coil configuration with unbalanced outer (P4) coil currents;
- a detailed finite element model of the region to complement a simpler overall model;
- mechanical fatigue tests on a prototype TF coil to prove the strength of the coil construction;
- a protection system to make direct measurements of poloidal flux and thus out of plane force, which terminates the pulse if safe limits are exceeded.

The study showed that the TF coils would be safe for operation at plasma currents up to 7MA, with some limits on shaping field imposed by the protection system.

Remote Handling Design

The remote handling tasks on the magnets were reviewed and classified as follows:

Class 1, routine tasks including turns changes on the shaping coils and changes at the shaping circuit linkboards;

Class 2, emergency tasks such as replacement of leaking hoses, change of tapping point on coil 1, raising and lowering of coils P3 and P4 for octant removal, removal of whole coil P1.

Design of modifications to coils for all Class 1 tasks has been completed and work has started on design of tools for Class 2 tasks.

Machine Instrumentation and Protection

The magnet protection system has been improved as described above to allow 7MA operation. The instrumentation system has also been extended to measure:

- deflections of and forces on vacuum vessel legs to study effects of plasma disruptions and prevent dangerous operation;
- relative rotation of P1 subcoils to check that new spring system was working.

Results of machine measurements have been analysed to:

- provide statistics on machine usage;
- check that correlations between machine parameters conform to theoretical predictions;
- aid understanding of machine behaviour, including suspected faults and new operating conditions.

Inspection of P1 Coils

At the end of 1988, the P1 coil were removed from the centre of the machine for inspection, as external measurements indicated unexpected rotations. On inspection, the main part of the coil was found to be undamaged, but:

- the keys connecting the coil stack to the upper and lower structure were tangentially displaced;
- the steel support rings were found to have rotated relative to the coils.

The following improvements were therefore made:

- stronger keys were fitted at top and bottom of the stack;
- the support rings were keyed to the coils to prevent rotation;
- stiffer inter-coil springs were fitted;
- low friction material was fitted between the coils to allow easier relative motion under the action of the springs.

Magnet Power Supplies

Further modifications and enhancements have been made during 1988 to toroidal and poloidal field coils power supplies as described below.

Current Imbalance in the Vertical Field Circuit

In late 1987, a new scheme was proposed in which a current imbalance between the top and bottom vertical field coils to produce a magnetic null (X-point) at plasma currents up to 7MA. This current imbalance is achieved by connecting a cable (current rating: 10kA) between the mid-point of the Poloidal Vertical Field Power Supply PVFA3-4 (2.8kV DC, 35kA DC) and the mid-point of the vertical field coils. The modified control of the power supply would allow two control loops, one for the radial plasma position control (total output voltage) and one for the X-point (current difference between upper and lower coils).

In addition, the configuration of the power supply, including the boost amplifier, had to be changed to make this symmetrical. The protection of the power supply needed modification as the two units PVFA3 and PVFA4 would carry different DC currents and, in addition, the low current rating of the mid-point cable needed suitable protection (instantaneous and thermal). The design, purchase of the required components (busbar, current transducers), modification of the control and protection system, and installation and testing were performed in a period of six months, during which the equipment was out of service for only four weeks for these modifications.

The Poloidal Vertical Field Boost Amplifier

This unit will enable the maximum voltage applied to the Poloidal Vertical Field coils to be increased from 5.6kV DC (with a temporary booster) to 12kV DC. This will greatly assist breakdown and initial rise of the plasma current. The amplifier consists of four series connected modules, each one including a 3.4MVA dry-type transformer and an air cooled thyristor rectifier

mounted in a HV deck (Fig.14). The four HV decks and control cubicle were delivered and installed in August 1988.

The commissioning of the equipment started during the October shutdown. This involved functional tests (protection, interlock and controls) and power tests on an inductive dummy load. By December 1988, the equipment had operated to its nominal current of 6kA. The local commissioning should be completed by February 1989 ready for operation on the JET coils in the 1989 campaign period.

Fig.14: Picture of the new boost amplifier.

Current Modulation Circuit

The current modulation circuit supplies current independently to the six central and to the four end subcoils of P1 poloidal coils, to increase the flux variation up to 42 Wb. The circuit was commissioned in late-1987, and during 1988 has permitted plasma currents to be reached of 7MA with 2s flat-top on limiters and of 5MA with X-point configuration.

New protections required as part of this development, were implemented with the Measurement and Protection Cubicle where voltage and currents of P1 are detected, manipulated and compared with the various thresholds set for protection. The noise level, which was higher than expected, required some modification, following which this system worked satisfactorily.

The original design of the current modulation circuit, foresaw the need for active stray field compensation. Proper resistors connected in parallel to both end subcoils should allow the correct current difference to flow at the beginning of the fast-rise and two large inductors were also necessary, in series with the PFX. In addition, the blocking diode snubbers needed modification. The design of these components is still in progress.

Plasma Control

The plasma position and current control system (PPCC) has been further developed and adapted for new operating scenarios as outlined below.

Radial Position and Shape Control

This part of the PPCC was modified to include control of the current difference in the upper and lower sections of the P4 coil. The difference current is controlled to be proportional to the reference for the shaping current in the P2S/P3S coils, using a presetable relative gain. Therefore, this facility can be regarded as an enhancement of the plasma shape control. It has allowed production of single X-point plasmas with up to 5MA current.

A digital version of the radial position and shape control system has been specified and implemented by CODAS. It includes additional features such as decoupling between radial position and shape (elongation) control and will be more flexible than the presently used analogue system. Preliminary tests have been carried out, but the commissioning is planned for 1989. This system is foreseen to replace the analogue system.

Vertical Stabilisation

Operation with single X-point plasmas has shown that the stabilisation system can fail when large perturbations occur, such as those seen during disruptions and H-mode transitions. Part of the problem was due to signal saturation arising from large amplitude helical plasma modes.

As a first measure of improvement, the stabilisation system was extended to simultaneously use magnetic signals from two opposite octants of the torus so that saturation due to helical plasma modes was avoided. Subsequently, single X-point operation became more reliable. However, large asymmetric perturbations can still provoke vertical instability. Several options for improvement are being considered. It is concluded that a significant enhancement of stability is possible by increasing the power and the response speed of the radial field amplifier and/or by using additional stabilising elements (saddle coils) inside the vessel.

The present stabilising system is also subject to failure in magnetic signal transmission and conditioning. A 'dual system' has been implemented which maintains feedback stabilisation in the event of a fault being detected in any one of the two signal conditioning branches of two opposite octants of the torus. The dual system is being implemented as a pilot system. Initial tests led to some modifications. Further tests are required before the system can be used for active stabilisation.

Other PPCC Developments and Related Studies

Some minor modifications were made in order to adapt the PPCC to new operating requirements. These include a re-calibration for currents exceeding 6.6MA; a facility for reading manually set parameters; and additional data acquisition. Future enhancements involve changes needed to minimise the interference from currents in the disruption control coils; adaptive control and decoupling in the vertical stabilisation system; and other improvements.

The PROTEUS evolution code has been included in the JET tools for development and analysis. This code has been developed by members of the Salerno University, Italy, and by the NET Team, Garching, F.R.G., and prepared for application in JET.

It has been used to assess the magnetic forces acting on the vessel during disruptions and vertical instabilities, and this work is still in progress. It is intended to apply the code also for the analysis of PPCC performance, in particular, of vertical stabilisation, and as an aid for further developments of the PPCC.

Additional Power Supplies

There are three systems of additional heating power supplies: the neutral beam (NB) and the ion cyclotron radio frequency (ICRF) systems, already in operation, and the lower hybrid (LH) radio frequency system, at present under procurement. In addition, there is further requirement for a Disruption Feedback Amplifier.

RF Power Supplies

During this year the eight new RF driver power supplies were installed and commissioned. These new power supplies were required to upgrade performance of the RF generators. Full performance tests were first carried out on dummy load. Tests on the real load could only be done when the RF generator tetrodes had been exchanged with the new more powerful models. Consequently, it was only possible for six of these eight new power supplies to be used for operation on the machine during 1988. The remaining two were only tested with the new converted generators during the shutdown at the end of 1988, but are now ready for use during the next operating period.

Lower Hybrid System Power Supplies

The contracts for Stage 1 of the LHCD power supplies and for protecting crowbars continued during 1988. In addition, Stage 2 was released for five additional protecting crowbars.

Stage 2 for the power supplies was reviewed and the dedicated power supply for the LH testbed was dropped. It was decided to make one of the Stage 1 power supplies switchable either to the testbed or to some of the klystrons used on the machine. This provided a considerable saving, but the disadvantage is that when the testbed is used a maximum of only 20 klystrons are available for machine use. A schematic of the power supply is shown in Fig.15 Stage 1 and Stage 2 each consist of one of these power supplies.

During the design phase, the overall system was designed in such a way to avoid a power step on the feeding 33 kV supply. For this reason, the output current was ramped up from zero to full load current over 100ms, during which the klystron worked as a diode. Only when the current out of the power supply had stabilized, after 100ms, the high frequency drive to the klystron was enabled. The reverse happened at the end of the pulse, and the current was ramped down over 100ms.

During the high frequency reapplications, the klystron worked again as a diode keeping the current from the power supply constant. In this way, another advantage became apparent. Due to the constant current from the power supply during the pulse, the voltage could be kept within required limits without need for an additional regulator modulator. One matching transformer fed three identical rectifiers. Each rectifier could supply 100A at 65kV nominal voltage. This was sufficient to feed four klystrons.

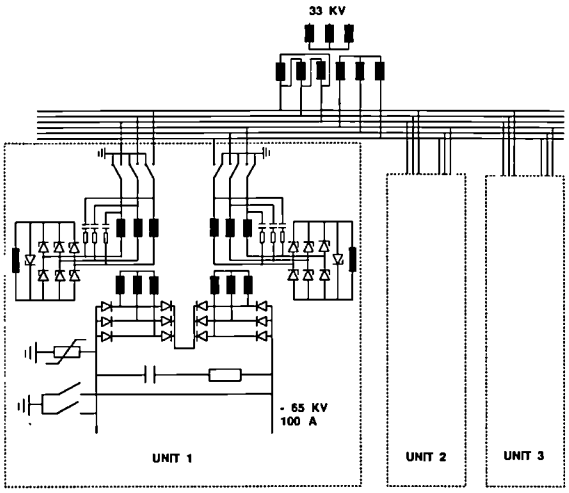

Fig.15: Schematic of the LHCD Power Supplies.

Stage 1 of the power supply is presently nearing completion and commissioning is in progress. The first two Stage 1 crowbars are being installed and commissioning is underway. Integrated tests with the power supply will follow immediately. Completion of Stage 2 of both contracts is expected during 1989.

Neutral Beam Power Supplies

From the beginning of 1988, the Octant No.4 power supplies were gradually brought into operation on the machine. At the same time, the reliability of the power supplies was improved. This resulted in the full neutral beam power being injected into the plasma. This was one of the main achievements during 1988.

To enable the injection of neutral beam power into 4MA and higher current plasmas, a special power supply was brought into service. This power supply is used

for active field compensation. It drives coils used to compensate stray magnetic field near the injectors.

During the shutdown at the end of 1988 the conversion of one of the neutral beam power supplies to 160kV was started. It is hoped to finish this work by the end of the shutdown and first experiments with 160kV injectors should take place in mid-1989.

A new contract was placed in 1988 for blocking diodes, which are necessary to decouple the transmission lines when the power supplies are converted to 160kV. In this way, capacitive energy stored in the two transmission lines can be decoupled during breakdown in one of the injectors.

Disruption Feedback Amplifier

The reference design used in the Call for Tender was specified. This design was based on a new component IGBT which is from the family of fast power transistors. The basic element is a module made up of an 'H' bridge in which each leg consists of two IGBT's in parallel; RC circuits ('spike killers') are connected across the IGBT for protection. One unit consists of 12 parallel modules decoupled by the inductance of the coaxial cable between the local area and the junction cubicle. One amplifier consists of two units connected in series. Each unit could supply independently four saddle coils connected in series and in parallel. The final configuration is based on four amplifiers each connected to two saddle coils in series.

Each amplifier has the following ratings:

Peak Voltage	:	1.5kV;
Peak Current	:	variable with frequency; 3kA in the range 0-1kHz; 3(kHz)/(kHz) in the range 1-10kHz;
Peak Power	:	4.5MVA;
Total Bandwith	:	0-10kHz.

The main components of the disruption feedback amplifier (see Fig.16) plant are: a rectifier transformer with two secondaries, which reduce the voltage from 33kV to less than 1kV, to supply two thyristor convertor units. L C filters are foreseen in front of the disruption feedback amplifier unit, which is a DC/AC power convertor, capable of four quadrant operation (invertor). Load connecting cables are planned between the amplifier and the junction cubicle that contains voltage and current transformers, load disconnectors and earthing switches.

Procurement is split into three stages: 1-design; 2-procurement of one amplifier; 3-procurement of three amplifiers. Call for Tender was issued inmid-1988; and the contract was placed in late-1988.

Power Distribution

Interaction of the JET Pulse with the CEGB 400KV Grid

During the year, tests were performed with CEGB to measure the effect of power steps on the 400kV grid. The assessment of the tests allowed CEGB not to insist on their previous request for active power compensation.

The power taken from the 400kV grid progressively increased up to 400MW; in all pulses, the reactive power

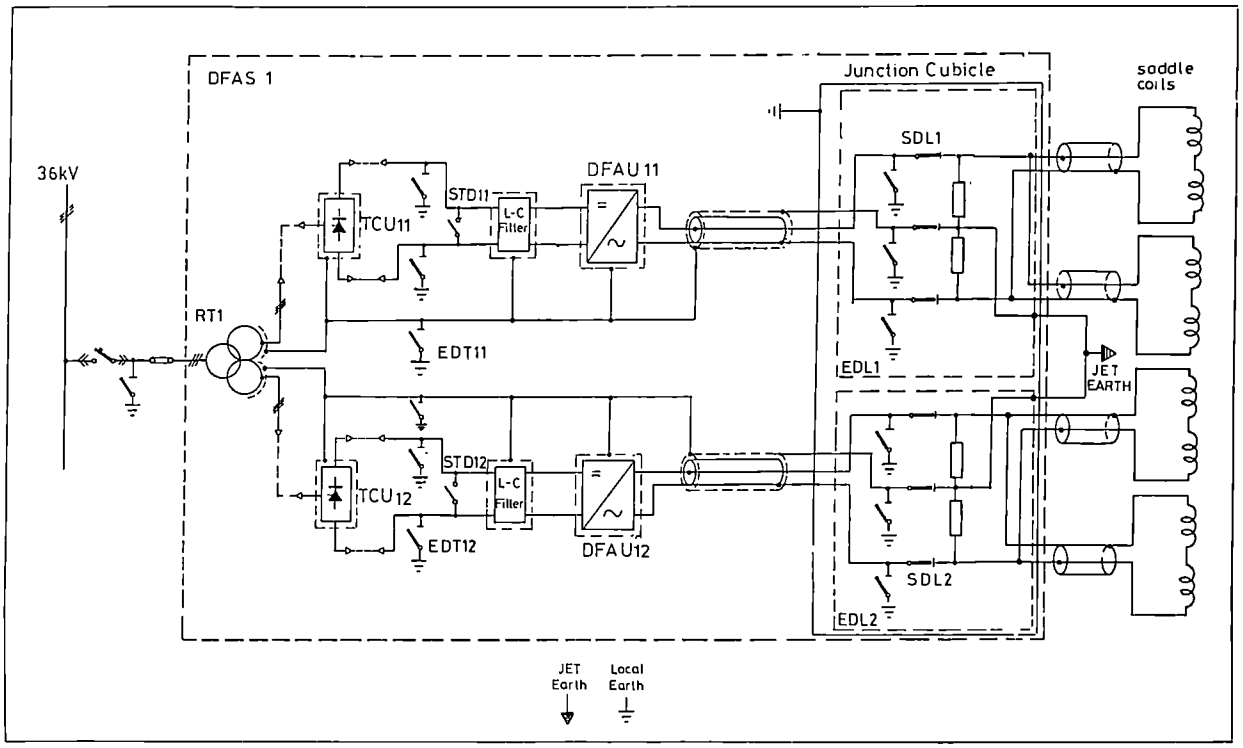

Fig.16: Schematic of the disruption feedback amplifiers.

was more or less equal to th active power: large voltage drops, ~6kV, were observed on both busbars 1 and 2. Therefore, it was sometimes necessary to increase the busbar voltage up to 35kV between pulses so that the voltage dropped to ~29kV during the pulse. The full operating range, from 36kV to 28kV, was almost completely used.

It was found that the coordination of the protections of the substation and of the loads needed review. To improve the situation it was decided to distribute more uniformly the loads among the three busbars. In addition, a reference pulse of JET's ultimate performance was defined: 7MA with 10s flat-top with full additional heating and LHCD.

A computer model simulation has shown peak active power very close to the CEGB contractual limit (575MW); however, the peak reactive power is 650MVA much higher than the CEGB contractual limit (475MVAR). Moreover, the voltage drop on all three busbars (more than 8kV) is too high. CEGB verified that the reactive power limit, already relaxed from 375MVAR to 475MVAR, could not be extended any further. Therefore, reactive power compensation is now necessary.

Further simulations with the computer model were undertaken:

- three identical compensators, 50MVAR at 33kV each, connected one per busbar, allowed a reduction of the peak reactive power, in the reference pulse defined above, to 530MVAR; the reduction is only 120MVAR because the busbar voltages, during the pulse, drop to 28kV;
- two other compensators, the same as the previous ones, were added to busbars 1 and 2, which were more loaded than busbar 3, reducing the peak reactive power to 470MVAR.

Therefore, from the computer simulations, 250MVAR appeared to be necessary; the uncertainty on the reference pulse and budget limits suggested preparation of a Technical Specifications in two Stages: the first for 150MVAR at 33kV (three compensators), and the second for 100MVAR (two compensators).

Each compensator consists of three elements which were star connected. The star-point is connected to the star-point of the transformer secondary, and therefore the voltage across each element of the star is well determined.

Each element is made up of a large capacitor bank a thyristor switch and a filter reactor connected in series. The thyristor switch consists of a series connected stack of thyristor pairs connected in anti-parallel, with each pair at a different voltage level. The Technical Specifications have been defined and a Call for Tender issued.

Other power distribution activation have included:

H V Distribution

- Additional load supply on the 3.3kV busbar for the new 6MW Chiller cooling system;
- Exchange of TS3 and TA3 with the higher rated TS4 and TA4 630kVA Transformers to supply J20 Building;
- Implementation of a temporary 33kV supply from the SEB 11kV grid during the outage of the CEGB 400kV supply;
- Commencement of the extension/arrangement of the 33kV distribution system;
- New 33kV Feeder for First Stage LHCD System.

415 V Experimental Services

- Installation and energisation of approximately 20 medium sized distribution boards includes assembly, wiring and testing;
- Overhaul of the J2 180kVA rotary UPS generator;
- Procurement and installation in J2 of a 10kVA uninterruptible power supply unit for essential computers.

415 V Building Services

- New supply for J20 Building;
- Extensive re-arrangement of the 415 V Building supplies following new locations of temporary offices, storage cabins and site facilities;
- Complete renovation of J4 Main Building lighting system.

Neutral Beam Heating System

1988 proved to be the most successful year to date for neutral beam (NB) injection into JET. The two beamlines installed on the tokamak have been brought into full simultaneous operation at 80kV culminating in a maximum injected power of 21.6MW of deuterium atoms. Furthermore, by the end of the year, a high degree of availability and reliability were achieved.

Neutral beam heating has made significant contributions to various aspects of the JET experimental programme, the results of which are described throughout the report. Major achievements include:

- the production of plasmas in the so-called hot-ion mode with measured central ion temperatures of up to 23keV and D-D reaction rates of up to $2.45 \times 10^{16} s^{-1}$. Additional interesting features of these plasmas were the spontaneous production of a high degree of peaking of the temperature and density profiles and enhanced confinement properties;
- the production of plasmas with H-mode confinement in both single and double-null configurations; the former produced a record value of stored plasma energy of 11.5MJ;
- identification of the presence of the bootstrap current of up to 0.8MA;
- combined heating experiments (20MW NBI+12MW ICRH) of both 5MA limiter plasmas, resulting in 9MJ of stored plasma energy, and 6MA plasmas with 13MW NBI + 9MW ICRH.

Other activities included: successful further development work on high heat transfer elements; continuation of studies relating to the conversion of one of the injectors to 160kV tritium injector; and engineering improvements to injector components including a quantitative assessment of their reliability.

Neutral Beam Operations

The second neutral beam injector was commissioned and brought into full operation during 1988. Following the repair of the high voltage supply damaged by fire in 1987, all 16 sources (8 per injector) were brought into full simultaneous operation in deuterium at their maximum rated voltage of 80kV. Fig.17 shows a resultant power waveform with 21.6MW being injected into JET (note that only one of the 16 sources exhibited a breakdown/ re-application during the pulse flat-top.

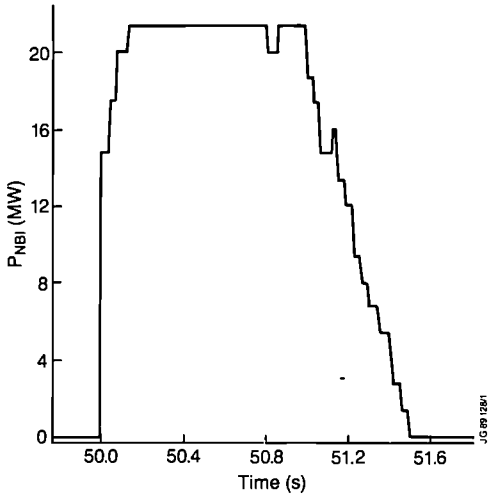

Fig.17: Injected power waveform for Pulse No:18569; 16 beam sources operating at 80kV in deuterium.

Although a high degree of reliability of the total system was achieved towards the latter part of year, two major failures occurred in the earlier part of the year.

The first of these was a further failure of the water cooled, thin walled nickel liner of the tokamak injection duct. This occurred due to the un-avoidable re-ionised particles being brought to a focus beyond the downstream end of the copper protection plates, which were installed in 1986 following similar incidents. Since routine safe operation at the same operating conditions (2MA plasma current) had previously been achieved, it is speculated that the modifications to the PI circuit carried out in 1987 have resulted in a reduced value of the vertical magnetic field in the duct region. As a result, injection experiments have been restricted to plasma currents ≥ 3MA. An ongoing programme of theoretical and experimental investigation into this problem is underway. Meanwhile the copper protection of the thin walled nickel liner is being extended further in order to protect completely the thin walled nickel liner over its exposed area.

The second major incident was a further failure of a water cooled neutraliser: as detailed below these components are being replaced by a more reliable version.

Apart from these two major failures the reliability and availability of the neutral beam (NB) systems and their associated power supplies has increased markedly throughout the year. Fig.18 shows the distribution of power levels obtained in all JET pulses with NB heating for the period January-September 1988.

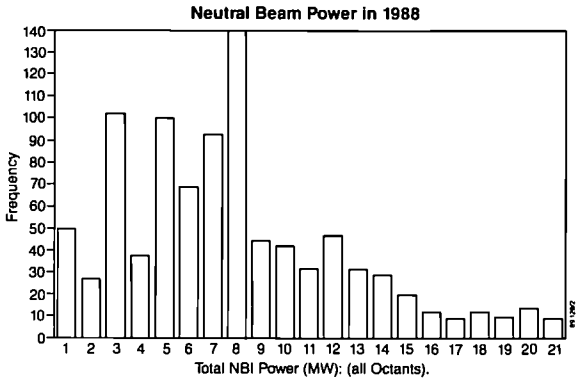

Fig.18: Neutral Beam power in 1988.

It should be noted that the second injection system was routinely available only for the period June-September. Fig.19 shows the loss of requested beam-on time due to all faults arising on the NB systems (plus power supplies) for the last three weeks of operation in 1988.

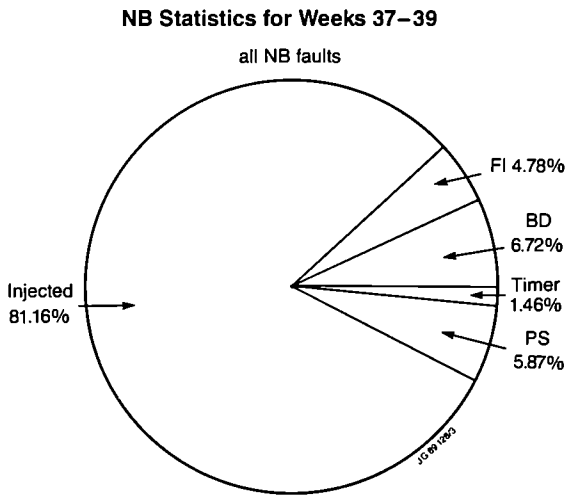

Fig.19: NB statistics for Weeks 37-39.

In addition to heating experiments on the tokamak, the Operations Group has also continued to carry out investigations relating to the operation of the injectors themselves. During 1986, it was found that the stray poloidal field of the tokamak was approximately one

order of magnitude higher than had been predicted and had a significant effect upon the alignment of beams. Since the observed beam deflection increased non-linearly with plasma current, an active compensation system was designed and installed to cancel the stray vertical field.

The successful commissioning and optimisation of this system has enabled injection to be performed over a wide range of plasma currents without the need mechanically to re-steer the sources. As part of this programme, experimental data on the power intercepted by various components of the injector has been analysed extensively resulting in reliable measurements of the beam alignment to within 0.4cm.

The conditioning (degassing) of the beam entrance duct into the tokamak has been studied further by direct measurements of the duct pressure using a specially installed vacuum gauge. This has given important and direct information on the behaviour of duct surfaces when bombarded by re-ionised beam particles, deflected into the walls by the poloidal field. In particular, large amounts of gas continue to be evolved from a carbonized duct over a series of beam pulses, as distinct from the situation without carbonisation. This is illustrated in Fig.20, which indicates an uncontrolled exponentiation in duct pressure. This is related to the magnitude of re-emission coefficient for ion induced desorption from surfaces exposed to the re-ionised beam particle flux. This can lead to 'beam blocking' in which the re-emittedgas causes further re-ionisation. This could result in extremely high power deposition in the duct and consequent component failure.

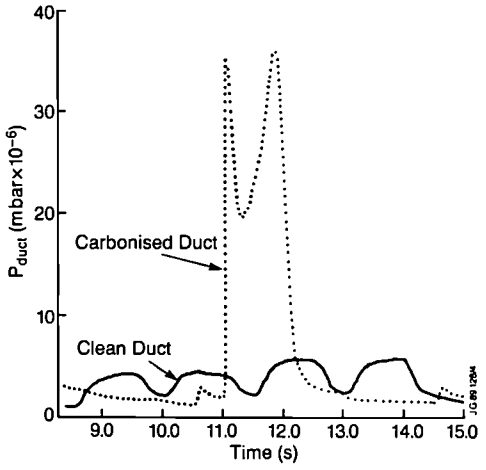

Fig.20: Typical duct pressure traces for 1 s, 2 beam pulses during duct conditioning sequence. In each case the duct had been exposed to a few beam seconds of conditioning.

Subsequent visual inspection of the carbonised duct revealed that the surfaces of the copper duct components were covered with a loosely bound layer of amorphous carbon resembling soot. This is in contrast to the hard carbon layer deposited on nickel and inconel surfaces inside the torus. The loosely bound deposits were wiped off manually and subsequent conditioning behaviour reverted to normal. Fig.20 shows the different behaviour of the duct pressure for the two cases. Normal behaviour is well described by a large, prompt gas release which lasts for ≤ 200 ms during the first beam pulse only, followed by ion induced desorption with an average re-emission coefficient of ~ 10. This greatly increases the effective time-constant for pump-out of the duct yet appears to be below the threshold for beam blocking.

A complete power loading survey was performed on the JET neutral injectors in synchronous operation. The input power was calculated from the acceleration voltage and current, and the power deposited on each beamline component was measured by thermal sensors either embedded in the component or in the water cooling circuit. Fig.21 shows the percentage of input power deposited on each major component (averaged over many pulses). The remaining fraction of the input power was assumed injected into JET. This may be a slight overestimate, as not all lost power can be measured.

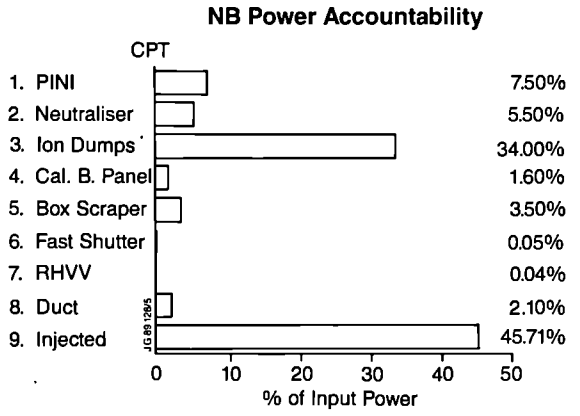

Fig.21: NBI power accountability.

Neutral Beam Testbed

Throughout 1988, the priority for the Testbed has been the simultaneous operation of two 140kV PINIs using the two existing 80kV 60A power supplies in their alternative design configuration of series operation to give 160kV at 60A. This and other aspects of the programme have suffered considerable delays due to a fire, initiated in one of the oil-cooled resistors attached to the high voltage supply, which prevented operation of the Testbed for the months of July and August. Nevertheless, heat transfer tests of a simulated divertor element for NET, plus two series of measurements on hypervapotron and a new 'multi-tube' high heat flux element have been carried out. In addition, re-conditioning of 80kV PINIs and experiments relating to the operation of a tritium injector have proceeded.

The cryoplant has demonstrated a high degree of reliability and availability, having routinely supplied cryogens

simultaneously to the three large cryo- pumps (two neutral injectors plus one pellet injector) and to the Testbed and various small users. A major extension to the cryo-distribution system has been initiated to accommodate future new users.

i) *160kV PINI Operation*

At the beginning of 1988, the two 80kV 60A HV power supplies were re-configured to the designed series mode of operation of 160kV 60A to enable simultaneous operation of two 140kV PINIs in parallel - this is the configuration to be used in the next phase of the tokamak injection systems.

Contrary to previous experience with single PINI operation at up to 160kV, simultaneous operation of two PINIs resulted in many and frequent problems with the HV power supply system and only after a great deal of time and difficulty was it possible to achieve two PINI operation at ~132kV (even though individually the PINIs had operated at ~150kV).

After extensive investigations and modifications, the main cause of the problems has been identified as that of radio-frequency interference (RFI), generated in the output circuit of the power supply during a real (or simulated) electrical breakdown in the accelerator. This RFI results in malfunction of various parts of the control circuits and associated microprocessors.

Additional screening of internal wiring and chassis, which has now been introduced inside the HV protection unit, has resulted in a considerable improvement in noise immunity and gives cause for optimism as regards future two PINI operation.

ii) *Test of Simulated NET Divertor Element*

Carbon tiles have been exposed to beam power densities of up to 1 kW cm^{-2} to determine their applicability as plasma facing components in a divertor for NET. Both graphite and graphite fibre composite materials have been used. The major new result to have been obtained is that the introduction of a layer of soft carbon foam material (papyex graphite) between the carbon tile and the copper supporting element improves the heat transfer across the mechanical joint by about one order of magnitude to give a heat transfer coefficient of 0.1-0.2 W cm^{-2}°C^{-1}. A further test of carbon tiles brazed on to a water cooled structure has been prepared for testing.

iii) *Development and Tests of High Heat Transfer Elements*

Water cooled structures capable of handling high total power at power densities >1 kW cm^{-2} are not only an essential part of injection systems but are directly relevant to many other aspects of next generation fusion devices. Tests and the development of such structures have continued in conjunction with the Neutral Beam Engineering Group.

a) Hypervapotron Elements

Fig.22 shows a section through a standard JET hypervapotron element which is incorporated into many of the beam line components. During previous tests, the maximum power density which could be safely handled was a decreasing function of the total power to the element. Although power densities up to 1.3 kW cm^{-2} could be handled safely at a total power of ~200kW, this reduced to ≤1 kW cm^{-2} at 500kW total power. From the results of tests using an element which was well instrumented with thermocouples, it was found that the above problem was a characteristic of the region of the element close to the central web which supports the rear closure plates. The measured temperature over the majority of the surface (and also close to the side walls) of the element was found to be considerably lower, and demonstrated steady state operation at higher powers, than in the central region.

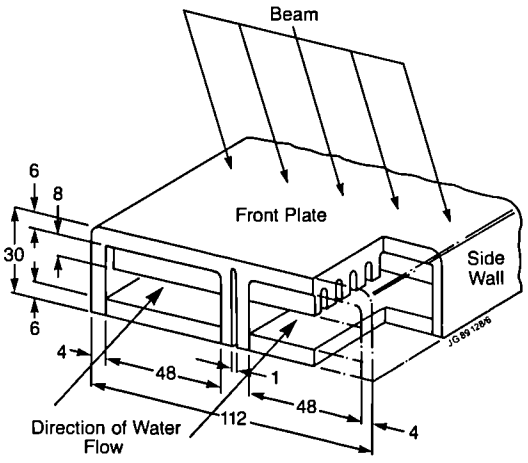

Fig.22: Section through a standard JET hypervapotron element.

It was concluded that the significant difference in behaviour across the width of the element was due to the difference in the attachment between the transverse fins and the central web as opposed to complete separation from the side walls of the element.

To test this hypothesis, a standard element was modified as indicated in Fig.23, in which the fin-side wall and a fin-central web configuration was essentially identical. The results of operational tests completely validated this hypothesis in that the central regions of the element did not deviate from those measured elsewhere in the surface. Furthermore, steady state operation was achieved with a total power in excess of 600kW and a power density of 1 kW cm^{-2}.

b) Multitube Elements

Due to the perceived shortcomings of the original JET hypervapotron elements described above, an alternative type of direct replacement element has been designed and tested. The essential features of this new design are shown in Fig.24. The cooling water flows across the face of the element through a densely packed array of cylin-

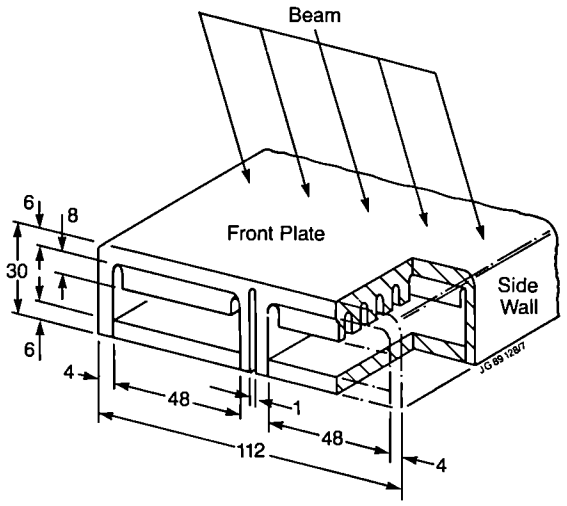

Fig.23: Modified standard JET hypervapotron element.

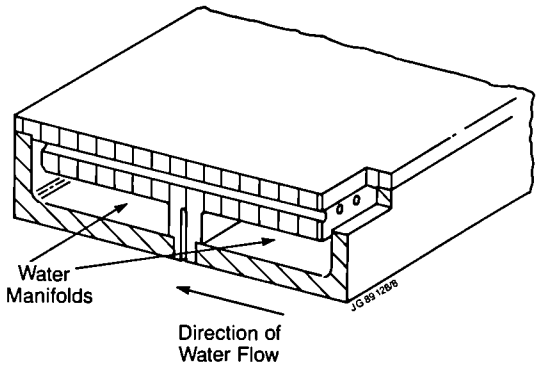

Fig.24: Direct replacment hypervapotron element.

drical channels 3 mm diameter and 3 mm below the front surface of the element.

Operational tests were successful, in that stable operation with no evidence of thermal runaway was obtained with an incident power density up to 1.25 kW cm^{-2} and a total power of 900 kW. A fully analytical model has been developed to predict the behaviour of the elment in the nucleate backing region. This model correlates well with the available experimental evidence.

Cryo-System

The cryoplant has been in routine operation throughout 1988 and has demonstrated a highly satisfactory degree of reliability and availability. To service additional new users of cryogens within the project, parts of the plant are being upgraded. In particular the liquid helium storage has been increased by the addition of a 10,000ℓ liquid helium dewar, while an additional recovery compressor and extra high pressure storage cylinders have been ordered. Major extensions to the distribution system for both liquid nitrogen and liquid helium have been designed with the requisite tender actions having been completed.

Cryo-pumps

The large open structure cryo pumps installed in the neutral injectors and the pellet injector have operated satisfactorily throughout the year. However, on two occasions significant unplanned pressure excursions and associated loss of liquid helium from the pumps in the neutral injectors were observed. Detailed examination and dedicated tests have shown that helium gas from helium discharges in the tokamak can be cryosorbed on the deuterium covered liquid helium surfaces. This gas is very weakly bound to the surface and a temperature fluctuation of < 0.3°K, due to a pressure change above the liquid helium, is sufficient to desorb the helium gas on the panels. It is relatively easy to avoid this problem by ensuring adequate vacuum isolation of the injectors from the torus, when the latter is using helium for operation or glow discharge cleaning.

Finally a fast regeneration cycle of the cryopumps has been tested. By using 'warm' gaseous helium to drive the liquid helium out of the pumps, a pump can be regenerated in $<$ 1hr and the complete regeneration cycle with the pump again ready for operation can be completed within about 2hours.

Engineering and Development Work

i) Operational Experience with Two BeamLines

Although both beam lines were brought into full simultaneous operation, several technical problems were encountered with various beam line components which required repair work.

- The second stage neutralizers continued to prove unreliable, when a further one suffered from delamination between electrodeposited layers, resulting in a water leak into the NIB vacuum system. It was decided to replace all of the original neutralizers with a new design using proven high reliability manufacturing techniques. Deep drilling was chosen to produce the water channels in copper plates which were subsequently pressed into the required shape. Thereafter, electron beam and friction welding were used for the manifold covers and transitions from copper to stainless steel. One complete injector will be equipped with this new design prior to operation in 1989. Those in the second beam line will be replaced during a subsequent suitable shutdown;
- Failure of two water cooled arc load resistors resulted in water leaks external to the vacuum system. These resistors ensure there is no gross imbalance in the distribution of the total arc current between the 24 filaments at the rear of each plasma source. One of the these failures resulted from a short circuit between the source back plate at anode potential and the retro-fitted molybdenum caps on the filament stems. The cap had worked loose due to thermal cycling and additional locking of all caps was foreseen to prevent recurrence. The reason for the second failure is unclear;

- Two single ply inconel bellows, one on the box scraper and one on a full energy ion dump, suffered fatigue failures due to flow induced vibrations, resulting in a large water leak into the NIB. These have been replaced by double ply stainless steel bellows, which have proved to be fully reliable in service;
- An unusual problem was experienced during injection experiments, when molybdenum was observed in the plasma during beam injection. This was traced to poor adhesion of the plasma sprayed molybdenum layer on the box scraper assembly. This layer, whose purpose was to prevent sputtering of copper on to the cryo-panels, had become detached due to thermal cycling and the resultant film had melted into many small droplets - some of which were accelerated into the torus by the beam. The poorly attached layer was subsequently removed by grinding.

ii) Design and Development Work

Preparation for future operation at 140kV has continued with the production of 140kV PINIs and the conversion of 80kV PINIs to their 140kV configuration;

- Due to the hitherto unknown unfavourable power density versus total power characteristic of the original hypervapotron, the operational safety margin of the full energy ion dumps for long pulse operation at 140kV is reduced significantly. A new design of full energy ion dump with generous operating limits has been completed and incorporates the improved hypervapotron elements described-above. Contracts have been placed for manufacture and assembly.
- Work on the conversion of a 140kV deuterium injector to a 160kV tritium injector for the JET D-T phase has also continued. One extensive and important area of work has been to establish the suitability of the existing beam deflection magnets for the tritium beams which require higher values of the deflection field than foreseen in the original design for 160kV D. An extensive series of measurements to produce a detailed map of the magnetic field at the required high values of excitation ($\sim$1kA) have been made. This field map was then used as input for a computer simulation of the trajectories of T beams in order to determine the focusing properties of the fringe fields and hence the expected power profile on the full energy ion dumps. The result of these calculations, which will be validated against measurements in the testbed using beams of He_4^+, indicate that 160kV operation with tritium is indeed possible. Extra cooling of the magnet coils to handle the extra excitation current has been provided by re-routing the internal pipework. In anticipation of operation in tritium, steps are being taken to drain the cooling water from the internal components of the NIB to minimise the possible accumulation of water which could become tritiated in the event of an internal water leak during tritium operation.

iii) Since it is uncertain whether the use of beryllium as a first wall material in JET will result in contamination of components inside the NIB, various measures have been taken in preparation for Be operation. These include the installation of a removable probe to measure the degree of Be contamination and the design of a decontamination enclosure capable of accommodating a complete central support column.

iv) A range of double-walled ceramic feedthroughs has been developed to meet safety and reliability criteria laid down for the introduction of tritium into JET. These feedthroughs will have a gas filled interspace which can be monitored to check the leak tightness of both the inner and outer containments. All instrumentation and magnet flanges will be fitted with these feedthroughs before the start of the active phase.

v) A quantitative reliability analysis has been carried out on the mechanical system of the beam lines. Using a two-stage Markov model, expressions for reliability and availability were obtained in terms of the historic failure rates and repair times. Furthermore using the Duane model to fit the time evolution of fault occurrences, it was possible to predict failure rates with a certain confidence limit for the near and medium (active phase) future. This allowed us to define a spares policy. This reliability prediction has proved to be encouragingly accurate. The analysis, summarised in Fig.25, shows that the reliability of the system has improved many fold with time, while the planned technological improvements (replacement rather than repair of liners, neutralisers, duct scraper, etc) should result in a further increase of reliability up to levels acceptable for operation in the active phase, (ie no more failures that can be handled by Remote Handling and the spares policy).

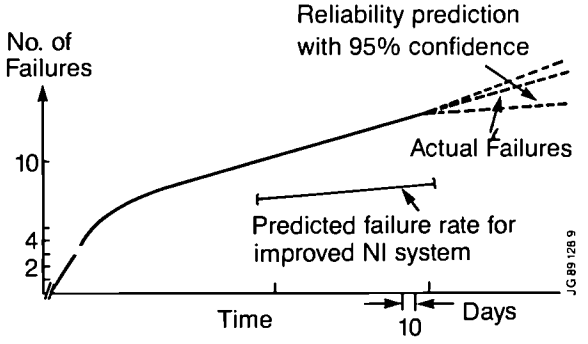

Fig.25: Reliability growth graph for the Octant No.8 NBI system.

Tritium Injector

It is intended to use one of the JET Neutral Beam Injections as a tritium beam injector during the final D-T phase of JET operation. The use of 160kV beams of tritium will provide fuelling in the central regions of the plasma and hence control of the isotopic fuel ratio. The

existing beam sources which deliver 30 A at 140 kV when operated in deuterium will deliver, without modification, the same current in tritium when operated at 160 kV and hence match the installed power supplies. Successful operation at 160 kV has already been demonstrated with beams of deuterium and helium,

Due to the higher neutralisation efficiency, the tritium injector will produce ~ 50% more neutral beam power than in deuterium, and the power handling of various components in the injector has been re-assessed. The only component which requires upgrading is the box scraper assembly defining the neutral beam at the exit of the NIB which can be readily accommodated.

Two important issues relating to the tritium injector have been examined experimentally in collaboration with TFTR (Princeton, U.S.A.). The first of these relates to the possibility of operating the plasma source in tritium but using deuterium in the neutraliser cell to minimise the usage of tritium. Although it was recognised that this would lead to the production of a mixture of D and T beams (due to diffusion of the neutraliser gas into the plasma source) a series of experiments was carried out on the JET Testbed using deuterium and hydrogen to quantify the problem. The results, in which the beam composition was measured using Doppler-Shift spectroscopy (a typical spectrum is shown in Fig.26), indicate that the degree of contamination of the source by the neutraliser gas is such that this scheme is of no practical value. An alternative method of reducing the overall tritium gas consumption of JET sources is being developed.

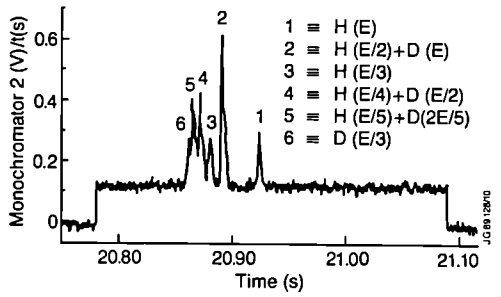

Fig.26: Doppler-shift spectrum using differing gases for source and neutraliser.

The second issue relates to the problem of high voltage insulators in the presence of tritium, where β-decay could lead to the build-up of surface charge and/or initiation of electrical breakdown. High voltage tests of JET and TFTR insulators in a tritium atmosphere have shown no observable degredation in performance.

In addition, studies have been initiated which relate to the degree of tritium retention to be expected in various beamline components plus procedures designed to minimise the possible production of tritiated water in the event of a water leak into the vacuum system during tritium operation.

ICRF Heating and LH Current Drive Systems

The purpose of the powerful ion cyclotron resonance frequency (ICRF) heating and lower hybrid (LH) current drive systems are quite different:

- The ICRF heating system is used for highly localized heating of the JET plasma ($\Delta r \approx \pm 15$ cm). The wide frequency band (23 to 57 MHz) allows variation in the position of heating as well as the ion species which is resonant with the wave (H or ^{3}He at present, D in the future D-T phase). The maximum design power is 20 MW. The system is not totally completed, but in 1988 a maximum power of 18 MW was coupled to the plasma.
- The LHCD (Lower Hybrid Current Drive) system (12 MW at 3.7 GHz) is still in the early construction phase. It will be used to drive a significant fraction of the plasma current by direct acceleration of the plasma electrons, in order to stabilize sawtooth oscillations, thereby improving the overall JET performance. This will be the main tool for controlling the plasma current profile. This subject as well as many aspects of the LHCD project are discussed in a later section of this report ('Current Drive and Profile Control'). In this section, discussion is limited to technical achievements made during 1988.

Technical Achievements with the ICRF System

i) Power Upgrade

The ICRF heating system is composed of eight units, each driving an antenna installed between the belt limiters in the toroidal vessel. Each unit is made of two identical sub-units, sharing a common high voltage power supply and a common low power RF drive. The output stage of each sub-unit is being upgraded to 2 MW instead of the original 1.5 MW by replacing the high power tetrode and modifying the output circuit. In 1988, 12 sub-units (out of 16) were upgraded and successfully commissioned. The remainder of the upgrade will be completed in 1989. This progressive transformation has allowed good use to be made of the guaranteed life of the power tetrodes and significant economies have been made in the operation budget.

ii) Remote Phase Control of the Antenna Array

The new system controls the phase of each coupling element of the antenna array[1]; a loop distributes (at a 'down'-converted frequency) a reference phase to each RF generator which is used to generate (after an 'up'-frequency conversion) an RF drive signal with a phase determined by the selected waveform. The phase waveform (as the power waveform) is generated from the JET Control Room, allowing generation of a great variety of phase patterns. This system was fully installed and commissioned in

1988. Phase control at lower frequencies gives excellent phase stability and control during plasma operation despite large fluctuations of the coupling resistance. Phase accuracy is better than ± 3 degrees.

iii) Operation on JET (new electronic devices and software).

The ICRF power plant has operated regularly above the 10MW level in a wide range of plasma conditions and frequencies[1]. A particularly severe test of the plant performance was the rapid change of plasma edge conditions imposed by the various facets of the JET experimental programme. The antenna loading resistance changed from above 6Ω, in limiter configuration and in monopole phasing, to less than 1Ω, in some X-point operations. In most cases, large variations of loading resistance during the pulse were produced by the crash of large sawteeth or by eigenmodes of the wave in the torus.

New electronic devices and software packages were implemented to cope with these variations. An algorithm for software matching was developed. The paramaters of the entire plant corresponding to a particular plasma condition can be stored in the computer and reset automatically for later use.

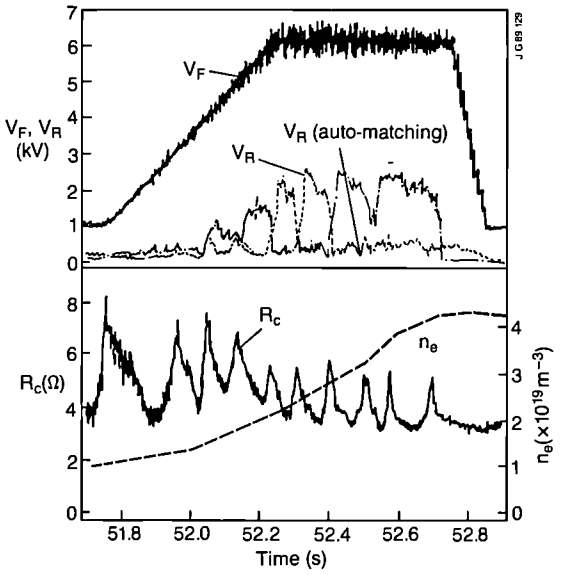

Fig.27: Typical evolution of signals during high power ICRF heating. V_F, V_R, R_C: forward and reflected voltages and loading resistance of one half antenna. n_e: plasma electron density. Total power 10MW. The auto-matching network provides a low reflection coefficient despite large variations in the load resistance and reactance.

A new electronic network automatically determines the frequency corresponding to the lower power reflected back to the generator. This system has been employed successfully during the year. In particular, the large load variation due to sawteeth could be compensated by a frequency variation automatically set by this system (see Fig.27).

In 1988, the ICRF system reached a record power of 18MW for 2s (see Fig.28) and 6MW for 20s. Nevertheless this value is somewhat less than the 20MW which was expected. Several difficulties prevented use of the plant to its full capability most notably:

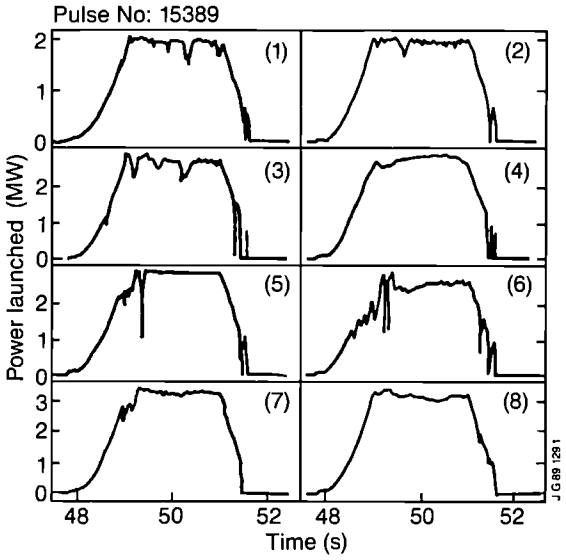

Fig.28: Power launched by each antenna during Pulse No:15389. The total power reaches about 18MW for 2s.

- *Power Supply and RF Plant Control Problem*

  The power upgrade pushed the auxiliary power supplies to their limits and their control circuits became more vulnerable. In particular, parasitic resonances due to sidebands generated by the new phase control system induced false alarms in several power supplies. These resonances were eliminated towards the end of the year and the amplifiers became technically capable of full power. The power was then limited by arcs on the antennae.

- *Antenna Arcs*

  Severe arcing occurred near the conical support at the end of the vacuum transmission line, where the RF voltage was at its highest. Some ceramic insulators were coated by a thick layer of sputtered metal and two antenna halves could no longer be used during the last two weeks of operation. All antennae have been modified during the shutdown to reduce the electric field strength in the critical area. Nevertheless, it is likely that this modification might not be sufficient to prevent totally the occurrence of arcs. Therefore, the generator tripping system had to be hardened to increase the reliability of arc detection (the observed damage came from long arcs which had escaped detection). A new tripping circuit has been superimposed on the new one, which recognises an arc from the assymmetry in the impedance of the two antenna halves, when such an arc occurs.

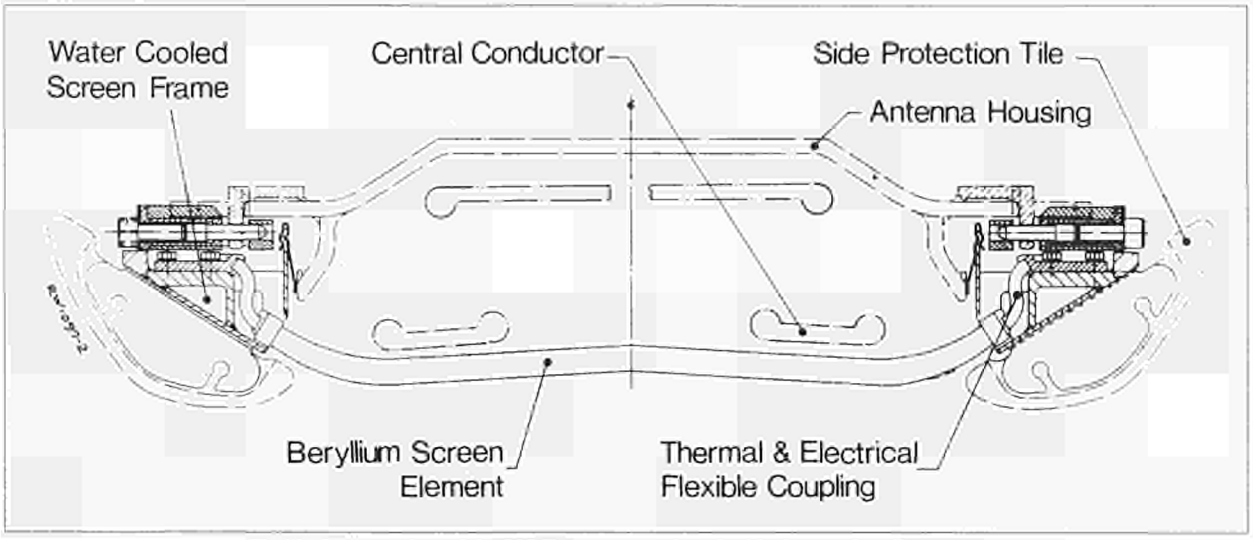

Fig.29: Cross-section of the ICRF antenna equipped with the new beryllium screen.

iv) Beryllium Screens[2]

JET undertook to procure a new set of screens made of beryllium elements:

a) to reduce radiation from the nickel ions released by the screens during heating. Nickel radiation is normally negligible during limiter operation but is believed to be the main source of problems for obtaining good H-modes with ICRF heating;
b) to reduce the risk of water leaks inside the torus.

The new design (see Fig.29) avoids circulating water in the screen elements and eliminates the highly stressed welds between the elements and the water manifold. The screen losses are much reduced due to the good electrical properties of beryllium and the heat can now be removed from the ends of the elements by the water flowing in the manifold forming a 'picture frame' for the screen. The beryllium elements have been fabricated and a proof assembly is under test (see Fig.30). The eight beryllium screens will be installed in the machine in September 1989.

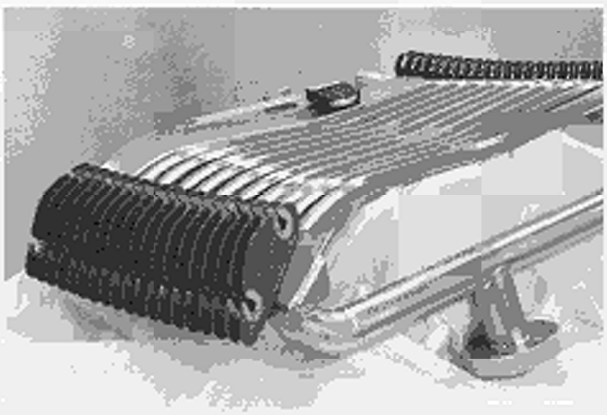

Fig.30: Proof assembly of the beryllium screen elements.

TableIV
Design Parameters of the LHCD System

Power Plant (15.6 MW generator output)
- 6 modules of 4 klystrons (650 kW, 3.7 GHz, 10 s).
- 1 circulator, 1 dummy load per klystron.
- Integrated power and phase control systems. Phase sensitive systems remote from the Torus Hall (no microwave diodes possible during the active phase).

Transmission Lines
- 24 waveguides (about 50 m each) single mode with optimized dimensions for low losses.
- SF6 filled (1 bar).
- Network (near the launcher) splitting from 24 inputs to 48 outputs. The network also accomodates the launcher movement and surveillance of the vacuum windows.

Launcher System (11 MW coupled, 10 s)
- Fills entirely one large JET port (Octant No.3).
- Moveable during the pulse (acceleration $\leq 2\,ms^{-2}$, velocity $0.4\,ms^{-1}$, stroke 26 cm).
- Multijunction concept which splits one input into eight outputs with proper phasing whilst providing some cancellation of the reflected power in each waveguides.
- Grill mouth: 384 waveguides; a protecting picture frame equipped with carbon tiles and water cooling between pulses.

Technical Achievements with LHCD

The design of the LHCD power plant, transmission lines and launching systems is now completed. TableIV summarises the main aspects of the system. The layout of the main elements can be seen in the section 'Current Drive and Profile Control' of this report.

In 1988, several important milestones were reached (see TableV). The 3.7GHz klystrons (Thomson) originally designed for a maximum power of 500kW for 20s were modified for operation at 650kW with a reduced pulse length of 10s. The klystrons and waveguides have now met the full technical specifications and two units are in operation on the RF testbed (see Fig.31).

TableV
Milestones of the LHCD Construction Programme

● 1987–88	– Placing major contracts. – Testing of components in collaboration with CEA Cadarache, France (under Article 14 Contract)
● Sept 1988	– Completion of the JET testbed: 2 klystrons+4 test stations. – Test of the klystron upgrade to 650kW.
● End 1988	– Tests of: windows, multijunctions, transmission lines, circulators, loads, control systems splitting network. – Installation of the main waveguide runs in the Torus Basement.
● Mid 1989	– Delivery of LOP and LOC, two prototype launchers (2MW each) of two different designs (Cadarache, France and JET) – Commissioning of the first two klystron modules and of the waveguide transmission network.
● Sept 1989	– Installation of LOP and LOC in JET
● Mid 1990	– Installation of the final launcher in JET.

Another notable achievement was the successful development of a circulator matching the power capability of the klystron. One of these circulators is on one of the testbed units and operates at the nominal power rating. A large variety of new microwave components and control systems have been designed and tested. Most notable developments are: the power and phase control units; loads to test the multijunction (combined loads for the eight outputs of a multijunction); vacuum loads to equip the hybrid junction in the launcher; etc.

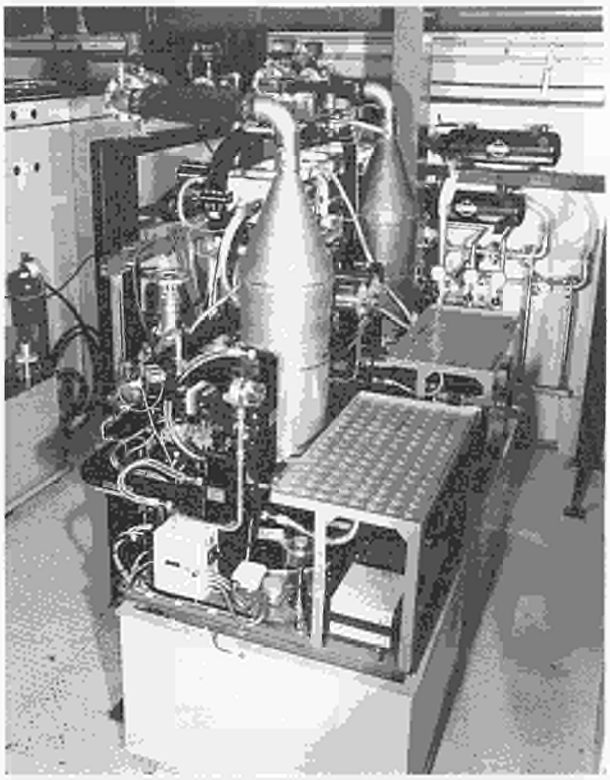

Fig.31: Testbed installation showing the two klystrons in the foreground.

The launcher is an extremely challenging construction. As many as 384 wave-guides are necessary to define precisely the parallel wavelength and launch the required power reliably. Each multijunction (Fig.32) divides the power in eight channels. Its waveguides are precisely machined to produce the necessary phasing between waveguides adjacent on a horizontal row and the cancellation of reflected waves. In the JET design, the multijunctions made of stainless steel are machined in three pieces, which are subsequently brazed together, copper coated for low losses and covered with a thin layer

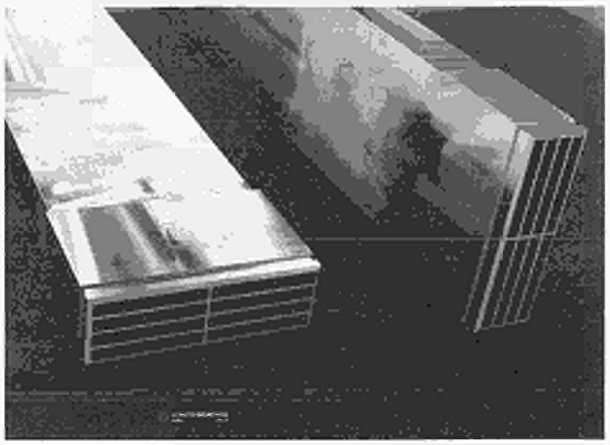

Fig.32: A multijunction.

of carbon to decrease the multipactor effect. All the multijunctions are welded together at the grill mouth. In a design from CEA Cadarache, France, the multijunctions are made of copper plates brazed in one operation. The multijunctions are insulated with respect to each other at the grill mouth. Both types of constructions have successfully passed HF power testing in vacuum. Each prototype launcher is made of eight multijunctions of the JET design (LOP) or of the CEA Cadarache design (LOC). Each launcher connected to a klystron module will be used during experiments on JET (end of 1989 to mid 1990) to gain insight on power transfer capabilities and impurity release.

At the end of 1988, the vessel and supporting structure of the launchers were in an advanced state of construction. In particular, it is expected to benefit from the full on-line positioning system during the initial phase of the experiment. Using hydraulic actuators, the launcher positioning system can be either programmed to follow a prescribed position waveform or connected to an electronic device using the information supplied by probes located in the picture frame to position the launcher at a prescribed value of the edge plasma parameters (electron density or power flux etc).

References

[1] G.Bosia, M.Schmid, J.Farthing, S.Knowlton, A.Sibley, T.Wade, E.Negro; '32MW ICRH Plant Operation Experience in JET'. Proceedings of the 15th SOFT Conference, Utrecht, The Netherlands (1988);

[2] C.I.Walker, H.Brinkschulte, M.Bures, N.Dragomelo, J.P.Coad, A.S.Kaye, S.Knowlton, J.Plancoulaine, 'The JET ICRF Antenna Screen: Experience with Actively Cooled Nickel Screen and Design of New Beryllium Screen', Proceedings of the 15th SOFT Conference, Utrecht, The Netherlands (1988);

[3] J.Dobbing, G.Bosia, M.Brandon, M.Gammelin, C.Gormezano, J.Jacquinot, G.Jessop, M.Lennholm, M.Pain, A.Sibley, T.Wade, 'Design of JET Lower Hybrid Current Drive Generator and Operation of High Power Test Bed', Proceedings of the 15th SOFT Conference, Utrecht, The Netherlands (1988);

[4] A.S.Kaye, H.Brinkschulte, G.Evans, C.Gormezano, J.Jacquinot, S.Knowlton, X.Litaudon, DMoreau, M.Pain, J.Plancoulaine, C.Walker, G.Wilson, 'Design of the JET Lower Hybrid Launcher', Proceedings of the 15th SOFT Conference, Utrecht, The Netherlands (1988).

Remote Handling

Further progress has been made in specifying, acquiring and commissioning major items of remote handling equipment. This equipment comprises special tools to suit the features and to provide access to JET components; end-effectors to lift and attach large components; large, high-precision transporters to carry the equipment to all parts of the JET machine; and control systems for this equipment:

During 1988, further efforts were devoted to analysis of tasks inside and outside the vessel to provide the basis for specifications of equipment and to supply material for data bases which will be used to direct operations.

The introduction of tritium into the machine, which will require that all work on the JET machine is performed by remote control from outside the Torus Hall, is now proposed for mid-1991. Until this time, increasing background radiation, the generation of slightly activated dust and the use of beryllium will necessitate special equipment and methods for gaining access and carrying out hands-on work safely inside the torus

Special Tools

Work this year has focused on requirements for the 1988/89 major shutdown requirements. The full range of sleeve welders and cutters required for JET has been identified, designed and manufactured. These are now being used on the machine for maintenance of the existing RF vacuum transmission lines and will be used to install the Lower Hybrid Wave System. New designs of orbital welder and cutter have been made to cover the 20-27 mm diameter pipes used by both Neutral Beam and RF systems. These tools are variations of the 50mm diameter tools designed in 1986/87 and successfully used for belt limiter and antennae first installation. Extensive use of these 50mm diameter tools has been made this year for the replacement of various antennae in the torus and some improvements to the designs have been incorporated resulting from the operational experiences.

The remote handling PROTIG weld power packs have been modified to facilitate control of the existing remote handling lip welding trolley and the new sleeve welders, all of which have resolver position feedback and new control requirements not found on the other weld tools. The facility for clamping and tack welding to cope with gaps which are out of tolerance has been incorporated in the new production trolleys.

Transporters

The articulated boom was used in the vessel under joystick control to replace 10 antennae. Trials of installation of a limiter segment and an antennae housing and screen were carried out in simulated remote conditions using the spare vacuum vessel octant in the Assembly Hall as a mock-up. These tests identified a number of improvements needed. As TV viewing of the fixing points of these components is virtually impossible, joystick control is not viable. A trial of installing a limiter using the teach-and-repeat facility of the boom was undertaken successfully, with dynamic repeatability better than 5 mm.

The control system has been refined and it is now pos-

sible to reach in resolved motion with any three joints and repeat with several joints at a time. This overcomes the difficulties encountered in inserting the boom through the port with the narrow gap available (~10mm). By rewriting part of the original BASIC software into FORTH the insertion time in repeat mode has been reduced to 40 minutes. This is expected to be halved by further software improvements.

Stiffer actuators, composed of two preloaded harmonic drives, were developed and two were installed and tested on the boom. Horizontal stiffness and load capacity of these joints improved by a factor 2-3.

The boom gaitering to avoid tritium and beryllium contamination was installed and tested. Enhancements have been pursued in the design of the end effectors. Actuated latches and increased clearances will make operation more reliable. A new end effector for the lower hybrid antennae has been designed and ordered after international tender. The large task of wiring from the Assembly Hall to the Torus Hall is complete and 80% commissioned.

The telescopic transporter for ex-vessel interventions (TARM) is being manufactured and is due for delivery in 1989. At JET, work has included specification and procurement of the TARM services (i.e. gas handling, welding sources, manipulator controls and cooling plant). The layout of installation and wiring on the crane and in the parking/testing stillage in the Assembly Hall has been completed. The articulated section, supplied by JET, is complete and the control software has been tested on some of these parts.

During 1988, the remote operated low level transporter (ROLLT) has been converted to full teleoperation status, and is now entirely controllable from a handbox, either locally or remotely. Fore and aft cameras with pan and tilts mounted on independantly controlled lifting mechanisms have been fitted. A comprehensive back-up facility will allow the truck to be retrieved from the Torus Hall in the event of a catastrophic failure. During the 1988 shutdown, the vehicle was used to replace the two most inaccessible turbomolecular pumps on the torus, confirming that its manoeuvring ability is excellent, and providing valuable information for later mock-up trials.

After seven years of service as a standard bridge crane, preliminary preparations for the crane's use as a remote handling transporter have started. This will involve three main areas:

- the fitting of precision resolvers to the crane, and eventually a system to enable closed loop velocity and position control of the cranes four major axes. This includes devising systems for remote lifting using special beams and frames, also possessing actuators and sensors. To eliminate cable reeler problems, a system correlating reeler motion with crane long travel will also be incorporated;
- reliability study to identify and eliminate inherent weaknesses;
- the integration of the crane with the planned Remote Handling Control System (RHCS), the man/machine interface, in particular.

The reliability study is underway, and the fitting of resolvers and provision of the crane management system will take place in early 1989.

Control Systems

The Remote Handling Control Room is now in operation with one completed Servomanipulator Master Station (SMMS). The equipment for completion of the second SMMS is available and will be installed shortly. Two production (non-prototype) Remote Handling Workstations have been completed and are in use in the Control Room. To improve response times, to ease maintenance requirements and to simplify the overall interconnection system, use is being made of an Ethernet link installed during this year. This facilitates all Local Control Unit data transfer to the Graphics Workstations and also handles all non real-time critical tasks such as camera selection and control. The system of Torus Hall wall mounted 'fixed' cameras, and their interconnection and control is now being implemented. Some of these camera assemblies will be used for the full size RH mock-ups in the Assembly Hall.

As a continuation of collaborative work with KfK Karlsruhe, FRG on real-time computer generated display of remote handling equipment, a software link was developed between the JET CATIA CAD system and the RH Graphics Workstation. This was written and developed by KfK personnel and will now be used for input of data for the next phase of work displaying the TARM in its Torus Hall environment.

Further improvements were obtained by enhancing the control software to include acceleration feed forward and speeding up the man-machine interface. Advanced functions for computer-aided manipulation are being developed. The teach-and repeat facility has been commissioned. Feasibility tests have been carried out for preferential constraints and the kinematics algorithm has been worked out for tool-weight compensation.

Mock-Ups

During the year, two full size remote handling task mock-ups were constructed and operated in the Assembly Hall. The JET spare octant was integrated into a mock-up facility to facilitate some in-vessel tasks. The tasks undertaken were belt limiter and antennae replacement. These tasks were undertaken in this first phase using the articulated boom under local or hands-on control and many modifications to both the remote handling and the JET components were recommended and are now being implemented as a result of these tests. This first phase of work has been completed and the mock-up facility has been disassembled for the duration of the major shutdown.

A special support frame for mounting and mock-up testing of neutral beam PINI removal has been built and also operated in the Assembly Hall. The first phase of hands-on testing with the remote handling lifting frames and tools, etc., was completed in July and the second phase of remote operations but with local control from the Assembly Hall, was implemented shortly afterwards. The mock-up is being operated fully remotely from the RH Control Room deploying the remote handling tools and the Mascot and with CCTV feedback from the boom extension and Mascot cameras.

In-Vessel Inspection System

The new IVIS designed to work at 350°C has been tested and used successfully in the vessel for several inspection campaigns, together with the new lighting system using light guides through the vacuum separation. To facilitate the scanning of the vessel and interpretation of images, a console with a graphical display and a facility for fast automatic retrieval of previously taken 'reference' pictures is being developed.

Machine Components

Work continued on ensuring remote handling compatibility. A simple method to upgrade the LEMO electrical connectors, which had proved unsatisfactory, was devised. Heating jackets for the vacuum flanges were developed and tested.

Active Handling

Based on the studies of active handling and remote maintenance requirements during the D–T phase, the conceptual design of the active handling facility has been completed. The new control area, to be built in the Assembly Hall adjacent to the Hot Cell, will provide facilities for decontamination, active maintenance on the remote handling tools, active waste handling and storage, maintenance on the articulated boom and the TARM and controlled access to the Hot Cell and Access Cell areas. This will include a change room and barrier facility.

Following detailed design, construction of the facility will commence in 1989 to allow commissioning prior to the start of the D–T phase. Whilst the main tasks will be in support of the remote handling intervention work, which will include specific tritium related problems, the area will also be used for beryllium related work.

Waste Management

Additional input data for the facility design came from studies on active waste arisings, completed earlier in the year. Part of this work involved assessments of all systems likely to produce active aqueous wastes. Analysis of the results led to a number of system modifications to minimise waste volumes. The conceptual design of an active drainage system has subsequently been completed. Disposal routes for both active and beryllium wastes have been considered and a QA system has been developed to ensure safe disposal.

Continuing assessment of secondary wastes has included the determination of decontamination requirements. The completion of the test programme on tritium related maintenance, conducted by JET in collaboration

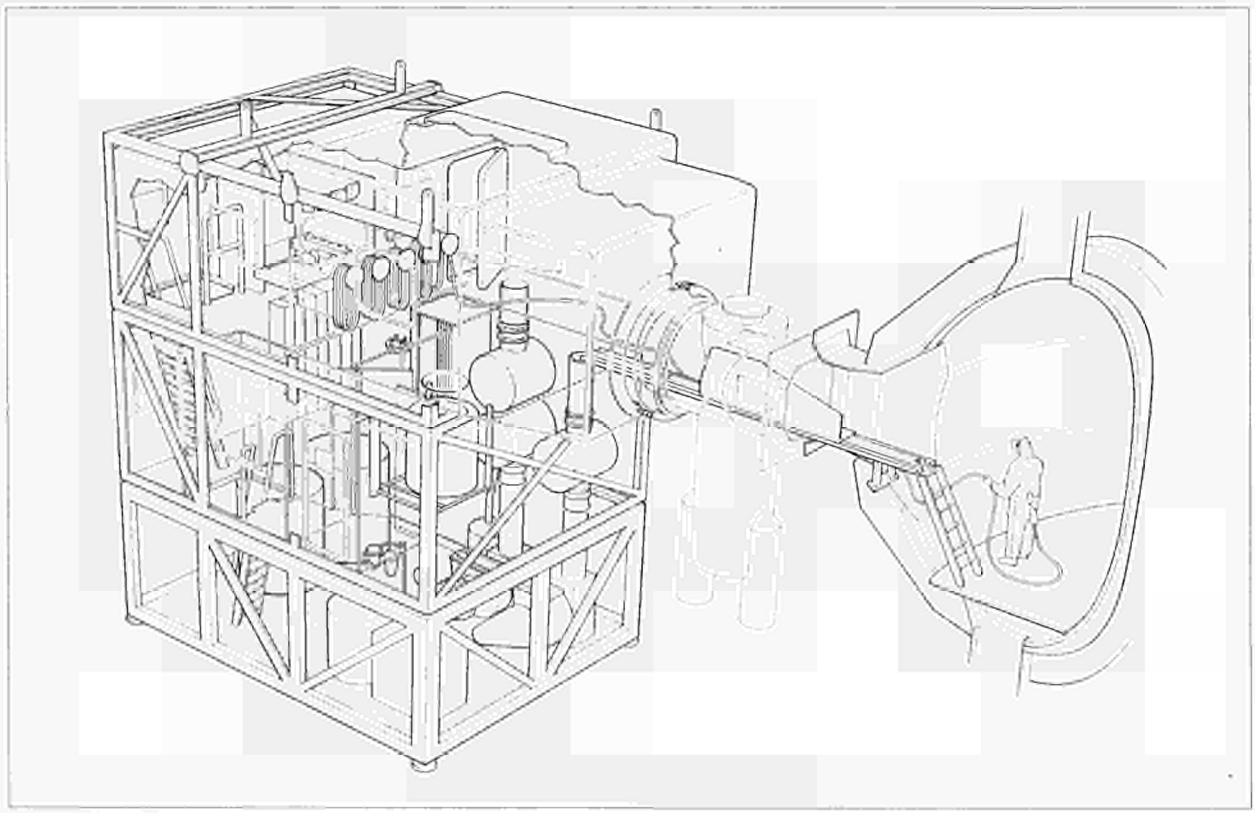

Fig. 33 JET Torus Access Cabin (TAC).

with TSTA staff at USDoE Los Alamos, USA has provided relevant data. Further decontamination investigations are planned and the results will be used to specify equipment for the decontamination facility.

Beryllium Operations

Further attention has been given to the special requirements of beryllium related maintenance. The Torus Access Cabin (Fig. 33), already used successfully in several interventions, will provide controlled access to the torus following plasma operations with beryllium. Ex-vessel maintenance will involve the use of flexible isolators and continuing development for the JET specific requirements has been carried out (see Fig. 34). A workshop is being established for their fabrication. Other control area facilities include an experimental laboratory for evaporation trials and a central beryllium handling facility for support operations and tile handling which has been designed and constructed in the Assembly Hall.

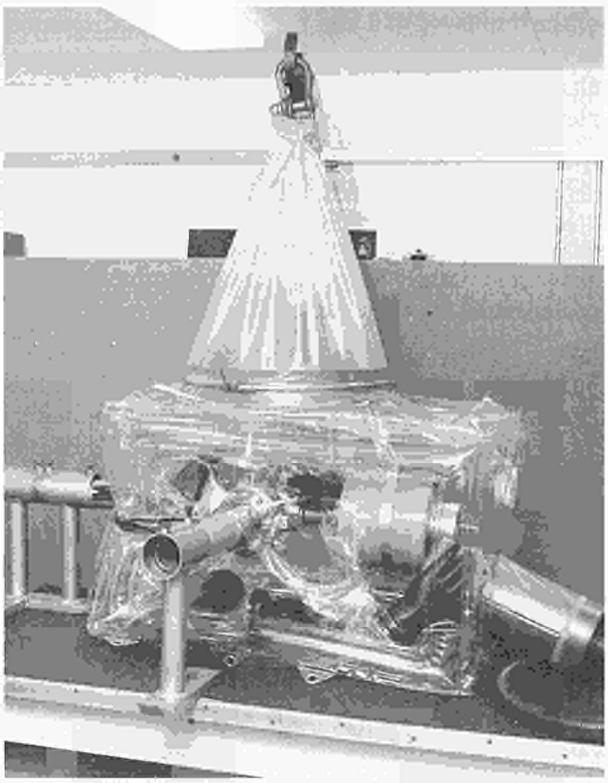

Fig. 34 Beryllium Isolator.

To standardise on design features and make all staff aware of the procedures necessary for safe operations with beryllium, notes for guidance which were generated last year have been updated. One of the difficult features of working with beryllium, is the time required for the analysis of samples. Using the standard technique of atomic absorption spectroscopy (AAS), this is usually a minimum of one hour/sample, though routinely much longer. To minimise machine downtime, JET has procured a new instrument, utilising the principle of laser induced breakdown spectroscopy (LIBS) (Fig. 35) developed at USDoE, Los Alamos, USA. Following agreement on the specification last year, the device was built by the Los Alamos National Laboratory and delivered to JET this year. It can analyse air-sample filter papers in around 30s.

Fig. 35 LIBS Beryllium Analyser.

Control and Data Aquisition System (CODAS)

The Control and Data Acquisition System (CODAS) Division is responsible for the design, procurement, implementation, upgrade and operation of the computer-based control and data acquisition system of JET. This system, based on a network of NORSK DATA minicomputers, allows centralised control and monitoring. The various components of JET have been logically grouped in subsystems such as Vacuum, Toroidal Field, Poloidal Field, etc. Each subsystem is controlled and monitored by one computer and the various computer actions are co-ordinated by a supervisory software running on the machine console computer. This supervisory function includes the countdown sequences for each plasma discharge. The allocation and configuration of all CODAS computers is given in TableVI and Tables VII and VIII provide other quantitative data.

The main developments during 1988 and the orientation for 1989 are summarised below.

TABLE VI

CODAS Computer Configuration at the end of 1988

Subsystem	Usage	Model	Memory (MByte)	Disks (MByte)
AH*	NI Additional Heating (Oct 8)	ND110	3.5	1×70 1×450
AN*	Analysis and Storage	ND560	4.0	1×70 1×140 2×450
AS	Assembly Database	ND110	2.0	2×45
CB	Message Switcher B	ND110	2.0	1×70 2×140
CP	Cable Database	ND530	6.0	1×70 1×450
DA*	On-line Diagnostic	ND520	4.0	1×70 1×140
DB*	On-line Diagnostic	ND520	4.0	1×70 1×140
DC*	On-line Diagnostic	ND520	4.0	1×70 1×140
DD*	On-line Diagnostic	ND530	4.0	1×70 1×140
DE*	On-line Diagnostic	ND520	4.0	1×70 1×140
DF*	On-line Diagnostic	ND520	6.0	1×70 1×140
DG*	On-line Diagnostic	ND520	4.0	1×70 1×140
DH	Diagnostic Conditioning	ND550	6.0	1×70 1×450
EC*	Experiment Console	ND570	6.0	1×70 1×140
EL	Electronic	ND110	2.0	1×70 1×140
GS*	General Services	ND110	2.5	1×70 1×140
XC	CODAS Commissioning	ND110	4.0	2×70 1×140
LH	Lower Hybrid	ND110	3.0	1×70 1×140
MC*	Machine Console	ND110	2.5	1×70 1×140
PF*	Poloidal Field	ND110	3.0	1×70 1×140
PL*	Pellet Launcher	ND110	2.5	1×70 1×140
PM*	Pulse Management	ND550	6.0	1×70 1×140 1×450
RB*	Radio Frequency Test Bed	ND110	2.25	1×70 1×450
RF*	Radio Frequency	ND100	3.0	1×70 1×140
RH	Remote Handling	ND110	2.5	1×70 1×140
SA*	Message Switching & JPF Collection	ND110	2.0	1×70 2×450
SB	Standby System/Backup	ND110	4.0	2×70 1×450
SD	Built-in, Pool, Computer dB	Compact	2.25	2×45
SS*	Safety and Access	ND110	2.0	2×70 1×140
TB*	NI Test Bed	ND110	2.5	1×70 1×140
TF*	Toroidal Field	ND110	2.5	1×70 1×140
TR	Tritium	ND110	2.5	1×70 1×140
TS	Test	ND530	4.0	1×70 2×450
VC*	Vacuum	ND110	3.5	1×70 1×140
YB	Integration	ND530	4.0	1×70 1×450
YC*	NI Additional Heating (Oct 4)	ND110	3.5	1×70 1×450
YD	Sc Dpt Development	ND570	6.0	1×70 1×450
YE	CODAS Development	ND520	6.0	1×70 1×450

* indicates on-line computers used for operation and testbed

New Subsystems

The development of the new Pellet Injector required the establishment of a testbed facility. This has been carried out on the CODAS commissioning computer (XC). This new subsystem is presently in operation and will be expanded during 1989.

The Lower Hybrid subsystem (LH) has been made available to users and hardware and software expansion will continue in 1989. Initial tests are presently in progress and the full control system should be commissioned before the end of 1989.

Expansion and Enhancements of Existing Systems

Data Acquisition

The hardware and software configuration of the link between the JET main-frame computer located at Harwell and JET site facilities has been completed. Its present status is shown on Fig.36. During the last period of operation, collection speed (from Subsystems to Storage and Analysis computer) of 65 kByte/s and transfer speed (from Storage and Analysis computer to JET main-frame) of 170 kByte/s were achieved routinely. The

TABLE VII

Quantative Information on CODAS Installation

Item	End 1987	End 1988
CODAS interface cubicle	138	149
CAMAC crates	223	232
CAMAC modules	3364	3420
Eurocard modules (signal conditioning)	6927	7250
Computer terminal (including PCs and IBM terminals for 1988)	333	534
CAMAC serial loop (fibre optic)	24	25
On-line computers	24	23
Off line and comissioning computers	14	15
Size of JPF	15MB	17.6MB
Number of diagnostics on-line with CODAS	27	35
Number of diagnostics under commissioning with CODAS	6	4

TABLE VII

Review of CODAS Electronics Stock Holding (installed, pre-procurement and spares)

	End 88	End 87	
1.	CAMAC system modules	895	873
2.	CAMAC digital I/O modules	840	814
3.	Timing system (CAMAC & Eurocard)	1,273	1,202
4.	CAMAC analogue I/O modules	1,154	1,086
5.	CAMAC display modules	409	360
6.	CAMAC auxiliary controllers	152	127
7.	CAMAC powered crates	273	262
8.	U-port adaptor	200	184
9.	CISS modules	959	856
10.	CCTV	510	544
11.	Cubicle frames	345	345
12.	Console devices (not CAMAC)	518	504
13.	Power supplies modules	1,709	1,614
14.	Intercom, Public address, Computer terminal Network	617	578
15.	Pool instruments	964	934
16.	Analogue I/O in Eurocard	2,741	2,485
17.	Digital I/O in Eurocard	4,897	4,718
18.	Eurocard sub-racks	970	860
		19,426	18,355
		Increase 1,071	5%

continuous growth of the JET Pulse File (JPF) size has required additional performance improvement. New software has been developed and tested. It should allow a JPF of 15MB to be delivered to the main-frame 90s earlier than before. As JET operates nearer its performance limits, the results of the detailed analysis made in the main-frame computer are becoming more necessary for its operation. Therefore, the data link performance improvements have a direct impact on the JET pulse repetition rate. The JPF growth and evolution of transfer time during the year is shown in Fig.37.

Studies of the possible benefits of applying data compression techniques to JPF data have started. A slightly modified version of the software used at TFTR has been tried showing that a compression factor of about three could be achieved. Such compression will be used in the main-frame Mass Storage System early in 1989. Additional studies, using data acquisition modelling, are underway to identify the benefits of data compression within the CODAS computer network.

Computer Configuration and Installation

The ageing disk storage media have been replaced with new devices based on Winchester technology which have higher reliability, better performance and much lower power consumption. All Central Processing Units (CPU) have been upgraded to higher performance models. A new version of the operating system has been installed on all CODAS computers and all software brought up to the latest revision level. All these changes have been implemented during the shutdown period and recommissioning will be formally completed in January 1989. Apart from application software upgrade and configuration changes, no major enhancements are planned for the coming years.

A secure area in J2 building has been set-up with independent air conditioning backup units, uninterruptible power supply (for computer and consoles) and special cable routing. This area is used for the Tritium (TR), Safety and Access (SS) and Remote Handling (RH) subsystem computers which have availability requirements different from the other CODAS computers used for operation. On SS, a new software for the Personnel Dosimetry Services complying with the new U.K. Health and Safety Executive (HSE) requirements has been developed. Commissioning and acceptance will be completed by April 1989. ETHERNET communication has been installed on RH and will be used by TR.

Plasma Control and Protection System

A new Direct Magnet Safety System for the poloidal field coils providing compensation channels for X-point operation has been integrated in the daily operation. The digital version of the plasma radial position feedback control has been tested and will be formally commissioned in 1989. An experimental unit for the dual vertical stabilisation system has been built for Magnet and Power Supply Division and, following initial tests, a revised version will be tested in 1989. Numerous and significant changes have been made to the Plasma Density Validation, Plasma Fault Protection System and Pulse Termination Network.

Networks

The CODAS Terminal Network has been considerably expanded to service the new building J20 (500 outlets installed) and the new Portakabins (150 outlets). A satellite station linked by fibre optics to the main Terminal Multiplexor has been brought into operation to service the additional channels. Three Personnel Computer net-

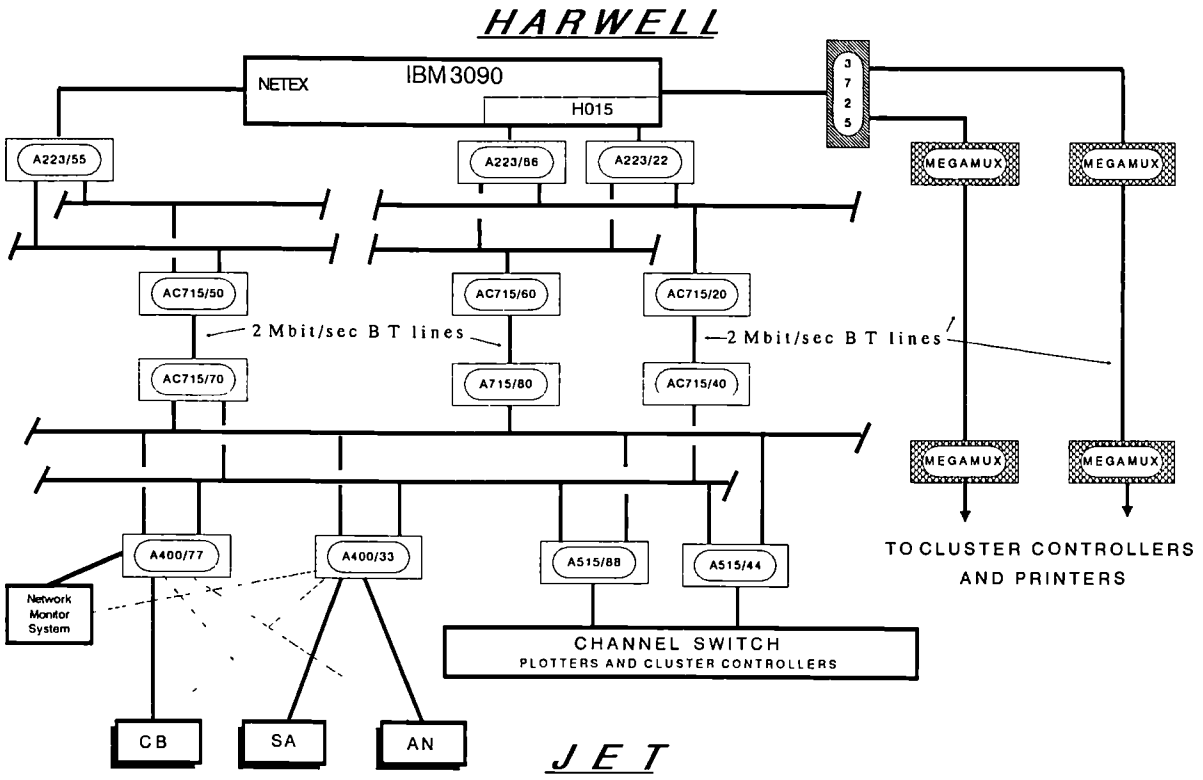

Fig.36: JET/Harwell Link

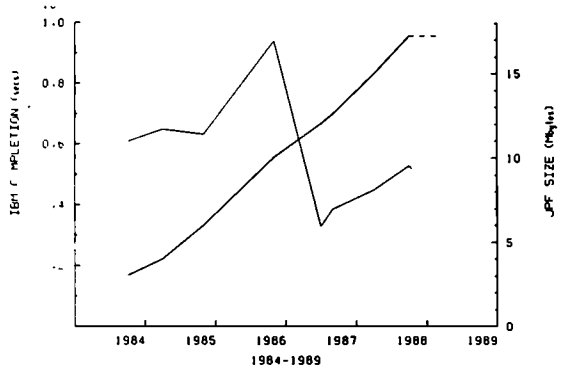

Fig.37: JPF Growth and Transfer Time over the Life of JET

works have been installed for Finance, Contracts and Personnel Services. Gateway facilities have been provided.

Central Interlock and Safety System

The Central Interlock and Safety System (CISS) is based on a network of Programmable Logic Controllers (PLCs) linked to a supervisor PLC. This system has been in operation since June 1983 and has never had a single failure to danger. The expansion of JET installation and additional modes of operation have required numerous changes to the hardware and software again this year. The operation of high performance plasmas has also required modification of the state transition in the supervisor to prevent hard termination in case of partial failure of additional heating subsystems.

Operation and Services

Support of operation has continued to absorb efforts of all members of the CODAS Division. A large number of upgrades and extensions to various systems have contributed improvement of comfort and efficiency of operation. During 1988, 337 hardware changes and 470 software upgrades were implemented.

The cable management service has issued 3,567 wiring schedules and entered 1,790 new devices (sockets, junction boxes, etc.) in the database. The user interface to this service has been improved and further enhancements are planned for 1989. The Electronics Group maintenance and repair services have operated smoothly and have been expanded to include cubicle construction.

Main Orientations of Future Activities

Expansion and New Systems

The design, implementation and commissioning of the CODAS part of the Tritium plant and of the Lower Hybrid Current Drive system (total of about 12 cubicles) and completion of the Remote Handling system will be the main targets for 1989.

Improvement of Reliability

As part of the preparation for tritium operation, a

general campaign of reliability improvement has started and will be pursued in 1989. A non- negligible effort is already invested in documentation improvement. Systematic fault analysis is under development to identify where available effort should be allocated. A gradual freeze of Hardware and Software installation will be enforced where reasonable.

Conclusions

This year, again, turnover of staff has been large and, in spite of an active recruitment campaign, the Division failed to reach its full staffing level. The average experience of all of CODAS (Team and Services) is less than 3 years. The size and complexity of the system requires a few months of familiarisation for a newcomer to become efficient.

JET Data Management Group

The JET Data Management Group is responsible for the provision of a Mainframe Computing Service for scientific and engineering computing. This includes provision of appropriate software and hardware systems. The Group is also responsible for the management of JET data and the organisation and control of routine data processing.

The Computing Service is based on an IBM 3090/200E dual processor mainframe with a vector facility. There are 70 GBytes of disc storage and a further 240 GBytes of IBM mass storage. The JET Mainframe Data Processing Centre is housed in a specially designed building at UKAEA Harwell Laboratory and operated for JET under contract by a team from that Laboratory. The JET mainframe is also connected to the Harwell Laboratory CRAY2 computer.

The JET Computing Centre has been operating since June 1987 and the computing load has grown significantly since that date, such that at peak times the system is reaching its capacity. However, by careful tuning of the system, good response time is maintained for interactive users and for the CAD systems in the JET Drawing Office. Also the prompt excecution of the intershot analysis is ensured. A background load of batch work is also serviced but the increasing long batch job work load, such as transport analysis and extensive structural analysis codes, now tends to be displaced outside daytime periods.

The Data Management Group provides the contact between the users, operators and system programmers, through the Help Desk Service, backed up by specialists in the Group. This ensures the smooth running of the system. The data communications between the JET site and the Computer Centre are mainly the responsibility of CODAS Division and significant improvements in these areas are reported in that section.

The Group is also responsible for the storage of JET data and currently ~ 110 GBytes of raw JET data (JPFs) are stored on the cached Mass Store, and a further 30 GBytes of analysed data are stored on the much enhanced PPF online data base system. During 1988, a complete higher level data selection and storage system, the Central Physics File (CPF), was established under the SAS environment. A subset of all data is extracted at time points of interest, determined by a newly developed Timeslice program, and stored in the SAS databases. These data are the basis for extended statistical analysis, and the source for other extracts such as the TRANSPORT bank. This complete system is a fully automated process.

In addition to mainframe computing, the Group, in collaboration with the Data Processing and Analysis Group, provides support for the increasing numbers of Personnel Computers (PCs) on site which are used both as stand-alone workstations and terminals to the IBM and NORD computers.

Diagnostic Systems

The status of JET's diagnostic systems at the end of 1988 is summarized in Table IX and their general layout in the machine is shown in Fig.38. The staged introduction of the diagnostic systems onto JET has proceeded from the start of JET operation in June 1983 and is now nearing completion. The present status is that, of 47 systems in total, 37 are in routine operation, 5 are being installed/commissioned, 4 have still to be constructed and 1 system is still under study. Operational experience has been good and many of the systems are now operating automatically with minimal manual supervision. The resulting measurements are of a high quality in terms of accuracy and reliability, and provide essential information on plasma behaviour in JET. Further details on specific diagnostic systems are given below.

Magnetic Measurements

The basic magnetic diagnostic has continued to provide routine and reliable measurements both for identification of the basic magnetic configuration in limiter and X-point discharges and for the signature of MHD behaviour. The analysis of very fast MHD phenomena and high frequency turbulence has progressed by taking data with previously installed coils with fast response ($\leq$ 125 kHz) and matching amplifiers. The need to follow the plasma movements during vertical disruptions has led to the successful commissioning of hard wired vertical and radial movement detectors based on the Shafranov moments. The design of fast dedicated disruption feedback control pick-up coils has been completed for installation during the 1988-1989 shutdown.

The installation of the PFX circuit that allows X-point operation at high current and is used to obtain 7 MA limiter discharges has led to an uncompensated contribution to the diamagnetic loop signal. This has been

TABLE IX
Status of the JET Diagnostics Systems, December 1988

System	Diagnostic	Purpose	Association	Status	Compatibility with tritium	Level of automation
KB1	Bolometer array	Time and space resolved total radiated power	IPP Garching	Operational	Yes	Fully automatic
KC1	Magnetic diagnostics	Plasma current, loop volts, plasma position, shape of flux surfaces, diamagnetic loop, fast MHD	JET	Operational	Yes	Fully automatic
KE1	Single point Thomson scattering	T_e and n_e at one point several times	Risø	Operational	Yes	Fully automatic
KE3	Lidar Thomson scattering	T_e and n_e profiles	JET and Stuttgart University	Operational	Yes	Fully automatic
KG1	Multichannel far infrared interferometer	$\int n_e ds$ on six vertical chords and two horizontal chords	CEA Fontenay-aux-Roses	Operational	Yes	Semi-automatic
KG2	Single channel microwave interferometer	$\int n_e ds$ on one vertical chord	JET and FOM Rijnhuizen	Operational	Yes	Fully automatic
KG3	Microwave reflectometer	n_e profiles and fluctuations	JET	(1) Fixed frequency operational (2) Swept frequency in commissioning	Yes	Fully automatic
KG4	Polarimeter	$\int n_e B_p ds$ on six vertical chords	CEA Fontenay-aux-Roses	Operational	Yes	Semi-automatic
KH1	Hard X-ray monitors	Runaway electrons and disruptions	JET	Operational	Yes	Fully automatic
KH2	X-ray pulse height spectrometer	Plasma purity monitor and T_e on axis	JET	Operational	Yes	Semi-automatic
KJ1	Soft X-ray diode arrays	MHD instabilities and location of rational surfaces	IPP Garching	Operational	No	Semi-automatic
KJ2	Toroidal soft X-ray arrays	Toroidal mode numbers	JET	Operational	Yes	Semi-automatic
KK1	Electron cyclotron emission spatial scan	$T_e(r,t)$ with scan time of a few milliseconds	NPL, UKAEA Culham and JET	Operational	Yes	Fully automatic
KK2	Electron cyclotron emission fast system	$T_e(r,t)$ on microsecond time scale	FOM Rijnhuizen	Operational	Yes	Fully automatic
KK3	Electron cyclotron emission heterodyne	$T_e(r,t)$ with high spatial resolution	JET	Operational	Yes	Not yet implemented
KL1	Limiter surface temperature	Monitor of hot spots on limiter, walls and RF antennae	JET and KFA Jülich	Operational	No	Fully automatic
KL3	Infrared belt limiter viewing	Temperature of belt limiters	JET	Commissioning	No	Will be fully automatic
KM1	2.4MeV neutron spectrometer	Neutron spectra in D-D discharges, ion temperatures and energy distributions	UKAEA Harwell	Commissioning	Not applicable	Semi-automatic
KM3	2.4MeV time-of-flight neutron spectrometer		NEBESD Studsvik	Operational	Not applicable	Fully automatic
KM4	2.4MeV spherical ionisation chamber		KFA Jülich	Commissioning	Yes	Semi-automatic
KM2	14MeV neutron spectrometer	Neutron spectra in D-T discharges, ion temperatures and energy distributions	UKAEA Harwell	Under Construction	Yes	Not yet installed
KM5	14MeV time-of-flight neutron spectrometer		SERC, Gothenberg		Yes	Not yet installed
KM7	Time-resolved neutron yield monitor	Triton burning studies	JET and UKAEA Harwell	Operational	Not applicable	Fully automatic
KN1	Time-resolved neutron yield monitor	Time-resolved neutron flux	UKAEA Harwell	Operational	Yes	Fully automatic
KN2	Neutron activation	Absolute fluxes of neutrons	UKAEA Harwell	Operational	Yes	Semi-automatic
KN3	Neutron yield profile measuring system	Space and time resolved profile of neutron flux	UKAEA Harwell	Operational	Yes	Fully automatic
KN4	Delayed neutron activation	Absolute fluxes of neutrons	Mol	Operational	Yes	Fully automatic
KP3	Fusion product detectors	Alpha-particles produced by D-T fusion reactions	JET	Under study	Yes	Automatic
KR1	Neutral particle analyser array	Ion distribution function, $T_i(r)$	ENEA Frascati	Operational	No	Automatic
KR2	Active phase NPA	Ion distribution function, $T_i(r)$	ENEA Frascati	Under construction	Yes	Automatic
KS1	Active phase spectroscopy	Impurity behaviour in active conditions	IPP Garching	Operational	Yes	Not yet implemented
KS2	Spatial scan X-ray crystal spectroscopy	Space and time-resolved impurity density profiles	IPP Garching	Operational	No	Not yet implemented
KS3	H-alpha and visible light monitors	Ionisation rate, Z_{eff}, impurity fluxes	JET	Operational	Yes	Semi-automatic
KS4	Charge exchange re-combination spectroscopy (using heating beam)	Fully ionized light impurity concentration, $T_i(r)$, rotation velocities	JET	Operational	Yes	Semi-automatic
KS5	Active Balmer α spectroscopy	T_D, n_D and Z_{eff} (B_p)	JET	Under Construction	Yes	Not yet implemented
KT1	VUV spectroscopy spatial scan	Time and space resolved impurity densities	CEA Fontenay-aux-Roses	Operational	No	Semi-automatic
KT2	VUV broadband spectroscopy	Impurity survey	UKAEA Culham	Operational	No	Fully automatic
KT3	Active phase CX spectroscopy	Fully ionized light impurity concentration, $T_i(r)$, rotation velocities	JET	Operational in'89	Yes	Not yet implemented
KT4	Grazing incidence spectoscopy	Impurity survey	UKAEA Culham	Operational	No	Fully automatic
KX1	High resolution X-ray crystal spectroscopy	Ion temperature by line broadening	ENEA Frascati	Operational	Yes	Fully automatic
KY1	Surface analysis station	Plasma wall and limiter interactions including release of hydrogen isotope recycling	IPP Garching	Operational	Yes	Automated, but not usually operated unattended
KY2	Surface probe fast transfer system		UKAEA Culham	Operational	Yes	
KY3	Plasma boundary probes	Vertical probe drives for electrical and surface collecting probes	JET, UKAEA Culham and IPP Garching	Operational	Yes	
KY4	Fixed Langmuir probes (X-point and belt limiter)	Edge parameters	JET	Operational	Yes	Semi-automatic
KZ1	Pellet injector diagnostic	Particle transport, fuelling	IPP Garching	Operational	No	Not automatic
KZ3	Laser injected trace elements	Particle transport, T_i, impurity behaviour	JET	Operational	Yes, after modification	Not automatic
Kγ1	Gamma-rays	Fast ion distributions	JET	Operational	Yes	Manual

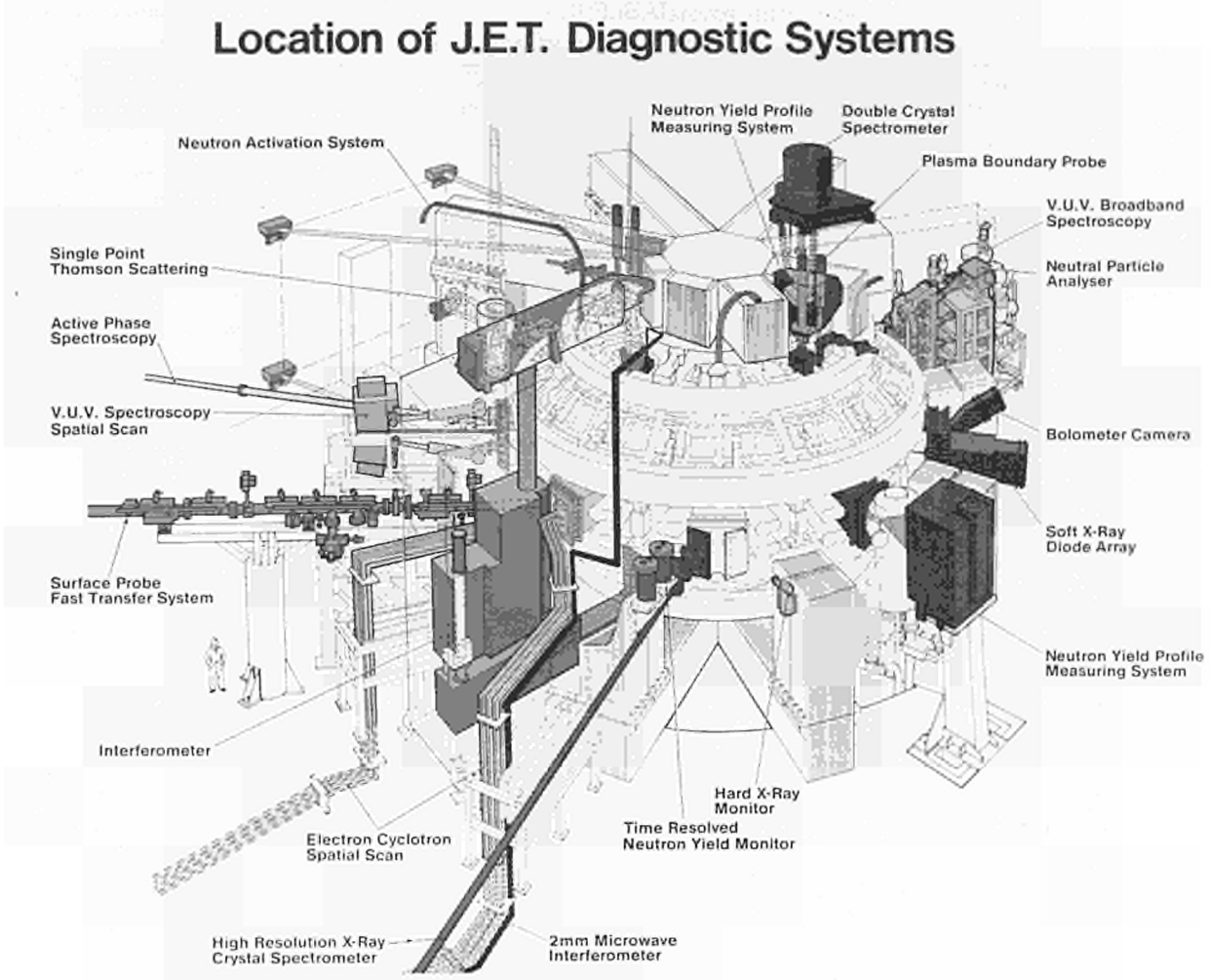

Fig.38: General Layout of Diagnostics in the Machine.

recognised and this contribution has been largely corrected. A similar problem has been found with the saddle loop signals and computer simulations are in progress to attempt to make this small correction to the equilibrium analysis.

Plasma Boundary Probes

Langmuir probes of all carbon construction in the plasma contact area have been in operation in all important regions in JET. In particular, the Langmuir probes mounted in a band of X-point target tiles have given important information on plasmas obtained in this mode of operation. The algorithm to fit automatically the non-linear Langmuir characteristics has been considerably improved. The fast moving (reciprocating) Langmuir probe drive which can scan 10 cm of the edge profile in 200 ms, has been used extensively (see Fig.39). It has given important details of the edge profile and, because this probe is designed to cross the last closed flux surface (LCFS), it gives unambiguously the position of this surface. Thus far, the applicability of this probe has been limited by uncontrolled movements of the plasma boundary which cause an excessive power loading to the probe in its rest position. A probe with a larger stroke of 25 cm is therefore under design.

The drive system for the plasma boundary probes which carries either the fast reciprocating probe or a rotating collector probe has been redesigned to improve the reliability. As a result these probes now operate reliably in a remote control mode.

Plasma Wall Interactions

Samples from limiters, inner wall, X-point tiles and special samples attached to the wall (all retrieved from the vessel after opening) have continued to confirm the basic understanding of the plasma wall interaction. In particular, detailed erosion/deposition measurements have been performed on the belt limiter tiles. Analysis of tritium originating from the $D+D \rightarrow T$ reaction and embedded in tiles has given preliminary information on the amount that will be found in the carbon protection of the JET vessel under active conditions. Studies have been made at JET of the release of loosely bound hydrogen isotopes (deuterium and tritium) from in-vessel

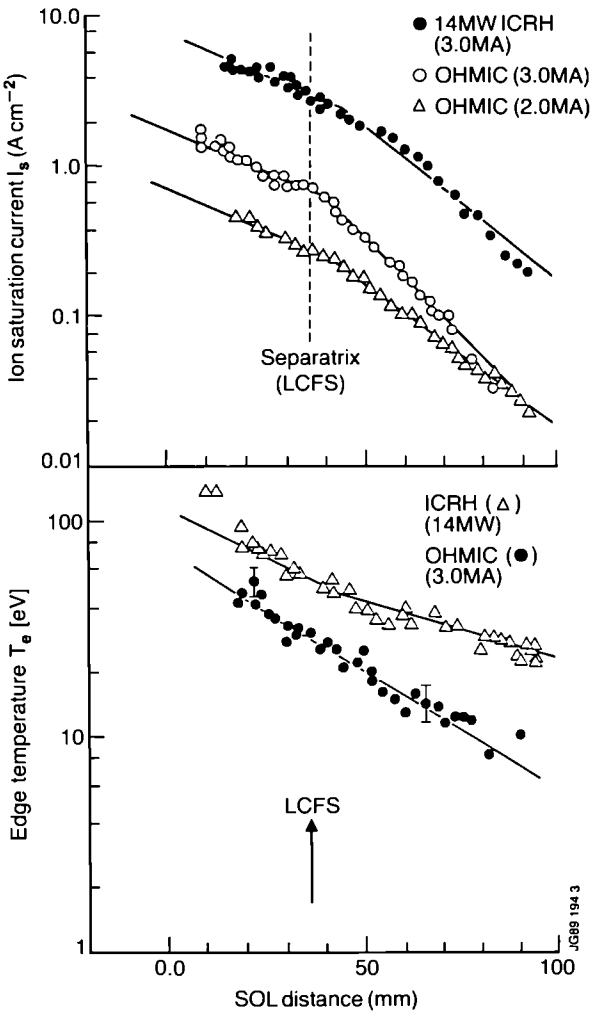

Fig.39: Radial profiles of the ion saturation current and edge electron temperature for ohmic discharges (2 and 3 MA) and ICRF heated discharges (14 MW) obtained with the reciprocating Langmuir probe. The change in gradient in the curves indicates the position of the LCFS. The SOL distance is determined from the magnetics diagnostic. At the location of the probe, the latter is subject to a systematic uncertainty of a few centimetres and so the fact that the LCFS does not occur at SOL distance equal to zero is not thought to be significant.

surfaces upon venting the torus to air on a number of occasions, and similar measurements have also been made on TEXTOR (at KFK Jülich, FRG).

The Fast Transfer System (KY2) designed to transport probes to the plasma, expose them with time resolution, retract them to the exchange station and then exchange them to the analysis system (KY1), has shown an increased reliability and flexibility. For the first time, observations on oxygen deposition have been reliably obtained, requiring cleaning of the surface before exposure by means of an Argon sputtering gun, checking by means of Auger Electron Spectroscopy (AES), followed by transport, exposure etc, with final analysis by means of AES and ion beam analysis using the reaction $^{16}O(d,p)^{17}O$.

When beryllium is used inside the torus, the surface analysis station will be required to handle Be-covered components: therefore, modifications are in progress to provide safe handling facilities for Be-covered probes. The surface analysis station can readily detect thin Be layers using AES, XPS or ion beam techniques. Increased shielding for the beam line is being provided so that the latter techniques can be operated in a more sensitive mode (using a D^+-ion beam).

Limiter Observations

Observations of limiter surfaces and the X-point target have been more important in 1988 than previously because JET has operated at higher power loads. Information from the camera systems has been used extensively to optimise the various modes of operation. This work was seriously hampered by the very limited view available on the X-point. However, it has been possible by using D_α filters to confirm the measurements of the Langmuir probes, identify the position of the outer separatrix, and to estimate the heat deposition during L and H-modes. One camera equipped with a filter carousel was aimed at the lower belt limiter and has observed the increased fluxes of carbon due to local heating of the edges.

The infra-red array detectors have not been successfully employed on the machine because of problems arising from the remoteness of the sensor head relative to the driving electronics. Delays in the supply of the detector heads has meant that only one (of 3) detectors has been obtained.

Electron Cyclotron Emission (ECE) System

The ECE system consists of an array of rapid scan Michelson interferometers and rapid scan Fabry Perot interferometers, a twelve channel grating polychromator, and an eight channel heterodyne radiometer. During 1988, the performance of the measurement system has been significantly enhanced and the quality of the ECE measurements improved.

A Real Time Processor for the Michelson interferometer was installed and commissioned early in the year. This instrument uses state-of-the-art signal processing hardware and software to analyse data from a Michelson interferometer during the plasma pulse. The full analysis of each scan, from raw data to temperature profile, takes ~10 ms, which is less than the 15 ms scan time of the interferometer. This makes it possible to analyse the data from every scan. Since its installation, it has routinely provided electron temperature profiles in real time. The line integral of the profile is transmitted to the control system for the JET high-speed pellet launcher where it is used as one of the safety interlocks. The profiles are also displayed in the Control Room (a typical example is shown in Fig.40) both in real time and as replays between plasma pulses.

The system incorporates a high-resolution Michelson interferometer (spatial resolution ~0.10 m for first harmonic measurements) and during the year this has been calibrated to an accuracy similar to that achieved with the other instruments, i.e. ~ ±10% in absolute level and

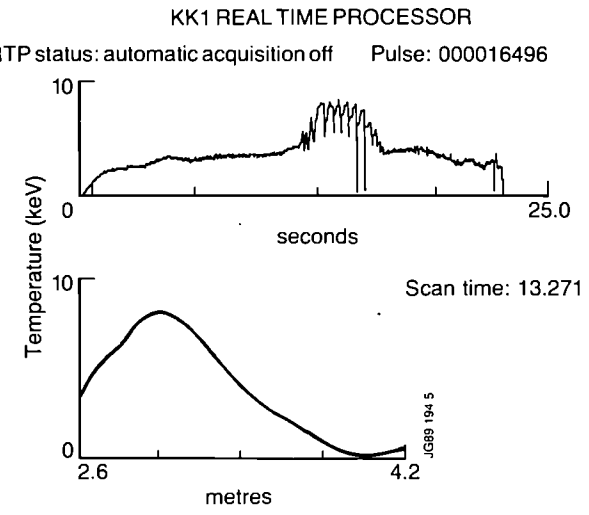

Fig.40: Diagram of the display provided by the Real Time Processor in the Control Room. The upper curve is the time history of the central electron temperature and the profiles are displayed on the lower left.

~ ±5% in relative profile shape. This has permitted its use for electron temperature profile measurements in the first harmonic (ordinary mode) of the electron cyclotron frequency. Using the first harmonic permits the profile to be measured across the whole plasma cross-section rather than being restricted to only the outer half, which is a limitation on the usual second harmonic measurements due to harmonic overlap. An example of a temperature profile obtained from the first harmonic is shown in Fig.41. Detailed comparisons with the standard (second harmonic, extraordinary mode) instrument are in progress. These will show under what conditions it is possible to exploit the wider spatial coverage of the

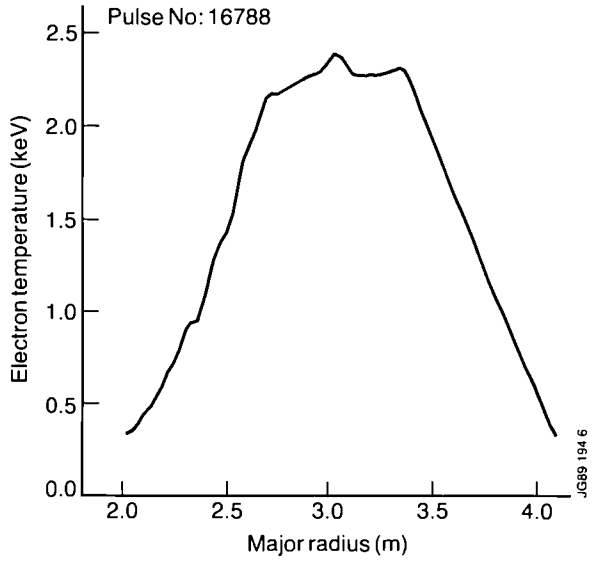

Fig.41: An example of an electron temperature profile measured by the high resolution Michelson interferometer using the first harmonic, ordinary mode. The structure on the profile is within the relative uncertainty of the system calibration (±5%) and so is not thought to be significant.

first harmonic measurements, including the upper density limit set by refraction and cut-off effects.

Considerable progress has been made with an upgrade of the heterodyne radiometer. The upgraded system will have 44 frequency channels, covering the frequency range from 73 to ~120 GHz, and will give a much wider coverage of the temperature profile with the same level of detail as the original system. Part of the upgraded system, which measures at higher radiation frequencies, has already been used. It has proved valuable for edge temperature measurements in X-point plasmas, in particular, for the investigation of the L-mode to H-mode transition. An example of an edge temperature profile constructed from five of the eight observation channels is shown in Fig.42.

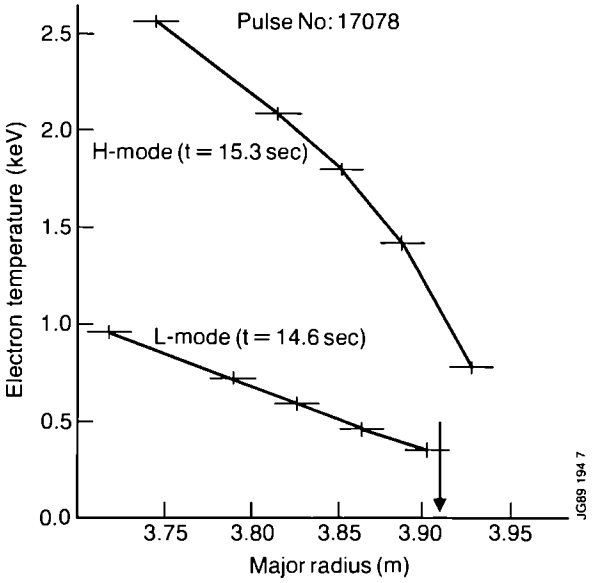

Fig.42: Edge electron temperature profiles measured by the heterodyne radiometer on a plasma exhibiting an L-mode to H-mode transition. The horizontal bars indicate the calculated spatial resolution. The arrow shows the position of the magnetic separatrix calculated from magnetic measurements.

Developments in several different areas have led to improvements to the quality of the ECE temperature measurements. More accurate calculations of the plasma internal magnetic fields (by the magnetic equilibrium code IDENTC) are now routinely available and used in the calculation of the frequency-to-space transformation for ECE data. This has resulted in a more accurate determination of the shape and location of the temperature profile. Under most plasma conditions, the error in spatial location of the profile is now believed to be no more than 0.05 m. Refinements in the calibration of the ECE measurements are continuing. A technique has been developed which reduces the uncertainty on the relative calibration between the heterodyne radiometer channels to ~1%. This technique uses the plasma pulses with ramped toroidal field, which are already used for improving the relative uncertainty of the Michelson interferometer calibration. The stability of the absolute

level of the Michelson interferometer calibration has been monitored by further in-vessel calibration measurements. These show that over a period of at least three years the spectral response of the whole measurement system has been stable to within ~5%. Independent verification of the absolute calibration has been made by a systematic comparison of plasma electron temperatures obtained from the ECE and the LIDAR Thomson scattering diagnostic. Fig.43 shows a comparison of the electron temperatures measured by the two systems for a large number of plasma pulses. This shows agreement to within ~10% which is the estimated systematic error on the absolute level of the ECE calibration.

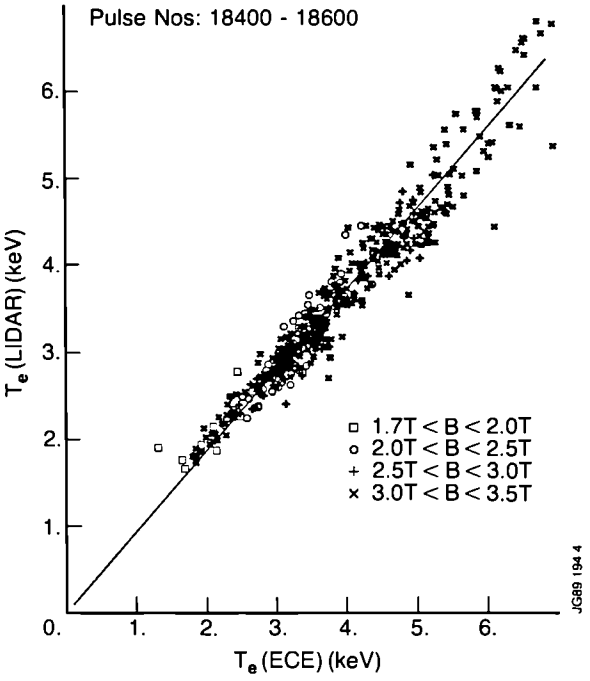

Fig.43: Electron temperature, averaged over the central 0.6m of the plasma, for a large number (~500) of pulses at various magnetic fields. The best fit line has a slope $T_{LIDAR}/T_{ECE} \approx 0.9$.

Microwave Transmission Interferometry and Reflectrometry

The microwave transmission interferometer has continued routine use for measurements of the line-of-sight electron density and for plasma control purposes. It has operated with high reliability and minor modifications of the system have significantly reduced running costs (by substantially increasing the time between klystron refurbishments).

Installation of the multichannel reflectometer was completed and substantial progress made with commissioning. This instrument probes the plasma along a major radius with radiation in the ordinary mode (E ∥ B) at twelve frequencies in the range 18–80GHz and so probes electron density layers in the range $0.4-8.0\times10^{19}m^{-3}$. It has two modes of operation: narrow band swept, for measuring the electron density profile; and fixed frequency, for measuring the radial propagation of density perturbations. During 1988, all channels, except the two operating at the highest frequencies, were brought into operation in the fixed frequency mode and some significant plasma data were obtained.

The reflectometer was used to study the sawtooth instability which has been previously extensively studied using measurements of the electron temperature and soft X-ray emission. Following the sawtooth collapse, both heat and density pulses propagate from the plasma centre towards the plasma edge. Investigation of the sawtooth instability with the multichannel reflectometer clearly showed the existence of a second density pulse propagating inwards (Fig.44). The measurements show that the speed of the heat pulse is several times greater than that of the density pulse and the results suggest that the interaction of the heat pulse with the limiter releases a burst of particles which act as a source for the inward propagating density pulse. It is also observed that the time for the pulse to propagate to the plasma edge is comparable with the period of the sawtooth oscillation.

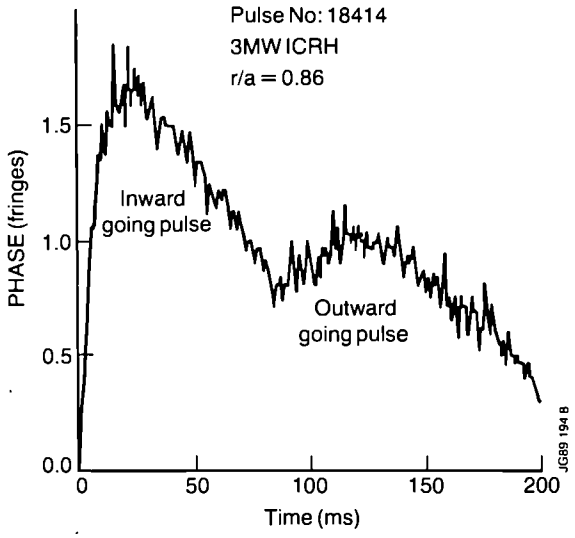

Fig.44: Response of the reflectometer channel probing the layer at r/a=0.86 following a sawtooth collapse. The inward and outward going density pulses are clearly seen.

Thus a realistic model of density pulse propagation must include both inward and outward going pulses, and must model a sufficient number of sawtooth oscillations to ensure that a steady state is obtained. By comparing the experimental data with the predictions of a comprehensive simulation code it has been possible to deduce a reliable value for the electron particle diffusion coefficient in the outer region of the plasma. The data for such a comparison are shown in Fig.45.

While the operation of the system in the fixed frequency mode is straightforward, the swept frequency operation is more complex and liable to disturbance by spurious signals arising from stray reflections in the microwave system. Tests with a moveable mirror carried

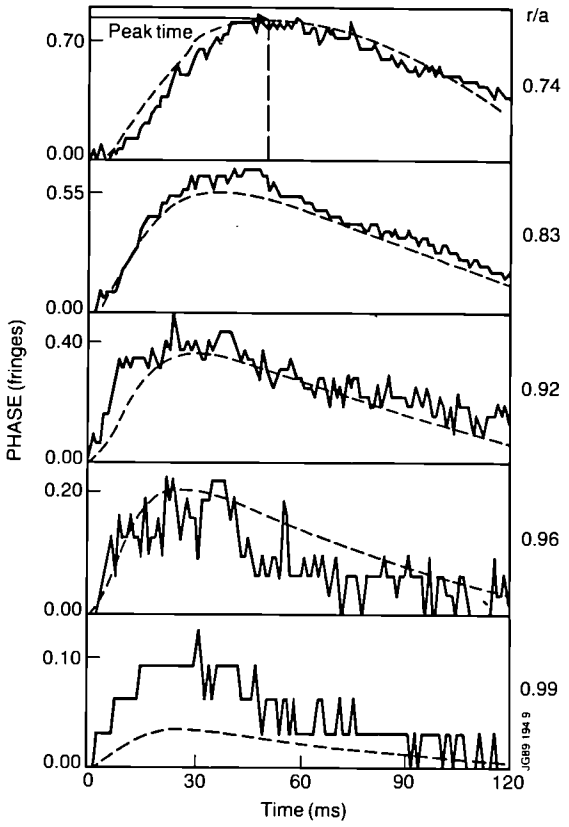

Fig.45: Comparison of model predictions (dotted curves) with measurements (solid curves) for five different reflectometer channels. The best fit is obtained with the particle diffusion coefficient $D_p(r) = (0.16 \pm 0.02)(1 + 2r^2/a^2)\ m^2 s^{-1}$ for r/a in the range $0.58 < r/a < 1.0$.

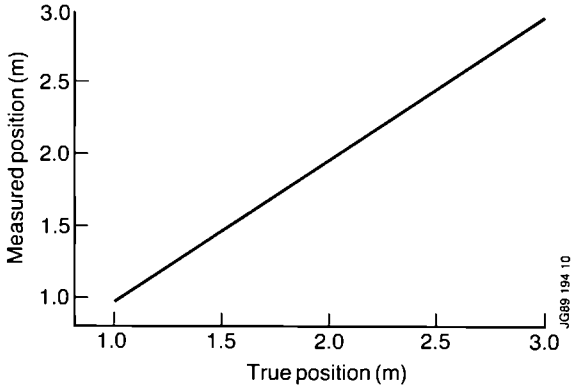

Fig.46: Laboratory test results obtained with one channel (39GHz) of the multichannel reflectometer system. In the tests, the location of a mirror is determined with the reflectometer operating in swept frequency mode and compared with its actual position.

out under laboratory conditions at the FOM Instituut voor Plasmafysica, Netherlands, have shown that the source, detectors and signal conditioning electronics are operating correctly and should be capable of determining the position of the different density layers to an accuracy of typically a centimetre (Fig.46). On the other hand, attempts to obtain the electron density profile on JET using the swept frequency techniques usually gave irregular and somewhat unrealistic profile shapes. Extensive investigations have been carried out and these have shown that the difficulties are due partly to spurious signals arising from reflections of the microwave signals in the throat of the diagnostic port, and partly due to fluctuations in the amplitude and phase of the reflected signals arising from fluctuations in the density.

Due to a possible interference with other diagnostics, the antenna in the vacuum vessel was not optimised and so the stray reflections were at a high level. A new optimised antenna will be installed in the 1988/89 shutdown and should substantially improve the performance of the system in the swept frequency mode.

The experiments on reflectometry in the extraordinary mode ($\underline{E} \perp \underline{B}$) have continued. Attention has concentrated on measurements of density fluctuations. A new technique, termed correlation reflectometry, has been developed. In this technique two (or more) independent reflectometers operating at fixed, but slightly different, frequencies probe the plasma along the same line-of-sight. The cross power (coherence) and cross phase spectra are deduced from the data and, under certain conditions, the dispersion curve and the correlation length of the waves characterising the density fluctuations are obtained. A preliminary correlation reflectometer has been constructed to test the feasibility of the technique and promising results have been obtained.

Thomson Scattering

The Single-Point Laser Thomson scattering system has been operated routinely during the year, and the data has been used in the assessment of the performance of the LIDAR system and in comparison with electron temperatures measured by ECE.

During 1988, the LIDAR system was brought into full operation and now routinely measures the spatial profile of the electron temperature and density every 2s throughout a JET discharge. The availability of the system has been ~90%, limited by some minor breakdowns of the ruby laser. In addition to the 0.5 Hz repetition rate, the system was operated occasionally close to 1 Hz in bursts of 4-5 pulses. With this mode of operation, the time evolution of the T_e and n_e profiles was investigated in more detail for some discharges with pellet injection, neutral beam and ICRF heating. Further, an event trigger (with a delay of 1 ms) has been installed on the laser which allows operation of the system if a time lapse of >1 s has occurred since the preceding, programmed laser pulse.

Steep gradients of the electron density (up to $7 \times 10^{20} m^{-4}$) occurring during H-modes, and structure on the electron temperature profile on some ICRF heated discharges (see Fig.47), were spatially resolved by applying a fast numerical deconvolution technique to the results. This increased the spatial resolution of the LIDAR system to considerably better than 10cm. Comparison with deconvolution of the same results with a

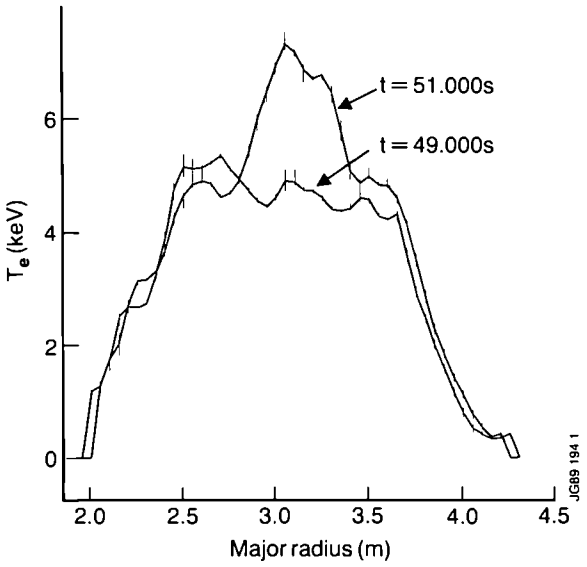

Fig.47: Clearly resolved structure in the LIDAR T_e profile, evidence of which also appears in soft X-ray and ECE profile data.

commercial maximum entropy method showed good agreement.

An investigation of the long term behaviour of the calibration indicates no significant changes either of the transmission of the collection optics and the spectrometer or of the sensitivity of the detection system. However, spectrally varying changes in the transmission of the torus windows, due to the build-up of an absorbing layer on the inside of the windows were observed, and gave rise to a temporary systematic error in the derived electron temperatures. A preliminary monitoring system using several spectral channels, which will eventually allow an automatic correction for the window transmission,operation and increased bandwidth was tested successfully.

The existing LIDAR system is presently being upgraded for 10Hz repetition rate. The new system will be based on an Alexandrite laser emitting at 760nm which is due for delivery in September 1989. During the 1988/89 shutdown of JET, the necessary modifications of the existing LIDAR system were started. The transient digitisers have been modified for 10Hz ($\approx$1 GHz) at the Risø National Laboratory, Denmark. A new data acquisition system is being set up to handle the large data rate. This will be done by installing a PC in each spectral channel which reads out the digitisers and performs some data reduction before passing the data to CODAS. Modifications of the spectrometer including the installation of a seventh spectral channel have been initiated and the Al-coated mirrors of the collection optics are being exchanged for broadband ($\approx$99%, 400nm-750nm) dielectric mirrors in order to increase the transmission of the optics. This allows operation of the Alexandrite laser at lower energy output (1-2 J) than the ruby laser while maintaining the SNR of the measurements.

Fast Ion and Alpha Particle Diagnostic

A thorough study was undertaken in 1987 of possible techniques to diagnose the energetic alpha-particle population that will be produced and confined in JET plasmas during the D-T phase of operation. This showed that a system based on collective Thomson scattering of a high power millimeter wave beam offered the best possibilities for JET. Before the D-T phase, the diagnostic would be used to diagnose the fast ion populations produced by ICRH which are important in experiments to simulate the effects of alpha particles.

During 1988, a detailed investigation of the proposed system and its possible application to JET was carried out. All relevant physical effects were examined: in particular, the basic theory of the scattering process, taking into account the dielectric effect of the plasma, was checked and some errors existing in the literature corrected; the effects of refraction on the paths of the launched and scattered beams and on the scattering parameters were calculated; possible spurious signals arising from absorption and re-emission through the electron cyclotron emission process were estimated; and the possible influence of density fluctuations was examined. On the technical side, an outline design of a suitable system was completed. The system would use a high power (~400kW, CW) 140GHz gyrotron, a combined quasi-optical and in-waveguide transmission system, and multichannel heterodyne detection. Possible suppliers for all the major system components have been identified. Substantial contributions in this work are being made by the Associated Laboratories: the Riso National Laboratory, Denmark is carrying out a detailed investigation of the effects of density fluctuations on the propagating microwave beams; ENEA, Frascati, Italy is investigating the possibility of diagnosing the bulk ion population using the same equipment; the ECRH group at the University of Stuttgart, FRG, carried out the scientific design of the high power transmission system; the FOM Instituut voor Plasmafysica has developed a ray tracing program; and the UKAEA Culham Laboratory is contributing to the design of the control system and power supplies for the diagnostic.

The work has shown that it should be possible to measure the spatial and velocity distributions of the confined alpha-particle populations with a spatial resolution ~10cm, a time resolution ~200ms with a signal:noise ratio of typically 20:1 assuming a total α-particle heating power ~5MW. In the fast ion measurements and in the alpha-particle simulation experiments much higher scattered signal levels are expected and the signal:noise ratio could be as high as 100:1. The scientific and technical design work is now nearing completion and it is expected that construction of the system will commence in 1989.

Neutron Flux Measurements

To understand tokamak plasma performance under conditions of high power additional heating, it is necessary

to demonstrate that numerical modelling can correctly predict the total neutron production. It is implicit that the neutron production is being measured accurately. At JET, the primary source of time-resolved neutron production data is the Fission Chamber system with its absolute calibration derived by means of the time-integrated Neutron Activation technique. The activation technique, in turn, depends on the application of neutron transport codes to relate the measurement of a neutron fluence in a foil of a chosen material placed just outside the vacuum vessel to the total number of D-D reaction neutrons emitted from the plasma. These neutron transport calculations have to be repeated whenever significant changes are made to the internal features of the vacuum vessel (protection tiles, belt limiters, etc). The measurement of foil activation is normally performed by studying selected γ-emission; the available nuclear reactions for 2.5 MeV neutron studies all have long half-lives which makes them inconvenient for routine use. The Delayed-Neutron Counters which have recently been commissioned permit this problem to be overcome. The delayed-neutron counting method uses fissionable materials (^{232}Th, ^{235}U, ^{238}U); the maximum useful counting period is two minutes and the same foils can be used in successive plasma discharges, so that automated operation is readily achieved. The Delayed-Neutron Counters have been carefully calibrated in relation to standard fast neutron energy spectra. The results obtained for JET discharges during the 1988, expressed as a calibration of the Fission Chamber system, are in very good agreement with previous best estimates. These new counters will permit more thorough calibrations of the Fission Chamber System, in future.

Neutron Emission Profiles

The Neutron Profile Monitor has been in routine operation throughout 1988. It is a 19 channel instrument, each channel being equipped with a neutron spectrometer (energy resolution, $\Delta E/E = 8\%$) which selects neutrons in the energy range 2 to 3 MeV and discriminates against background gamma-radiation. Each spectrometer can operate at selected event-rates up to at least 100 kHz.

Several concerns have to be addressed with this instrument, including the ambient temperature (30°C), the local magnetic field (time-varying up to 0.1 T) and the rapid variations in count-rate. Accordingly, much effort has been devoted to checking the correct operation of this diagnostic and to obtaining absolute efficiency calibrations for each channel. For ohmic discharges, the neutron yields obtained from the profile monitor agree well with those given by the Fission Chambers. For additionally heated discharges, the Profile Monitor efficiency apparently increases: the full explanation for this effect is not known but the increase is at least partly due to the sensitivity of the spectrometer efficiency to neutron energy and to the non-isotropy of the neutron emission from D-D reactions. Examination of the neutron profiles for ohmic discharges has shown that the ion temperature profile is very similar to the electron temperature profile as given by the Lidar diagnostic (Fig.48). Neutral beam-heated discharges are less easy to characterize because the contours of constant neutron emission strength for such discharges are not magnetic flux contours, due to beam particle trapping effects. Despite the interpretational difficulties mentioned above, the plasma regions responsible for the bulk of the neutron emission are very well defined for all discharge types.

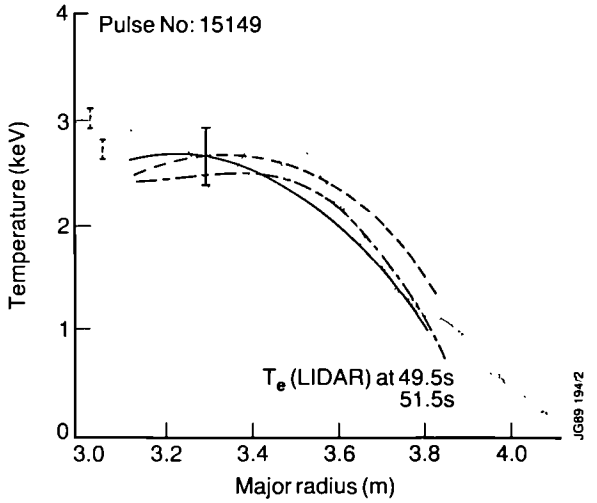

Fig.48: Showing ion and electron temperature profiles for a typical 5 MA discharge. The electron temperature profiles are from ECE (thin, dotted line) and Lidar (thin, dashed lines) diagnostics. The ion temperature profiles (heavy lines) and derived from the Neutron Profile Monitor using three different analytical procedures. The error bar shows the typical absolute accuracy.

Neutron Spectrometers

A time-of-flight neutron spectrometer and several ^{3}He ionization chamber spectrometers are used for high resolution ($\Delta E/E \sim 4\%$) neutron energy spectrum measurements and a NE213 liquid scintillator spectrometer is used for broad band studies. Now equipped with adjustable aperture collimators for intensity control, these spectrometers constitute a system which can cater for most circumstances. In particular, the time-of-flight spectrometer offers a time resolution of 1 s for high intensity discharges, compared with 4s for the ^{3}He spectrometers.

The early ohmic and ICRF-heated discharges in deuterium were studied with the ^{3}He spectrometer and the deuterium dilution (n_d/n_e) was shown to be typically 0.4. This work has now been extended to beam-heated discharges, although at the present time it has proven necessary to make some simplifying assumptions in the form of analysis used.

High-power combined (ICRF and Neutral Beam) heated plasmas have been carefully examined for evidence of the synergetic effect whereby beam ions are heated by the second harmonic of the waves when tuned to hydrogen. It is clear that no strong high-energy deute-

ron tail is formed and that the extra neutron emission attributable to synergy does not exceed 30%. In general, RF heating does generate very high energy tails of those ions to which it is tuned (fundamental or second harmonic) but the high-energy neutrons which an energetic deuteron tail would necessarily produce are sufficiently few in number as to render their observation difficult.

Tritium Burnup

The study of the confinement and slowing down of the 1.0MeV tritons emitted from D-D reactions is of considerable importance because these tritons are expected to behave in the same way as the α-particles emitted from D-T reactions in respect of their single particle (as opposed to collective) properties. The major difference is that the tritons undergo T-D fusion reactions and emit 14MeV neutrons as they slow down and so can be investigated through their related neutron emission. The triton burn-up measurements are being continued as the additional heating powers applied to JET plasmas are increased. The present status of these measurements is that both the absolute yield of 14MeV neutrons and the time-dependence of the emission can be simulated within experimental errors by numerical modelling, provided the electron temperatures provided by the Lidar diagnostic are employed. When the ECE temperatures are used, agreement falls just outside the experimental errors and the possibility of non-classical losses or anomalously fast slowing down cannot be discounted. The existence of such effects has been noted, but only for the brief period of time following a major internal relaxation.

Charged Fusion Products

The prototype detector mounted inside the vacuum vessel to study the emission of 14.6MeV protons from $^3He + D \rightarrow p + \alpha$ reactions was replaced with an improved system provided with adjustable collimation for intensity control. With this new detector, it was possible to confirm the main feature observed with the prototype, ie. the sudden and strong increase of detected protons at the moment of a sawtooth crash, and to obtain reliable proton energy spectra, which show the proton emission to be due to expelled ^3He ions undergoing reactions in the field of view of the detector and not confined protons being expelled and then scattering into the field of view. Some confusing observations made with the prototype were further investigated and were found to be of instrumental origin, owing to the earlier lack of intensity control. Work on this particular diagnostic has now been redirected towards construction of a simple radiation-resistant device for the detection of α-particles in the active phase of JET operations.

Gamma-Ray Studies

This work was motivated by the desire to monitor the 16.5MeV γ-emission from ^3He-D fusion reactions, as this is the only means of measuring the fusion reaction rates between ICRF-heated ^3He ions and the bulk deuterium in high plasma current discharges. An initial investigation has been completed, with fusion powers of about 60kW being generated (Fig.49) but with evidence of a saturation of the thermonuclear Q at high heating powers.

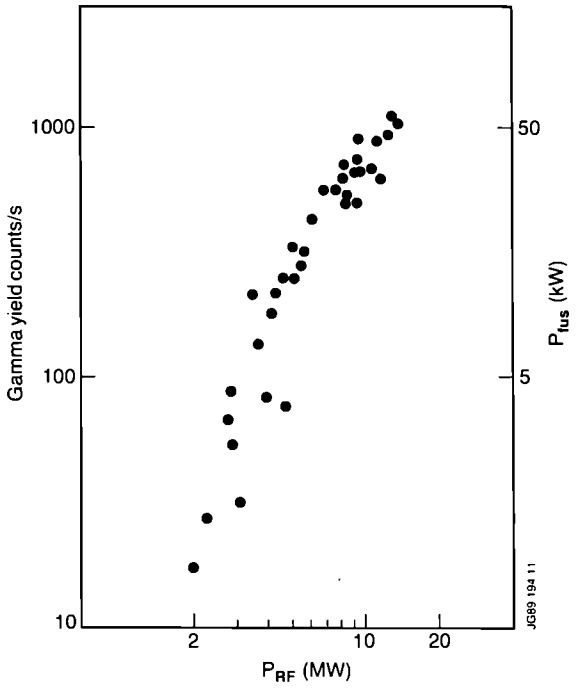

Fig.49: Variation of count-rate of 16.5MeV gamma rays (l.h.s) and related fusion power (r.h.s) from D(^3He,p)^4He reactions with applied rf power tuned to minority ^3He ions.

Gamma-ray emission has also been detected from interactions between the heated ions and the major plasma impurities, notably carbon. Acceleration of ions into the MeV energy region has been observed (protons to 10MeV). When two or more γ-lines originating from different energy threshold reactions are seen, then an effective temperature can be assigned to the high-energy ion tail. Provided the impurity species ion density is known, the ion density for the tail can be estimated. Gamma-ray emission offers a sensitive means of detecting the presence of high-energy particle distributions.

Single-shot Pellet Injector

After extensive modification [1], the injector has been used to produce pellets of pure deuterium or hydrogen, or of known mixtures of the two gases. The pellet composition has been doped with up to 1% neon impurity; a higher concentration of neon has not been feasible because the neon condenses out at higher temperatures than H/D leading to non-uniform ice (and hence unknown pellet composition) or malfunction of the cryostat due to blockage. Using such doped deuterium pellets, a neon impurity concentration of 0.1% in the JET plasma has been detected spectroscopically.

Single pellet injection events have been analysed to determine simultaneously the electron thermal and particle diffusivities, and also the ion thermal diffusivity, by measuring the inward propagation of temperature and density perturbations caused by a shallow penetrating pellet. The quality of data and analysis which has been carried out shows that this will develop into a powerful technique for study of local transport behaviour and for study of interference and correlations between simultaneously occurring processes in the plasma. The ability to deposit locally known quantities of impurity will enable extension of the above analysis to deduce simultaneously the impurity transport characteristics in JET.

The feasibility of determining the magnetic field topology by spatially resolved imaging of the ablation cloud of a neon doped pellet is being investigated. Further measurements to elucidate the 'snake' phenomenon[2] are in progress, including making a 'snake' with a neon doped pellet, rendering it spectroscopically bright.

Neutral Particle Analysis (NPA)

Increased application of high NB and ICRF heating power has entailed analysis of increasingly non-Maxwellian distributions of the observed neutral particle outflux. During heating of deuterium plasmas with deuterium beams, neutral analysis of the hydrogen minority has been employed to deduce the ion temperature profiles for use in interpretation of ion thermal transport. Simultaneously, the non-Maxwellian deuterium spectra have been measured, with emphasis on the high energy part of the distribution, for interpretation in terms of a Fokker-Planck description of slowing down of the injected beam ions.

Similarly, in minority ICRF heating experiments, the measurement emphasis is on determination of the temperature of the majority ions and, simultaneously, to study the heating mechanism by measurement and interpretation of the minority ion distribution to high energies. For these priority measurement objectives to be successfully executed in the neutron intensive environment of the future, the present apparatus will be replaced with one that is more immune to neutron induced noise, and capable of simultaneous measurement of H, D, and T particles to higher energies. Such an enhanced NPA system, capable of measurement up to 250 keV, has been prepared [1] for installation in 1989.

Interferometry and Polarimetry

The compensating interferometer at 0.119 mm, installed on the two lateral channels in 1987, has added to the measurement capability of the multichord far-infrared interferometer system. Up to 1 cm radial movements of the mirrors mounted on the JET vacuum vessel have been observed, and compensated to within 0.02mm allowing accurate chord-integrated measurements of the electron density on the main 0.195 mm interferometer. The capability to make othogonal chord-integrated measurements has allowed testing of an assumption routinely made in Abel inversion of density data, that the density is constant on flux surfaces. Measurements confirm that the assumption is well founded, and that deviations from constancy of greater than 3%, in a chord- integrated sense, may be excluded. A system for automatic feedback tuning of the 0.119mm alcohol vapour laser was developed at JET in the course of the above enhancement, and subsequently sold to the manufacturers of the laser.

Polarimetric measurements of Faraday rotation, and determinations of current density profiles in different regimes of JET operation, have been pursued vigorously during this period. These indicate that the value of the safety factor on the magnetic axis, $q(0)$, is always considerably less than unity in a sawtoothing discharge, not even the collapse of a monster sawtooth elevates $q(0)$ to unity. These radical observations merit further careful confirmation. Enhancements of the polarimeter are in preparation, increasing the number of chords from six to eight, measurement along orthogonal chords, and more accurate measurements of the Faraday rotation angle. These improvements will permit more accurate deduction of the magnetic geometry (in particular, the elongation of the flux surfaces near the magnetic axis) giving a more firm assessment of the behaviour of $q(0)$. The enhanced capability to measure the currentj density profile, $j(r)$, is indispensable for the proper evaluation of the benefits of Lower Hybrid Current Drive experiments which are due to commence soon.

Soft X-ray Diode Arrays

The diode array system consists of 100 soft X-ray detectors arranged in a vertical and horizontal camera in a single poloidal plane with additional detectors installed in five arrays distributed toroidally around the machine, nearly on the median plane. The detectors in the cameras have various different arrangements of absorption filters. A radiation shield has been installed to reduce the effects of neutrons on the detectors. The diagnostic is used to investigate MHD properties of the JET plasma and also to measure radiation profiles with coarse energy resolution. An extensive set of computer programmes has been developed both to display the large quantities of data produced and to carry out tomographic analysis of the camera data. Development has started on a real-time tomography system which will produce 3-D X-ray reconstructions during the plasma pulse.

Since the cameras are installed in the same poloidal plane as the pellet injectors, they provide valuable information on the pellet-plasma interactions and make accurate measurements of the pellet's velocity. The pellet-plasma interaction zone has a region of greatly increased local X-ray emission, as can be clearly seen in Fig.50. The absolute intensity of the X-ray emission has been shown to be in good agreement with a standard model of pellet ablation.

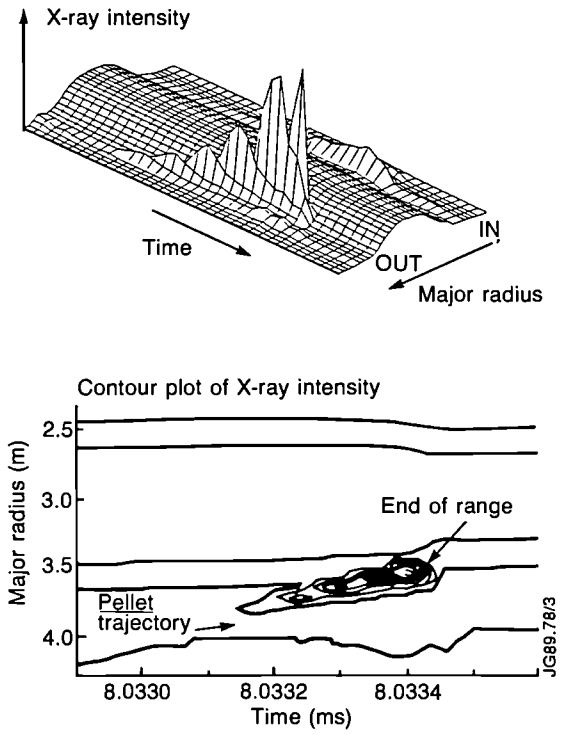

Fig.50 Contour and 3-D plots of the pellet ablation, as seen by the vertical camera. X-ray intensity is plotted versus time and major radius. The peak at the inner edge is an H_α ghost and should be ignored.

Other more complex phenomena have also been observed in pellet ablation experiments. Further observations on the snake, which is a small region of plasma on the $q=1$ surface with greatly enhanced density, have confirmed our earlier observations on its $m=n=1$ topology and its ability to survive the sawtooth crashes. Detailed analysis has also shown that the impurity concentration within the snake is similar to that of the background plasma.

One of the striking observations of the pellet ablation process is the pronounced drop in X-ray emission which occurs as the pellet crosses the $q=1$ magnetic surface. This is thought to occur because of the reduced number of plasma electrons which are available to interact with the pellet on a rational q surface. More detailed analysis has shown that the shear on the $q=1$ surface is also important and the variation in emission has been used to determine a local value of the shear at $q=1$. This value was found to be very low implying either a central q-value close to unity or a local flattening of the q-profile at $q=1$.

Continuing studies of the sawtooth instability have concentrated on analysis of monster sawteeth, partial sawteeth and the sawtooth instability growth rate. The monster sawtooth crash has a similar structure to normal sawteeth, but the inversion radius is considerably larger. The measurements also show that the collapse has a dominant $n=1$ component. Partial sawteeth have been shown to involve processes which lead to a flattening of the profiles around $q=1$ but with an essentially unaltered centre. The instability growth rate has been studied by determining the centroid of the soft X-ray emission calculated from the profiles reconstructed from the camera data. The time behaviour of the centroid is in good agreement with the behaviour of the perturbed magnetic field at the plasma edge and corresponds to the growth rate of an ideal MHD mode. No satisfactory explanation of the sudden onset of the instability has yet been found.

The cameras have also been used to investigate impurity diffusion, following the injection of metallic impurities into JET with the laser ablation blow-off technique.

Soft X-ray Pulse Height Analysis (PHA)

The three detector pulse height analysis (PHA) system has continued to work well and has provided impurity concentrations and electron temperatures. In future, it is intended to use this system with different detectors to measure the X-ray emission from the high energy tail produced on the plasma electron distribution by the lower hybrid heating system.

Further work has been carried out with a radiation code which fits the PHA spectrum and also calculates the expected radial X-ray power emission for the X-ray diode arrays for the same impurity concentrations. This work has had particular success in explaining the very peaked X-ray profiles observed after pellet injection (Fig.51) into JET and also hollow profiles observed during H-mode operation.

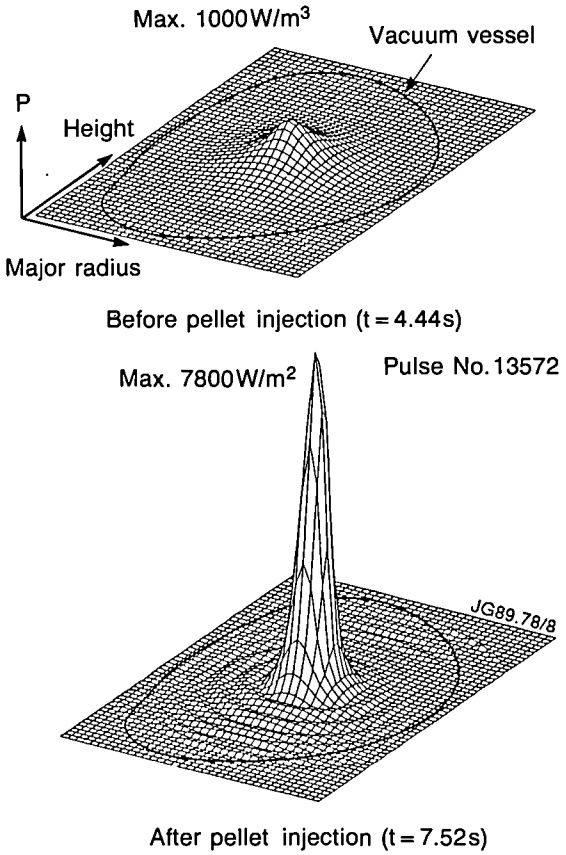

Fig.51 Isometric plots of the soft X-ray emissivity in the poloidal plane before and after the injection of a deuterium pellet.

Laser Injected Trace Elements

This new diagnostic started operation in June 1988. It utilises the ruby laser pulse available from the Single Point Thomson Scattering System. A flipped-in mirror optically transfers the selected pulsed beam to an evacuated chamber on a lower vertical port. Then, it is focussed onto the upper surface of a glass slide, coated with a 5 μm thick metal layer. At any time, there are twelve slides on a movable target-holder. Materials used include: Mg, Al, Ti, Fe, Co, Ni, Cu, Zr and Mo. One slide is sufficient for 30-40 shots. Typically $2\text{-}3\times10^{18}$ atoms are evaporated. The ejected atoms are propelled towards the plasma where they undergo successive ionisation and excitation; a certain percentage arrive at the centre, within a few milli-seconds. They decay there in a time characteristic for the impurity containment of the particular discharge. Such controlled impurity release is not detrimental to the plasma and can be used for various diagnostic purposes. Several diagnostic systems like VUV and X-ray spectroscopy, X-ray diode array and pulse height analysis and bolometry are used to collect and analyse the data.

Fig.52 illustrates the time development of injected Co and intrinsic Ni and O during an H-mode (Pulse No: 18627). The constancy of the cobalt emission during the H-mode demonstrates the ability of this plasma phase to accumulate impurities. The behaviour of the intrinsic impurities indicates a continuous source which is 'integrated' by the plasma. During the next operational period, it is planned to start systematic transport studies of various JET scenarios.

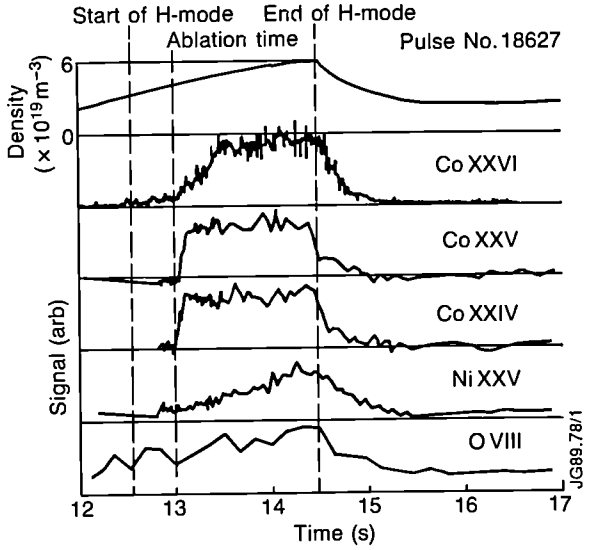

Fig.52 The time development of the line average electron density and the emission from cobalt, nickel and oxygen lines following the injection of some cobalt by the laser blow-off system. The injection takes place during an H-mode.

Wide Band X-ray Spectroscopy

The active phase double crystal X-ray monochromator, built by EURATOM-IPP Association, Garching, FRG,

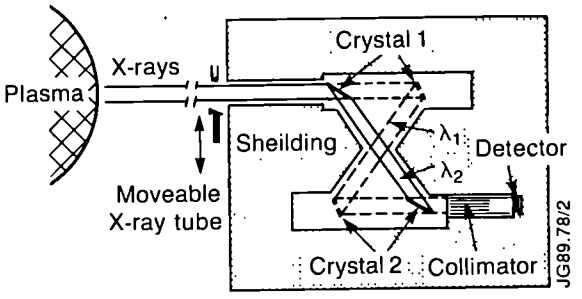

Fig.53 Schematic of the double crystal monochromator.

was fully commissioned during mid-1988. The detector is protected from high fluxes of neutrons and γ-rays by placing the instrument outside the JET biological shield, and by using two crystals in the parallel (non-dispersive) mode. This arrangement allows a labyrinth radiation shield to be built around the optical path (Fig.53). Impurity line radiation in the band 0.1 - 2.3 nm is monitored, with absolute calibration, for wavelength and intensity, and with spectral resolving power ($\lambda/\Delta\lambda$) of between 500 and 5000 depending on choice of collimator. This performance allows intensity, line profile and line shift measurements of a wide range of impurities ($Z \geq 7$, N) and ionisation stages (K-shell for light impurities such as Oxygen; K and L-shell for medium-Z impurities such as Nickel). Observable ionisation stages range in radial position from $r=0$ to about $r=1.1$ m. The instrument can operate in a spectral scan mode as shown in Fig.54 or in monochromatic mode illustrated by the Co XXVI time evolution in Fig.52. Intrinsic impurities, O, Cl, Cr, Fe, Co and Ni, have been observed for a wide range of JET operating conditions.

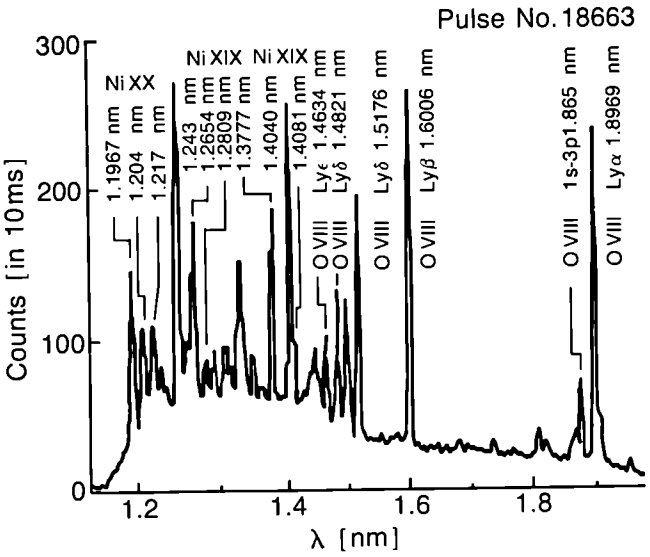

Fig.54 Broad-band spectrum from the double-crystal monochromator, showing Neon-like Ni lines, and H-like and He-like O lines in the range 1.13 to 1.95 nm.

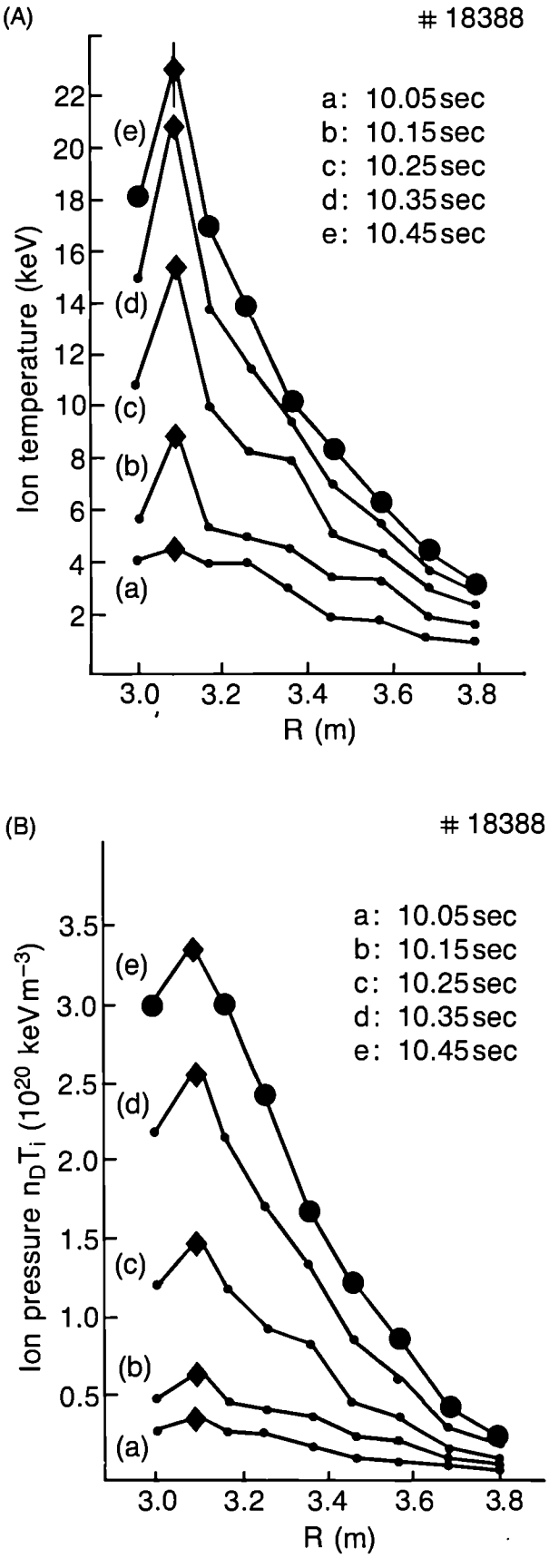

Fig.55 Evolution of (A) ion temperature and (B) ion pressure during a low-density high-temperature inner wall discharge ($I=3MA$, $P_{NB}=19MW$).

Charge Exchange Spectroscopy

During 1988, considerable progress was achieved in the performance of the JET charge exchange spectroscopy diagnostic. The measurement of the central ion temperature was implemented as a routine on-line diagnostic, which was available for the majority of neutral beam heated plasmas and, in addition, for dedicated experiments where a minimum of neutral beam power was provided for diagnostic purposes.

The most significant progress was achieved by commissioning a multichord viewing line system which enabled the temporally and radially resolved measurement of ion temperature and toroidal angular frequency profiles. Highly peaked ion temperature profiles (Fig.55A) were observed in the case of neutral beam heated low-density plasmas, with temperatures on-axis exceeding 20 keV. Densities of the dominant light impurities carbon and oxygen were derived from absolute measurements of charge exchange photon fluxes and used to reconstruct radial deuteron concentration profiles and hence the ion pressure $n_d T_i$ (Fig.55B). Minute details of the profile behaviour were recorded in a high sampling rate by the CX chords covering the outer plasma regime. During long neutral beam pulses in magnetic limiter configuration, the instantaneous changes into broad temperature profiles with pedestals typical for the transition into high confinement regimes (see Fig.56) were observed.

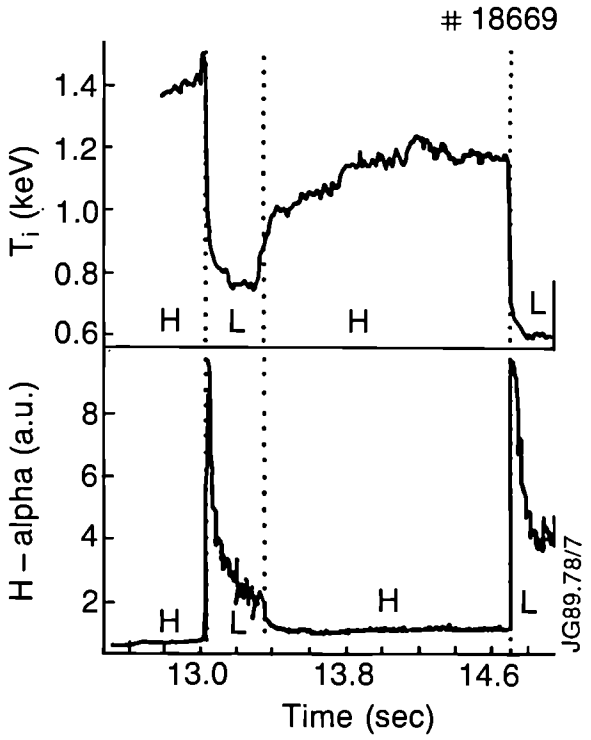

Fig.56 Ion temperature T_i, at $R=3.82m$ and the H_α signal from the plasma edge during a series of H- and L-modes.

In addition to the analysis of thermal low-Z impurities, the light emission of the bulk plasma deuterons may be used to derive deuteron density and deuteron temper-

ature. The very intense spectrum emitted at the Balmer Alpha wavelength (Fig.57) consists of two main features representing the bulk plasma and the Doppler shifted spectrum representing the fast injected deuterium atoms which experience a strong local electric field and Stark splitting. The high energy neutrals are excited by the impact with plasma ions and, therefore, proportional in intensity to the local effective ion charge Z_{eff}. The local value of Z_{eff} can be derived directly from the intensity ratio of beam and thermal spectrum. This novel diagnostic technique, which was discovered at JET in early 1988, should ultimately provide local magnetic fields as well as effective ion charge and will be fully commissioned in the forthcoming operation period.

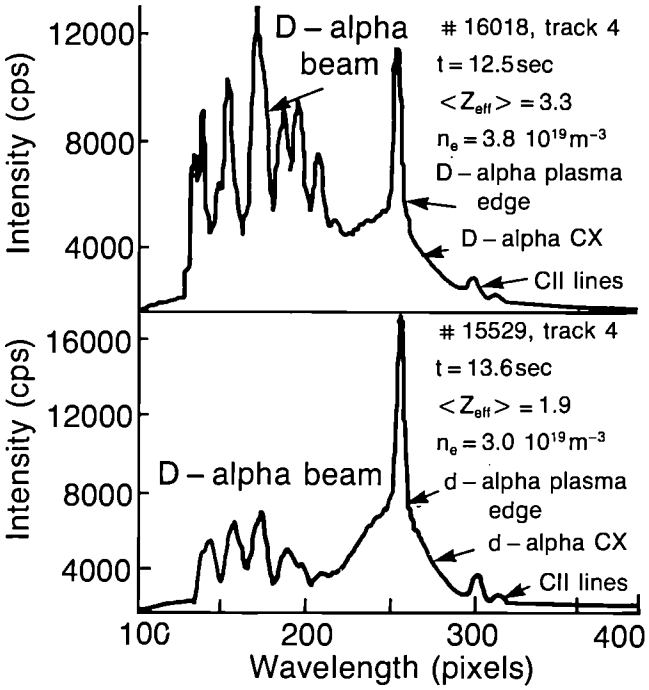

Fig.57 Balmer Alpha spectra of plasma edge, thermal deuterons and fast injected neutrals for two JET pulses with comparable densities but different effective ion charge Z_{eff}.

References

[1] JET Joint Undertaking, Progress Report 1987.
[2] A Weller et al., Physical Review Letters, 59(1987)2303.

Summary of Machine Operation

During 1988, JET operation (weeks 1 to 40) was essentially made up of four periods:

a) The first period (weeks 1 to 11) was intended to follow on from 1987 operation, but a leak in the Octant No 4 duct scraper shortly before the close of the 1987 operation required a vessel entry in week 1, to effect repairs. Throughout this first period, the neutral beam (NB) heating system suffered a number of problems so that only limited use of the Octant No 8 injector was made, and the Octant No 4 injector did not achieve synchronous operation.

Unfortunately, torus vacuum leaks and in-vessel water leaks required two further vessel entries in this period. In spite of these problems, improved operation was achieved leading to a high pulsing frequency and a high average daily time available for pulsing.

b) The second period (week 12 to 19) began with one week of maintenance and recommissioning. The major innovation in this period was the synchronous operation of the Octant No 4 NB injector. This allowed extended performance of the additional heating system (15MW ICRF and 10MW NB) and permitted the previous high values to be exceeded.

Other notable achievements were:

i) routine and successful use of pellet injection in the current rise phase to produce peaked density profiles;
ii) P1 central coil operation commissioned to 55kA (design 60kA);
iii) by means of chillers, the TF magnet long pulse performance was extended to 16s at 67kA coil current;
iv) relatively straightforward reconditioning of the vessel following disruptions by glow discharge cleaning, and/or pulsing in helium.

c) The third period (weeks 20 to 30) began with extended maintenance/commissioning activity to include the remedial work necessary in the vessel, as well as the installation of new protection tiles. Other activities were: the modification of the P1 cooling system, the modification of the vertical field control to allow different currents in the P4 coils upper and lower, and the continued upgrading of the ICRF generators (from 3 to 4MW).

There were several notable achievements:

i) regular operation of both NB injectors to a peak power 18MW,
ii) successful operation of the poloidal coils with the new P1 cooling and the P4 current imbalance,
iii) a 5MA single X-point plasma was achieved,
iv) record RF energy was transmitted (6MW for 20s),
v) regular use of IVIS at 250°C for in-vessel inspection,
vi) regular use of pellets to create peaked density profiles, and the successful heating of such plasmas.

d) The fourth period (weeks 31 to 40) followed directly from the third, with one week of in-vessel and NB remedial work. The main success of this period was the achievement of the simultaneous operation of all 16NB sources.

Large additional heating power (greater than 30MW)

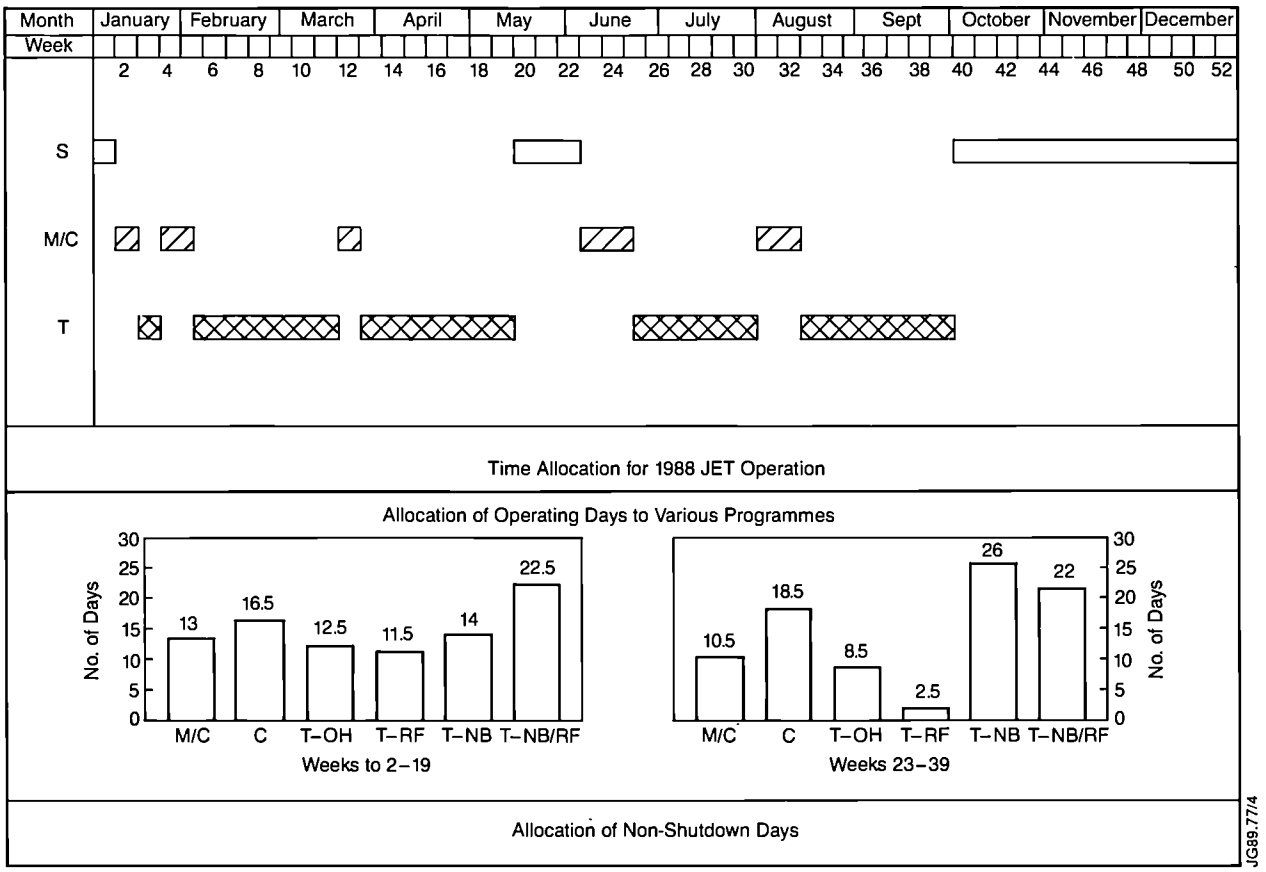

Fig 58: Allocation of time to different activities of the operating programme for 1988 (S=Shutdown; M/C=Machine Commissioning; T=Tokamak Operations).

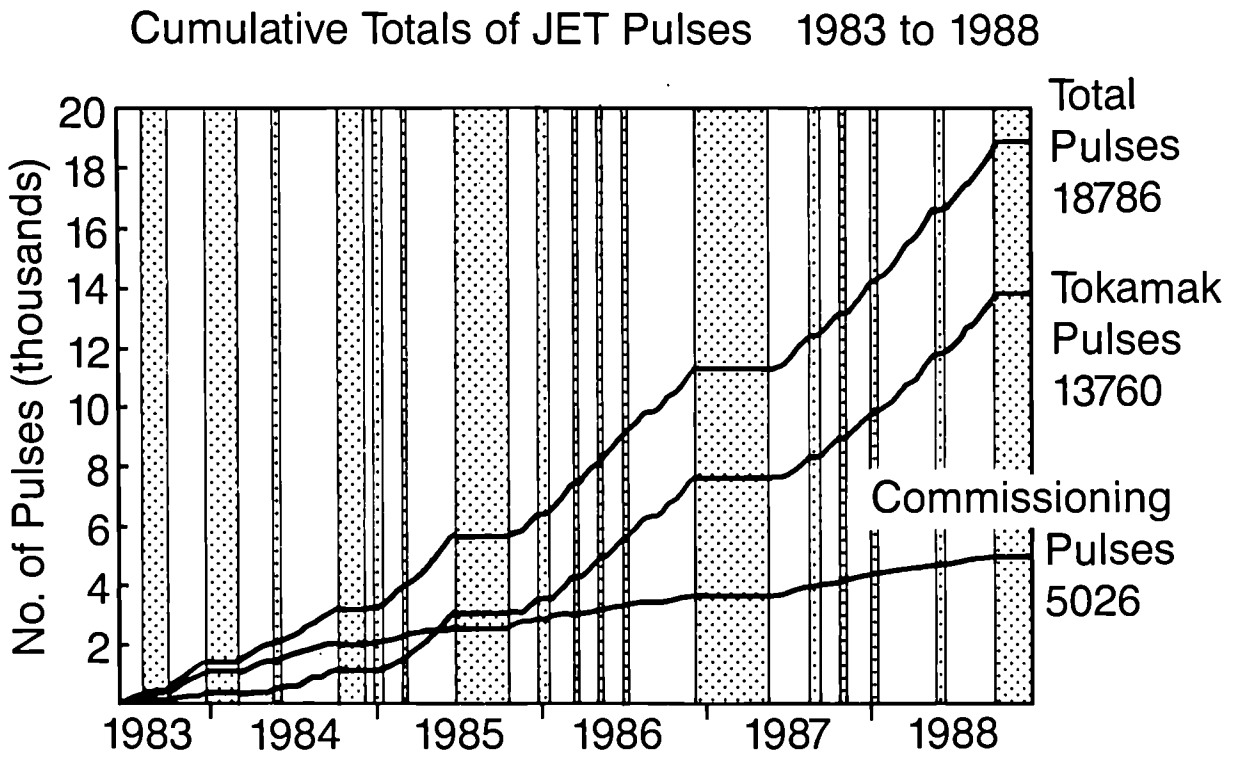

Fig 59: Cumulative total of JET pulses.

were applied regularly, producing plasmas with high energy content, and high ion temperatures (greater than 20keV) in inner wall plasma operation.

Other achievements were:

i) vertical stabilisation of high elongation ($\epsilon \sim 2$) plasmas;
ii) 7MA for 2s flat-top, and routine high current (5 and 6MA) discharges including 5MA single-null X-points, and 3.5MA double-null X-point,
iii) long duration H modes (up to 4s);
iv) commissioning of the digital radial position control system was started;
v) increased purity of plasmas with neutral beam injection and, in particular, with pellet injection.

The machine was operated for 154.5 days during the January-September period. About 77% of these days were devoted to experimental operation with a distribution among different heating programmes as follows:

17.6% Ohmic (OH) heating;
11.7% Radio-frequency (RF) heating only;
33.5% Neutral Beam (NB) heating only;
37.2% Combined (NB and RF) heating.

The allocation of time to the different activities and the number of days in the various tokamak operational programmes is shown in Fig.58.

The organisation of operation time remained essentially the same as for 1987 but the frequent overnight use of a special HV (standby) isolation reduced the time spend in the power supplies isolation and re-energisation activities, thus liberating more time for tokamak operation.

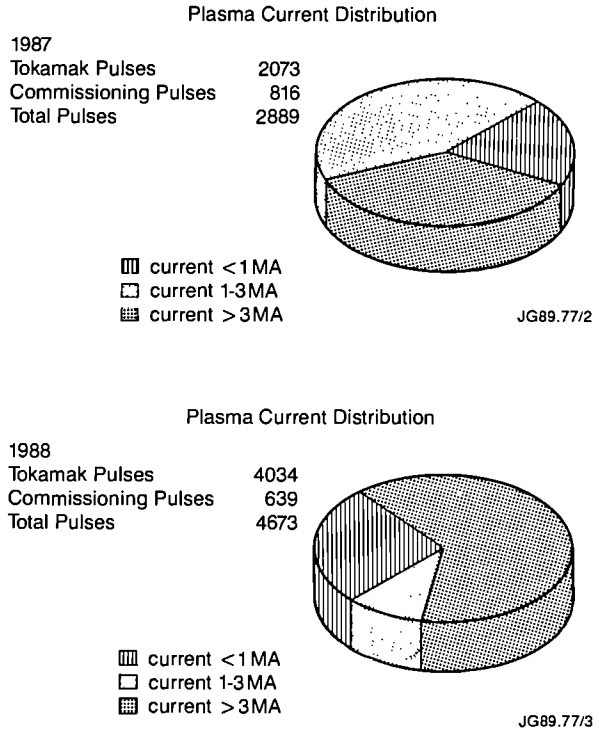

Fig 60: Relative plasma current distribution for 1987 and 1988.

The total number of pulses was 4673 in 1988 bringing the total number of pulses to 18786 (see Fig.59). The relative number of commissioning pulses continues to decrease. Even more significant is the cumulative number of discharges with plasma current exceeding 3MA, which for 1988 was 2398 bringing the cumulative total to nearly 4800 (see Fig.60).

Summary of Technical Achievements

There was no major shutdown during the early part of 1988 and therefore, the machine and associated systems were operated with basically the same configuration as that already achieved in 1987. Minor modifications were nevertheless implemented with the aim of increasing the level of performance in the X-point configuration. New wall protection tiles were installed inside the vacuum vessel in the vicinity of the X-point. These tiles were wider than the normal ones, specially shaped and carefully aligned to allow a total energy deposition in a single-null configuration up to 50MJ per pulse. More importantly, the power supplies to the vertical field coils were split into two units to allow, by means of a mid-point connection with the coils, imbalanced currents between the upper and lower vertical field coils. It had been found that such a current imbalance would produce a more favourable pattern of poloidal field crossing the toroidal field coils and therefore, reduce the lateral forces acting on the toroidal field coils. All these modifications allowed plasma currents up to 5MA to be obtained in the single null configuration: a value previously considered well beyond reach!

Another technical innovation which proved most effective in operation, was the systematic use of glow discharge cleaning with helium. This technique, pioneered in TEXTOR at KFA, Julich, F.R.G., appears to be highly effective in depleting the walls of deuterium and also removing impurities, such as oxygen. The technique was used extensively to recover from plasma disruptions, and also to enhance the pumping capability of the walls. The latter phenomenon allowed high ion temperatures to be reached in the so-called hot-ion mode.

The pellet injector supplied under a JET-US DOE Collaboration Agreement operated reliably and succeeded in producing discharges with highly peaked density profiles with central electron densities exceeeding $10^{20}m^{-3}$.

The neutral beam injection system which includes two boxes each with eight 80kV, 60A injectors encountered a number of technical problems throughout the year which limited their performance. However, towards the end of the operation period these problems were largely solved and the neutral beam power injected into the plasma reached 21.6MW, a value in excess of the design value of 20MW.

The most significant technical achievements of 1988 are summarised below:

With a material limiter:

- Plasma currents up to 7MA with 2s flat-top;
- Plasma currents up to 6MA with 6s flat-top;
- Plasma currents of 3MA for 24s flat-top duration;

With a magnetic limiter (X-point configuration):

- Plasma currents up to 5MA

Plasma heating systems:

- Total power delivered to the plasma in excess of 34MW;
- Quasi-steady state conditions achieved at 3MA with 6MW of RF heating power for 20s duration.

From October onwards, the machine was shutdown. The two main tasks during the shutdown were to reinforce the vacuum vessel and to inspect and, if required, to repair the ohmic heating coil. The vessel reinforcement was decided early in 1988 as an outcome of the so-called '7MA Study' and consists in welding inside the vessel, at the inboard wall, inconel rings to stiffen and strengthen the vessel against disruption forces. At the end of 1988, the welding work was close to completion.

The ohmic heating coil inspection was made necessary because of the excessive rotational displacements observed on the individual subcoils making up the coil stack. The inspection revealed only minor damage. This damage was repaired and other modifications implemented to avoid the reoccurence of the phenomenon.

Scientific Achievements during 1988

Introduction

For 1988, a new system of operation of the scientific programme was introduced. The programme operated for a series of Campaign periods, each of eight weeks duration (composed of six weeks tokamak operation and two weeks of maintenence/commissioning). Two Programme Leaders were nominated with responsibility for formulating near programme proposals (one campaign ahead) and outline plans (two campaign periods ahead). These proposals were presented to the JET Experiments Committee for discussion and approval. These proposals were within the broad outline of the JET Development Plan and subject to guidelines provided by the Experiments Committee.

Programme Leaders for 1988 were as follows:

January–May 1988 (inclusive):	**P P Lallia and P R Thomas**
June–October 1988 (inclusive):	**P E Stott and A Tanga**

Four Task Forces were introduced to carry through the programme, as follows:

Task Force	Task Force Leaders
(a) **Full Performence and Operational Limits** (including High Current; Low q; Inner Wall Operation; Optimization of Density Limits; etc)	J Jacquinot
(b) **X-Point and H-Mode Phenomena**	M Keilhacker
(c) **Pellet Fuelling and Density Profile Effects**	P Kupschus/ G Schmidt
(d) **High Temperature Performance and High Neutron Yield** (including Hot Ion Mode, Monster Sawteeth; Disruptions; High Additional Power, High Neutron Yield, etc)	J G Cordey

Task Force Leaders were nominated with responsibility for (i) interacting with and advising Programme Leaders on programme requirements within that task area; (ii) devising and setting out a detailed programme for allocated time within a campaign period; (iii) driving through that task programme (including acting as Control Room representative); (iv) analysing data (in conjunction with Topic Leaders, if appropriate); (v) disseminating information in the task area through internal meetings and publications (in conjunction with Topic Leaders, if appropriate).

In addition, Topic Groups were formed, as follows:

Topic Group	Topic Leader
(a) **Global Power Balance and Heat Transport**	A Taroni
(b) **Particle and Impurity Transport**	A Gondhalekar
(c) **Plasma Edge Effects and Impurity Production**	G McCracken
(d) **MHD Phenomena** (including Sawteeth and Stabilisation Effects)	J Wesson
(e) **Heating Physics and Current Drive**	D F Start

Topic Group subjects are of longer term interest than the immediate tasks undertaken by the Task Force Groups. The Topic Groups are responsible for analysis of results within many areas across the Task Force spectrum, but they also have responsibility for advising Programme Leaders on programme requirements which are topical and relevant to the Groups areas of activity. In addition, the Groups disseminate information through internal meetings and in external publications.

It is within this system of operation and under these headings, that the scientific achievements for 1988 are described in the following sections.

Full Performance and Operational Limits

The main priority of this Task Force was the develop-

ment of high current plasma targets suitable for high power heating of plasmas resting on the belt limiters. The Task Force optimized conditions to use new equipment installed on the machine to its best advantage. This included belt limiters, eight new antennae, a second neutral beam injector, new amplifiers for the poloidal field coil system, multipellet injector, etc.

The highlights in the Task Force's performance have been the achievement of 7MA discharges, high power heating of 5MA plasmas with low $Z_{eff}(2-2.5)$ and long pulses of high temperature plasmas (20s with T_{eo} and T_{io} greater than 5keV) [1]. On the scientific side, the most dominant results were the observations of the saturation of the incremental confinement time with plasma current[2], good performance obtained by heating 5MA discharge with ICRH during the current rise[3](monster sawtooth equivalent) and the achievement, (in collaboration with Task Force C) of improved confinement obtained with peaked plasma profiles heated by pellets and reheated with ICRH.

The main areas of activity are described in the following paragraphs.

Discharge Optimisation for High Current and Flat Top

Current ramps at constant toroidal field B_t are limited by instability at rational q values which can lead to stationary modes and subsequent disruption. This limits the current ramp rate to ~0.25MA/s at 6MA when $q=3$. By ramping B_t and I_p simultaneously, so that q is maintained approximately constant at $q=2.5$, a higher ramp rate was possible (eg. 0.75MA/s up to 7MA). In such a case, sawteeth were present throughout the current rise and the loop voltage on axis was typically 1V. The saving of resistive Volt-seconds allowed a flat-top of 2s at 7MA or 8s at 6MA (see Fig. 61).

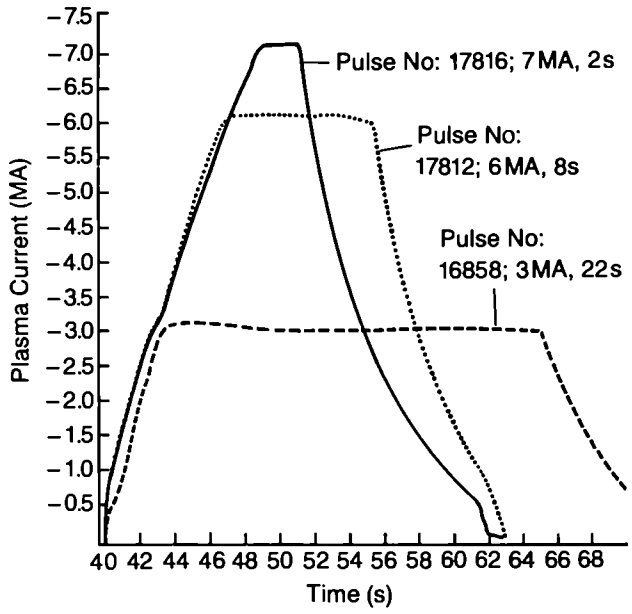

Fig. 61 High current or long flat top discharges. The 7 and 6MA pulses were obtained by ramping simultaneously plasma current I_p and toroidal field B_t.

At lower current (~3MA), a flat-top of 22s was achieved. This discharge was used to demonstrate ICRF heating for 20s (Fig. 62) and fuelling using up to 32 pellets (2.7mm diam.). A constant electron temperature of 7keV was maintained for 20s without change of impurity concentration after the first 2s.

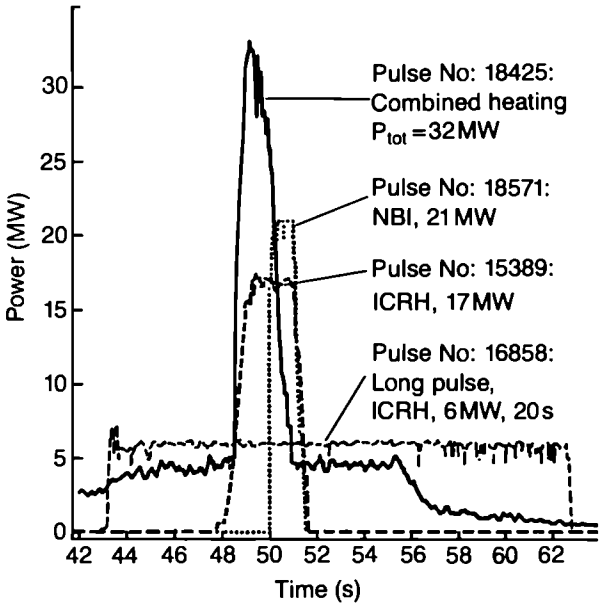

Fig. 62 Power traces corresponding to highest performance of the heating systems either used alone or combined.

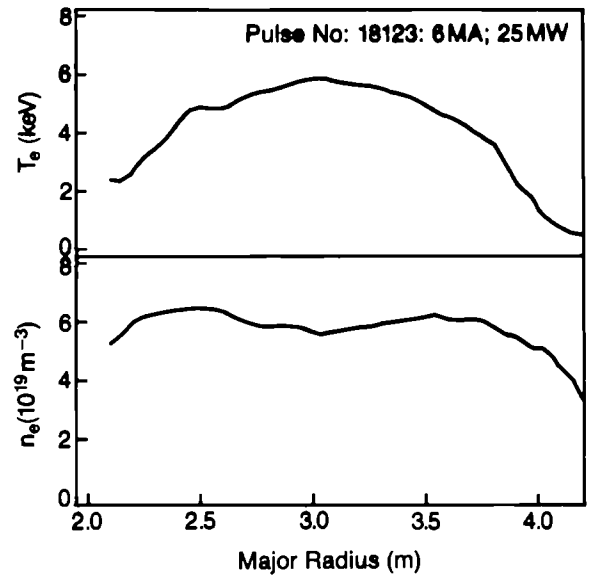

Fig. 63 Density and temperature profile during combined heating (25MW) of a 6.2MA plasma. Note the flat n_e profile and the weakly peaked T_e profile.

Combined Heating of High Current Plasmas

During combined ion cyclotron resonance frequency (ICRF) and neutral beam (NB) heating of high current plasmas the following effects were seen.

Profiles

- In the ohmic phase of 6 or 7 MA plasmas, the density and the temperature profiles were flat in the inner 70% of the plasma radius. With high power heating (see Fig. 63), the density profile remained flat, the electron temperature became parabolic before the sawtooth crash and the ion temperature could exhibit moderate peaking;
- With 3 MA plasmas using combined heating with more than about 7 MW of ICRF heating, long or monster sawteeth were routinely obtained and the electron temperature profile became triangular with peak temperatures up to 12 keV;
- With peaked density profiles created by pellet injection at the end of the current rise up to 3 MA, ICRF heating sustained high ∇T_e and ∇T_i (see Figs. 64 and 65) in the plasma core ($r/a \leq 0.5$). The density profile also remained peaked in the core.

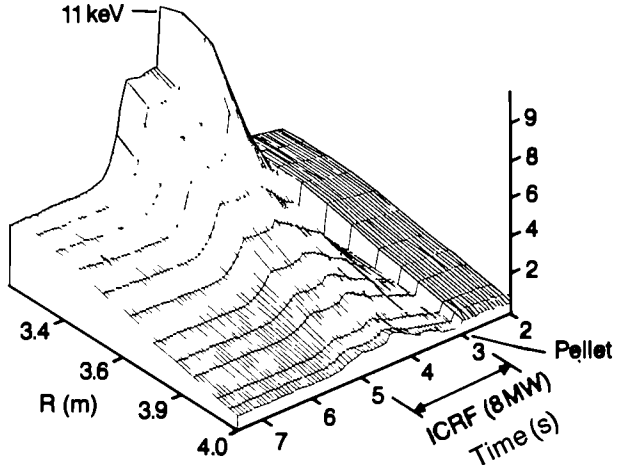

Fig. 64 Electron temperature during the ICRF reheat of deep pellet fuelling. Note the peaked $T_e(R)$ which suddenly relaxes to a 'monster' at ~4.5 s.

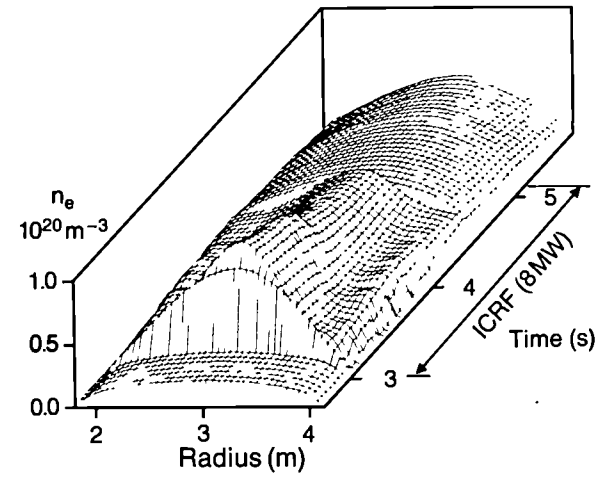

Fig. 65 Electron density profile after pellet injection and reheat by ICRF. Note the peaked n_e profile which relaxes at the same time as $T_e(R)$.

Typical Parameters

The typical parameters of the plasma in this series of experiments and the heating systems are summarised as follows:

Plasma

- $1 \leq I_p \leq 7$ MA
- $10^{19} \leq \bar{n}_e \leq 7 \times 10^{19}$ m^{-3}
- $1.55 \leq b/a \leq 1.6$
- $q_\phi \geq 2.5$
- $2 \leq Z_{eff} \leq 4$; <1.5 with pellets

Heating Systems

ICRH

- usually dipole ($R \sim 2$ to $4\,\Omega$)
- V_{max} at antenna ≤ 32 kV
- $P_{tot} \leq 18$ MW; H or ^{3}He minority

NBI

- 80 keV Deuterium, (injection angle 16° at $R_0 = 3$ m)
- $P_{tot} \leq 21$ MW

Stored Energy, Scaling with Plasma Current

The database of the diamagnetic energy stored in limiter full bore plasmas (at 3, 5 and 6 MA) is plotted versus input power in Fig. 66 and compared to Goldston (Aachen) scaling in Fig. 67. Overall, the data is well represented by the scaling given by Rebut and Lallia as well as by the Goldston (Aachen) scaling. Despite considerable scatter in the data, some general trends emerge:

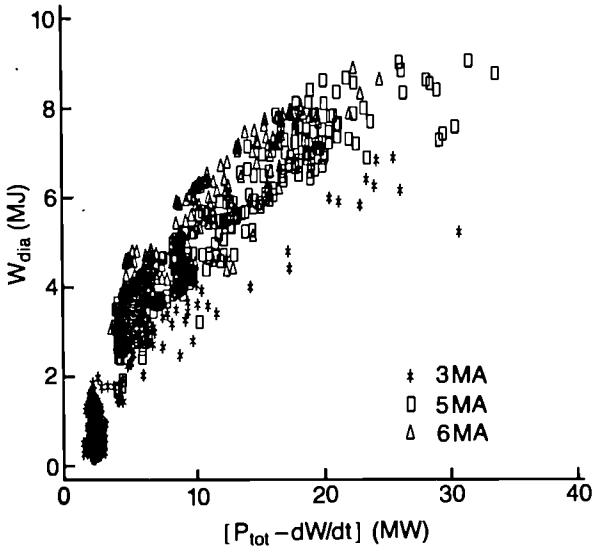

Fig. 66 Stored energy (diamagnetic) obtained with combined heating of full bore plasmas on the belt limiter for 3, 5 and 6 MA.

- At moderate values of I_p/B_t, eg for $I_p = 3$ MA and $B_t = 3.1$ T. The stored energy can exceed the Goldston value by ~50%. The improvement is mainly due to

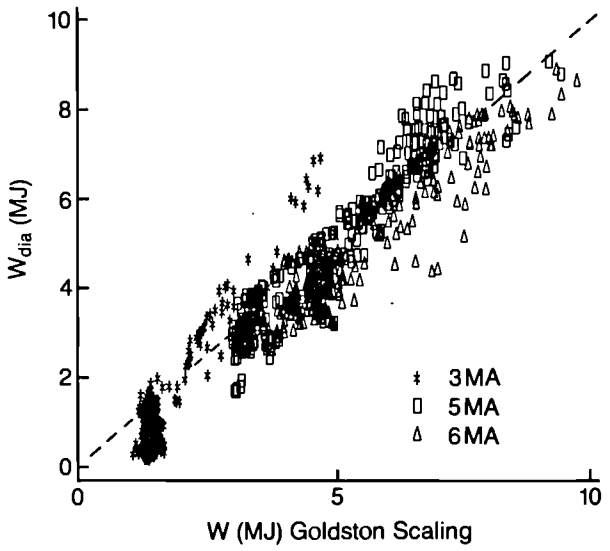

Fig. 67 Comparison of 3, 5 and 6 MA data with the Goldston (Aachen) scaling. 3 MA performs better and 6 MA is worse.

lengthening of the sawteeth and the production of fast particles by ICRH;

- At high values of I_p/B_t (eg for $I_p = 6$ MA and for high power levels), the stored energy can be inferior by ~20% compared to the Goldston value. Two effects can lead to this result.

  NBI Power Deposition: It has not been possible, at high power, to maintain a density low enough to allow central deposition of the 80 keV beams. The calculations of Fig. 68 shows that after 1 s only of 25 MW heating in a 6.2 MA plasma, the NBI power deposition, which was initially located centrally, has moved far off-axis, thus reducing the heating efficiency.

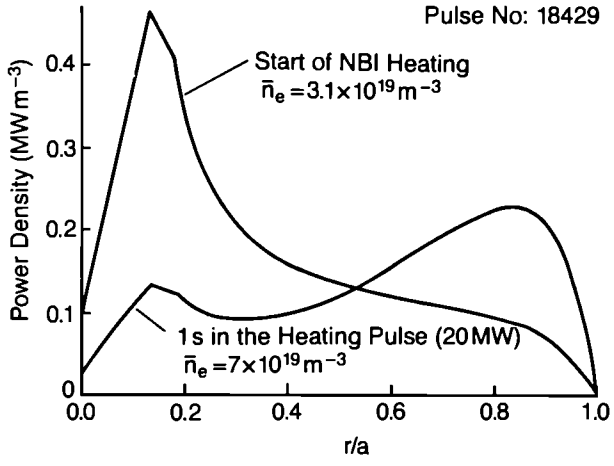

Fig. 68 Heating power density by NBI at 80 keV at the beginning of the heating pulse and 1 s after.

Sawtoothing Volume: This volume is large at low q and contributes to an effective broadening of the power deposition of both NBI and ICRH.

Radiated Power: In these conditions, the radiated power amounts to ~60% of the input power. Although this radiation occurs at the plasma edge (carbon and oxygen), it can significantly reduce the heating efficiency in this condition of off-axis heating with a large sawtoothing volume.

These effects have been taken into account by a local transport calculation using the Rebut-Lallia transport coefficients [4]. The results simulate well the temperature profiles and the evolution of the stored energy (Fig. 69).

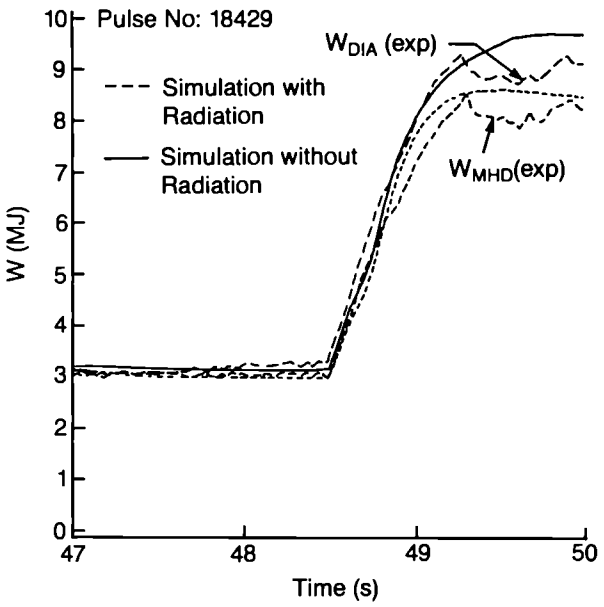

Fig. 69 Simulation of 25 MW, 6.2 MA heating pulse by a local transport code using the Rebut-Lallia transport coefficients. The code uses the measured electron density and radiated power and self-consistent power deposition profiles.

When impurity radiation is taken into account, the stored energy is reduced by ~15% in the 6 MA plasma case. The same calculation also gives a good representation of the monster sawtooth regime but does not fit the very peaked profiles obtained with pellet injection and ICRF heating.

NB Heating Regimes

The performance of NB heating for high current full bore plasmas is hindered by lack of beam penetration in the uncontrollable high density. The control of the density rise during heating is much better for lower plasma current (eg. 3 MA) particularly in double-null X-point or for small bore plasmas limited by the inner wall. In these two cases, the beam power deposition remains highly peaked in the plasma centre, ion heating is dominant and the ions can be decoupled from the electrons (see Task Force D report). Ion temperatures of about 23 keV have been observed with D-D reaction rates of about $2.5 \times 0^{16} s^{-1}$. The small bore inner wall plasmas can give an improvement of about 60% over Goldston scaling (Fig. 70). The density profile resembles TFTR

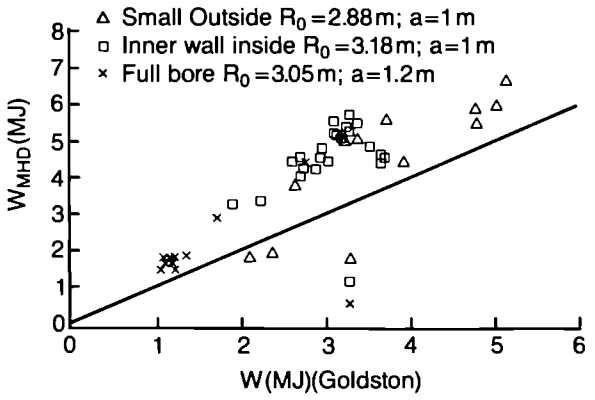

Fig. 70 Diamagnetic energy stored in various 3 MA plasmas heated by NBI. The small bore inner wall plasmas give an improvement over Goldston scaling.

supershots. Small-bore plasmas on the outer limiters appear to have a similar confinement time τ_E although the improvement over the Goldston scaling is less.

ICRH Regimes

Gas Fuelled Limiter Discharges

Enhancement of the diamagnetic energy up to 50% over the Goldston L-mode scaling is also achieved by ICRF heating alone[5](see Fig.71). This is obtained when all the following conditions are met:

- Peaked deposition profile: on-axis ICRF heating with H or ^{3}He minority;
- Long sawteeth: $\tau_{st} \geq \tau_E$ (the best conditions with monster sawteeth when $q_{cyl} \geq 3.3$ or $I_p/B_t = 1$ MA/T,
- Low or moderate densities, $n_e \leq 4 \times 10^{19}$ m^{-3}.

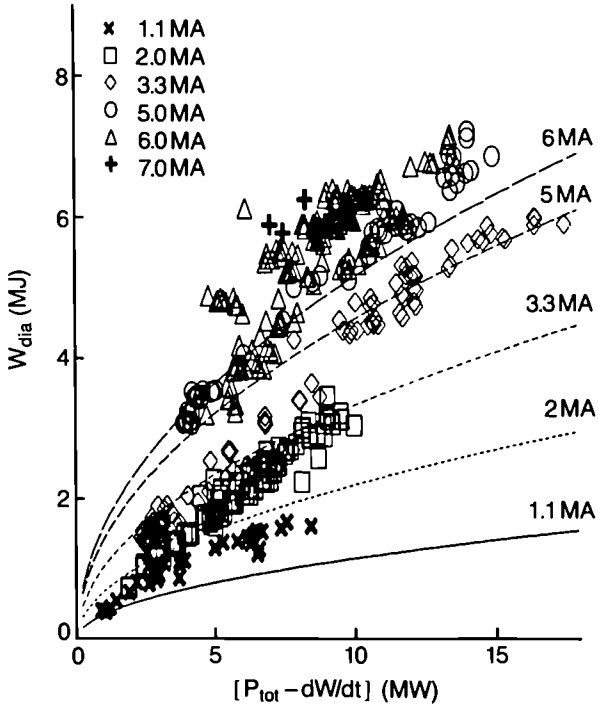

Fig. 71 Diamagnetic stored energy versus input power for ICRH on full bore limiter plasma (H minority). Improvement by up to 50% over Goldston scaling is obtained at 3 MA.

Comparison between the stored energy deduced from the diamagnetic loop (W_{dia}) and from the Shafranov (W_{MHD}) shift or the kinetic stored energy (W_{kin}) shows that most of this enhancement comes from fast particles accelerated by RF. More precisely the fast particle energy in the perpendicular direction has been estimated from: $W_{f\perp} = 2(W_{dia} - W_{kin})/3$. Fig. 72 compares $W_{f\perp}$ to a value W_{fo} based on Stix's quasi-linear treatment $W_{fo} = P_{RF}\tau_{so}/2$, where P_{RF} is the coupled power and τ_{so} is the classical Spitzer slowing-down time by electron drag using the central value of n_e and T_e. Good agreement of the two quantities is found (inclusion of profile effects resolves the difference by a factor of 2 shown in Fig. 71). The result suggests that these fast particles have a classical slowing down time[6]. The perpendicular energy of the fast particles is on average 1 to 2 MeV, a range similar to the α-particles average energy in a reactor. Therefore, these experiments offer a reactor relevant simulation of α-particle heating physics. This case is equivalent to about 10 MW of α-particle heating sustaining the plasma against losses. No obvious instabilities are observed. On the contrary, the confinement is somewhat better than Goldston scaling values.

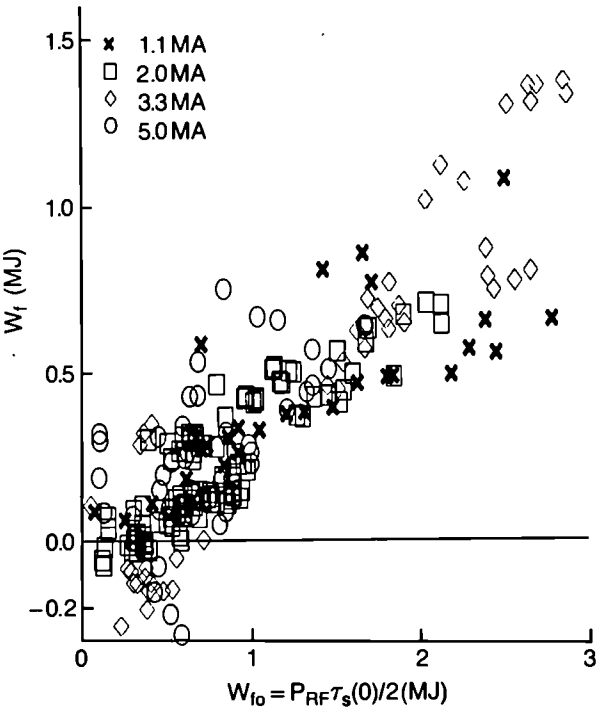

Fig. 72 Perpendicular energy in ICRH generated fast particles versus $W_{fo} = P_{RF}\tau_{so}/2$ where τ_{so} is the Spitzer slowing down time in the plasma centre.

Incremental Confinement Time and Fusion Parameter

Although global confinement increases with current at fixed power input, it is clear (see Figs. 71 and 73) that the incremental confinement time, $\tau_{inc} = \Delta W/\Delta P$, no longer increases when the plasma current exceeds $I_p/B_t \sim 1$ (eg. $q_{cyl} \sim 3.5$). This value of I_p/B_t also corresponds to a transition between a long sawtooth regime ($\tau_{st} \geq \tau_E$) to a

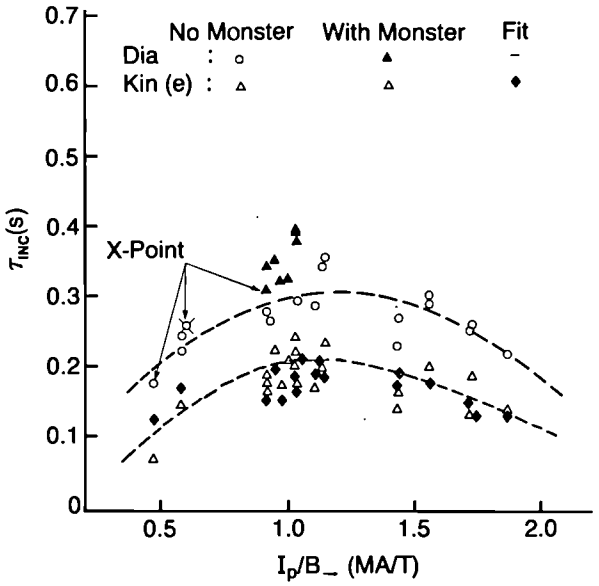

Fig. 73 Incremental confinement time (diamagnetic energy and electron energy content) versus I_p/B_t. Although the global confinement keeps increasing with I_p at fixed power input τ_{inc} is maximum when $I_p/B_t \sim 1$.

short sawtooth regime ($\tau_{st} \leq \tau_E$). A simple model describing the effect of sawteeth[2] on τ_{inc} fits with the observation, if we assume that $\chi_{e,i}$ decrease as $I_p^{-0.5}$. Therefore, the sawteeth as well as the lack of beam penetration of high density seem to be responsible for the relatively poor performance in the fusion parameter ($n_d \tau_E T_i(0)$) diagram of high power operation in 6MA high current discharge.

Heating after Deep Pellet Fuelling or during Current Rise to 5MA

Deep (on-axis) pellet injection at the end of the current rise, before onset of sawteeth, produces:

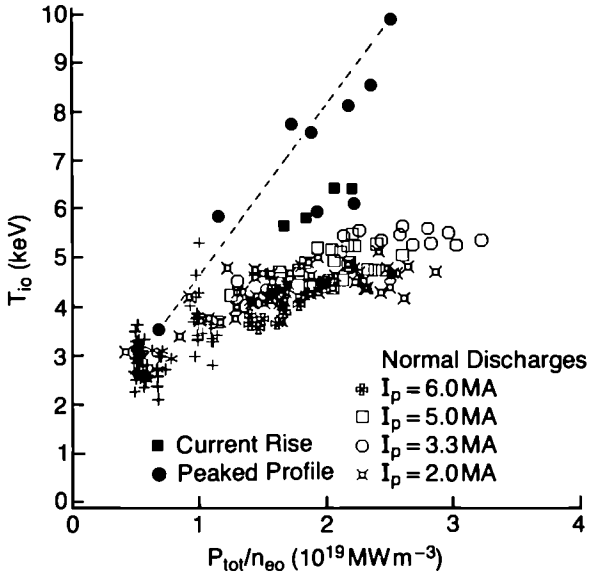

Fig. 74 Central ion temperature during ICRF heating. Best results are obtained with deep pellet fuelling (3MA) or current rise heating (5MA).

a) a peaked density profile which can last for several seconds;
b) a delay in the onset of sawteeth.

On-axis ICRF heating following pellet injection gives rise to improved ion and electron heating [4,7]. Peak electron temperatures of 12keV and peak ion temperatures of 10keV have been obtained in this mode (Figs. 74 and 75). The fusion parameter value ($n_d \tau_E T_i(0)$) obtained is comparable to those achieved with 3MA H-mode or 3MA hot ion mode plasmas. The heat transport coefficient in the plasma core ($r/a \leq 0.5$) is reduced by a factor 2 for electrons and by a factor 5 for ions. It is remarkable that a reduced heat transport can be maintained despite an exceptionally high pressure gradient. High electron temperatures are also obtained by heating during the rise to 5MA (see Fig. 75) before onset of sawteeth. However, the improvement in ion heating is less than with pellet fuelled discharge (Fig. 74).

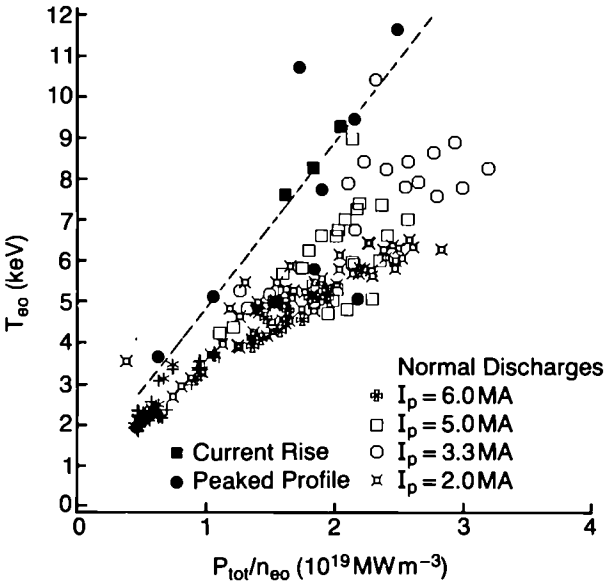

Fig. 75 Central electron temperature during ICRF heating regimes: (a) flat top gas fuelled, (b) current rise to 5MA, (c) after deep pellet injection.

The evolution of the product $[n_e(0)\, T_e(0)]$ during the current rise and during the flat-top of 5MA discharges is shown in Fig. 76. The product $[n_e(0)\, T_e(0)]$ is improved by about 50% in the current rise case. This discharge which also had a favourable dilution factor $n_d/n_e \sim 0.75$ appears to be a promising target for D fundamental cyclotron heating in a D-T mixture [5,8]. Projections based on this discharge yields a fusion Q of 0.5 to 0.7 [8].

Conclusions and Summary

In summary, the following conditions were achieved in Task Force A experiments:

- Discharge optimisation produced discharges of 7MA for 2s and 3MA for 22s;
- Up to 32MW of additional heating power was

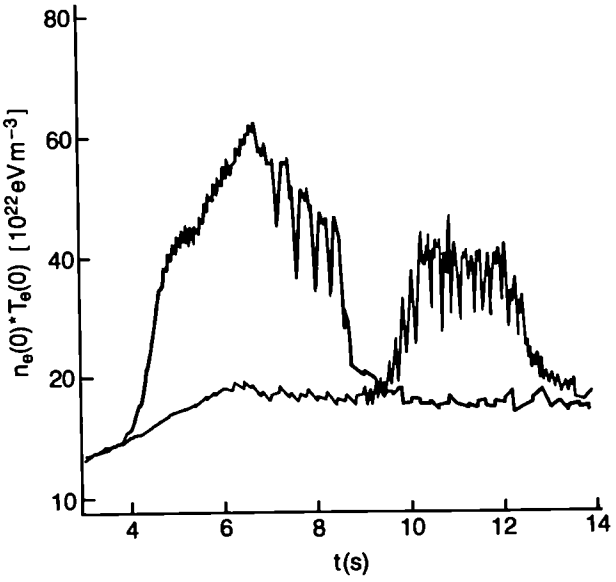

Fig. 76 Product $[n_e(0)\,T_e(0)]$ versus time during current rise heating or during flat-top heating. The RF power is 11 MW in both cases. The plasma current starts at 40s and reaches 5 MA at 47s. In the current rise heating case, the RF reached full power at 44.5s; at this time I_p is 4 MA.

References

[1] Jacquinot, J. et al, Bull. Amer. Phys. Soc. 33, 2031 (1988).

[2] Bhatnagar, V. et al, Proc. 15th EPS Conf. on Plasma Phys. and Con. Fus. (1988) Europhysics Conference Abstracts I, 358.

[3] Bures, M. et al, to be published in the Proc 16th EPS Conf. on Plasma Phys. and Cont. Fus. (Venice, Italy, 1989).

[4] Taroni et al, 12th International Conference on Plasma Physics and Controlled Nuclear Fusion Research (IAEA) (Nice, France, 1988).

[5] The JET Team, Plasma Phys. and Cont. Fus, 30, 1467 (1988).

[6] Erikson, L. G. et al Nuc. Fus. Lett. (1989) to be published.

[7] Schmidt, G., 12th International Conference on Plasma Physics and Controlled Nuclear Fusion Research (IAEA) (Nice, France, 1988).

[8] Cottrell, G., to be published in Proc. 16th EPS Conf. on Plasma Phys. and Cont. Fus. (Venice, Italy, 1989).

injected in 3 and 5 MA plasmas;

- The performance of high current discharges is presently limited by:
  - power spreading in a large volume due to sawteeth;
  - lack of density control and poor beam penetration with 80 kV beams;
  - dilution $n_d/n_e \leq 0.5$, except in a number of 5 MA discharge; including current rise experiments where a more favourable values up to 0.75 were obtained;
- Up to 50% improvement over Goldston scaling was obtained with:
  - on-axis ICRH at 3 MA (long sawteeth, W_f large) and maximum values of $T_e = 12$ keV, mainly due to fast particles;
  - small-bore plasmas heated with NBI to maximum values $T_i(0) = 23$ keV;
- α-particle heating in a reactor was well simulated by ^{3}He minority heating;
- The best fusion parameter ($n_d\,\tau_E\,T_i(0)$) in limiter plasmas and H modes were similar with:
  - on-axis ICRH of peaked profile created by deep pellet fuelling, eg. $n_d = 6\times10^{19}$m^{-3}, $T_{eo} = 11.5$ keV, $T_{io} = 9$ keV;
  - NBI heating of small bore inner wall plasmas in the hot ion regime;
- The product $n_e(0)\,T_e(0)$ reached 6×10^{20}m^{-3} keV both in current rise experiments and in the pellet case and project, with a D-T mixture (D at the fundamental resonance), to a fusion Q of 0.5 to 0.7;
- The high-current mode of operation should benefit significantly from the installation of 140 keV NBI, Be gettering/limiter, LHCD (sawtooth stabilisation).

X-Point and H-Mode Phenomena

First H-mode results in JET at plasma currents up to 3 MA and with neutral beam injection (NBI) heating up to 10 MW were presented in the 1987 Report. By using differential currents in the main equilibrium coils, the current capability of single null X-point discharges and H-mode operation has been extended to currents of 5 MA, full toroidal fields of 3.4T and neutral beam powers of 20 MW. With the global energy confinement time, τ_E, increasing roughly linearly with current, τ_E, in the range 0.8-1 s and stored plasma energies of more than 10 MJ have been achieved with ~10 MW of additional heating. H-modes have also been obtained in the double null configuration with currents up to 3 MA. Present JET H-mode plasmas are restricted to NBI heating (80 keV deuterium injection) of deuterium plasmas in a single null X-point configuration.

Operational Limits for H-Mode Operation

Fig.77 shows poloidal flux contours for a 5 MA single null X-point discharge. To achieve an H-mode, minimum separations of the separatrix from the inner wall, δ_{IW}, and from the lower belt limiter, δ_{BL}, are required. The precise clearances required depend on vessel conditioning, plasma parameters and, in particular, on the heating power used. Typical values are

$$\delta_{BL} \gtrsim 0.05\,\text{m} \qquad \delta \gtrsim 0.05 - 0.08\,\text{m}$$

The separation of the X-point position from the target plates was generally a few centimetres, but can be

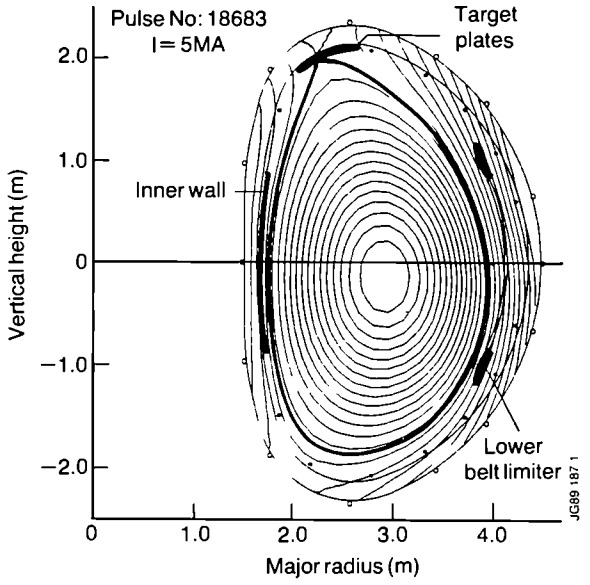

Fig.77: Poloidal flux contours for a 5 MA single-null X-point discharge.

reduced practically to zero. The most stringent requirement for achieving an H-mode is the heating power level. In JET, the threshold power, P_{th}, increases with toroidal magnetic field, B_T, as shown in Fig.78 for 3 MA single null X-point discharges. Typical values with NBI are

P_{th} = 5 MW for B_T = 2.0 – 2.4 T
P_{th} = 8-12 MW for B_T = 3.0 – 3.4 T

A low density limit is set for H-modes by the appearance of locked modes.

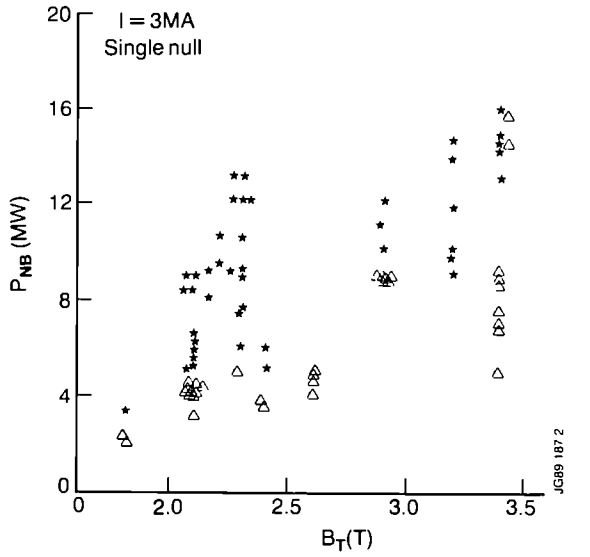

Fig.78: H-Mode threshold power as function of toroidal magnetic field (I = 3 MA, single null X-point).

H-Mode Characteristics

(i) Time Evolution of H-Mode Discharges

The characteristic time evolution of various plasma parameters for JET H-mode discharges is shown in Fig.79 for a 3 MA discharge (Pulse No:15894). Characteristic of most JET H-modes is the absence of very low level of ELM activity through-out the H-mode phase. This results in a continuous rise in plasma density and a corresponding increase in bulk plasma radiation which finally terminates the H-mode (longest H-phase ~4s) when the bulk radiation reaches about 60% of the input power. The increase in the total energy content of the plasma, W, during the H-phase results largely from the plasma density increase, while the central electron temperature, T_{eo}, is roughly constant or even decreasing slightly with time.

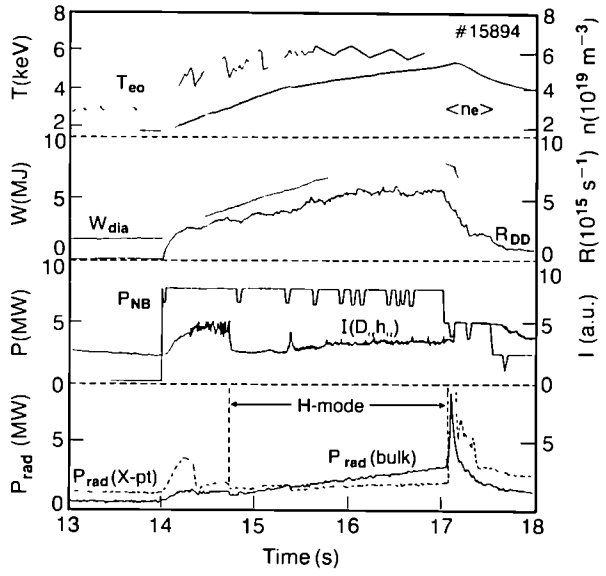

Fig.79: Time evolution of electron temperature on axis T_{eo}, volume-averaged plasma density $<n_e>$, total plasma energy W, total reaction rate R_{DD}, neutral beam power P_{NB}, D_α intensity $I(D_\alpha)$, bulk radiation P_{RAD}(bulk) and X-point radiation P_{RAD}(X-pt) for a 3 MA H-mode discharge (B_T = 3.1 T).

The level of ELM activity depends on the separation of the plasma boundary (separatrix) from the lower limiter and the inner wall. Provoking ELMs can be used to control the rise in plasma density which can be kept approximately constant throughout the NBI pulse. However, this occurs at the expense of simultaneously reducing the energy confinement time.

(ii) Evolution of Plasma Profiles

Typical radial profiles of n_e, T_e, T_i, P_{RAD} and j during an H-mode phase are shown in Fig.80 for Pulse No:15894. Fig.80a shows radial profiles of electron density n_e (r) and temperature T_e (r) at t = 16.0s (1.25s into the H-phase). The most characteristic feature of these profiles are the steep temperature and density gradients at the plasma edge (or pedestals) which form at the L → H transition. Flat or even slightly hollow density profiles are a common feature of both JET limiter (particularly at low values of q_{cyl}) and X-point discharges[1] employing NBI heating. In the H-mode case,

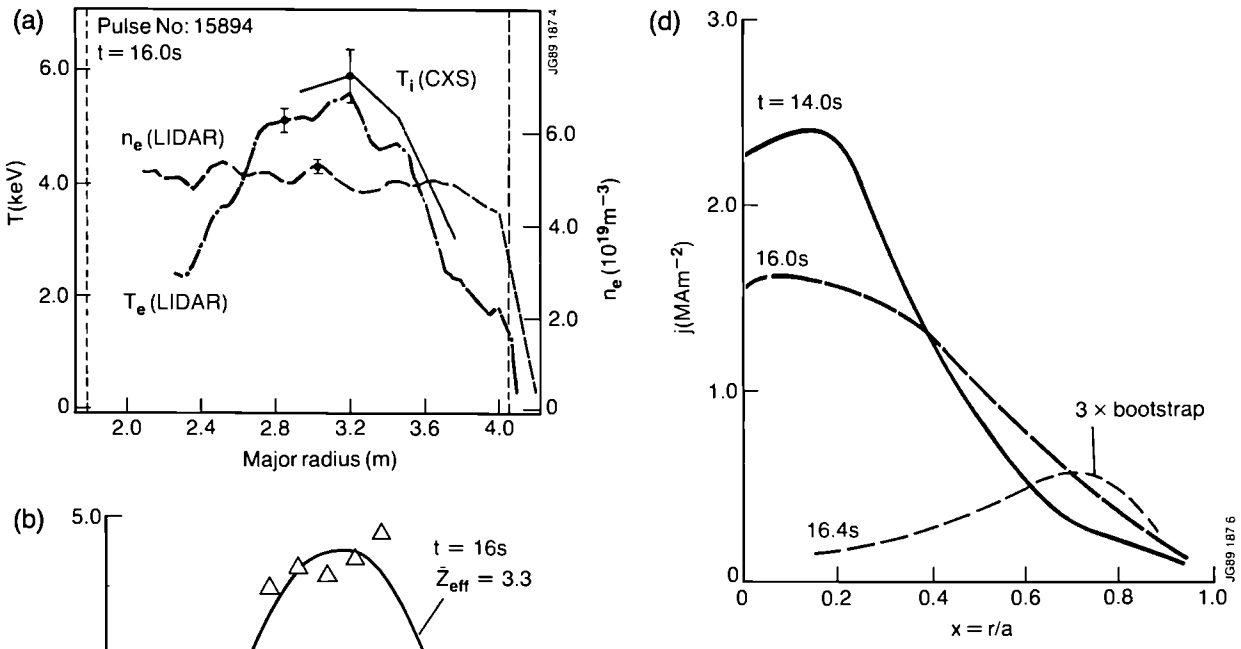

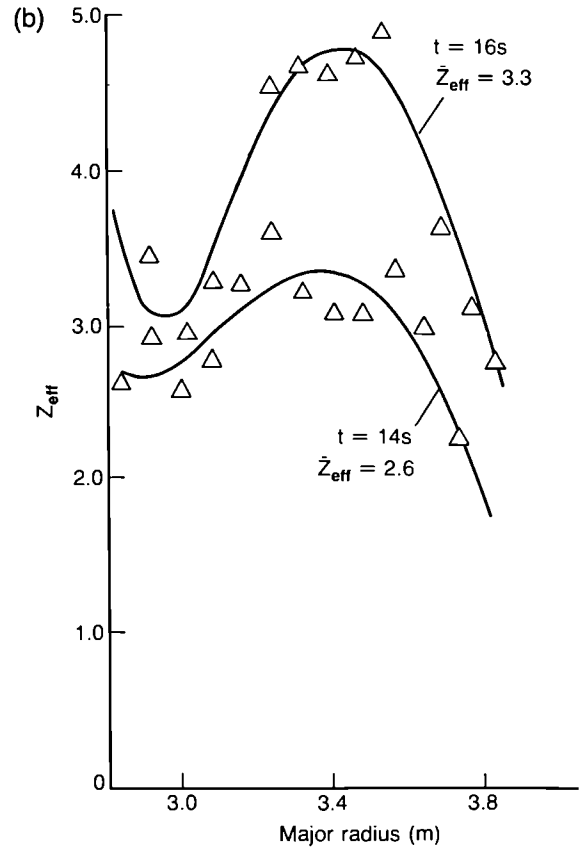

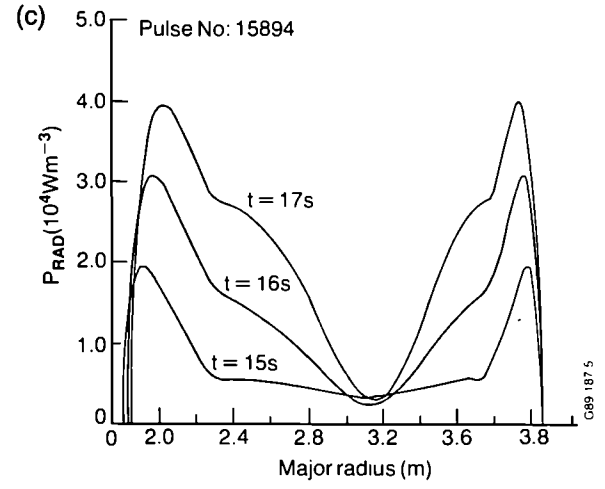

Fig.80: Radial profiles of (a) electron density, n_e, electron temperature T_e and ion electron temperature, T_i; (b) Z_{eff}; (c) bulk plasma radiation, P_{RAD} (bulk), and (d) current density during the H-phase of the discharge shown in Fig.79. The dashed line in Fig.80a indicates the radius of the 95% flux surface.

the density increases continuously, the profile shape changes little. The electron temperature profile is also broad and changes little with time. Fig.80a also displays the central ion temperature profile from charge-exchange spectroscopy, which within the accuracy of the measurements, the two temperatures are consistent.

Fig.80b displays Z_{eff} radial profiles determined from visible bremsstrahlung emission at 523.5 nm. During the limiter phase, the profile Z_{eff}(r) is peaked on axis, with an average value Z_{eff} of ~2.5. Following the formation of the X-point, Z_{eff}(r) becomes hollow on axis (profile at t=14.0s) with little change in Z_{eff}. The second profile shows the H-phase at t=16.0s. Z_{eff}(r) remained hollow, but Z_{eff} increased to ~3.3, due to the increase in impurity and particle confinement.

The evolution of the radiated power profile is shown in Fig.80c for t=15.0, 16.0 and 17.0s. Again the profiles are hollow throughout the H-phase but tend to fill in with time. Most of this radiation is emitted by light impurities, the major contribution coming from oxygen. The observed profiles of radiated power and Z_{eff} indicate hollow profiles of the light impurity densities [2]. Typical concentrations on-axis are 1-3% of the electron density for O and for C and $10^{-5}-10^{-4}$ for Ni. The deuterium density is typically ~$0.6n_e$ due to dilution by light impurities.

Fig.80d shows the evolution of the current profile, j. During the H-phase, the current density at the plasma periphery rises markedly. This is expected since (a) the resistivity is reduced in the edge region due to the increased edge electron temperature and (b) a large bootstrap current[3] develops due to the increased edge

pressure gradient. A corresponding decrease of the central current density is also observed, although experimental uncertainties preclude any definitive conclusion.

(iii) Edge Plasma

Plasma edge parameters play a decisive role in the transition to an H-mode and in the resulting improved plasma confinement properties. Fig.81 shows a plot of T_{edge} versus n_{edge} for 3 MA single null X-point discharges (B_T=2.2 T). The measurements are at various times during OH, L and H-phases determined by the timing and frequency of the laser pulse (0.5 Hz). The domain of edge parameters for an H-mode displays a well-defined lower density limit of $\sim 2\times10^{19}m^{-3}$ (increasing to $\sim 3\times10^{19}m^{-3}$ at B_T=3.0-3.5 T) and a minimum edge temperature of $\sim$0.5 keV.

These boundaries may be interpreted in terms of the collisionality of the edge plasma and the requirement to limit edge cooling by ionisation of neutral particles re-entering the plasma from the wall. The former condition, namely that the ion neoclassical collisionality parameter $\nu_i^* < 1$, is plotted in Fig.81, and shows that H-modes correspond to low collisionality in the plasma edge. The latter condition requires that the ionisation mean-free path of incoming neutrals, λ_{mfp}, be small compared to the thickness of the edge layer, δ_B. The boundary $\lambda_{mfp} < \delta_B$ is also plotted in Fig.81, where δ_B is taken at the width of an ion banana orbit.

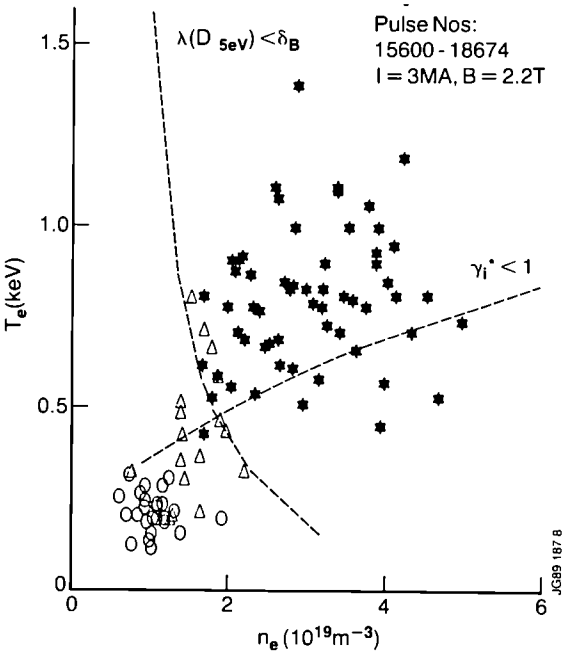

Fig.81: Edge temperature T_e (χ=0.95) versus edge density n_e (χ=0.95) for OH(o), L-(Δ) and H-mode (*) discharges (I=3 MA, B =2.2 T).

(iv) Divertor Plasma

The plasma in the vicinity of the X-point target plates (divertor plasma) has been investigated using eight Langmuir probes mounted in the target plates (see inset in Fig.82), with a reciprocating Langmuir probe (at R=3.25 m), and with a 2-dimensional view of the radiation from the divertor region.

Fig.82 shows profiles of density, temperature and ion saturation current in front of the target plates for a 4.6 MA discharge (OH and H-phase with P_{NBI}=14 MW). Although a single-null discharge, the inner divertor plasma is colder and denser than the outer. More power is carried to the outer divertor, suggesting that the main source of power flow into the scrape-off layer is in the vicinity of the outer mid-plane, i.e. closer to the outer divertor target. The unequal temperatures lead to thermo-electric currents in the scrape-off layer[4]. Current densities $I(O) \lesssim 10^5 Am^{-2}$ have been measured during the H-phase (see Fig.82) corresponding to more than 10% of the mean current density in the discharge. The scrape-off layer current flows from outer to inner divertor and returns through the target plates, thus flowing in the same direction as the plasma current.

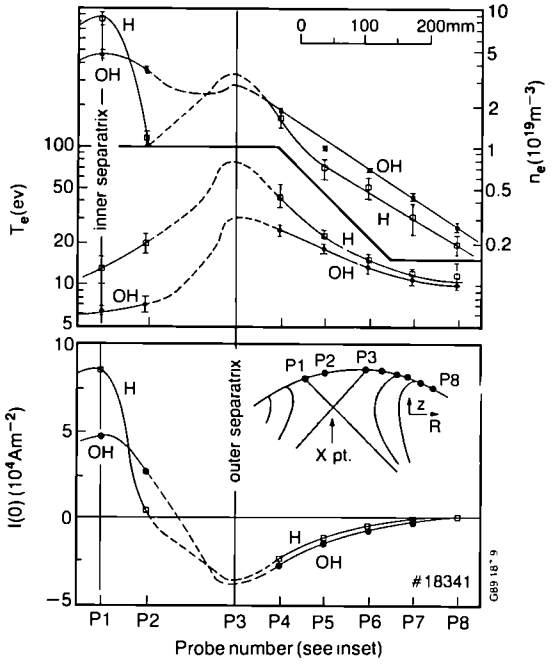

Fig.82: Profiles of density, temperature and ion saturation current in front of the target plates, measured with Langmuir probes mounted in these plates.

The power estimated to be carried by plasma to the target plates increases from 0.8 MW in the ohmic phase to 1.9 MW at the end of the H-phase. For most of the discharge, i.e. L and H-phases, this is about 15% of (P_{tot}-dW_{dia}/dt) but about 25% total during the ohmic phase.

The collisionality of the divertor plasma may have a bearing on whether an H-mode can be achieved. This has been considered for JET[5] and results suggest that flows in the scrape-off layer have a low Mach number, or are nearly stagnant, near the separatrix but are stronger and towards the divertor further away from the

separatrix. Flow reversal occurs near the separatrix and plasma also leaves the divertor. This outflow from the divertor, which is stronger during the H-phase, might correspond to an influx of deuterium into the bulk plasma. This would lead to a density increase, as observed in JET and other tokamaks during H-phase. Additional impurity flow from the divertor could ensue.

Energy Confinement

The dependence of global energy confinement on plasma current and heating power has been considered for ELM-free H-modes in the single null X-point configuration. Fig.83 shows the plasma energy W from diamagnetic measurements (Fig.83a) and global energy confinement time $\tau_E = W/[(P_{tot}\text{-}dW/dt)]$ (Fig.83b) as a function of the total net input power $[P_{tot}\text{-}(dW/dt)]$ for plasma currents of 2, 3, 4 and 5 MA. The limited amount of data at the highest current of 5 MA was obtained when the discharges were not fully optimised. In all experiments, the power range in which ELM-free H-modes could be obtained was limited to $P_{tot} \lesssim 14$ MW.

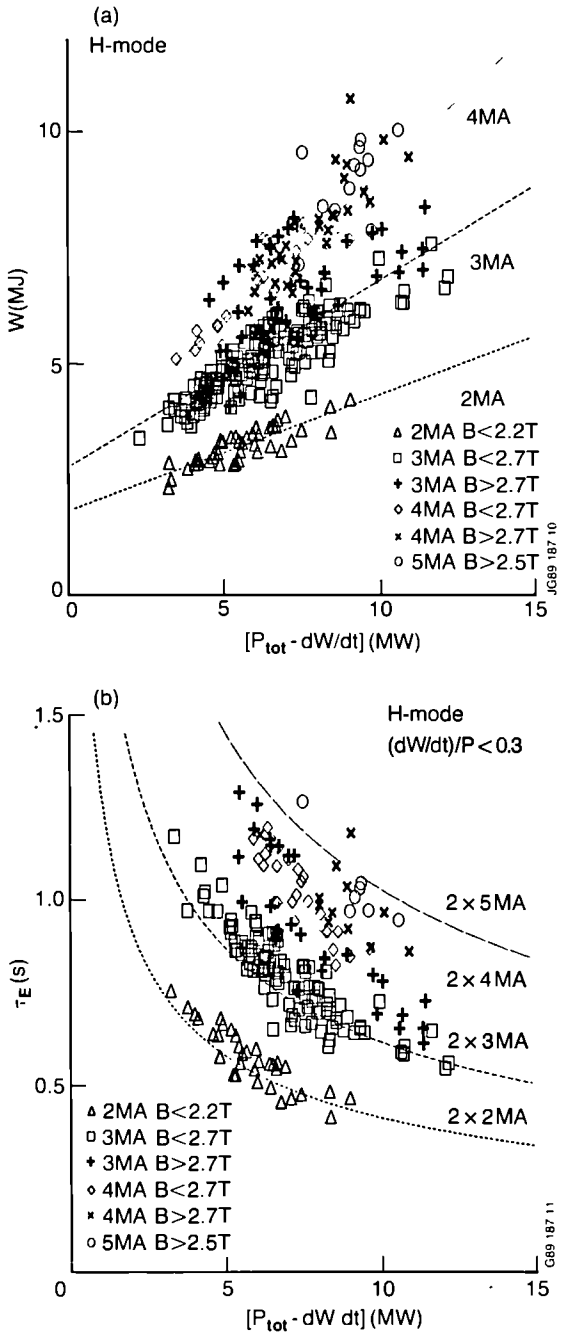

Fig.83: (a) Plasma energy and (b) global energy confinement time in ELM-free H-mode plasma versus total net input power for currents of 2, 3, 4 and 5MA.

The data in Fig.83 exhibit two main trends: a roughly linear increase of W and τ_E with plasma current; and a degradation of confinement with heating power. Part of this degradation can be attributed to increased impurity radiation and poor NB penetration at the higher densities. Data at 3MA and 4MA indicate that the energy confinement is higher at higher B_T. A comparison of L-and H-mode confinement described, for example, by Goldston scaling[6], shows an improvement in τ_E by at least a factor of 2, and even greater at higher B_T.

Fig.84 is a plot of the confinement quality factor τ_E/I versus q_{95} for various toroidal fields (for heating powers in the range $8\,\text{MW} \leq P_{tot}\text{-}dW/dt \leq 10\,\text{MW}$). The decrease in confinement for $q_{95} \gtrsim 3$ is probably caused by a reduction in the confinement value as the sawtooth inversion radius moves outwards.

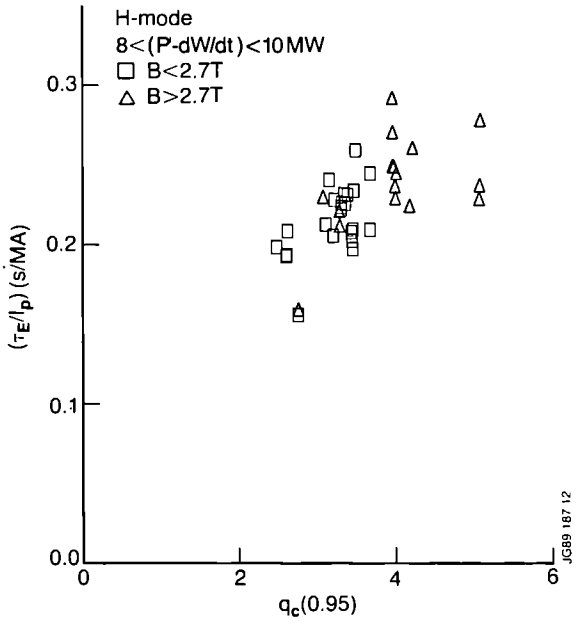

Fig.84: Confinement quality factor τ_E/I versus safety factor at the 95% flux surface ($8\,\text{MW} \leq P_{tot}\text{-}(dW/dt) \leq 10\,\text{MW}$).

A regression analysis of these data has been performed (taking one observation per shot, at times close to when W is maximal and $0 \leq (dW/dt)/P < 0.3$; 102 shots in total) shows the following confinement scaling for JET ELM-free H-mode plasmas:

$$\tau_E\,(\text{s}) = (0.63 \pm 0.15) I^{0.76 \pm 0.08} B_T^{0.48 \pm .08} \langle n_e \rangle^{0.18 \pm 0.09} P^{-0.69 \pm 0.05},$$

where $<n_e>$ is the volume-averaged electron density and P_{tot}=-dW/dt. The constant is fitted at I=3MA, B=2.5T, $<n_e>=4\times10^{19}m^3$ and P=10MW. It was assumed that the variables τ_E, W_{dia}, I, B, $<n_e>$ and P were measured with constant relative (random) errors of 10%, 10%, 1%, 1%, 5% and 5%, respectively. Fig.85 shows the observed versus fitted energy confinement times. At constant $q_{cyl}\sim B_T/I$, the confinement time scales with current as

$$\tau_E \sim I^{1.2\pm0.1}.$$

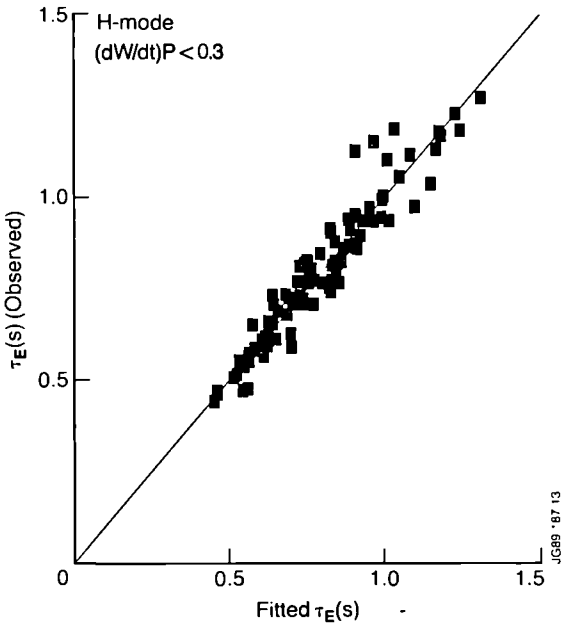

Fig.85: Observed versus fitted energy confinement times from an ordinary least squares fit.

As shown in Fig.83a, the data can also be described by an offset linear scaling law of the form

$$W=W_0+P_{tot}\tau_{inc}$$

where τ_{inc} represents the confinement time at high heating powers. The present data set would suggest that τ_{inc} increases roughly linearly with current at a rate of ~0.14s/MA.

The steep temperature and density gradients at the plasma edge (pedestals) characteristic of H-phase suggest separation of edge and central confinement properties. Therefore, the kinetic energy of the plasma has been split into the contributions from the edge pedestal

$$W_P=3\left[\int_{v_p}^{v} n_e\, kT_e\, dV+n_{e,p}\, kT_{e,p}\, V_p\right]$$

and from the plasma core $W_c=W_{tot}-W_p$, where V_p is the plasma volume inside a certain radius r_p chosen to be r=0.195a.

Fig.86 shows this analysis for 3MA H-mode discharges, in which W is plotted versus (P_{tot}-(dW/dt). W_c, like W_{tot}, is of offset linear form, indicating degradation with input power. However, the pedestal energy W_p(0.95)

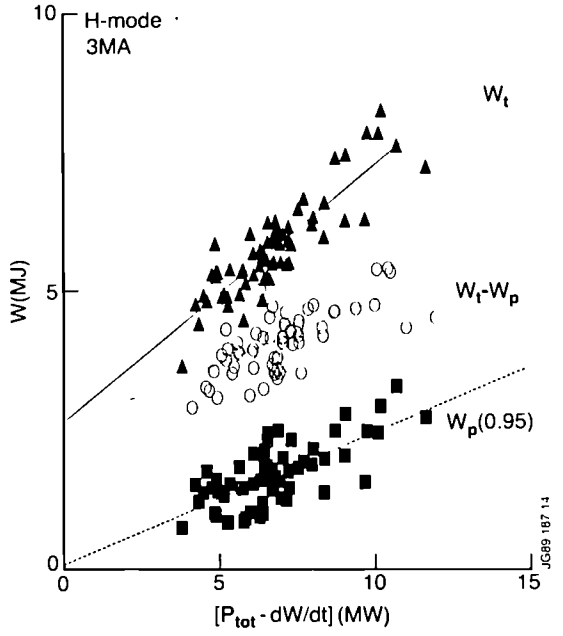

Fig.86: Plasma energy in pedestal and plasma core, respectively, versus total net input power for 3MA H-mode discharges ($B_T\leq2.7T$).

shows no offset, indicating little or no degradation with heating power. In conclusion, H-mode confinement (up to 12MW) comprises a power independent contribution from the plasma edge and a power dependent contribution (degraded, L-mode like confinement) from the plasma core.

Particle Control and Future Prospects for H-mode Operation

With good energy confinement properties of the ELM-free H-mode discharges, favourable values of fusion product ($n_{Do}T_{io}\tau_E$) up to $2.5\times10^{20}m^{-3}$keVs have been achieved. However, particle confinement improved similarly (impurity injection experiments indicate that impurity confinement times improve by at least a factor of three) making density control difficult. Beam penetration was also affected, radiation losses increased and finally terminated the H-phase. At the highest NBI power (14-20MW), strong radiation occured from a well-defined region near the X-point, and a thermal collapse resulted (reminiscent of plasma approaching the density limit) and lead to very ELMy-H-modes with inferior confinement.

The effect of high density and Z_{eff} on the projected values of the fusion amplification factor, Q_{DT}, for JET H-modes with 15MW of 140kV deuterium NBI has been calculated. It is clear that for τ_E in the range 0.6-1 s and volume-averaged electron densities $<\bar{n}_e>\sim5\times10^{19}m^{-3}$, the projected performance is significantly below the optimum which would occur at lower density and correspondingly higher temperature. It is clearly beneficial to increase τ_E (provided the density does not increase faster) but it is essential to control the plasma density, improve plasma purity and central heating.

So far, the plasma density has been controlled only by provoking sufficient ELM-activity obtained by reducing the separation between the plasma in the inner wall and/or the outer belt limiter. This allows the density $< n_e >$, total plasma radiation P_{rad} and concentration of metal impurities in the plasma centre to be kept approximately constant for 1 or 2s but at the expense of a considerable reduction in energy confinement time τ_E

Attempts to improve central heating by using ICRH have, so far, been unsuccessful. In the double-null configuration up to 8MW ICRH (hydrogen minority, 33.5MHz, monopole phasing) has been coupled to the plasma both alone and in combination with a similar level of NBI. A strong increase in radiation resulting from enhanced impurity influxes (mainly nickel, possibly also oxygen) has allowed only short, or very ELMy, H-modes with τ_E close to typical L-mode values. To overcome these difficulties, the present nickel antenna screens will be replaced with beryllium in 1989. The introduction of beryllium as a limiter material should also reduce radiation and, possibly, Z_{eff}. In 1989, one NBI box should be upgraded to 140kV/D which should give better penetration and inject fewer particles.

However, to maximise JET prospects, it may be necessary to introduce active particle control. First, sweeping the X-point position will be examined to help reduce particle and impurity influxes. Ultimately, however, it might be necessary to pump in the vicinity of the X-point where particle flows are most concentrated.

References

[1] Smeulders, P., et al., 'Hollow Profiles and High-β Effects During H-Mode in JET', JET Internal Report JET-IR(88)11, JET Joint Undertaking, (1988);

[2] Behringer, K., et al., 'Impurity Transport in JET during H-Mode, Monster Sawteeth, and After Pellet Injection', (Proc. 15th Europ. Conf. on Contr. Fus. and Plasma Heating, Dubrovnik), 12B (I) (1988) 338;

[3] Bickerton, R.J., Connor, J.W., Taylor, J.B., 'Diffusion Driven Plasma Currents and Bootstrap Tokamak', Nat. Phys. Sc., **229** (1971) 110;

[4] Harbour, P.J., Workshop on Plasma Edge Throy in Fusion Devices, Augustusburg, G.D.R., 26th-30th April 1988. To be published in 'Contributions to Plasma Physics', (Akademie-Verlag, Berlin, G.D.R.);

[5] Keilhacker, M., and the JET Team, 'The JET H-Mode at High Current and Power Levels', 12th IAEA Conference on Plasma Physics and Controlled Nuclear Fusion Research (Nice, France, 1988) to be published in Nuclear Fusion Supplement;

[6] Goldston, R.J., 'Energy Confinement Scaling on Tokamaks: Some Implications of Recent Experiments with Ohmic and Strong Auxiliary Heating', Plasma Phys. and Contr. Fus., (Proc. of 11th Eur. Conf. on Plasma Physics and Controlled Fusion, Aachen, F.R.G., 1983), 6 (1984) 87.

Pellet Fuelling and Density Profile Effects

The multiple injection of 2.7 and 4mm deuterium pellets has been undertaken into JET plasmas under various scenarios for limiter and X-point discharges with currents up to 5MA in ohmic, neutral beam and RF heating situations. This has been carried out as a collaborative effort between JET and a US team under the umbrella of the EURATOM-USDoE (US Department of Energy) Fusion Agreement on Pellet Injection, using a jointly built three-barrel, repetitive multi-pellet injector. The Pellet Agreement involves joint experiments during two major operational periods of JET, one of which was completed in September 1988. With the introduction of routine use of pellet injection and expansion of various pellet injection scenarios, within several task forces have resulted in a large amount of data - about 350 pulses with about 1250 pellets. However, there is a backlog in evaluation of this large amount of data.

The best plasma performance with pellet injection and additional heating revealed a new enhanced confinement regime. This was obtained by injecting a 4mm pellet (sometimes combined with one or two 2.7mm pellets to keep the electron temperature low) early into 3MA, 3.1T limiter discharges while centrally depositing the pellet mass, with central density n_e (0) initially well in excess of 10^{20} m^{-3}. The maximum n_e (0) reached about 10 milliseconds after the pellet event was 2×10^{20} m^{-3} but more common values were 1.4×10^{20} m^{-3}. The achieved peaking factors n_e (0)/$< n_e >$ taken 0.2s after the pellet event were ~ 3 and the radial density exhibited a centrally enhanced core with $r \leq 0.5a$ on top of a flat pedestal for times in excess of 1 s. As shown in Fig.87, increasing this peaking factor is closely related to the requirement of depositing the pellet mass near the plasma axis, within say $r \leq 0.3$m. To model the evolution of these density profiles, particle diffusion coefficients for the central core out to the pedestal have to be lowered by almost a factor of 3 - already assuming an inward Ware pinch [1]. Subsequent central heating of this dense and initially clean core by ICRF heating - using H and ^{3}He minority schemes - in the 10MW range, yielded T_e (0) up to 12keV and T_i (0) up to more than 10keV. Electron and ion temperatures and their profiles, exhibited a distinct core and tracked each other quite closely [2], (see Fig.88). n_e (0) slowly decreased (up to 1.5s) to 0.6×10^{20} m^{-3}.

This suggested an enhanced central energy confinement in limiter discharges whereas the global L-mode type confinement was only modestly improved. To model the temperature profiles, the radial total heat conductivity in the central core must be lowered by about

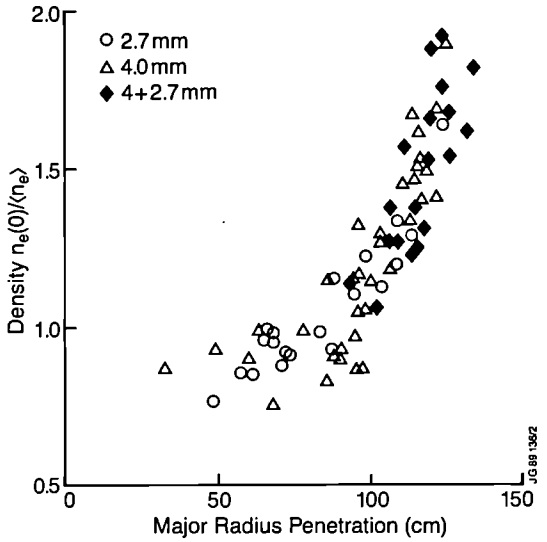

Fig.87: Ratio of density peaking factors, $\alpha = n_e(0)/\langle n_e \rangle$, before and 0.2s after the pellet event; α after the event in absolute value has to be multiplied by about 1.5 .

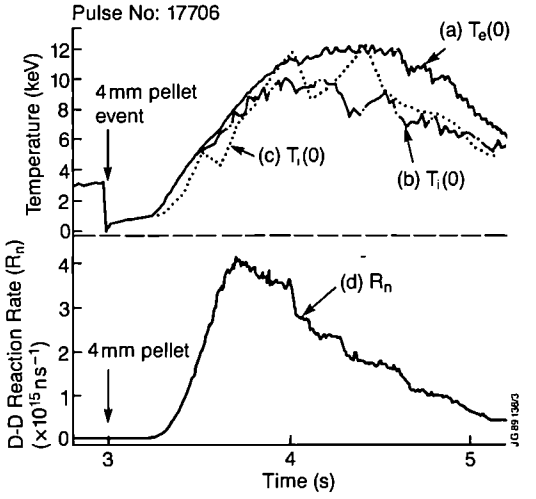

Fig.88: (a) $T_e(0)$ from ECE; (b) $T_i(0)$ from the Crystal Spectrometer; (c) $T_i(0)$ from the Charge-Exchange Spectroscopy; and (d) total neutron rate versus time (4 mm pellet event at 3 s into the pulse) for Pulse No. 17706.

a factor ×2 compared to the normal L-mode discharge [3]. Fig.88 shows the time behaviour of $T_e(0)$, $T_i(0)$ and the total D-D neutron rate for one of the better discharges, demonstrating that the lifetime of this high performance plasma state is so far limited to about 1 s. Other discharges exhibited spectacular crashes of the temperatures by several keV within milliseconds rather than the more gentle roll-over in this example. In this plasma core, electron pressures of more than 1 bar have been reached, i.e. usually a factor of 2 - 3 higher than similar non-pellet shots with gradients ~4 bar m^{-1}. The total plasma pressure here was close to 2 bar corresponding to a maximum central toroidal beta β_T of about 5 %, approaching locally ballooning stability limits. At this time, it cannot be concluded whether this improved confinement or its later decay is primarily due to the particular shaping of the density/temperature profiles - η_i mode enhanced transport is suspected not to occur in the early part of the pulse - or due to that of the plasma current profile linked to the pellet disturbance.

The non-sawtoothing, well confined part of the discharge exhibited strong central impurity accumulation. There are indications that this accumulation stems from a sort of neoclassical pinching and, therefore, central concentrating effect of impurities already present in the core plasma rather than from the influx of additional impurities from the wall and limiter which are expected to need more time to reach the plasma centre. The resulting total neutron rate from D-D reactions of up to $4.5 \times 10^{15}\ s^{-1}$, increased strongly with RF power and exceeded that of similar non-enhanced shots by factors of 3 to 5. Fusion products ($n_D(0)\ T_i(0)\ \tau_E$) of $\sim 1\text{-}2 \times 10^{20} m^{-3} keV\,s$ were obtained but combined power with neutral beams (up to 28 MW total) generally degraded the performance though leading to higher neutron rates up to $7 \times 10^{15}\ s^{-1}$. In the latter case, a high fraction of the neutrons was estimated to be generated by beam-beam and beam-plasma interactions, whereas the fact that, with ICRF heating only, this type of high performance plasma can be equally well obtained using the ^{3}He and H minority schemes - thus eliminating the possibility of a major contribution of direct second harmonic heating to the deuterium ions - points towards a predominantly thermo-nuclear generation of neutrons. In these discharges, as shown in Fig.88, the neutron rate increased steeply with time from the onset of the heating pulse along with the ion temperature but reached its peak value and decayed before the latter saturated at its maximum level; although still under investigation, this effect seems to be caused by the dilution of deuterium ions due to the impurity concentration on axis. More details have been published, previously [4 - 9]. Apart from the basic physics of this enhanced mode, there is also a technical and operational interest. Despite being transient in nature, this mode may have the potential for ignition of a fusion plasma which might then have to continue in a different confinement mode.

Attempts to extend this type of discharge to higher plasma currents has not yet been successful. Despite careful choice of size and respective timing of pellets to control the central electron temperature (needed to permit central mass deposition) over the long ramp of current build-up, the plasma often developed quasi-stationary modes (QSM's or locked modes). These usually destroyed the density peakedness quite rapidly and easily led to disruptions especially, with subsequent additional heating. A number of reasons have been identified [10] but no safe recipe for the avoidance of QSM's has yet been found. In view of these interesting results, there was not sufficient time available to promote the otherwise developed 4 and 5 MA scenarios and employ

additional heating. A similar situation has arisen for the injection of pellets into the discharge flat-top.

Suitable plasmas for the injection of 6 mm pellets ($\Delta < n_e > \approx 0.7 \times 10^{20}$ m^{-3}) requiring $T_e(0) \approx 5$-6keV and a total plasma energy greater than 5MJ have not readily been available and the few attempts made under marginal conditions have so far ended in disruptions.

In injecting 4mm pellets into single and double-null X-point discharges (most at 3MA), strong peaking before neutral beam injection was achieved; the onset of the H-mode was expectedly delayed due to the higher particle content but the limited penetration of the 80keV deuterium beams prevented the heating of the core, and ICRH cannot yet couple central power due to the incompatability of antennae and X-point geometry. So, the question of whether the central enhanced mode can be combined with the H-mode remains open. 2.7mm pellets have been injected into already established H-modes without noticably disturbing the typical H-mode boundary. Pellets were also contributing to the clean fuelling of small inner wall high-T_i shots and have increased by about 20 % the highest neutron rate so far obtained on JET.

Some preliminary attempts were made to fuel long-pulse RF heated limiter discharges in a centrifuge injector like manner with 2.7 and 4mm pellet strings. One case is indicated in Fig.89 where 32 pellets of 2.7mm were fired at about 1300m s^{-1} with a rate of 4s^{-1}. No development of a peaked profile has yet been found, the profiles exhibited rather more the features of gas fuelled discharges. These fuelling experiments will be continued.

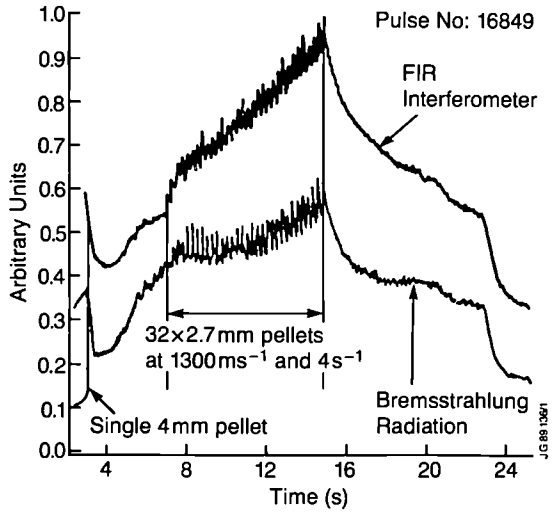

Fig.89: Bremsstrahlung and FIR-interferometer signal for demonstration of fuelling experiments: Pulse No. 16849, 4mm pellet at 3s and 32 2.7mm pellets at 4s^{-1} starting at 7s into the plasma pulse.

References

[1] L.R. Baylor et al., IAEA Technical Committee Meeting on Pellet Injection and Toroidal Confinement, Gut Ising, F.R.G., 24th-26th October 1988, to be published

[2] G.L. Schmidt et al., 12th IAEA Conf on Plasma Physics and Controlled Nuclear Fusion Research, Nice, France (1988) paper IAEA-CN-50/A-4-1

[3] A. Taroni et al., 12th IAEA Conf. on Plasma Physics and Controlled Nuclear Fusion Research, Nice, France (1988)

[4] P. Kupschus et al., 15th European Conf on Controlled Fusion and Plasma Physics, Dubrovnik, Yugoslavia (1988), Europhys. Conf Abstr, Vol 12b. 1, p143-146 (1988)

[5] S. Milora et al., 15th European Conf. on Controlled Fusion and Plasma Physics, Dubrovnik, Yugoslavia (1988), Europhys. Conf. Abstr., 1, p147-150

[6] A. Gibson, Invited paper to the 15th European Conference on Controlled Fusion and Plasma Physics, Dubrovnik, Yugoslavia (1988), Plasma Phys. and Contr. Fusion, **30**, 11, 1467-1478, (1988)

[7] J. Jaquinot, invited paper, 15th European Conference on Controlled Fusion and Plasma Physics, Dubrovnik, Yugoslavia (1988), Plasma Phys. and Contr. Fusion, **30**, 11, 1467-1478, 1988

[8] P. Kupschus et al., 'JET Multi-Pellet Injection Experiments', IAEA Technical Committee Meeting on Pellet Injection and Toroidal Confinement, Gut Ising FRG, 24th-26th October, 1988, to be published

[9] P. Kupschus, Invited paper, 'JET Multi-Pellet Injection Experiments', 30th Annual APS Meeting, Div of Plasma Physics, Hollywood Fla, U.S.A., (1988)

[10] B. Tubbing et al., 30th Annual APS Meeting, Div. of Plasma Physics, Hollywood, Fla, U.S.A., (1988)

High Temperature Performance and High Neutron Yield

Two different types of high fusion yield experiments were undertaken during 1988.

(i) ion cyclotron resonance heating of a minority ^{3}He distribution in a deuterium background, whose main objective was to confirm ICRH theory. However, these experiments also have important implications for the confinement and slowing down of α-particles in a reactor since the key dimensionless parameters are similar;

(ii) optimisation of D-D fusion yield using combined heating neutral beam (NB) injection and ion cyclotron resonance heating (ICRH). In these experiment, neutron yields in excess of 10^{16}n/s were achieved with a variety of plasma configurations. Very high ion temperatures (up to 23keV) and high electron temperatures (up to 12keV) were obtained.

The main results from the two series of experiments are briefly described below.

^{3}He-D Experiments with ICRH

A full description of these experiments and comparison with theory has been given previously[1,2], but a short synopsis is presented below. In these experiments, up to 15 MW of ICRH was used to heat a small ^{3}He minority with concentrations between 1 and 10%. The toroidal field was 3 T and the current was varied between 2 and 4.5 MA. At peak power, a reactivity of $2\times10^{16}s^{-1}$ was measured, which was equivalent to 60 kW of fusion products and hence a fusion Q value of 0.5%. The scaling of the reactivity with the ICRH power is shown in Fig.90. The reactivity increases strongly with the power ($\propto P^{5/3}$), with some evidence of a weakening of the dependence at higher power levels. Increasing the current from 2 to 4.5 MA did not increase the yield further, presumably due to the lack of any improvement with current of the central plasma parameters, principally, the electron temperature.

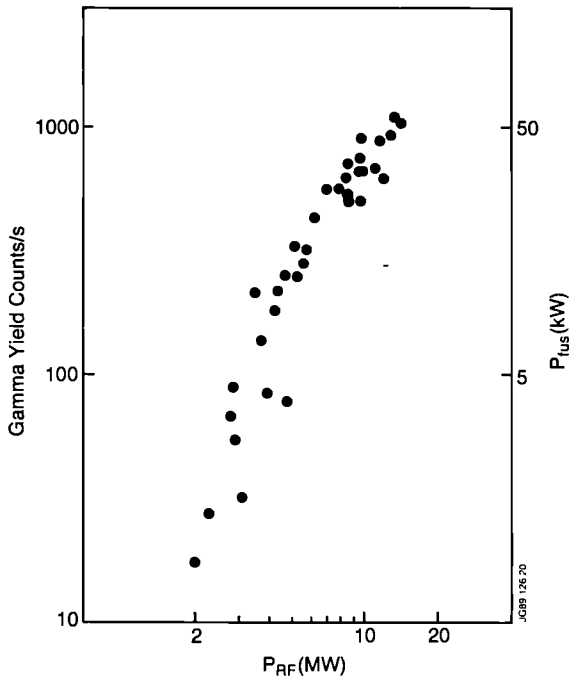

Fig.90: Variation of γ-ray count rate and fusion power from ^{3}He-d reactions in the energy range (12-20) MeV with applied RF power for a number of discharges. Plasma parameters: $I_p=(2\text{-}4)$ MA, $B_T=(3.2\text{-}3.4)$ T, $\eta=(1.6\text{-}4)$%. The highest count rate observed corresponds to 60 kW of fusion power.

To confirm the theoretical model of minority ICRF heating, the measured fast ion energy content was compared (Fig.91) with the calculated fast ion energy content using a single Stix model[1]. The predicted and measured reactivities were compared (Fig.92) and both were in good agreement.

One other interesting feature of these experiments was that a record monster sawtooth length of ~3.2 s duration was obtained (Fig.93). The reasons for the extended

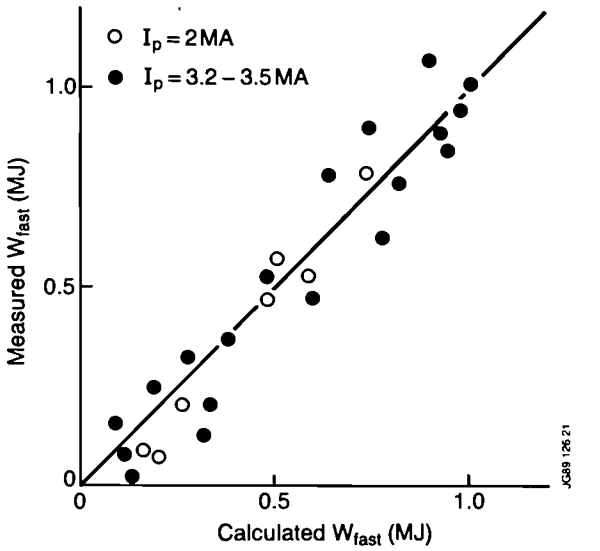

Fig.91: Comparison of measured and predicted total fast ion energy contents of the discharges in the data set. For all discharges, it was assumed that a fraction ($\mu=0.65$) of the ICRH power launched by the antenna was coupled to the fast ^{3}He minority ions.

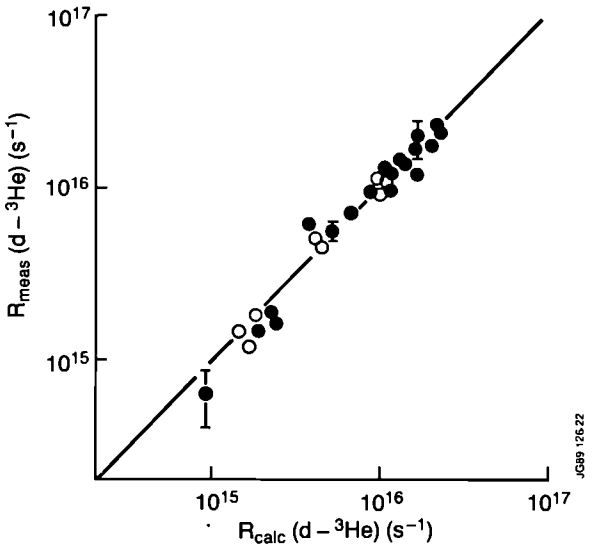

Fig.92: Comparison of measured and calculated ^{3}He-D fusion reaction rates for the complete data set. Open circles: Plasma current, $I_p=2$ MA, filled circles: $I_p=(3.2\text{-}3.5)$ MA. Toroidal field: $B_T=(3.2\text{-}3.4)$ T. The calculated points were obtained with a value of deuterium dilution factor ($n_d/n_e=0.3$.

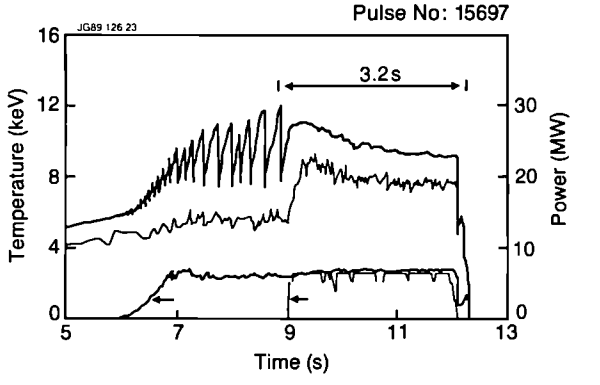

Fig.93: Behaviour of the central electron and ion temperatures during the longest period of sawtooth stabilization observed.

sawtooth period are still not clear. Fast particles have been proposed as a mechanism[3] and also changes in the current profile due to the strengthening of the bootstrap current[4].

As mentioned previously, these experiments have important implications for the confinement and slowing down of α-particles in a reactor. To ensure that a substantial fraction of the α energy is transferred to the background plasma, the α-particle confinement time must exceed the slowing down time τ_s. In terms of the α-particle diffusion coefficient D_α, this implies that $D_\alpha < a^2/4\tau_s$ for good α-particle confinement (a is the minor radius).

Values of $a^2/4\tau_s$ for these experiments are given in Table X and for several proposed devices. Clearly, the ^{3}He-D experiments are a more stringent test of fast particle confinement than α-particles in many of the reactor designs.

TABLE X

Machine	T_e(keV)	n_e ($\times 10^{20} m^{-3}$)	τ(s)	$(a^2/4\tau_s)$ (m^2/s)
JIT	25	1	1.3	2
ITER	15	1.5	0.39	2.6
Ignitor	6	10	0.014	3.1
JET (Q=1)	10	1.2	0.26	1.4
Experiments in JET				
ICRH (He^3min)	6.6	0.5	0.25	1.4

High Temperature and Fusion Yield D-D Experiments

For present JET parameters, the dominant contribution to the D-D reactivity comes from fusion reactions between the injected fast deuterons and the background deuterons. To optimise this term, high electron temperatures are required to maximise the fast ion slowing down time, and hence this means working at low density $<n> \sim 2\times10^{19} m^{-3}$. After extensive discharge cleaning in helium, it was found that low densities could be maintained in the presence of high power heating for plasmas located on the inner wall or with an X-point region. For plasmas located on the belt limiter, the density rise during additional heating could not be controlled despite extensive helium pre-conditioning. Hence, most of the effort was expended on inner wall and double-null X-point plasmas. The double-null X-point configuration was used in preference to the single-null to facilitate coupling of the ICRF power to the plasma. The current in these experiments was varied between 3 and 4MA. With the toroidal field at 3.4T, up to 33MW of additional heating power (21MW NBI and 12MW ICRH) was used.

Very high temperatures were achieved in these discharges. In several pulses, both the electron and ion temperature were maintained above 10keV for ~2s. A typical example is shown in Fig.94. In pulses with only NBI heating, the ion temperatures exceeded 20keV for periods of up to 1s with the electron temperature ~8keV. This is the traditional hot-ion mode of operation. The ion temperature profile was highly peaked under these conditions, as shown in Fig.95.

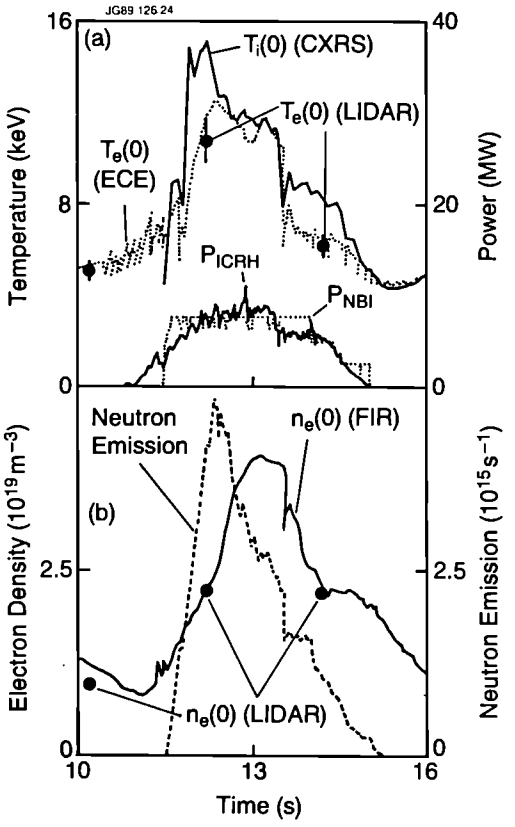

Fig.94: Data for JET Pulse No.16066, (a) central temperatures and additional heating powers versus time, (b) the central electron density and neutron emission rate versus time.

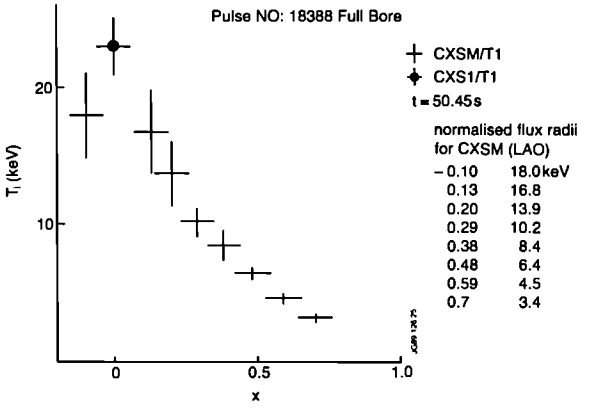

Fig.95: Ion temperature profile charge exchange recombination spectroscopic measurements for a high power (20MW) neutral beam heated discharge.

A study of global confinement properties of these pulses has been made previously[5]. Despite the wide variation of temperatures within the data set, the energy content of the thermal plasma is the same at a given power, as shown in Fig.96. The local confinement analysis of these shots has been undertaken, and indicates that the confinement in the central region where the ion temperature gradient is steep is better than in the outer region where the gradient is lower. The central region is only a small fraction of the total volume so that the improved central confinement is not seen globally.

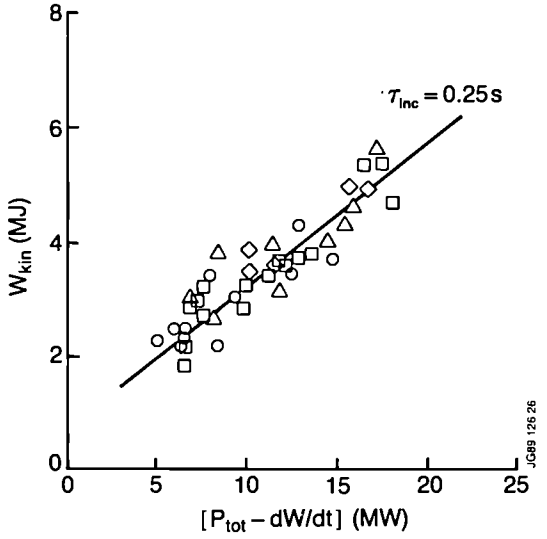

Fig.96: Kinetic energy content versus heating power

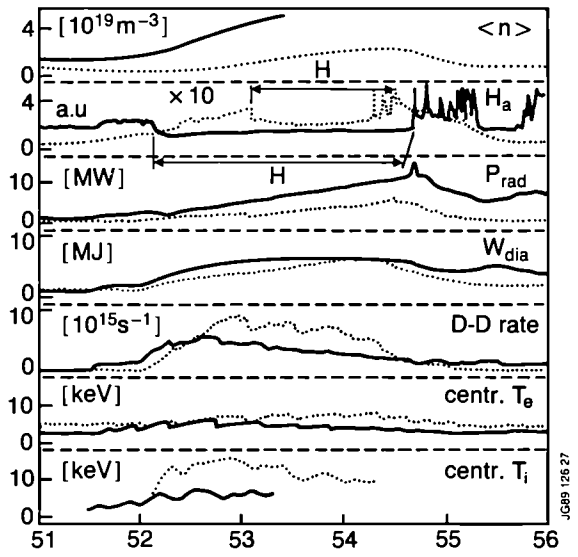

Fig.97: Comparison between an H-mode at medium density (Pulse No:17386, solid line) and one at low density (Pulse No:18757, dashed line). Both discharges have 10MW NBI from t=52s. Note that the H_α signal for the low density case is multiplied by 10.

In some of the double-null plasmas, a transition from the hot-ion mode to an H-mode occurred when the density was above a critical level ($<n> \sim 1\times10^{19}$m^{-3}). Although the confinement characteristics of these double-null H-modes were identical to the single-null H-modes, the temperatures were much higher in these hot-ion double-null H-modes ($T_i \sim 14$keV, $T_e \sim 7$keV) and the density much lower ($<n> \sim 1\text{-}2\times10^{19}$m^{-3}). A comparison of the time behaviour of the main parameters of a low and high density H-mode at the same power level is shown in Fig.97. The low density H-mode reaches the same contained energy as the high density H-mode but has a higher neutron yield due to the higher electron temperature and hence a larger beam-thermal neutron yield component.

In this double-null X-point configuration, a 3.5MA H-mode was obtained with 11MJ of stored energy using 9MW of ICRH and 12MW of NBI, demonstrating that

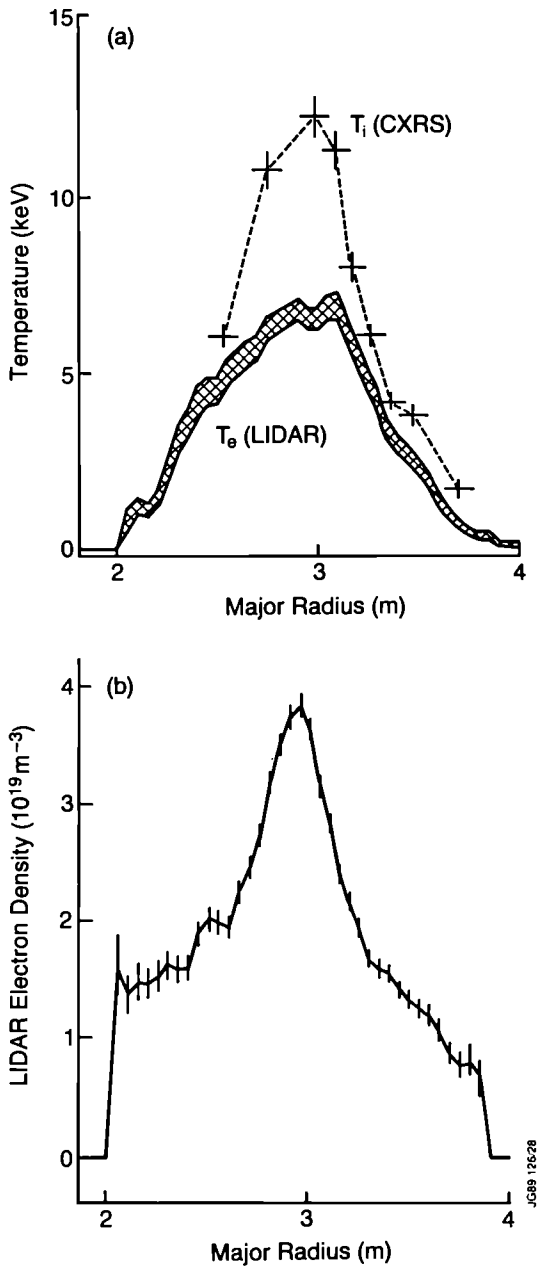

Fig.98: (a) Electron and ion temperature profiles and (b) the electron density profile for the 'supershot', JET Pulse No.16981.

H-modes can be obtained with a significant component of ICRF heating.

By pushing the plasma to a smaller minor radius on the inside wall, plasmas similar to the TFTR 'supershots'[6] have been produced. Fig.98 shows the temperature and density profiles in one of these pulses (Pulse No:16981). The characteristic narrow electron density and broad temperature profiles can be seen. This pulse has been identified in Fig.96. The global energy confinement is similar to other high temperature JET pulses in spite of the different plasma dimensions.

Extensive studies have been made of the neutron emission from these discharges. Since the major neutron component came from the beam-thermal fusion reactions, the yield was found to scale $\propto P_{NB}\,\tau_E\,n_D$ which reduces to an approximate quadratic scaling with power shown in Fig.99. The solid points are neutral beam only and the open points with the addition of ICRF heating. Although there is clear evidence from Fig.99 that the neutron rate can be improved with ICRF heating, the efficiency is not very high. There is clear evidence of the acceleration of the injected deuterons by the second harmonic ion cyclotron waves and the formation of an extended tail. The tail is much smaller than that predicted by simple theory, and the reasons for this poor efficiency in the tail heating are being investigated.

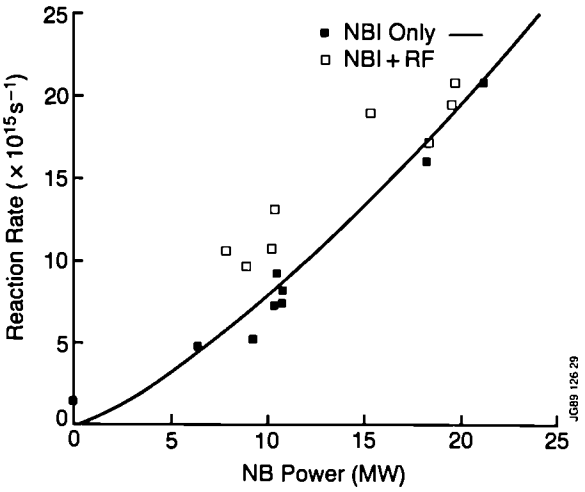

Fig.99: Reaction rate versus neutral beam power, solid points NBI only, open points with the addition of ICRH.

References

[1] D.A. Boyd, et al, JET Report JET-P(88)42;
[2] L.G. Eriksson et al, JET Report JET-P(88)53;
[3] F. Pegoraro et al, XIIth IAEA Conference on Plasma Physics and Controlled Nuclear Fusion Research, Nice, France (1988);
[4] J.G. Cordey, C.D. Challis and P.M. Stubberfield, Plasma Physics and Controlled Fusion **30**, 1625, (1988);
[5] P. Thomas et al, XIIth IAEA Conference on Plasma Physics and Controlled Nuclear Fusion Research, Nice, France (1988).

Global Power Balance and Heat Transport

Several lines have been followed at JET to study the crucial issue of energy confinement. Global energy confinement studies have been carried out on data collected in the JET transport database, which contains information from most JET discharges. Analysis has been carried out based on the bulk of collected data and on selected data corresponding to similar operating conditions.

A deeper understanding of the mechanism of energy confinement has been attempted by means of local transport analysis using interpretive transport codes. These studies have been performed at various levels of complexity with different codes. Predictive transport codes have been extensively used to test empirical and theoretical models of the local heat fluxes q_e and q_i.

Analysis of Global Energy Confinement

JET results have extended the parameter range for confinement scaling studies further than other devices. In particular, high power ($P_{tot} \gtrsim 30$MW) heating experiments have been performed for plasma currents 3-6MA using either the toroidal carbon belt or the inner-wall carbon protection tiles as limiters. There is no significant difference in confinement according to which configuration is used.

Whereas the confinement of ohmic and moderate power cases scales roughly as the square root of density, the confinement at high power has no clear density dependence. Indeed, in some cases, the confinement decreases with density, although this may be an effect of radiation. The confinement degrades with power in the sense that typical confinement times are in the range 0.3-0.9s for ohmic discharges, 0.3-0.5s at 15MW and 0.2-0.3s at 30MW. Some scans, particularly with ICRH alone and a low density target plasma, show a rapid approach to an asymptotic value of confinement time with increasing power (i.e. an incremental confinement behaviour). However, at the highest powers with combined neutral beam and ICRF heating, it is not clear whether an asymptotic value has been reached or whether the confinement continues to degrade with power. In particular, it is not possible to distinguish unambiguously between power law and incremental type models.

The bulk of JET data fits equally well either the Goldston auxiliary heating or the global form of Rebut-Lallia scaling laws but with a large scatter of ± 30% (see Fig. 100). The 3MA data tends to be better than predicted by either model whereas the 6MA data is worse. The behaviour at low q is influenced by sawtooth activity taking place within a large region, as can be shown by computations with predictive transport codes. A series of results show that important questions on the scaling of the plasma energy content with global external

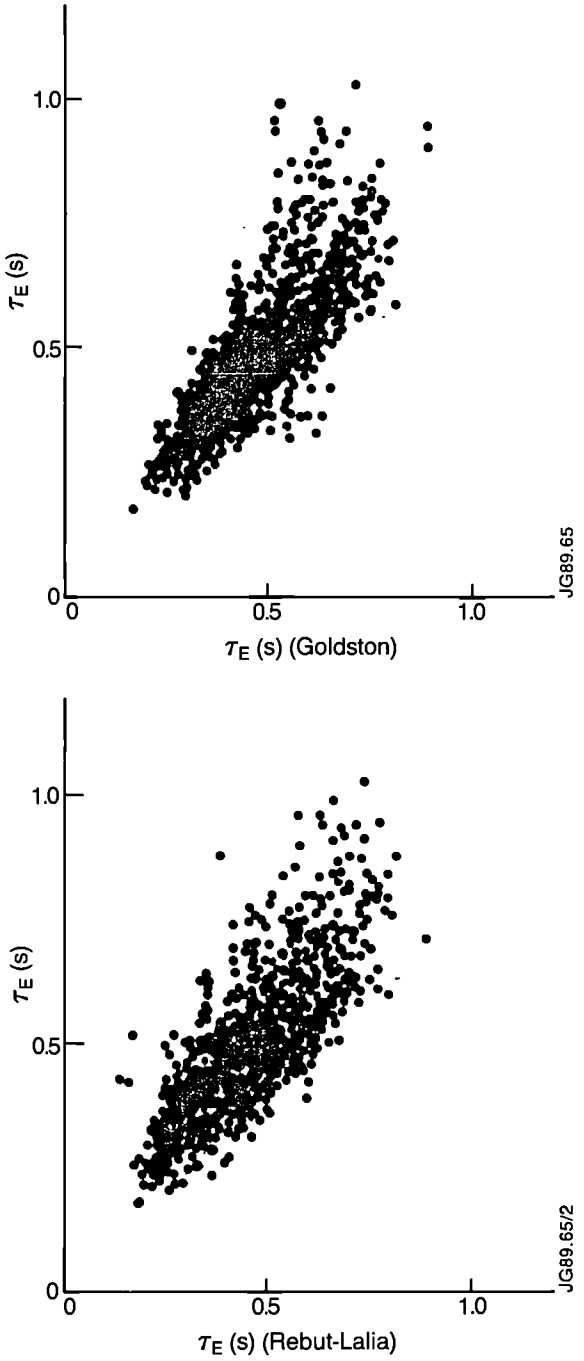

Fig.100: Observed confinement time τ_E (exp) versus that predicted by the (a) Goldston scaling and (b) Rebut-Lallia scaling. Data refer to 1988 discharges with $P_{tot} \geq 1.1\ P_{OH}$, excluding H-modes.

parameters remain open and that global scaling law are not sufficiently accurate for reliable extrapolations to ignition devices.

The analysis of discharges where sawtooth activity was spontaneously suppressed for as long as 3 s (the so-called 'monster' sawteeth) shows that even in the absence of sawteeth the incremental confinement time τ_{inc} (defined as the slope in the stored energy versus input power plot) increases less than linearly with current:

- The H-mode discharges, obtained with single and double-null magnetic configurations with $I_p = 2\text{-}5$ MA, show energy confinement times 2-3 times the Goldston scaling, with a similar degradation with power;
- The results from plasmas with small minor radius and small or large major radius show little variation in confinement;
- Various regimes of 'improved' confinement have been found.

High central densities, $n_{eo} \approx 1.4 \times 10^{20}$ m^{-3}, and peaked density profiles $n_{eo}/\bar{n}_e \approx 3$, can be produced by deep pellet fuelling. With injection before the onset of sawteeth, the decay of the density profile is slow and, furthermore, ICRF heating can be successfully applied. Despite the high density, high central electron temperatures up to 11.5 keV have been produced with only 10 MW of ICRF power. The electron temperature profile is highly peaked, with $T_{eo}/ < T_e > \approx 4$. Whereas normally with ICRF heating alone, T_i saturates at 5-6 keV, in these pellet shots T_i follows T_e and reaches 9.5 keV. Although the global energy confinement time is only 10-25% higher than in comparable discharges without pellets, the central confinement is enhanced by a factor $\gtrsim 2$.

Low density target plasmas and improved density control during additional heating can be achieved with plasmas limited on the inner wall carbon tiles after extensive conditioning with glow discharge cleaning (GDC) in helium followed by tokamak discharges in helium. Subsequent discharges with deuterium prefill gave a target discharge which is almost entirely carbon with $n_e \approx 5 \times 10^{18}$m^{-3}. With neutral beam heating, the density rises, and the profile peaked due to deep beam refuelling. The ion temperature rose to 23 keV whereas the electron temperature rose to 8-12 keV, for $P_{tot}/n_{eo} \approx 11$ MW/10^{19} m^{-3}. The confinement times were typically 1.3-1.5 times the Goldston prediction. The beam penetration could be improved by reducing the minor radius and this gave strongly peaked density profiles and confinement 1.7 times Goldston. High ion temperatures ~ 23 keV were produced.

Local Energy Transport Analysis

Studies of local energy transport have been carried out for a wide range of plasma regimes: sawtoothing L-mode discharges with ICRF, NBI and combined heating; discharges with ICRF off-axis heating; discharges with 'monster' sawteeth; H-mode cases; experiments at $I_p = 3$ MA with pellet injection; and hot ion modes. The most important results are summarised in the following paragraphs.

The total heat flux $q = q_e + q_i$ across a surface has been calculated from deposition profiles and the time derivative of the stored energy density profile for a series of 'monsters' at 2.5-3.5 MA heated by ICRF, and the results compared with $n_e \nabla T_e$. For each current and radius, a linear relationship was found with slope, χ_{inc}, and offset q_p which represents a non-diffusive 'heat pinch'

and/or convection. At half radius, $\chi_{inc} \approx 2 m^2 s^{-1}$ independent of current, but at three quarter radius, $\chi_{inc} \approx 7.5/I_p(MA)\ m^2 s^{-1}$. This current dependence in the outer region, where ion transport is important, accounts for the favourable global scaling with current. ICRF modulation experiments have been carried out in similar monster discharges, and the amplitude and phase of the perturbed T_e profile allows determination of the electron incremental thermal diffusivity $\chi_{e,inc}$, in addition to the proportion of direct electron heating to collisional heat transfer from the minority species. In the central region, where electron transport dominates, $\chi_{e,inc} \approx 2 m^2 s^{-1}$, consistent with results of heat flux analysis showing no significant reduction of the thermal conductivities χ_e and χ_i as the magnetic axis is approached.

Transport coefficients have been determined from the inward propagation of perturbations caused by a pellet which penetrates only the outer regions of the plasma. The T_e and n_e perturbations propagate inwards on different time scales and, therefore χ_e and D_e can be determined. $\chi_e \approx 3 m^2 s^{-1}$ was found for both the OH and H-mode phases of a divertor discharge, in agreement with the results of sawtooth heat pulse propagation. $D_e = 0.3\text{-}0.6 m^2 s^{-1}$ for OH and H phases. These results are interesting, not only because the transport coefficients have not changed but also because the ratio of χ_e/D_e indicates that the underlying mechanism for the observed anomalous transport might be micromagnetic stochasticity rather than E×B convection.

Analysis of discharges with pellet injection show interesting behaviour, where a novel, transient JET plasma regime is observed when strong additional heating is applied towards the end of the current rise. Strongly peaked sawtooth-free profiles of T_e and T_i are established, with T_{eo} and T_{io} higher than in comparable 'monster' cases. Temperature peaking correlates with density peaking. A sharp variation of ∇T_e, ∇T_i (when available) and ∇n_e is observed at a radius $x_p \approx 0.5$ (see Fig.101). Transport analysis shows that the local energy confinement improves for radius $x < x_p$ (leading to an improvement (< 25%) in the global value of τ_E): both electron and ion thermal conductivity are reduced by a factor 2-3 for $x < x_p$.

It is tempting to relate the observed regime to the suppression of the so-called η_i-mode, as a consequence of density peaking. The value of η_i uncertain, but, in cases where T_i profiles have been measured, these are similar to those of T_e. Thus, the evaluation of η_e is likely to be a reliable estimate of η_e, under reasonable assumptions of the n_i profile. All estimates of η_e and η_i show that these reach very low values (< 0.5) just after pellet injection, increasing gradually in time to values in excess of 3 in the region $x < x_p$ before the end of the good confinement phase (see Fig.101). This may indicate that η_i exceeds the predicted threshold limit η_{ic} without noticeable change in energy transport, or that η_{ic} is larger than 1.5, a value usually assumed. Notice that $\eta_e \gg 3$ for $x > x_p$ in these

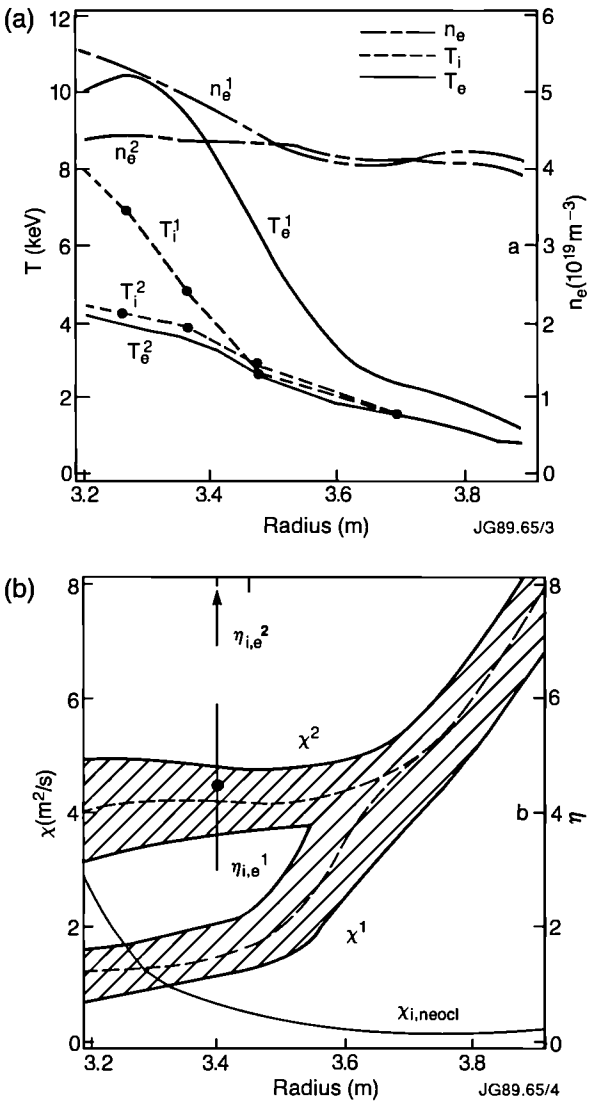

Fig.101: (a) Experimental profiles of T_e, T_i and n_e for a pellet shot (Pulse No:17279). 1 refers to the phase of enhanced confinement (t = 44.6s), 2 to the following 'normal' phase (t = 45s); (b) corresponding 'experimental' thermal conductivity χ and values of η_e and η_i at r=3.4m, t = 44.6s. The neoclassical (Chang-Hinton) value of χ_i at t=44.6s is given for comparison.

experiments, and through almost the entire plasma cross-section for most JET discharges without pellets.

Other observations yet to be explained are: the strong reduction of electron energy transport; the fact that sufficiently vigorous central heating is required to produce the increase in ∇T_e and ∇T_i, not observed so far with NBI alone; the MHD events at the end of the enhanced confinement phase; the correlation, observed so far, with the evolution of the current density profile.

The analysis of the hot ion regimes in JET shows that the main transport losses in these discharges are through the ion channel: χ_i increases with radius and can be an order of magnitude larger than χ_e. For $\rho > 1/4$ (ρ being the normalised radial coordinate), χ_i is larger than the neoclassical value by at least a factor 20. The anomaly of χ_i is a general result. In most cases where the electron

and ion heat fluxes can be separately determined, it is found that $\chi_i \approx \alpha \chi_e$ with $\alpha \gtrsim 1$. No quantitative relationship between the observed χ_i and the one predicted by the so-called η_i instability has been established, so far. Qualitatively one can say that peaked density profiles and improved confinement are generally correlated.

Predictive 1½-D equilibrium-transport codes have been extensively used to test models of the local heat fluxes q_e and q_i. The aim has been to assess the performance of the models on the basis of the capability to reproduce:

- the observed global scaling laws for the energy content W (or equivalently the energy replacement time τ_E);
- the shape of electron and ion temperature profiles;
- the time evolution of the profiles.

Particular attention has been dedicated to models of q_e and q_i proposed at JET, such as the critical temperature gradient model of Rebut and Lallia (1988) and the critical pressure gradient model of Thomas (1988). Predictions of microinstability based models, such as the so-called η_i model of χ_i have also been tested.
The main results can be summarised as follows.

- It is particularly difficult to distinguish between the Rebut-Lallia and Thomas models when ohmic and L-mode discharges (including 'monsters' and off-axis heating cases) are considered. Both, simulate well the 'resilient' T_e profiles observed in JET discharges without adhoc modifications in the external region of the plasma. Such modifications, leading to increased transport, are required if the microinstability based models quoted above are used;
- The Rebut-Lallia model can also simulate the transition from L to H modes, provided the formation of a temperature pedestal inside the separatrix is prescribed (see Fig.102). This is consistent with the analysis of H-mode results showing that the main improvement in confinement in the H-mode is in the edge plasma;
- Uncertainties remain with respect to the validity of all the considered models in the vicinity of the magnetic axis. These uncertainties may reflect an intrinsic deficiency of the models but are also related to the inadequate evaluation of important quantities such as local power deposition profiles, non-thermal energy content and local shear;
- All simulations performed confirm that χ_i is the same order as χ_e or larger. The theoretical models of χ_i based on the so-called η_i- instabilities tested have not been successful in quantitatively explaining the observed ion heat fluxes in the various JET regimes;
- A predictive transport code has also been used to simulate the propagation of a perturbation $\tilde{T}_e$ in electron temperature following a sawtooth crash. The $\tilde{T}_e$ evolution depends on the linearised expression of the heat flux q_e and is not simply related to the local value of χ_e. Results so far refer to the Rebut-Lallia and the Thomas models. One important feature of χ_e^{HP}, the value of χ_e derived experimentally from heat pulse propagation measurements, is its weak (or no) dependence on input power. This feature is better simulated by the Rebut-Lallia model. A relative strong dependence of χ_e^{HP} on Z_{eff} implied by the analysis of experimental data is not observed in numerical simulation. This might show a possible line of improvement for the considered models;
- Both models predict an inverse dependence of χ_e^{HP} on plasma current. These also predict that χ_e^{HP} depends weakly on plasma minor radius except close

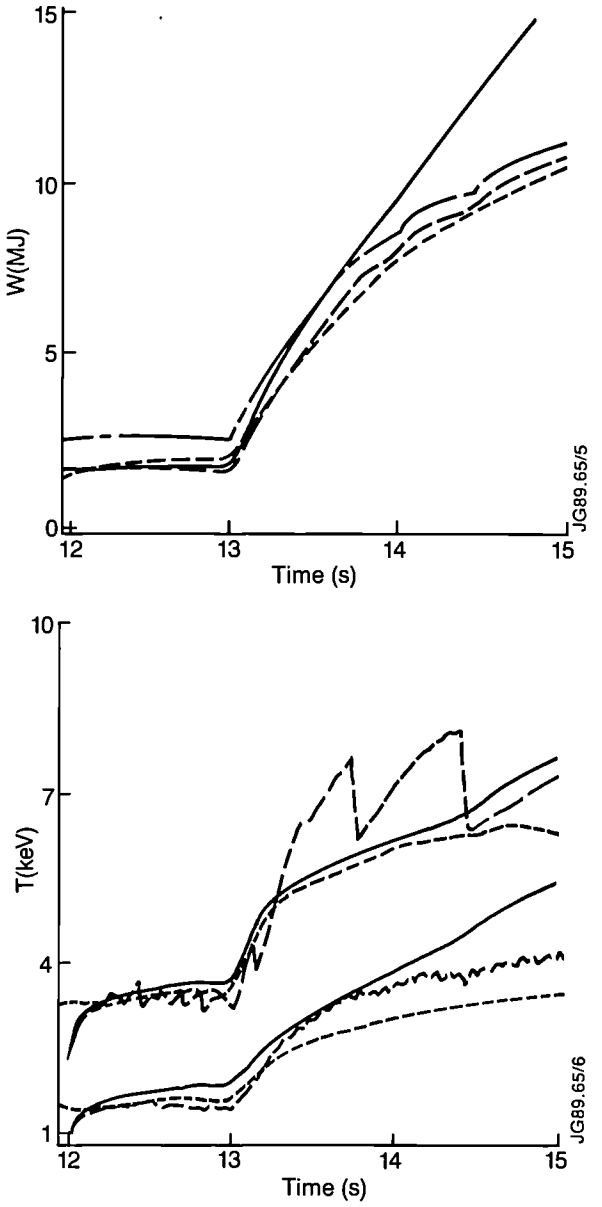

Fig.102: Results of the simulation of an H-mode discharge at 4 MA (Pulse No:16297): a) time evolution of energy content from models (PT—, RL ...) and measurements (magnetic ---, diamagnetic - - -); b) time evolution of central and average T_e from models (PT—,RL ...) and ECE (- - -)

to the plasma boundary region, where it increases sharply. This is qualitatively consistent with available experimental results but more work is required and is being carried out for quantitative comparisons.

Particle and Impurity Transport

Plasma and heating performance in JET is aimed at maximizing the fusion product, $(n_D(0)\ T_D(0)\ \tau_E)$, while maintaining an average electron density $<n_e> \cong 4\times10^{19}\mathrm{m}^{-3}$. This requirement suggests maximizing the profile peakedness, $n_e(0)/<n_e>$, and plasma purity, $n_D(0)/n_e(0)$.

The factors controlling the observed density profiles for electrons, deuterons and impurities are:

(a) density transport behaviour;
(b) neutral beam injection (NBI);
(c) elements of particle removal, (i.e. pumping by limiter and wall materials in inner-wall, outer-limiter and X-point operation).

Electron Density Transport

Electron density dynamics in JET have been measured in different ways to determine the appropriate transport description and the corresponding coefficients. The model electron flux is expressed as $\Gamma_e(r) = -D_e(r)\ \nabla n_e + \Gamma_p$, where Γ_e is the electron flux, D_e is the diffusivity and Γ_p is a convective flux, $\Gamma_p = n_e V_p$. The electron density profile is then controlled by the continuity equation:

$$dn_e(r)/dt = -\mathrm{div}\ \Gamma_e(r) + S_e(r)$$

where $S_e(r)$ and $n_e(r)$ are the electron source and density profiles, respectively. The coefficients $D_e(r)$ and $V_p(r)$ have been determined by various measurements and analysis, as follows:

- Electron density profile evolution by modulation of electron sources, when ICRF (edge source) or NBI (core source) power is applied, giving $D_e(r)$ and $V_p(r)$[1,2];
- Rate of increase of central electron density during density ramp-up using gas injection fuelling, yielding $V_p(a)$[1], where a is the minor radius;
- Refuelling of the centre between sawteeth giving $V_p(r \le r_c)$[1], where r_c is the sawtooth mixing radius;
- Propagation of density pulses produced by sawtooth crashes, using reflectometry[3], yielding D_e in the region $r > r_c$;
- Density profile evolution from a hollow shape, $(dn/dr > 0)$, to a peaked state after pellet injection, giving $D_e(r_1)$ and $V_p(r_2)$[4];
- Density profile relaxation following pellet injection[4], giving $D_e(r)$ and $V_p(r)$;
- Langmuir probe measurements of the plasma edge giving $D_e(a)$[5].

The observations may be summarized as follows:

- Electron density dynamics in JET can be described well by the given flux model;
- The deduced electron density diffusivity may be expressed as a sum of neoclassical and anomalous contributions, $D_e = D_e^{NEO} + D_e^{AN}$ where $D_e^{AN} \gg D_e^{NEO}$. D_e has a low value in the plasma core and rises to a maximum at the edge. The form $D_e(r) = D_0(1 + 2r^2/a^2)$, with $0.3 \le D_0(\mathrm{m}^2/\mathrm{s}) \le 0.5$, fits most data satisfactorily;
- The inferred pinch velocity may be expressed as a sum of neolassical and anomalous contributions, $V_p = V_p^{NEO} + V_p^{AN}$ where $V_p^{AN} \gg V_p^{NEO}$. Moreover, V_p^{AN} has a different spatial variation than V^{NEO}, except near the plasma centre. $V_p(r) = -V_0(r/a)^{2-3}$, with $0.4 \le V_0(\mathrm{m/s}) \le 1$;
- $D_e \neq f(n_e, n_e(r), S_e(r), P_{AUX})$. The density diffusivity seems not to depend on average electron density, on the shape of the density or the source profiles, nor on the kind of heating applied, whether Ohmic, ICRF and NBI, or the power level;
- The diffusivity appears to have a dependence on the electron temperature or its gradient, $D_e = f(T_e, \nabla T_e)$, and the volume average $<D_e>$ appears to be inversely proportional to the plasma current, $<D_e> \propto I_\phi^{-1}$[6].

An assessment of the behaviour of the profile controlling elements in a reference high performance JET plasma has been made with a view to determining the density profile that might obtain under present machine conditions, and the additional measures needed for obtaining more peaked profiles. With core fuelling restricted to the projected NBI, and without means of active recycling control, it is unlikely that significant profile peakedness can be achieved in steady state, $n_e(0)/<n_e> < 2$. Electron density profiles with peak-to-average ratio $n_e(0)/<n_e> \sim 3$ would be possible with simultaneous core fuelling using PI and NBI, and edge pumping to reduce the recycling coefficient to ≤ 0.85 in order to maintain steady state [7].

Impurity Transport

To assess the behaviour of deuteron concentration, $n_D(0)/n_e(0)$, it is necessary to determine the sources and transport of impurities in the plasma. Assessments of mechanisms of impurity production and of the source strength in terms of plasma edge properties has been carried out. Impurity transport modelling has been performed for a variety of plasma regimes and in a wide range of parameters in order to infer ion charge state distributions and to interpret measured spectral line intensities. This procedure gives an estimate of $<D_z>$

for the impurity ions, assuming a form for $V_p(r)=2<D_z>r/a^2$[8]. $<D_z>$ thus deduced is indistinguishable from that measured directly for electrons by methods described above.

This conventional procedure for impurity transport analysis is precarious, and is not suited to solving the problem in hand, which is to determine the interaction between density profiles of the many particle species present in the plasma in order to determine how fuel concentration will respond when one of the profiles is perturbed. This will occur when new sources are added, such as pellet injection and NBI for core fuelling, or helium ash source in the plasma core, or when a new impurity species is introduced at the edge, such as new wall/limiter materials. Thus, there is need for direct measurements of impurity density profiles, simultaneously with electron and deuteron density profiles, from which impurity dynamics may be deduced.

Impurity density profile evolution and associated transport for high-Z impurities may be deduced from time dependent tomographic measurements of soft X-ray emissivity profiles when the impurity species is known and when a reliable model for the ion charge state distribution can be employed. In analysis of nickel injection experiments in JET[9], the ionization states of nickel responsible for the observed soft X-ray emission at energies E>2keV, Ni^{+25} and Ni^{+26}, are described well by the coronal equilibrium. Fig.103 shows the time evolution of the radial soft X-ray emissivity profile in the horizontal mid-plane after a trace amount of nickel is injected into the plasma at 10.99s. Evolution of the emissivity profile, and therefore, movement of the injected nickel can be followed with good spatial and temporal resolution. Impurity transport analysis of these measurements has been made using a model flux as before, $\Gamma_z=-D_z\,\nabla n_z+n_z\,V_p$, where $V_p(r)=2D_z\,r/a^2$. The calculations yield that the observed slow evolution of the emissivity profile for $\Gamma \leq r_{q=1}$ between sawteeth implies small nickel transport in this region during this period, that major redistribution of nickel occurs in the q=1 region during a sawtooth, that nickel across $r_{q=1}$ mainly during the sawtooth cash, that $D_{Ni}(r \leq r_{q=1}) \cong 0.04\,m^2/s \cong D_{Ni}^{NEO}$, and $D_{Ni}(r > r_{q=1}) \cong 1\,m^2/s \gg D_{Ni}^{NEO}$ during the quiescent period between sawteeth.

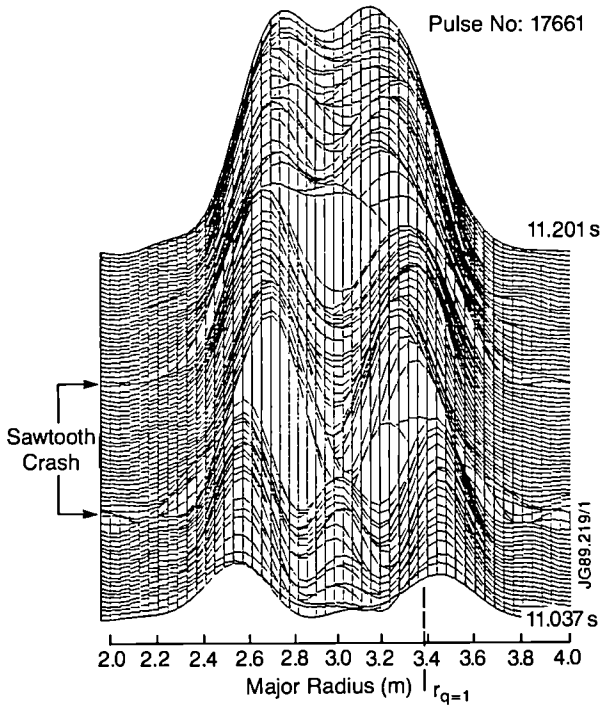

Fig.103: Evolution of the radial profile of soft X-ray emissivity. The background has been subtracted to show the contribution due to injected nickel only.

Temporal evolution of density profiles for the dominant low-Z impurity, carbon in JET, has been deduced from measurements of visible Bremsstrahlung (VB) emissivity profiles, and from charge-exchange recombination spectroscopy (CXRS) of carbon[10]. Absolute continuum emission at 523.5nm wavelength is measured, using a 15 chord poloidal array, to deduce $Z_{eff}(r,t)$ by Abel inversion. From other measurements, it is known that carbon and oxygen are the main contributors to Z_{eff}, and that $n_c/n_o \cong 3$. Then, $n_c(r,t)$ can be deduced with good temporal resolution in the region with $T_e > 200$eV. Fig.104 shows a sequence of profiles of n_c/n_e after pellet injection, using the VB measurement. For comparison, a profile from the CXRS measurement is also shown. At present, only qualitative inferences about carbon density transport have been drawn[10]. The VB measurement, with good temporal and spatial resolution, is well suited for quantitive analysis of low-Z impurity dynamics in JET.

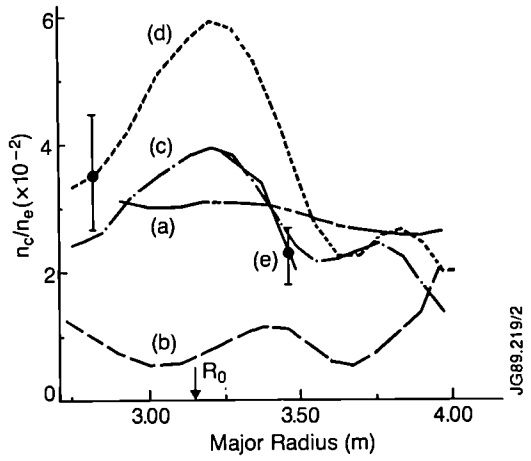

Fig.104: Sequence of radial profiles of carbon concentration, using the VB measurement, for a pellet injection fuelled plasma. (a) is the pre-pellet equilibrium profile, (b), (c) and (d) are respectively at 0.1s, 0.9s and 1.2s after pellet injection. Profile (e) is from the CXRS measurements, and corresponds to (c) temporally.

Correlations of Thermal and Particle Transport

The different regimes (OH, L-mode, H-mode) observed in JET are at present classified according to their quite different observed global energy and particle confinement behaviour. An important next objective is to devise

a measure by which to distinguish between different confinement regimes. This should determine if they represent a transition from one dominant mechanism of radial thermal and particle losses to another, or merely changes in the transport coefficients or in the boundary conditions and source profiles. Moreover, it is necessary to exclude from the large number of contending transport models. Accurate measurements of correlations between thermal and particle transport in the different confinement regimes are necessary in order to be able to separate the different regimes. To this end, measurements are in progress to determine radial thermal and particle diffusivities, χ and D, simultaneously, and in the same spatial region. Three transient methods have been employed to deduce electron diffusivities[11]:

(a) analysis of inward propagation of electron temperature and density perturbations produced when a small pellet is injected into the plasma;
(b) measurement of velocity and damping of electron temperature and density pulses propagating outwards following sawtooth collapse;
(c) time dependent transport analysis applied to slightly non-stationary plasmas.

TABLE XI

Some Elements of the Radial Transport Matrix

OH Limiter Plasma [11]				
	χ_e (m^2/s)	D_e (m^2/s)	$-\Gamma_p$ ($10^{18}/m^2 s$)	$\rho=r/a$
a	2.8 ± 0.3	0.4 ± 0.1	2 ± 0.7	$0.5\leq\rho\leq0.6$
b	2.9 ± 0.4	0.4 ± 0.2	—	$0.6\leq\rho\leq0.8$
c	—	$0.4^{+0.2}_{-0.1}$	$1.4^{+5}_{-0.5}$	$\rho\approx0.67$

NBI Heated H-mode Plasma				
	χ_e (m^2/s)	D_e (m^2/s)	χ_i (m^2/s)	$\rho=r/a$
a	3 ± 0.5	0.3–0.6	1–3	$0.4\leq\rho\leq0.6$
b	3 ± 0.6	—	—	$0.5\leq\rho\leq0.7$
c	2(d)	0.2–0.3 0.3–0.4	—	$\rho\approx0.5$ $\rho\approx0.67$

where
(a) Perturbations of n_e and T_e by pellet injection[11].
(b) Sawtooth density and heat pulse propagation[3,15].
(c) Time dependant transport analysis, 'flux-gradient' method[11]. Inferred χ is for single fluid plasma.
(d) $I_\phi=2MA$, $B_\phi=2T$, different from that for the other data.

Table XI summarizes the observations[12], and shows that χ_e and D_e deduced using the three methods are in agreement. The pellet injection method entails modelling of propagation of perturbations as shown in Fig.105. Different models for the electron thermal flux have been tested. The pellet injection measurements seem to

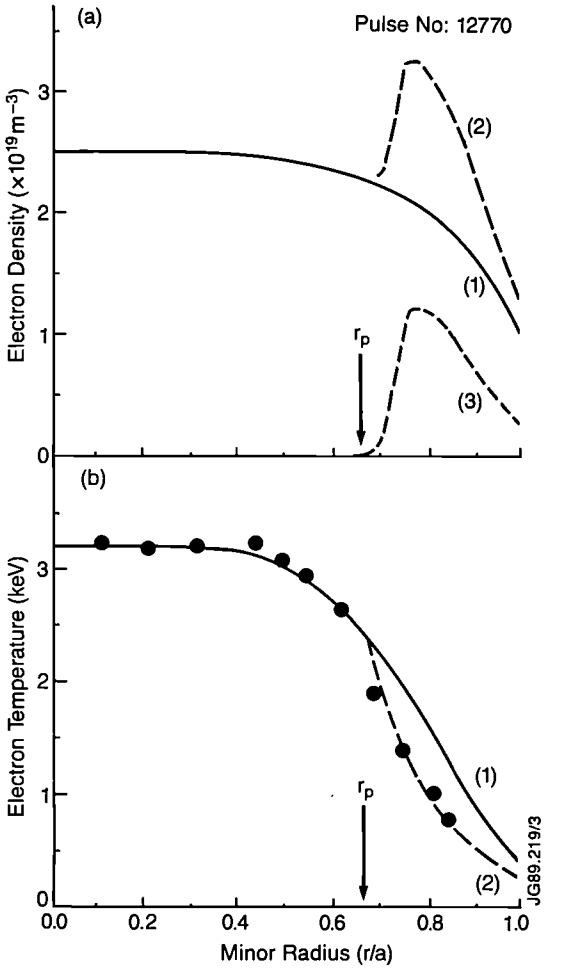

Fig.105: Electron temperature and density profiles immediately before (1) and (2) pellet injection, and the calculated pellet deposition profile (3). The perturbed profiles (2) are those used as the initial conditions for the transport calculation. The circles are the data points from the ECE measurement (KK2).

exclude the non-linear χ_e model ($Q_e=-n_e\chi_e\,\nabla T_e$, with $\chi_e\propto(\nabla T_e)^6$) in favour of the diffusive with constant heat pinch description of thermal fluxes in JET, ($Q_e=-n_e\chi_e\nabla T_e+Q_p$, where Q_p is the heat pinch). The ion thermal diffusivity χ_i can also be determined using pellet injection, by analyzing propagation of an ion temperature perturbation. Since the ion temperature cannot at present be measured with the required resolution, propagation of perturbations of thermonuclear neutron emission is employed, as witnessed by a multichord neutron camera viewing a poloidal cross-section of the plasma from above, to deduce χ_i[12]. Thus, simultaneous direct measurements yield $\chi_e=2.9\pm0.4\,m^2/s$ and $D_e=0.4\pm0.2\,m^2/s$, giving $\chi_e/D_e=7.2\pm3$ at $0.5\leq r/a\leq0.7$ in ohmic heated plasmas on the outer belt-limiter. H-mode plasmas, limited by a magnetic separatrix formed during X-point operation, with $\cong8$MW of NBI heating, are indistinguishable from OH plasmas in respect of χ_e, D_e and χ_e/D_e. The ion thermal diffusivity has also been determined in the specified

region for the H-mode plasma, yielding $1 < \chi_i(m^2/s) < 3$, simultaneously with $\chi_e = 3 \pm 0.5\, m^2/s$, giving $0.3 \leq \chi_i/\chi_e \leq 1$.

The large value of χ_e/D_e would suggest that micromagnetic stochasticity[13,14], rather than $\tilde{E} \times B$ convection, may be the key mechanism in the observed anomalous radial thermal transport in JET. The similarity of OH limiter plasmas and NBI heated H-mode plasmas in respect of electron thermal and particle transport behaviour in the plasma interior suggests that the same underlying mechanism of anomalous transport is operative in the two cases, although they are quite different in respect of magnetic configuration, temperature range, and density profile shape. The intrinsically better particle confinement (versus energy) witnessed here, which will similarly affect recycled impurities and helium ash, may make fuel dilution rather than energy confinement the critical issue in future reactor oriented tokamak experiments.

References

[1] A. Gondhalekar, et al., Bull. Am. Phys. Soc. **30** (1985) 1525, and JET Report, JET-P(85)31;

[2] A. Cheetham, et al., 13th Eur. Conf. on Controlled Fusion and Plasma Physics, Schliersee, FRG (1986), Europhys. Conf. Abstracts, Vol.10C, part I, p240;

[3] A. Hubbard, et al., 13th Eur. Conf. on Controlled Fusion and Plasma Physics, Schliersee, FRG (1986), Europhys. Conf. Abstracts, Vol.10C, part I, p232;

[4] A. Gondhalekar et al, Proc. 11th IAEA Conf. on Plama Phys. and Contr. Nucl. Fusion Research, 1986, **3** (1987) 457;

[5] P. Stangeby, et al., Plasma Phys. and Contr. Fusion **30** (1987) 1839, and JET Report, JET-IR(87)18;

[6] J. O'Rourke, Private Communication;

[7] A. Gondhalekar, et al., Bull. Am. Phys. Soc., **32** (1987) 1839, and JET Report, JET-IR(87)18;

[8] K. Behringer, et al., Proc. 11th IAEA Conf. on Plasma Phys. and Contr. Nul. Fusion Research, 1986, **1** (1987) 197;

[9] N. Hawkes, et al., 16th Eur. Conf. on Controlled Fusion and Plasma Physics, Venice, Italy, (1989);

[10] P.D. Morgan et al., 16th Eur. Conf. on Controlled Fusion and Plasma Physics, Venice, Italy, (1989);

[11] A. Gondhalekar, et al., to be published in Plasma Physics and Controlled Fusion, (1989);

[12] A. Cheetham, et al., Proc. 12th IAEA Conf. on Plasma Phys. and Contr. Nucl. Fusion Research, 1988, Paper IAEA-CN-5o/I-2-2;

[13] J.D. Callen, Physical Review Letters, **39** (1977) 1540;

[14] P.H. Rebut, et al., Proc. 11th IAEA Conf. on Plasma Phys. and Contr. Nucl. Fusion Research, 1986, **2** (1987) 187;

[15] B.J.D. Tubbing, et al., Nuclear Fusion **27** (1987) 1843, and N.J.Lopes-Cardozo, et al., Nuclear Fusion **28** (1988) 1173.

Plasma Edge Effects and Impurity Production

The JET plasma boundary is important as it controls recycling, and hence the density of the plasma. There is also increasing evidence that the extent of the recycling plays a role in determining the global energy confinement of the plasma. With the availability of increased additional heating power, the effect on the plasma boundary parameters and on the impurities has been extensively studied during the present campaign.

The recycling plasma ions cause the release of impurities from the wall by a variety of processes. As the power increased, the impurity level has also become an increasing problem. At low powers the impurity production increased roughly linearly with total heating power. At the highest power levels attained, there is evidence of enhanced impurity production, which may be correlated with localised areas of high surface temperatures. These effects are discussed in the following sections.

Plasma Boundary Parameters

(i) Ohmic Plasmas

Extensive measurements have been made with the new belt limiters. A new reciprocating probe drive has been installed at the top of the torus. This probe has Langmuir elements facing both ion and electron drift directions, and can make up to three reciprocating radial movements of 100 mm, in a period of 400 ms at any time during a discharge. Using the probe with the belt limiter configuration, radial profiles of flux, edge density, electron temperature and floating potential have been obtained for ohmic, ICRH (up to 18 MW) and X-point discharges. Profiles have been recorded from a position about 25 mm inside the last closed flux surface (LCFS) defined by the belt limiters, out to ~ 100 mm in the limiter shadow. Some data on the scaling of edge density and temperature with line average density (ohmic discharges) and total input power (ICRH discharges) show that results are similar to scalings made for the discrete limiters, although absolute values at the LCFS are lower.

Fig.106 shows typical radial profiles $I_s(r)$ using the reciprocating probe for ohmic and ICRH discharges[1,2], with Langmuir elements facing ion and electron drift direction. The radial position shown is relative to the LCFS predicted by magnetic measurements. However, the true radial LCFS position is believed to be where the profiles show a sharp break, and the floating potential shows a peak before falling rapidly to a negative value. This is 15-30 mm radially further out than the position predicted by magnetics (for limiter discharges). The difference is not unreasonable in view of the uncertainty of the limiter contact point and the finite mesh used in the magnetic calculations. In the limiter shadow, all profiles show an exponential fall with radius, although some

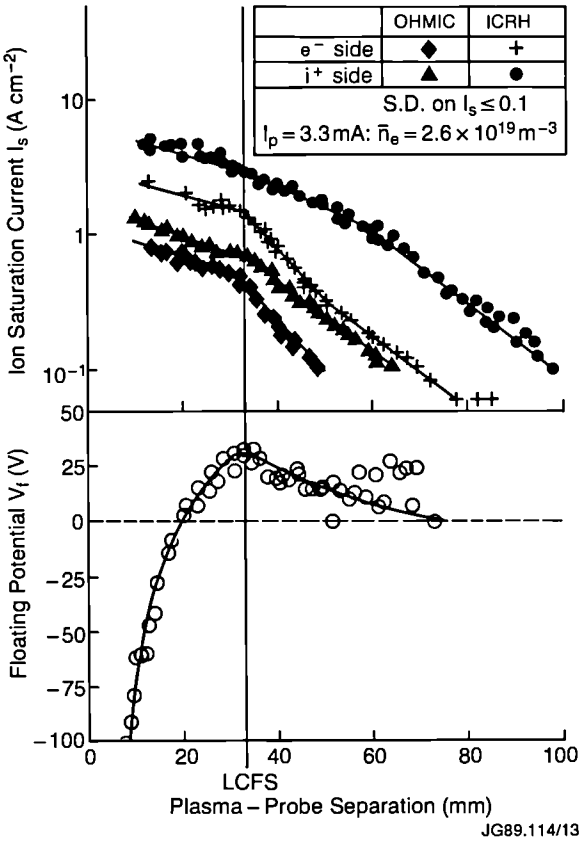

Fig.106: Radial profiles of saturation ion current I_s and floating voltage V_f on the ion and electron drift facing sides of the reciprocating probe in ohmic and ICRF heated discharges.

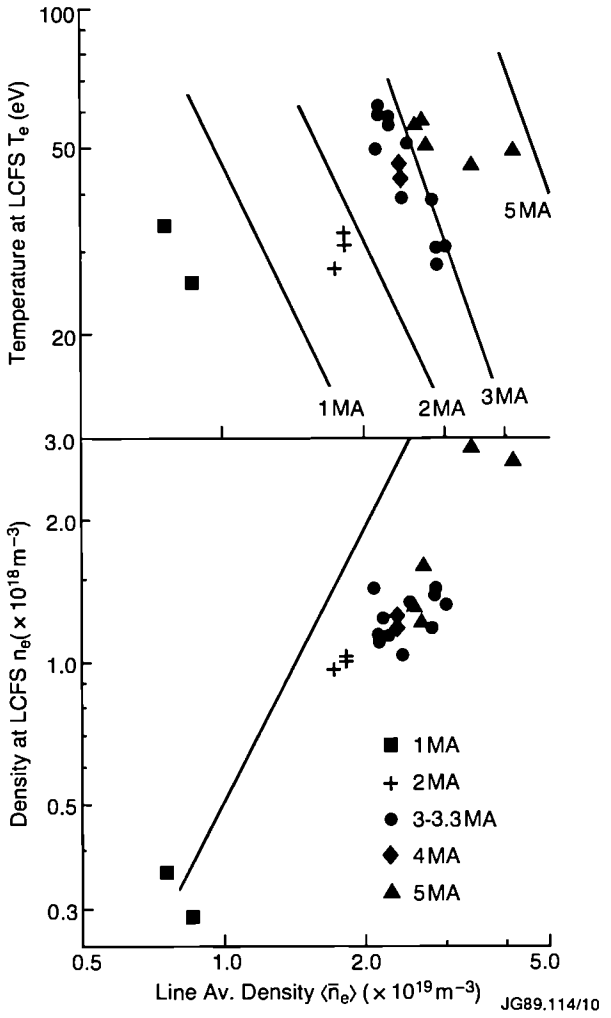

Fig.107: Scaling of T_e and n_e at the LCFS with line average density, $\bar{n}_e$. The points are data from the belt limiter discharges, solid lines are from the earlier discrete limiter scaling.

structure has been observed, particularly in ICRH discharges.

The scaling of the edge parameters n_e (a) and T_e (a) with average plasma density[2], using the belt limiters is compared in Fig.107 with data previously obtained with discrete limiters. In general, the new data is more scattered, but the densities and temperatures are slightly lower than previously.

(ii) Scaling of edge parameters with ICRH power

Fig.108 illustrates the effect of increasing ICRH power on edge density n_e (a) and temperature T_e (a) at the LCFS[3]. The edge density rises almost linearly with total input power, P_T, from an initial 2MW (3.3MA ohmic plasmas), up to 18MW ICRH. Also plotted is the line average density $\bar{n}_e$, which after an initial rise, shows only a small increase with P_T. However, T_e (a) then rises linearly with P_T as $\bar{n}_e$ (P_T) levels off. This behaviour is expected from the simple ID model presented previously,[4], which predicts an almost linear dependence of T_e (a) on P_T, but an almost inverse square dependence on $\bar{n}_e$.

(iii) Neutral Beam Heating

Neutral beam injection produces an increase in density and, in general, steady state conditions are not obtained. Initially, the edge temperature rises, but as the density rises the temperature falls again as expected from scaling behaviour deduced during ohmic heating. No systematic scaling measurements as a function of input power or initial density have been undertaken.

(iv) Measurement of electric fields in the SOL

Experimentally, the electric field in the plasma shows significant increases during RF application[5]. Triple probe measurements have been made 15mm radially outside the LCFS. The potential difference between the probes increases from ~ 2Vcm^{-1} to ~ 40Vcm^{-1} over a poloidal distance of 30mm. Rectifying effects at the probe tips were previously shown to be negligible[6].

Electric field variation with RF power has been studied for different gas minority species. The field increases approximately linearly with RF power but is much lower for H than for ^{3}He minority heating (see Fig.109). Components measured in two directions show the field is oriented at an angle of 60° to the plasma current for the ^{3}He minority heating. For H minority

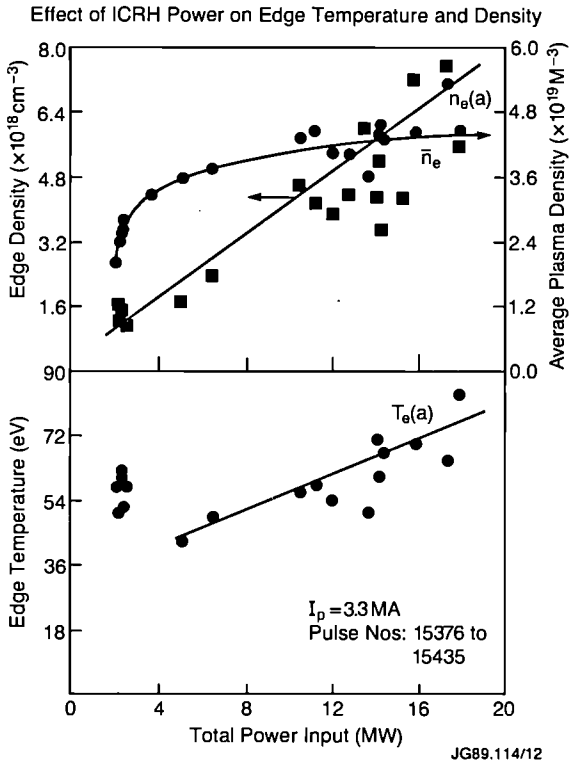

Fig.108: The effect of ICRH power on temperature and density at the last closed flux surface. The change in volume average density $\bar{n}_e$ is also shown.

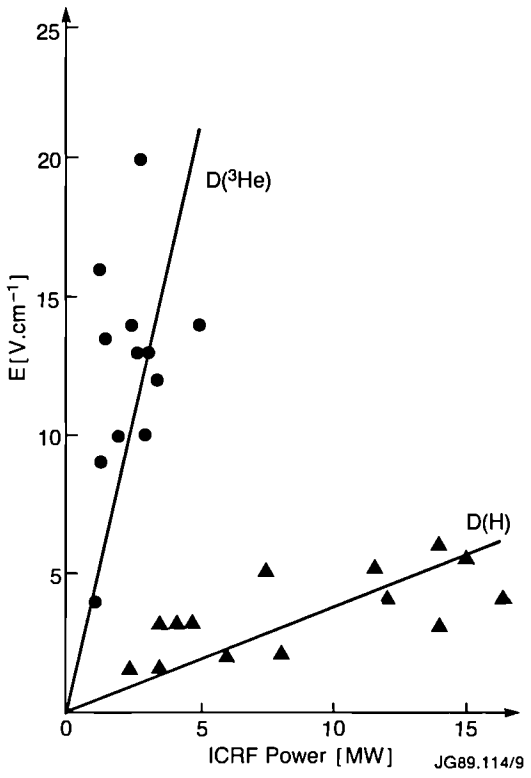

Fig.109: Electric field strength in the scrape-off layer during ICRH for the different minority species ^{3}He and H (I_p=3 MA, B_T=3.4 T)

heating, data are more scattered and the field direction varies from 80 to 200° to the current direction. The field occurred independent of whether or not the antenna closest to the the probes was energised, implying a significant toroidal field extent. Such a field is expected to cause a radial drift ~400 ms^{-1}, comparable to the diffusion velocity in the boundary. Such drifts could cause local outflows, possibly explaining the enhanced ion sputtering and impurity production during ICRH.

(v) Measurements of radial profiles during X-point operation

The reciprocating probe enters the torus just outside the vertical centre-line of the plasma and ion side probes have a connection length of ~2-3 m to the X-point tiles. Only a limited data-set is available for profiles taken during X-point, and X-point with neutral beam injection (NBI = 5-7 MW, H-mode)[7]. Density and temperature profiles are shown in Fig.110. The separatrix is at 0, (i.e. according to the magnetics), indicated by a small peak in the V_f(r) data.

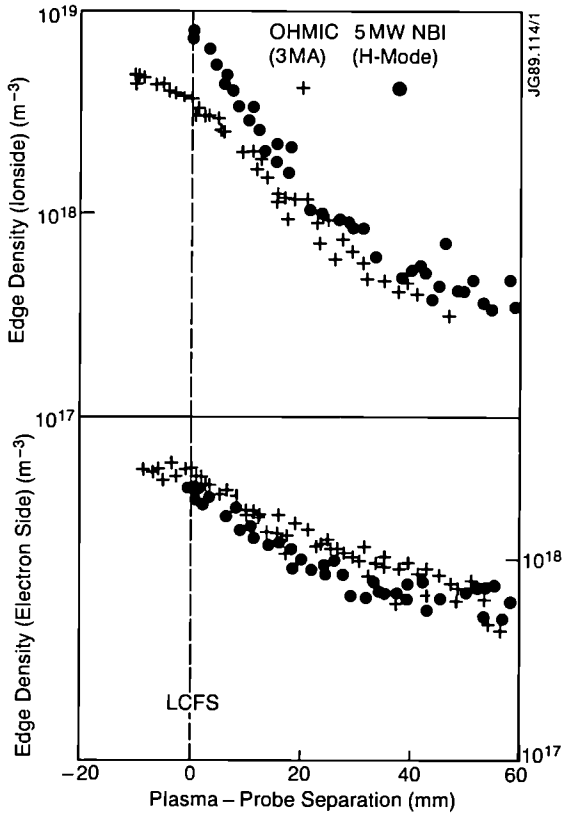

Fig.110: Temperature and density profiles in an ohmic 3 MA discharge and in the same discharge during an H mode after 5 MW NBI has been turned on.

There is no major difference in ion and electron side T_e(r) profiles. However, the ion side n_e(r) profile is steeper than that from the electron side. This could be due to flow from the high density X-point region; from an increasing Mach number with radius; or due to the

probe moving from a collisional to collisionless region. It is unlikely to be due to connection length effects.

The divertor plasma in the vicinity of the X-point target plates has been investigated with an array of eight Langmuir probes mounted in the target plates and with a 2-D view of the radiation from the divertor region. Fig.111 shows profiles of density, temperature and ion saturation current in front of the target plates for a 4.6MA discharge (OH and H-phase with NBI = 14MW). The inner divertor plasma is colder and denser than the outer. More power is carried to the outer divertor, suggesting that the main source of power flow into the scrape-off layer is in the vicinity of the outer mid-plane (ie closer to the outer divertor target). The unequal temperatures lead to thermo-electric currents in the scrape-off layer. Current densities $\leq 10^5\,Am^{-2}$ measured during the H-phase (see Fig.111) correspond to >10% of the mean current density in the discharge [7]. The scrape-off layer current flows from the outer to the inner divertor and returns through the target plates, thus flowing in the same direction as the plasma current.

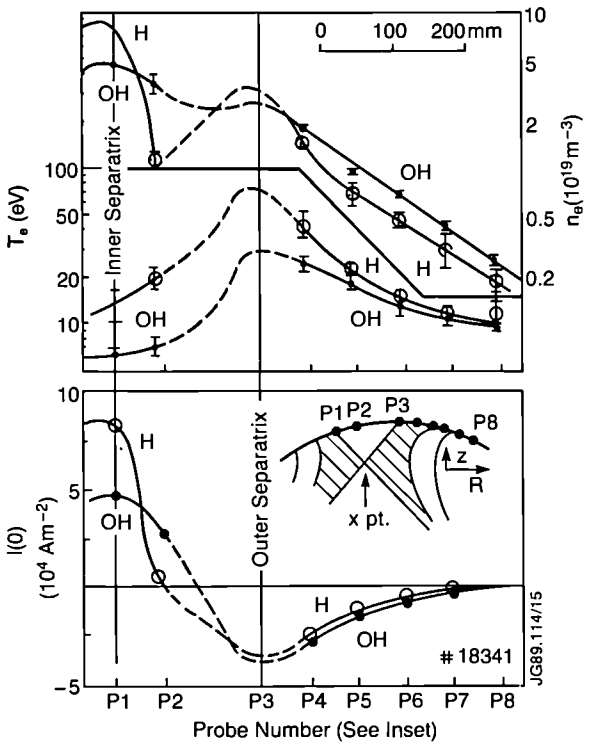

Fig.111: Profiles of density, temperature and ion saturation current in front of the target plates, measured with Langmuir probes mounted in these plates during the ohmic phase of a I_p = 4.6MA discharge and during an H mode with 14MW of NBI.

The estimated power carried by the plasma to the target plates increases from 0.8MW (in the ohmic phase) to 1.9MW (at the end of the H-phase). For most of the discharge (ie L and H-phases), this is about 15% of (P_{tot}-dW_{dia}/dt) but about 25% during the ohmic phase. The separatrix location in the divertor is dependent on plasma conditions. Profiles of I_{SAT} and D_α show that the point where the outer separatrix intersects the divertor target moves to smaller R as the discharge changes from OH to L to H phases. The movement shown is ~1 cm. There is an outward movement when a sawtooth arrives in the plasma edge evident in the D_α profile. These results suggest a β-dependence of separatrix location in the divertor.

Recycling and wall pumping

During the 1988 campaign, the wall pumping effects, observed earlier, continued to be seen. The pumping of the walls and limiters under the present machine conditions and in different modes of operation are shown in Fig.112. The density decay behaviour in a discharge where gas puffing was stopped is shown for three boundary conditions: (a) belt limiters; (b)inner bumper limiter, and (c) elongated plasma limited by the top and bottom wall tiles. The density decays, indicating wall pumping, in all three cases.

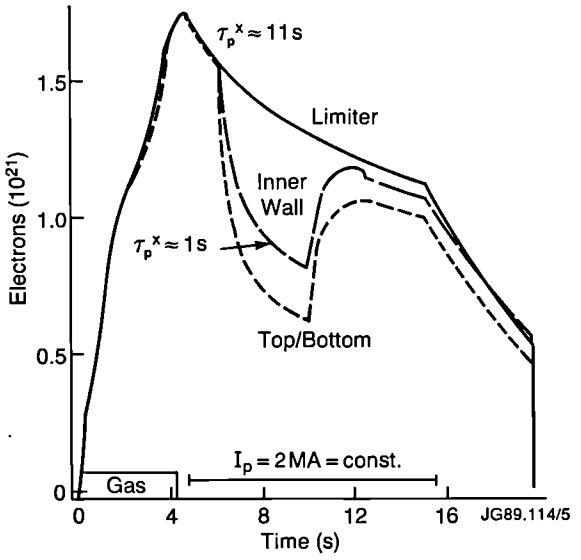

Fig.112: Total electrons in the plasma as a function of time for three discharges, defined by the limiter, the inner wall and the top/bottom of the vacuum vessel.

There are two different pumping mechanisms[8]: (i) the density decay when the plasma resides at a certain surface, and (ii) the density decay when the plasma is moved from one place (eg the limiter) to another (inner wall or top/bottom).

The first mechanism is responsible for a permanent particle loss at a slow rate of on average 5×10^{19} electrons/s. Part of this can be associated with H-C co-deposition on limiter and wall surfaces which are far enough outside the erosion zone. The second mechanism pumps particles at an initial rate of 10^{21} electrons/s and happens only in a transient phase of 1s after moving the plasma. This can be explained by the increase in edge density when the limiter is on the high field (inner

wall) side of a tokamak. The radial expansion of magnetic flux tubes at the plasma edge on the inboard side enhances the screening of recycled neutrals such that the fuelling efficiency is much reduced and, thus, the plasma density decreases provided the particles can stay in the wall for a time of the order of the plasma particle confinement. This effect is expected to be strongest for plasmas limited by the top/bottom of the wall (expansion of field lines) consistent with the experimental observations (see Fig.112).

During helium discharges, hydrogen isotopes are released from the wall and limiter, leading to increases in density. After about five helium discharges, the hydrogen isotope inventory in the walls and limiters is substantially depleted. In subsequent hydrogen isotope discharges, there is enhanced hydrogen pumping by the walls and much larger gas puffing rates are necessary for a given density. This effect saturates after about five discharges.

Impurity production mechanisms

There are three impurities routinely observed spectroscopically in JET: carbon, oxygen and nickel. The carbon levels currently in JET range from 2% to over 10%. The level depends strongly on average density, plasma current and input power. In ohmic discharges, Behringer[9] has shown that a consistent pattern is observed with the concentration decreasing as the density increases. This behaviour is also characteristic of metal impurities though the dependence on density is much stronger with metals[10]. The carbon concentration increases as the plasma current increases. This general behaviour is consistent with the global behaviour of the edge density and temperature and is in good quantitative agreement with physical sputtering by plasma ions at the limiter.

During some phases of JET operation, oxygen concentrations have been at the few per cent level and at high densities it has been the source of a major loss of power by radiation. However, during the year, the oxygen level has been consistently low, typically $\leq 0.5\%$[11]. This may be attributed to the consistent use of helium glow discharge cleaning before each operational day. At its present levels, under most operating conditions, oxygen plays only a minor role in the radiation and Z_{eff}, compared with carbon. The concentration of nickel over the last operational period has been generally in the range 10^{-6} to 10^{-4} of the electron density[12]. At these levels, the contribution to radiation and Z_{eff} can be neglected. During RF heating, nickel levels have occasionally risen to $\sim 0.1\%$ radiating up to 3 MW. Earlier work[13] established that the nickel comes directly from the Faraday shields of the RF antennae. It has also been shown that metal injected into the plasma can be deposited on the limiters and the carbon antennae protection tiles. When the source of nickel stops the nickel is progressively removed from the surface of the limiters by a process of erosion and redeposition[14].

The mechanism of nickel injection into the plasma during RF heating is not understood. There are no data on incident fluxes of ions to the Faraday screens or on their energies. However, the role of the electric field discussed earlier is probably significant. The metallic flux into the plasma is quite reproducible and depends roughly linearly on RF power (5×10^{19} atoms/MW)[13].

Measurements of fluxes from the belt limiter

The fluxes of fuel and of impurities into the plasma from the limiter and the wall are routinely measured using neutral or low ionisation states and calculated values of the photon efficiency. The carbon flux, measured by CIII, is roughly constant with increasing $\bar{n}_e$ (at a given plasma current), while the oxygen flux depends strongly on the condition of the machine. The oxygen flux is always high after an opening of the vacuum vessel, but can drop rapidly to well-conditioned values after only one or two weeks of operation.

Since February 1988, observations have been made of the spatial distribution of emissions from the low ionisation states of fuel and impurity species around the belt limiters. These measurements have been made with a CCD camera with a carousel of narrow-band interference filters centred on strong spectral lines of these species[15]. The spatial distributions of DI, HeI, CI, CIII, or OI and OII have been observed in a variety of plasma conditions and auxiliary heating levels. Some results are shown in Fig.113(a).

The shape of the poloidal distributions varies depending on the species. The lower ionization states (eg. HeI, CI, CII, OI and OII) do not extend any significant distance poloidally away from the belt limiter (<5 cm), whereas the DI and CIII distributions can extend up to 20 cm away from limiter in the poloidal direction. In the case of DI, significant transport away from the limiter is expected via charge-exchange reactions whilst in the case of CIII, the poloidal extent reflects the toroidal transport of the C^{++} ions along the field lines. The distribution of carbon species in different charge states has been modelled using the Monte Carlo model LIM which follows ionisation heating and transport[16]. Good agreement with the experimental results has been obtained, as shown in Fig.113(b).

Impurity Production in High Power Discharges

As the ICRH input power is increased the central density of the plasma increases without external gas puffing. The resulting edge density rise is somewhat greater, being roughly proportional to the total input power (Fig.114). The increase in density is such that the electron temperature in the boundary remains constant at T_e (a) ~ 55eV. The carbon sputtered from the limiter, measured by the CI, increases roughly in proportion to the edge density (see Fig.114). This is expected since a constant electron temperature implies a constant sputtering yield and a constant photon efficiency for the radiating atoms. Similar results are obtained observing CIII light.

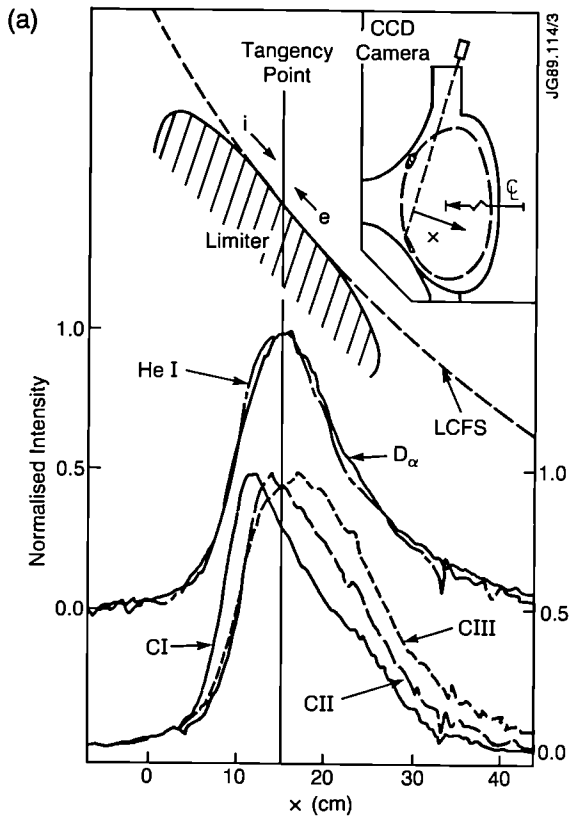

Fig.113(a): Spatial distributions of the low ionisation states of C I, C II, C III, He and D_α around the lower belt limiter in a 3.1 MA discharge with $\bar{n}_e = 1.5 \times 10^{19} m^{-3}$

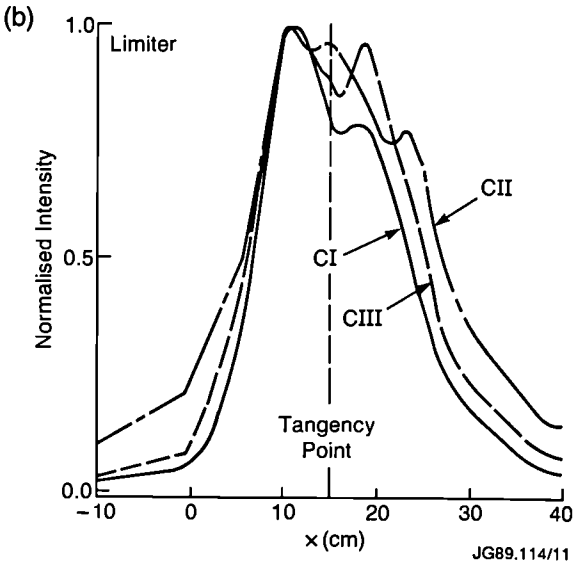

Fig.113(b): Spatial distributions of C I, C II and C III as predicted by the LIM code.

Since the sputtered carbon flux is proportional to the edge density, it is in turn proportional to the total input power (Fig.114). During high power operation, this scaling breaks down, as enhanced carbon erosion occurs at 'hot spots' that appear at the limiter tile edges, typically

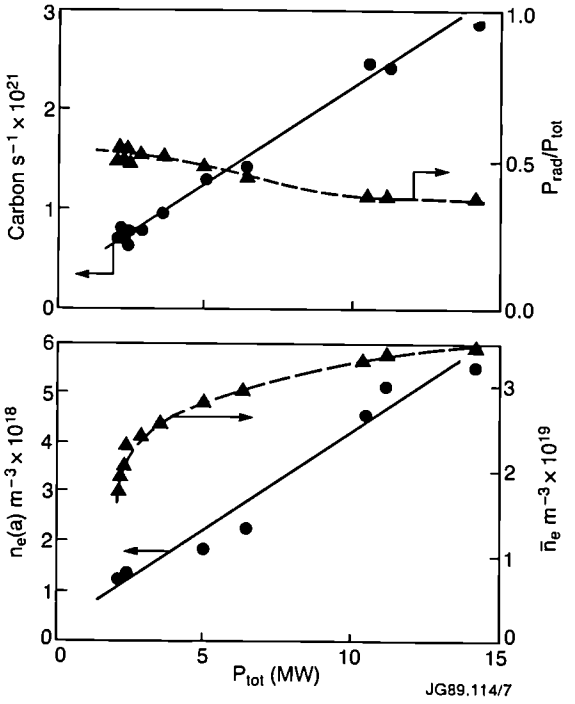

Fig.114: The ICRH power scaling of the carbon influx from the lower belt limiter, the radiated power fraction P_{rad}/P_{tot}, the edge density n_e (a) and the volume-averaged density $\bar{n}_e$ in a 3.3 MA discharge.

with an area of ~10cm^2. In Fig.115, the C III emission associated with a single hot spot on the lower belt limiter and the edge plasma conditions, measured by the built in Langmuir probes are shown as a function of time. With ~28MW of combined ICRH and NBI heating, the edge density rises and the electron temperature remains constant, as observed at lower powers. The CIII

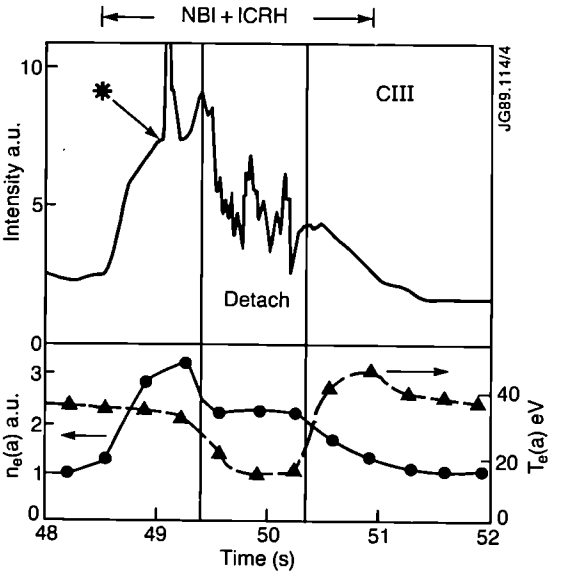

Fig.115: The C III intensity associated with a hot spot on the lower belt limiter and the edge plasma conditions during 28 MW combined ICRH and NBI heating. $I_p = 5$MA, $B_T = 3.2$T, discharge balanced between upper and lower limiters. '' denotes hot spot temperature - 1600°C.*

emission rises in proportion to the edge density up to ~0.5s after the start of the heating, where the signal abruptly rises and saturates. The temperature of the hot spot at this time has risen to ~1600C estimated from the black-body emission measured with the CCD camera. As a result of the massive influx of carbon, the discharge detaches, the total radiation abruptly jumps from ~40% to ~100%, and the edge density and temperature drop significantly. Once the heating power is reduced, the discharge re-attaches and the edge signals and radiated power revert to more typical values.

From the C III observation, it appears that enhanced erosion is occurring at ~1600C probably due to radiation-enhanced sublimation[17]. Unfortunately, the majority of the limiter surface is not observed and it may be that some spots are hot enough for thermal sublimation to be important.

In X-point discharges, there is also good evidence for suddenly enhanced carbon influxes and plasma detachment. Measurements of the tile temperatures with CCD cameras indicate that they frequently exceed 2100°C during H modes. The edge temperature T_e falls to ~2eV and n_e to ~$10^{19}m^{-3}$ and due to the low ionization probability, a substantial fraction of neutrals escape from the divertor. The CCD observations show that the zone where ionisation is likely to occur moves from the divertor to the SOL at the inner wall.

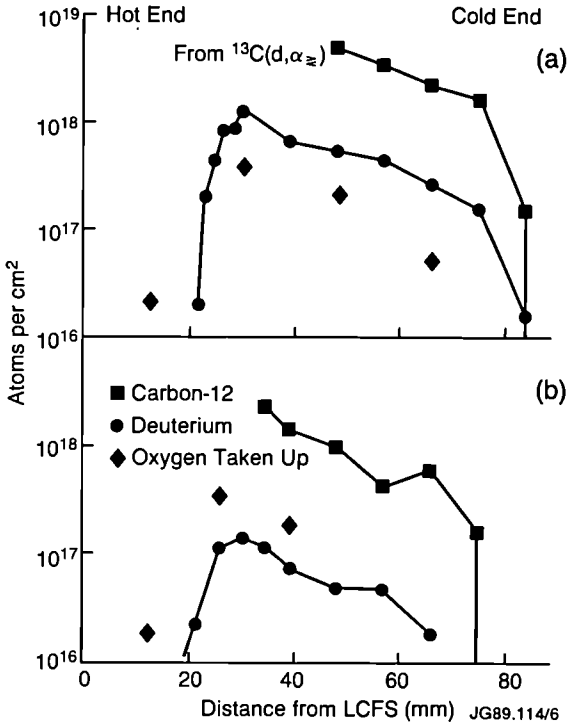

Fig.116: Radial distribution of carbon, deuterium and oxygen deposited on a carbon probe exposed to a single 3MA discharge (a) constant plasma current exposure (b) current rampdown phase.

Erosion and Redeposition

Although of no great concern in JET, erosion of the walls is expected to be a major problem in the next step fusion devices. Due to its long pulse length and relatively high edge temperature, limiter erosion is readily detected in JET. The subject is important not only due to the effect on wall components but because an understanding of erosion and the redeposition helps understanding of the impurity transport in the boundary and is relevant to wall pumping and tritium inventory.

The measurement of erosion and redeposition has been approached in two ways. Firstly, ^{13}C markers have been implanted in probes which are exposed with the Fast Transfer System on a shot-by-shot basis. When the experiment was first performed in 1986, after exposure of the probe to two 5MA pulses both erosion and redeposition were observed on the same area (up to 20mm from the LCFS) [18]. The experiment has been repeated in 1988 in the new belt limiter geometry and probes have been exposed in a time-resolved manner to single 3MA discharges. Erosion is the dominant effect within approximately 25 mm of the LCFS in each phase (ramp-up, flat-top and ramp-down), though some differences in the behaviour during each phase were observed which will be examined further in 1989. Fig.116 shows the radial distribution of the deuterium collected on such a (carbon) erosion probe from the flat-top phase (upper part) and ramp-down (lower part) of a 3MA discharge. In each case the deuterium level is undetectable from the LCFS out to ~25mm from the LCFS. The amount of carbon deposited, as derived from the position of the 13 marker is also shown; the markers are not detectable closer than 30mm from the LCFS. Redeposition of carbon was observed on other parts of the probe.

A second approach has been to make accurate macroscopic measurements of limiter tiles before assembly in JET and then to repeat these measurements when they are taken out at the end of a campaign. Detailed measurements have been made on the discrete limiter tiles exposed during 1986[14]. Erosion was dominant near the last closed flux surface and redeposition occurred at larger minor radii. Typical net changes were ~0.1 mm for both erosion and deposition. Analysis of the redeposited layer showed it to be a layered structure containing nickel and chromium, identified spectroscopically as coming from the Faraday screens of the ICRH antennae. The erosion and redeposition pattern has been compared with a 1-D model. Good agreement between the experimentally measured transition radius from erosion to redeposition and the predicted value is obtained. The absolute value of the measured net erosion is about a factor of 3 less than the theoretical estimate. This is reasonable in view of the integration over many discharges with different conditions.

Recent measurments have been made on the belt limiter tiles exposed during 1987-88 and removed in May 1988. A pattern of erosion and redeposition has again been detected (Fig.117). The net erosion is lower (~ 20μm maximum), consistent with a the larger area. (The

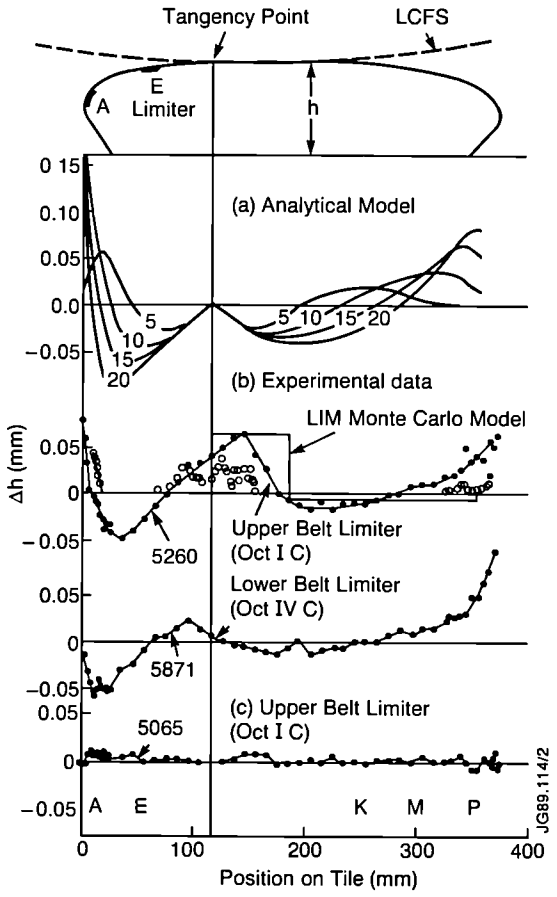

Fig.117: (a):Calculated erosion of limiter tile using analytical model [14] which neglects ionisation in the SOL. Ion current density = 2 Acm^{-2} deuterons, T_e (a) = 50eV, exposure times 5×10^4 s, for different λ_Γ and $\lambda_T = 2\lambda_\Gamma$; (b) spatial distribution of erosion and redeposition on the JET belt limiter after exposure to ~ 4000 discharges in 1987-88. Physical measurements °°°°°; measurements of deposition obtained by sectioning •••••. Monte Carlo calculation using LIM code for T_e (a) = 50eV, $\lambda_\Gamma = 20$mm, $\lambda_T = 40$mm, $D_\perp = 1\,m^2s^{-1}$ n_e (a) = $3 \times 10^{18} m^{-3}$; (c) distribution on belt limiter after 470 discharges; physical measurements.

limiters were exposed to a similar number of discharges to the tiles in 1988). The erosion appears to be toroidally uniform and to be similar on top and bottom belt limiters.

One striking difference between the results from the belt limiters and the earlier discrete limiter is that there is now deposition near the last closed flux surface. This is attributed to reionisation within the scrape-off layer due to higher densities during 1988 operation. New calculations using the Monte Carlo model (LIM) for impurity transport[19] supports this explanation (see Fig.117).

Tritium Inventory

For both safety and economic reasons, it is important to establish the tritium inventory in JET during the D-T operation phase. It is also important to understand the isotopic exchange of tritium with deuterium and hydrogen so that the optimum tritium/deuterium ratio can be established as soon as possible in the D-T phase. The hydrogen and deuterium and tritium inventories have been studied experimentally. Firstly, gas balance measurements have been made by measuring the total gas input and the total gas released from the vacuum vessel both per discharge and over a series of discharges[20]. Measurements made in 1987 - 88 show that typically during the 10 minute period after a discharge 10-30% of the gas is released (ie 70-90% of the gas remains trapped in the vessel). There is a clear correlation between the amount of gas trapped in the vessel and the amount of gas injected. As the amount injected is increased, the fraction which is trapped increases. Although there are small differences between different types of discharge, the overall trend for NB heating, ICRH, pellet injection and X-point discharges is similar (see Fig.118). Integrating over a number of discharges and a longer period of time, the amount of deuterium trapped in the vessel is ~ 50%. When account is taken of the deuterium pumped away as hydrocarbons, the estimated amount left in the vessel is ≈ 40%. This work is being continued to build up a better data base.

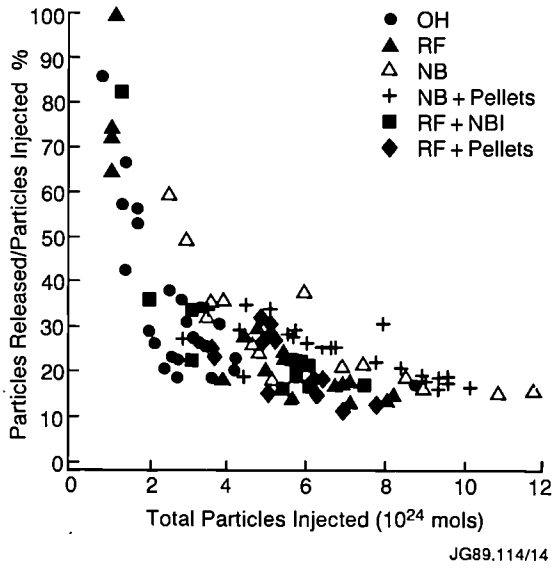

Fig.118: The fractional gas released from the tokamak integrated over a 10 min period after the end of a discharge, as a function of the total number of molecules injected. Results are presented for ohmically heated, ICRH, NBI and pellet injection.

A second approach is to measure the amount of gas trapped in the surfaces of the wall and limiter after a campaign. Samples are only available by venting the torus, so these measurements are normally made during maintenance periods. A detailed analysis of the deuterium in the walls after the 1986 campaign has been made by Coad et al[21]. Samples of wall, limiter tiles and inner bumper limiters were taken. Approximately 5% of the total deuterium injected into the tokamak has been accounted for. Similar samples have also been analysed for tritium[22]. This tritium is produced by (d, d) reactions and the total amount generated can be quite

accurately estimated from the integrated neutron yield. Over the 1986 campaign, 1.7×10^{18} tritium atoms were generated. The tritium analysis was undertaken by vapourising the carbon in an oxygen atmosphere and counting the beta particles from the tritiated water using a liquid scintillation counter. The poloidal distribution of the tritium trapped in the wall is shown in Fig.119. The fraction of the tritium accounted for was in the range 4 - 7%, ie very similar to the deuterium. Less extensive results are also available from samples removed after the 1987 and 1988 campaigns. Analysis of these samples is continuing. In general, the analyses confirm that a much higher fraction of the deuterium used and the tritium created is retained in the vessel.

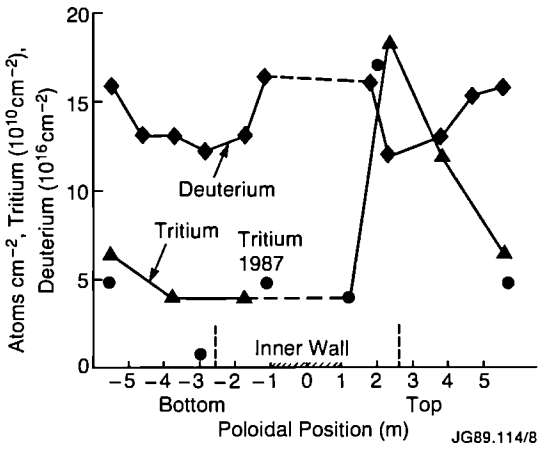

Fig.119: The poloidal distribution of tritium in the walls of JET measured after the 1986 and 1987 campaigns. Analyses of the tritium was carried out using liquid scintillation counters.

A significant amount of deuterium and tritium is released when the JET vacuum vessel is vented to atmosphere[23]. The amount released has in 1987/88 was typically from 7 to 16% of the inventory if the vessel was vented directly after an operational period. However carbonisation reduced the gas release by about a factor of 7, and the amount released into the Torus Hall can be reduced by a factor of 10 to 20 by double venting the torus. Control of the amount of gas (particularly tritium) released may be important after long campaigns using high plasma heating powers, and during the tritium phase.

Altogether the long term gas balance measurements, the amount trapped in the walls and the amount released during venting roughly tally. At present, there appears to be ~10 - 20% of the inventory unaccounted for, but this may be resolved when the different measurements are made over the same time interval.

References

[1] J A Tagle, S K Erents, M Bures, H Brinkschulte, G M McCracken and L de Kock, J Nucl Mat **163-165** (1989)

[2] S K Erents, J A Tagle, G M McCracken, G Israel, H W Brinkschulte and L de Kock, J Nucl Mat, **163-165** (1989)

[3] S K Erents, P J Harbour, S Clement, D D R Summers, G M McCracken et al 16th EPS Conf of Plasma Physics and Controlled Fusion, (Venice, Italy 1989)

[4] S K Erents, J A Tagle, G M McCracken, P C Stangeby and L de Kock, Nuclear Fusion **28** (1988) 1209

[5] S Clement, J A Tagle, M Laux, S K Erents, M Bures, P C Stangeby, J Vince and L de Kock, 16th European Phys Soc Meeting, (Venice, Italy 1989)

[6] S K Erents, J A Tagle, G M McCracken, H Brinkschulte et al, J Nucl Mat **145-147** (1987) 231

[7] P J Harbour, R Behrisch, S Clement, P Coad, L de Kock et al, J Nucl Mat, **163-165**, (1989)

[8] J Ehrenberg, J Nucl Mat, **163-165** (1989)

[9] K Behringer, B Denne, M J Forrest, N Gottardi, M von Hellerman et al, J Nucl Mat, **163-165**, (1989)

[10] K. Behringer, Nuclear Fusion 26 (1986) 751.

[11] P Morgan et al, 16th Eur Phys Soc Conf on Plasma Physics and Controlled Fusion, (Venice, Italy, 1989)

[12] K. Lawson, Private Communication, (1989).

[13] K Behringer, J Nucl Mat, **145-147**, (1987) 145

[14] G M McCracken, D H J Goodall, P C Stangeby, J P Coad, J Roth, B Denne and R Behrisch, J Nucl Mat, **163-165** (1989)

[15] C S Pitcher, P C Stangeby, G M McCracken and D D R Summers, 16th Eur Phys Soc Conf on Plasma Physics and Controlled Fusion (Venice, Italy, 1989)

[16] P C Stangeby, C Farrell and L Wood, Contributions to Plasma Physics, **28**, (1988) 501

[17] J Roth, J Nucl Mat, 145-147 (1987)

[18] R Behrisch, J P Coad, J Ehrenberg, G F Neill, J W Partridge et al, J Nucl Mat, **163-165** (1989)

[19] G M McCracken, R Behrisch, J P Coad, D H J Goodall et al, 16th Eur Phys Soc Conf on Plasma Physics and Controlled Fusion (Venice, Italy 1989)

[20] R Sartori, G Saibene, J L Hemmerich and M A Pick, 16th Eur Phys Soc Conf on Plasma Physics and Controlled Fusion (Venice, Italy, 1989)

[21] J P Coad, R Behrisch, H Bergsaker, J Ehrenberg, B Emmoth et al, J Nucl Mat **163-165**, (1989)

[22] D H J Goodall, G M McCracken, R A Causey, J P Coad, O N Jarvis and GSadler, J Nucl Mat **163-165** (1989)

[23] J P Coad, J Orchard, J Monaghan, J Nucl Mat, **160**, (1980) 95

MHD Behaviour

The MHD Topic Group has concentrated its programme of work on the understanding and control of disruptions

and on furthering understanding of sawtooth instabilities and their stabilization in tokamak plasmas. In addition, the effect on MHD instabilities of introducing pellets into the plasma have been studied. These features are described in more detail in the following sections.

Disruptions

Recently, investigation of disruptions in JET focussed on the behaviour associated with the decay of the plasma current. The observed rapid current decay appears to be due to a sudden cooling of the plasma and this had led to further understanding of two related phenomena: the negative voltage spike, and the generation of runaway electrons.

Negative Voltage Spike

It is surprising that following the rapid drop in plasma temperature in the disruption, the plasma current increases momentarily. The negative voltage associated with this current increase has always been considered an important element of tokamak disruptions. Fig.120(a) shows the current increase and negative voltage spike during a 1.8 MA disruption.

The increase in plasma current and the negative voltage spike are brought about by a rapid flattening of the current density profile during the disruption process. The flattening of the current is expected to precede the final temperature collapse. The fact that the voltage spike follows the collapse was initially difficult to understand. An explanation has now been proposed. The current flattening results in a current increase in the central region of plasma with a reverse current induced at larger radii. This reverse current and its associated negative voltage are trapped until the temperature collapse allows a sudden release by rapid diffusion through the cold plasma. Fig.120(b) shows the result of a simulation in which this process is modelled by flattening a peaked current density profile ($q(a)/q(o)=5$) over 75% of the minor radius. The current profile is allowed to evolve resistively in a plasma initially at 5 eV, the temperature falling as the current falls to model the effect of the reduction in ohmic heating. It is seen that the calculation is in reasonable agreement with experiment.

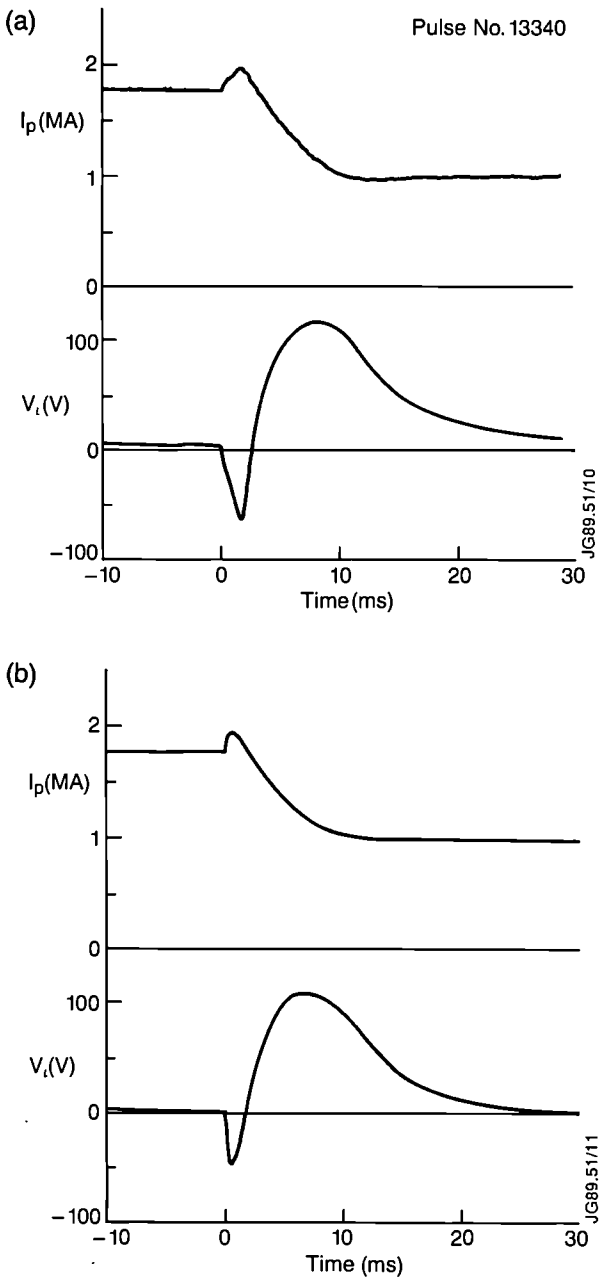

Fig.120: (a) The current increase and negative voltage spike during a 1.8MA disruption and (b) simulation of this process.

Runaway Electrons

The large electric fields induced in the disruption generate runaway electrons. This is seen in the 1 MA current plateau in Fig.120(a). It has been suggested that the disruptive fall in temperature is due in part to a rapid ($\sim 100\mu$s) influx of impurities. The model predicts a drop in temperature to <10 eV and an increase in electron density by a factor ~ 5. The electron distribution function is non-Maxwellian in such a cooling process, making the calculation of runaway generation complex. A simple model has been used to estimate the number of runaways and the fraction of the total current which they carry. Fig.121 shows contours of constant runaway current fractions in the n_e, T_e plane for a 1.8 MA disruption. The temperature is in eV and the density normalised to the value before disruption. For 50% runaway current and an increase in electron density by a factor of 5, the required temperature is 6 eV. This is consistent with the impurity influx model of disruption.

Sawtooth Oscillations

Studies of sawtooth activity have focussed on understanding the phenomena and problems highlighted by earlier investigations. Further analysis of two-dimensional reconstructions of plasma behaviour dur-

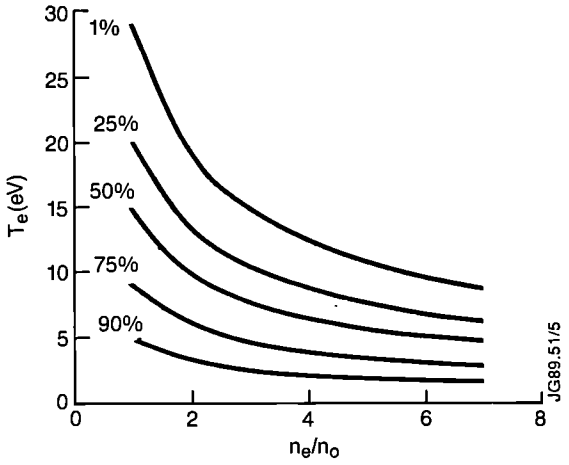

Fig.121: Contours of constant runaway current fraction in the n_e, T_e plane for a 1.8MA disruption.

ing sawtooth activity has confirmed the previous picture of the sawtooth instability, but inevitably, has raised more questions about details of the behaviour of the m=1 mode. In addition, considerable efforts have been devoted to determine the evolution of the q-profile and to understand its influence on sawtooth activity.

Sawtooth activity in JET is accompanied by a wide range of MHD activity and the rise phase of the sawtooth is interrupted by a variety of phenomena (Fig.122).

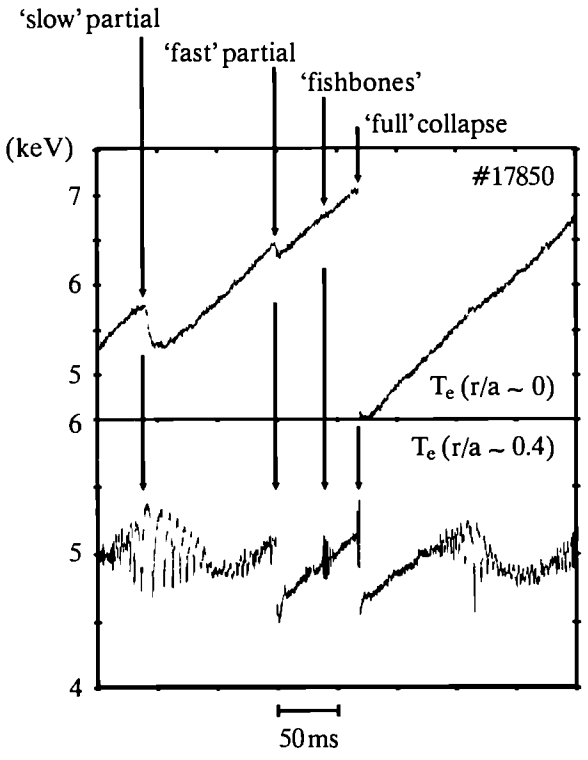

Fig.122: Behaviour of the electron temperature at two radii during a sawtooth cycle in a JET discharge with auxiliary heating. Major commonly observed phenomena are indicated.

Two-dimensional tomography of soft X-ray (SXR) emission has become a standard analysis technique for the investigation of such phenomena and the recent development of new analysis tools for electron cyclotron emission (ECE) data [1] has permitted two-dimensional reconstructions of the detailed behaviour of the plasma during sawtooth activity to be derived both fromECE and SXR observations. The agreement between reconstructions using the two methods has not only increased confidence in the accuracy of both (in particular, confirming that SX emission does represent the behaviour of the electron temperature) but has stimulated a more careful analysis of a number of phenomena. Fig.123 shows a comparison of reconstructions of full sawtooth collapses derived by the two methods [2]. The ECE reconstructions confirm the, now well-known, formation of a hot crescent-like structure as the hot plasma core is displaced by a cold 'bubble [3]. Successor oscillations are due to the rotation of the residue of this hot crescent. In some cases, successor oscillations show, clear evidence of island-like structures in addition [1]. How such islands interact with the sawtooth instability is not clear, but in these cases there is evidence that they can exist well before the onset of the sawtooth collapse and that, like the 'snake' perturbation, they survive the collapse.

Partial relaxations have been subdivided into two broad categories, 'fast' and 'slow' which reflect the significant difference in timescales involved, although there are many other differences between the two types of relaxation. One common feature is that both give rise to a structure resembling a magnetic island. This structure then forms a flat annular region around the core (Fig.124), suggesting that reconnection of the magnetic field lines occurs in this region, but does not involve the plasma core [4].

Full and partial relaxations are observed in both ohmic and auxiliary heated discharges, but 'fishbone'-like bursts [5] are observed only during additional heating experiments and are believed to be driven by fast particle populations accelerated by neutral beam injection (NBI) or radio-frequency heating (ICRH). However, detailed analysis of this phenomenon in JET is at an early stage and, as yet, no direct evidence for their interaction with fast particle populations has been obtained. An understanding of these bursts is of some importance, as in earlier tokamak experiments, they were considered to be responsible for substantial degradation of energy confinement.

Sawtooth-free periods, or 'monster' sawteeth, have now been extended to 3.2s periods in discharges with NBI and ICRF heating. In addition, by heating during the plasma current rise phase, it has been possible to produce sawtooth free periods routinely at 5MA. Global analyses have confirmed previous results [6] that only a small ($\leq \sim 20\%$) gain in energy confinement time is obtained, and that the main advantage of this phenomenon is expected to be a significant gain in fusion reactivity due to the peaked temperature profiles and the

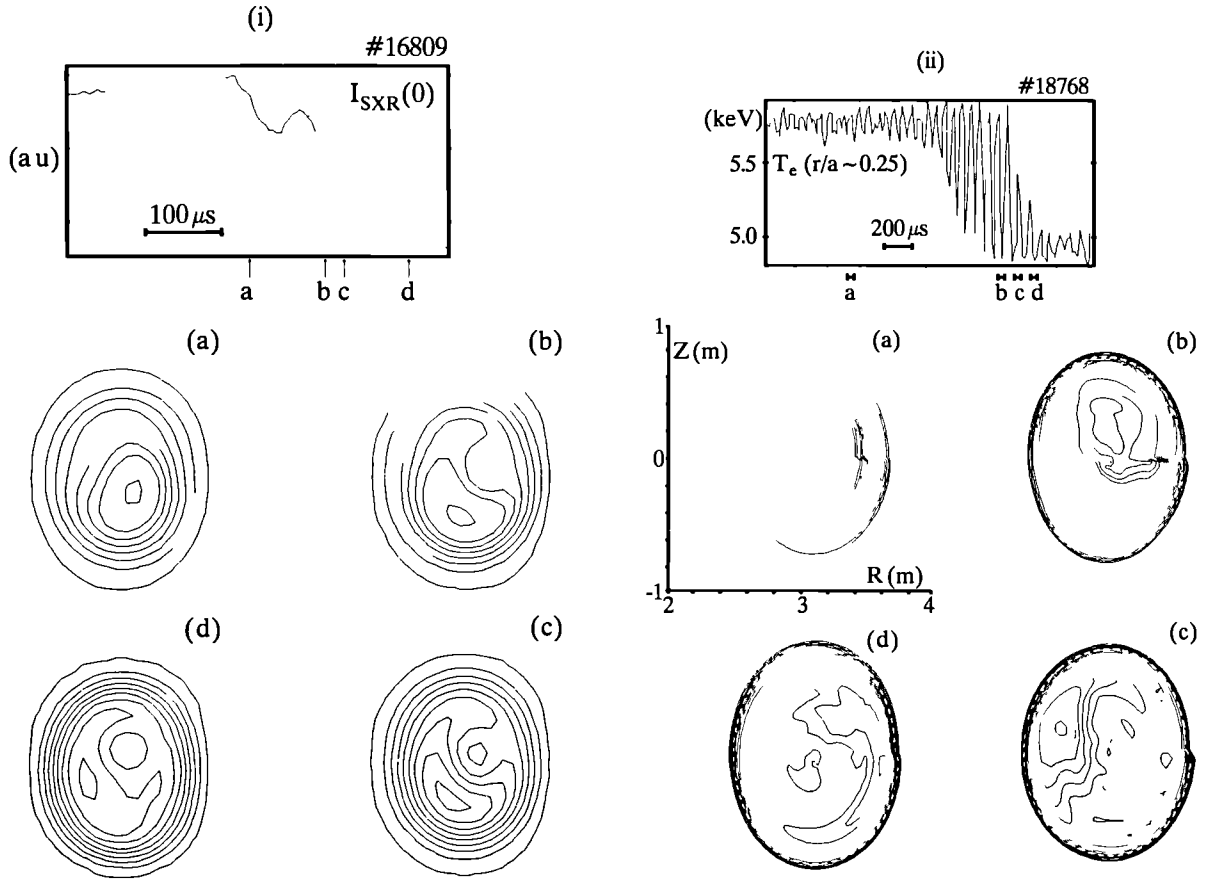

Fig.123: Comparison of sawtooth collapses in JET using (i) SXR and (ii) ECE reconstruction techniques. In both cases a characteristic displacement of the plasma core and formation of a crescent-shaped hot region can be observed. This is followed by a rapid cooling of the displaced core. Successor oscillations are due to the rotation of the plasma residue of the crescent-shaped region.

confinement of fast particles in the plasma core. Particular emphasis has been placed on the determination of the q-profile during such sawtooth-free periods, and the evolution of the central q value, q_0, has been deduced from measurements of plasma-induced Faraday rotation using a far-infrared polarimeter [7]. The results (Fig.125) show that q_0 falls throughout the sawtooth-free period, reaching values ~0.6-0.7. Resistive diffusion calculations using the TRANSP code confirm this conclusion. The question of the mechanism responsible for the observed stabilization is not settled, but it appears that the stabilisation may be due to energetic trapped ions [8].

Despite substantial theoretical attention, both at JET and at many other laboratories, fundamental questions about the nature of the sawtooth instability remain open. While the sawtooth instability, as revealed by SXR and ECE measurements, closely mimics the predicted behaviour of the quasi-interchange mode [9], the rapid growth rate of the instability just before the sawtooth collapse and the nature of the energy redistribution mechanism remain unexplained. In addition, the fundamental assumption that $(q_0\text{-}1) \leq 10^{-2}$, which underlies the theory of the quasi-interchange mode, is challenged by the experimental observation that, in normally sawtoothing discharges in JET, $q_0 \sim 0.8$ (in confirmation of results obtained in TEXTOR). A re-evaluation of resistive theory, including diamagnetic and trapped particle effects, is therefore underway [10]. A central aspect of this analysis is that the sawtooth collapse leads to a relaxation of the shear at the $q=1$ surface rather than a reconnection to $q=1$ in the plasma centre.

Sawtooth Stabilisation and Enhanced Global MHD Stability of Ignited Plasmas

The suppression of sawtooth oscillations in JET regimes with strong additional heating has been attributed [11] to the stabilising effect on $m=1$ internal modes of a minority population of energetic (trapped) ions. When their mean magnetic drift frequency ω_{Dh} is larger than the mode frequency, these ions respond to $m=1$ perturbations with a restoring force. Stability occurs when the work against this force is larger than the energy that is available to the perturbations from the bulk plasma. This translates into a stable domain [12] in the β_P-β_{Ph} plane, if the energy available is measured in terms of the plasma poloidal beta, β_P, and the work in terms of the energetic ion, β_{Ph}. Above a maximum value of β_P, no stability is possible, however large the value of β_{Ph}, as the mode frequency increases with β_P and reaches the

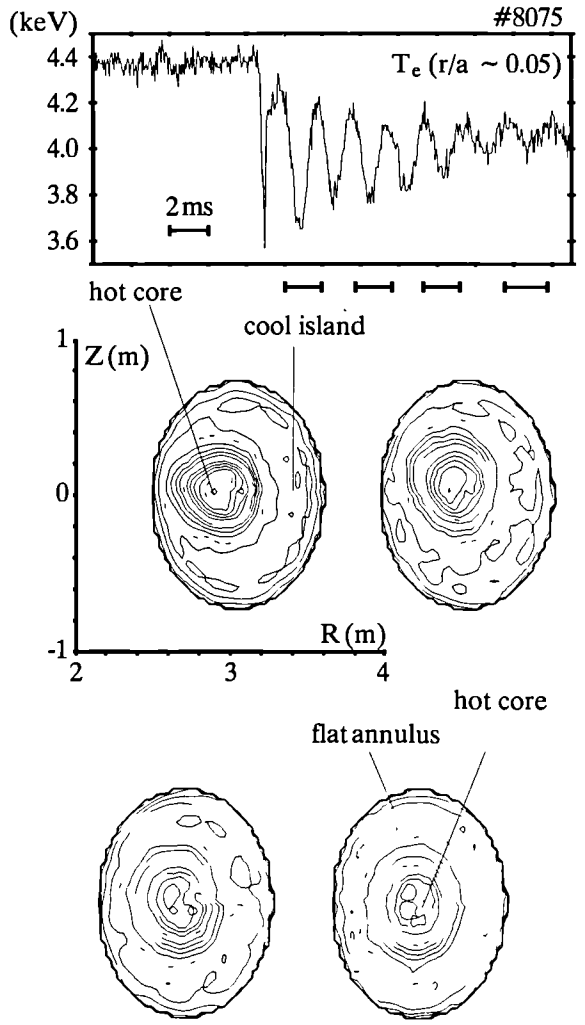

Fig.124: ECE reconstruction of the decay of successor oscillations to a 'fast' partial collapse. The collapse gives rise to an island-like structure which gradually leads to the formation of a shoulder on the temperature profile, apparently by the occurrence reconnection in an annular region about the plasma core.

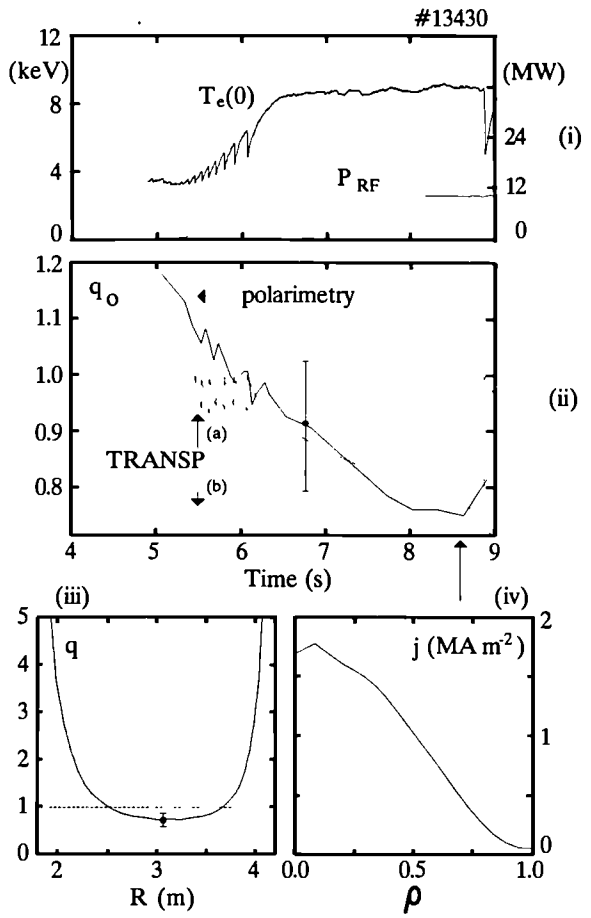

Fig.125: (i) Behaviour of the central electron temperature during a period of sawtooth stabilization. (ii) Evolution of the central value of the safety factor, q_0, as deduced from Faraday rotation measurements (polarimetry), and calculations of the resistive diffusion of current (TRANSP) under two different assumptions (a) with reconnection at sawtooth collapses (b) without reconnection at sawtooth collapses. Safety factor (iii) and current density profiles (iv) are shown just before the termination of the stable period (arrowed).

point where the energetic ions cease to exert a restoring force. A similar frequency increase with β_{Ph} limits the stable domain at large values of β_{Ph}, where the work on the energetic ions eventually changes sign. The stable domain disappears if the bulk ion diamagnetic frequency ω_{di} becomes comparable to ω_{Dh}. In the region just outside the stability boundary, the resonant energetic ions, whose magnetic drift frequency matches the mode frequency, lead to growing oscillations. When $\omega_{di} << \omega_{Dh}$, their frequency is of the order of ω_{di} at small β_{Ph} [13] and of the energetic ion magnetic drift frequency at large β_{Ph}, where it is determined by the resonant ions [14]. When $\omega_{di} \simeq \omega_{Dh}$, their frequency is tied to ω_{di}. These growing oscillations are interpreted as representing the initial phase of the fishbone bursts observed in a number of experiments including JET. Further inside the unstable domain these oscillations turn into fluid type kink modes.

The theory developed agrees qualitatively, and to a certain extent quantitatively, with experimental data. The major uncertainties arise from the energy content and the space and velocity distribution of the energetic ions. In particular, consistent with experimental findings, centrally peaked heating profiles have been shown to be advantageous for stability, while large currents, causing the q parameter to fall below unity over a large portion of the plasma cross-section, have been shown to make the stabilisation due to the energetic ions ineffective.

These results have prompted the realisation that an ignited plasma may spontaneously enhance its stability against $m=1$ modes, the energetic ions then being the charged reaction products such as α-particles. The stability domain in the $\beta_P - \beta_{P\alpha}$ plane [12] is shown in Fig.126 for $\omega_{di}/\omega_{D\alpha} = 5 \times 10^{-2}$, $r_0/a = 0.36$, where $q(r_0) = 1$ and a is the effective minor radius of the plasma column.

The outcome of this work has indicated that in future ignition experiments the stable values of β_P can be as much as 3-4 times higher than the threshold value obtained within the ideal MHD approximation [12].

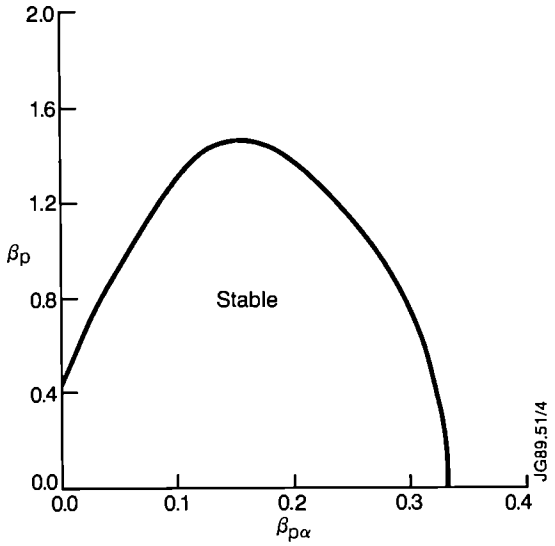

Fig.126: The stability domain in the β_P-$\beta_{P\alpha}$ plane.

However, this enhancement is lost if the region where $q<1$ is too large, (say $r_0/a \gtrsim ½$) and when ignition is sought at high central temperatures ($T_0 \gtrsim 25$keV) [15]. In this latter case, fish-bone oscillations with frequency $\omega \sim \omega_{D\alpha}$ may scatter newly born fully energetic α-particles significantly and affect the ignition balance.

Pellet Ablation and $q(r)$

X-ray and visible light emission measurements have been used extensively in JET to monitor the ablation processes which occur during D_2 pellet injection. It has been observed that the region close to the pellet has a very enhanced level of emission and the absolute value generally agrees well with calculations based on a standard model of pellet ablation. However, for pellets which cross the supposed position of the $q=1$ surface, a large drop in radiation occurs (Fig.127). The radius of this position has been found to be well correlated with the position of the sawtooth inversion radius determined from tomographically reconstructed soft X-ray camera data,

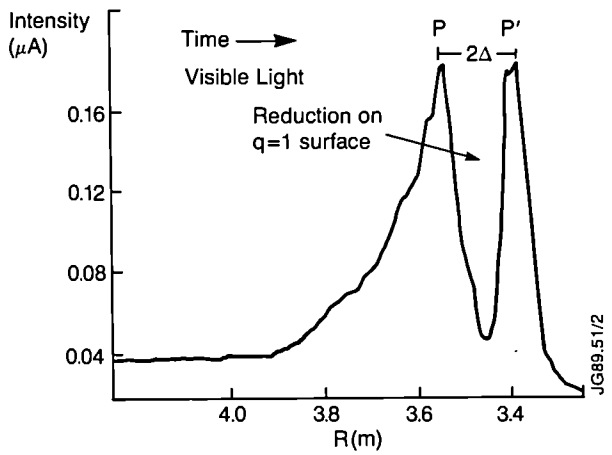

Fig.127: Visible light emission during pellet ablation.

confirming the identification with the $q=1$ surface. The position of the $q=1$ surface within the sawtooth cycle has been shown to move gradually outwards by $\approx 30\%$ and the inversion radius corresponds to the position of $q=1$ surface at the start of the sawtooth cycle.

Effects of Shear and Determination of (dq/dr)

The physics of pellet ablation is well understood: the plasma electrons move along their magnetic field lines and lose energy in the ablation cloud surrounding the pellet and protecting it from direct heating (Fig.128). The ablated material expands radially up to a critical radius and then flows along the field lines. The relative velocities are such that the plasma electrons can make many (≈ 10) toroidal transits around the torus while the pellet ablation cloud crosses a flux surface. On a non-rational q-surface, electrons from many parts of the flux surface can interact with the pellet. However, for integer q, the flux tube closes on itself, thereby reducing the reservoir of available electrons. The cold ablated electrons cool the plasma slowly compared with the time taken for the pellet to cross a magnetic surface and q is not expected to be disturbed or modified on this timescale. On the integer q-surfaces, the effects of shear must also be considered and it can be shown that for an appreciable reduction in ablation rate the shear must be quite small and that this is only likely to happen on the $q=1$ surface. This also provides a satisfactory explanation for the lack of observation of a drop in ablation rate on surfaces other than $q=1$.

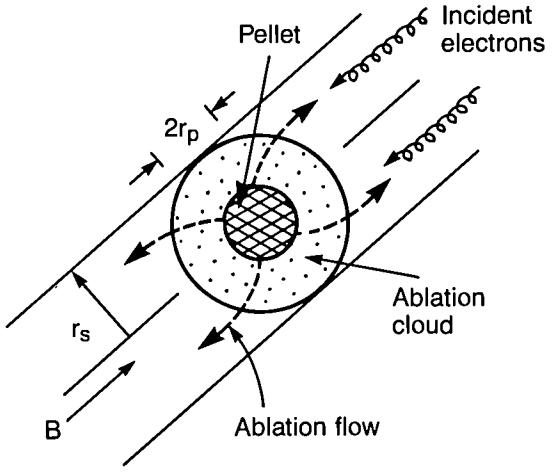

Fig.128: Pellet ablation processes.

Values of (dq/dr) at $q=1$ can be found from the width of the region with reduced ablation and the calculated pellet radius at $q=1$. Typical values obtained are $dq/dr = 5\times10^{-5}$, and if $q(r)$ varies parabolically, an extremely low value of central q is found of $q_0 \sim 0.99$. The values of dq/dr through the sawtooth cycle were found not to change appreciably (with quite large errors) (Fig.129). An alternative interpretation of the results would be that q has a local flattening in the region of the $q=1$ surface and then the extrapolation to find q_0

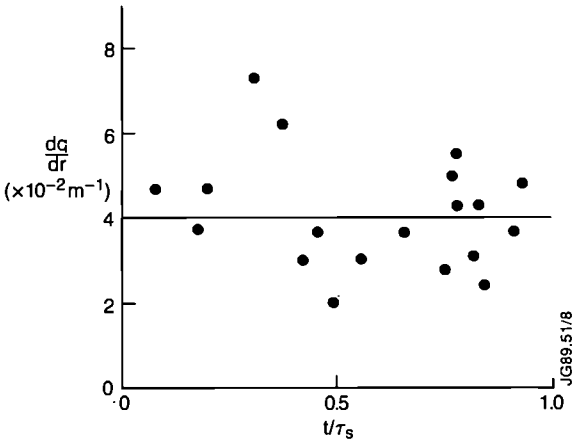

Fig.129: (dq/dr) deduced from pellet ablation.

cannot be made. In either case, the results have important implications for the theory of the sawtooth instability.

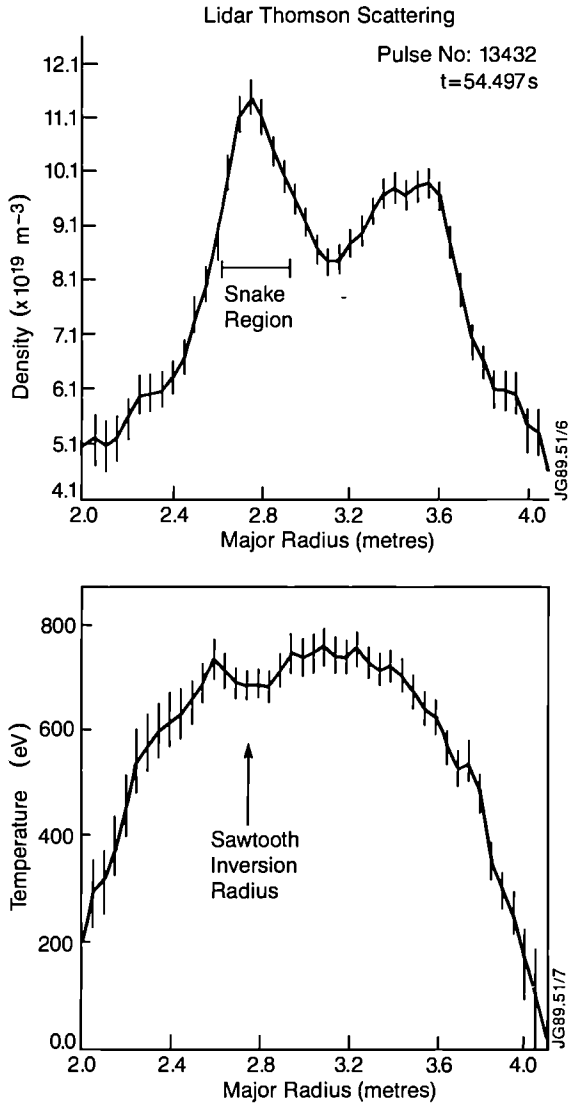

Fig.130: Density and temperature profiles across the mid-plane of JET 19ms after the injection of a pellet.

Snakes

The extremely long lived density perturbation, or 'snake', first seen by the soft X-ray cameras following single pellet injection into JET, has now been observed following multiple pellet fuelling of JET discharges. The snake is a local density perturbation at a rational q-surface, normally the $q=1$ surface. It can persist for longer than 2s, suggesting that a magnetic island is formed at the rational q-surface, with ablated pellet particles being deposited inside this island. Further investigations have now been carried out using the LIDAR Thomson Scattering System, which makes simultaneous measurements of the electron temperature and density profiles. LIDAR profiles across the horizontal mid-plane of JET at 19ms after the injection of a pellet are shown in Fig.130. The formation of the snake is seen from the local density enhancement and temperature depression. These are found to occur at the sawtooth inversion radius. This indicates local cooling at the $q=1$ surface and this is expected to lead to a helical current perturbation and the formation of a magnetic island.

Plasma Rotation

A detailed study of plasma toroidal rotation, measured by Doppler shift of C^{6+} ions, during large amplitude MHD activity has revealed a strong coupling of the ions to MHD modes. Depending on the MHD modes

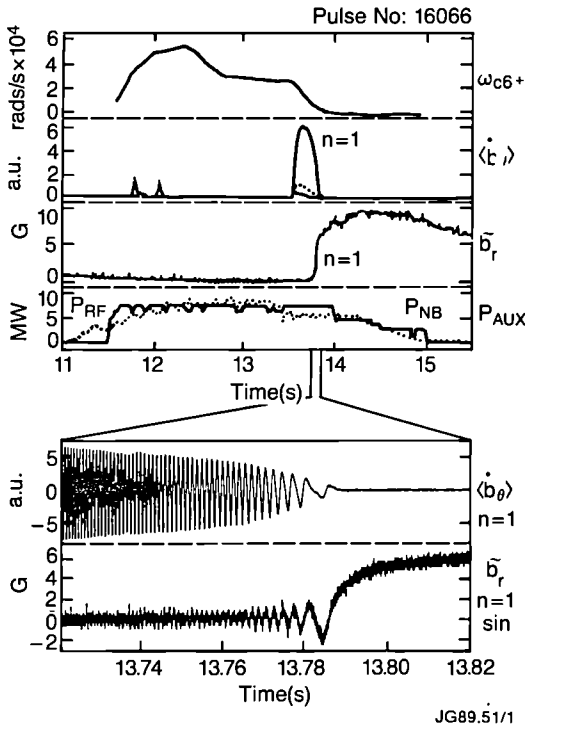

Fig.131: The top trace is the central ion rotation frequency, the second trace is the rectified and smoothed amplitude of MHD oscillations, the third trace is the locked mode amplitude, and in the fourth box are the neutral beam and radio frequency auxiliary heating powers. The expanded time traces show the oscillating MHD activity as the mode locks together with one component of the locked mode amplitude.

present, this force can couple: across all of the plasma cross-section; across only the central region, roughly within the $q=1$ surface; or across only the outer region outside the $q=1.5$ surface. The force flattens the ion toroidal rotation frequency profile (v_ϕ/R) across the coupled region of plasma. The frequency of rotation in this region agrees with the MHD oscillation frequency measured by magnetic pick-up coils at the wall. The strength of the force between the ions and modes becomes evident when mode locking occurs during high power neutral beam injection, which brings the mode to rest through induced eddy currents in the wall of the vessel. Fig.131 shows such a large amplitude mode locking to the wall together with the central ion rotation frequency. A monster sawtooth collapse at about 13.5s drives a large MHD mode unstable. Almost immediately, the central rotation frequency begins to drop as the mode frequency slows down. The mode locks at about 13.79s and the ion toroidal rotation profile across the plasma radius (Fig.132) comes to rest (within the errors of the measurement in about 200ms). This time lag is believed to be due to the inertia of the ions.

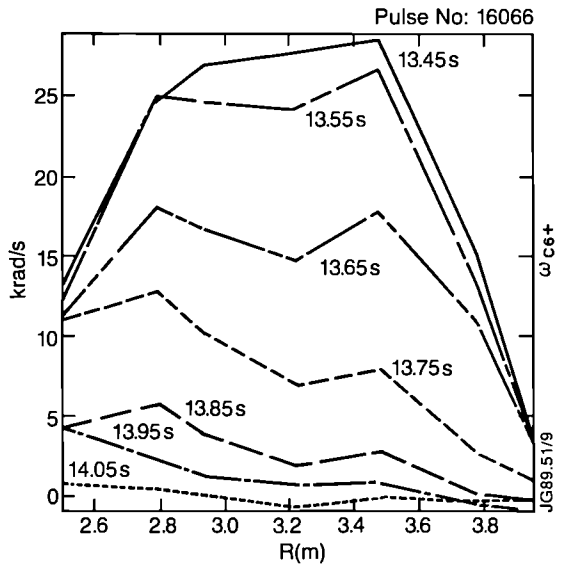

Fig.132: The ion toroidal rotation profiles across the plasma radius during the drop in the rotation frequency at mode locking.

References

[1] E. Westerhof and P. Smeulders, to be published;

[2] D.J. Campbell et al, Proc. 16th European Conference on Controlled Fusion and Plasma Physics (Venice, Italy, 1989), to be published;

[3] A.W. Edwards et al, Phys. Rev. Lett. **57** (1986) 210;

[4] D.J. Campbell et al, Proc. 12th Int. Conf. on Plasma Physics and Contr. Nucl. Fusion Res., Nice (1988), to be published;

[5] M.F.F. Nave et al, Proc. 16th European Conference on Controlled Fusion and Plasma Physics (Venice, Italy, 1989), to be published;

[6] D.J. Campbell et al, Phys. Rev. Lett. **60** (1988) 2148;

[7] J. O'Rourke et al, Proc. 15th European Conference on Controlled Fusion and Plasma Heating (Dubrovnik, Yugoslavia 1988) **1** 155;

[8] F. Pegoraro et al, Proc. 12th Int. Conf. on Plasma Physics and Contr. Nucl. Fusion Res., Nice (1988), to be published;

[9] J.A. Wesson et al, Proc. 11th Int. Conf. on Plasma Physics and Contr. Nucl. Fusion Res., Kyoto (1986) 23;

[10] R.D. Gill et al, Proc. 15th European Conference on Controlled Fusion and Plasma Heating (Dubrovnik, Yugoslavia, 1988) **1** 350;

[11] B. Coppi, J. Hastie, S. Migliuolo, F. Pegoraro and F. Porcelli. Phys. Lett. **A132** 267 (1988)

[12] F. Pegoraro, F. Porcelli, B. Coppi, P. Detragiache and S. Migliuolo. XII International Conference on Plasma Physics and Controlled Nuclear Fusion, Nice (1988), paper IAEA-CN-50/D-4-6

[13] B. Coppi, F. Porcelli. Phys. Rev. Lett. **57** 2272 (1986)

[14] L. Chen, R.B. White, M.N. Rosenbluth. Phys. Rev. Lett. **52** 1122 (1984)

[15] F. Pegoraro, F. Porcelli, B. Coppi and S. Migliuolo. 16th European Conference on Controlled Fusion and Plasma Physics (Venice, Italy 1989), paper PA A32

Heating Physics and Current Drive

Additional heating on JET has now reached power levels of 21 MW from neutral beam injection (NBI) and 18 MW from ion cyclotron resonant heating (ICRH) although not simultaneously. Such intense heating has produced central electron and ion temperatures of 11.5 keV and 23 keV, respectively, and a fusion power of 60 kW from ^{3}He-D reactions. A similar reaction rate ($\sim 2\times10^{16}s^{-1}$) has also been obtained from beam-driven D-D fusion reactions in low density plasmas limited on the inner wall. Long pulse operation of the ICRH has been demonstrated using the water cooled antennae which allowed 6 MW of power to be coupled for 20 s. Commissioning of the system for phase-correlating the eight RF antennae has been completed in readiness for fast wave current drive experiments. A phasing application, which has already proved useful and will be employed frequently in future, is the 'super dipole' mode of operation in which the strip lines of each antenna are fed in phase but a π-phase difference is applied between adjacent antennae. This generates a radiation spectrum that has zero power at $k_\parallel = 0$ but which is substantially narrower than the spectrum produced by normal dipole operation. As expected the nickel impurity release and the coupling resistance are intermediate between those with normal

dipole and monopole phasing modes. The nickel impurity production is strongly influenced by misalignment between the magnetic field lines and the slots in the antenna Faraday screens [1]. By reversing the toroidal field, the angle between the field and the slots was changed from 5° to 25° resulting in a threefold nickel density increase for the same RF power. Correspondingly, the central electron temperature was reduced from 6 keV to 4.5 keV (Fig.133), and there were 30% reductions in both the coupling resistance and the incremental confinement time.

The effect of ^{3}He minority ion concentration on electron and majority ion heating by ICRH has been investigated with both ^{4}He and deuterium plasmas and

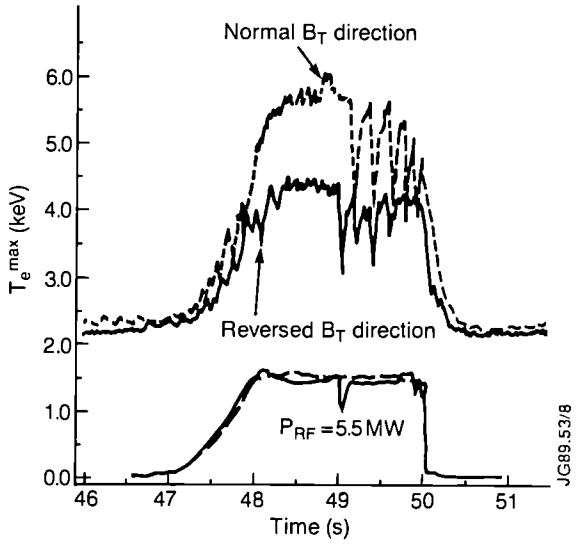

Fig.133: Time evolution of central electron temperature during ICRH with normal and reversed toroidal field directions.

with monopole and dipole phasings [2]. The heating was on-axis for maximum efficiency. The discharge employed a plasma current I_p = 3.5 MA and toroidal field B_T = 3.4 T, such that I_p(MA)/B_T(T) ~ 1 for optimum confinement. The central ion temperature, T_i(0) is plotted against the ratio of RF power to electron density, P_{RF}/n_e, in Fig.134, for values of the minority concentration n^3_{He}/n_e ranging from 1% to 11%. The higher values of T_i (0), up to 8 keV for 12 MW of power, are clearly achieved with the higher minority concentration. Such a trend is expected since the minority ion tail temperature will be least under these conditions thereby enhancing the collisional power transfer to the majority ions at the expense of electron heating. The latter is expected to be strongest at low minority concentration and this tendency was also observed. The different antennae phasings and majority ion species all gave essentially similar results.

^{3}He minority ions in D plasmas have also been used for RF power modulation experiments during sawtooth-free periods ('Monster' sawteeth). Fig.135 shows the response of the central electron temperature T_e (0) to 4 Hz

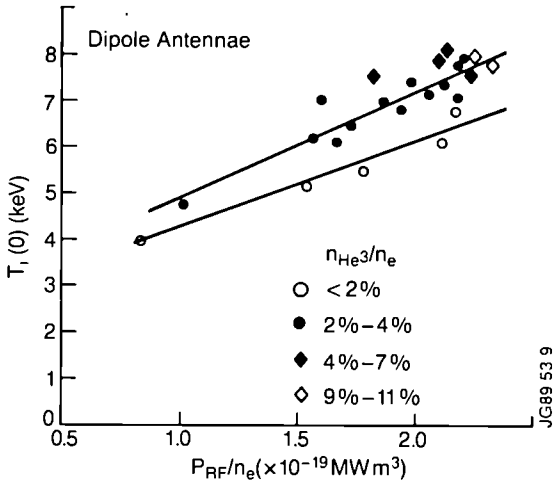

Fig.134: Central ion temperature versus P_{RF}/n_e for various ^{3}He minority ion concentrations.

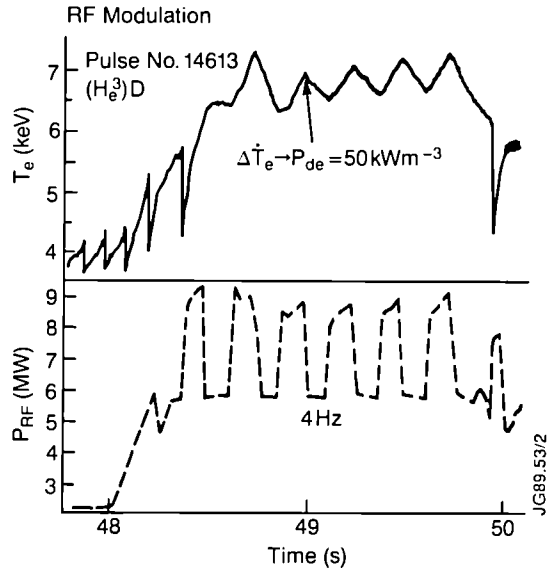

Fig.135: Response of the electron temperature to 4 Hz modulation of the ICRF power. The discontinuity in (dT_e/dt) corresponds to a modulated direct heating power density of 50 kW/m^3.

square wave RF power modulation between 6 MW and 9 MW. The sharp change in the time derivative of T_e (0) at the power switch-up and switch-down times is due to the direct electron heating component from mode conversion, electron Landau damping (ELD) or transit time magnetic pumping (TTMP), as opposed to indirect electron heating from collisions with the hot minority ions. The magnitude of the discontinuity in the derivative gives a direct heating power density of 50 kW/m^3 in the plasma centre. The amplitude of the 4 Hz oscillation in T_e has an almost gaussian profile centred on axis with a width of 30 cm. The phase delay increases monotonically with minor radius. Both the phase and amplitude can be reproduced by a simple electron heat diffusion model which gives a thermal diffusivity, χ_e = 1.5-3 m^{2}s^{-1}

and a power deposition of width 20cm. This localisation of the heating is in good agreement with the predictions of self-consistent, combined full-wave and Fokker Planck calculations.

The above results were obtained with relatively high ^{3}He minority concentration $n_{^3He}/n_e = 8\%$. With low concentrations ($\sim 2\%$), the ^{3}He temperature response is quite different. The amplitude has a hollow profile at a modulation frequency of 4Hz and a 'normal' peaked profile at 16Hz as shown in Fig.136. Such a hollow profile could be produced by off-axis heating and a large reduction in χ_e in the plasma core, but this explanation is inconsistent with the observed phase profile which has a minimum on axis. A possible, though not unique, interpretation is that the width W of the minority heating profile is slightly modulated ($\Delta W/W \sim 4\%$) perhaps as a result of the modulated energy of the minority ions causing a modulation in their banana orbit widths. Such a width variation can provide the on-axis power depletion which appears to be necessary to reproduce the data using a heat diffusion model. The best theoretical fits to the data are shown in Fig.136.

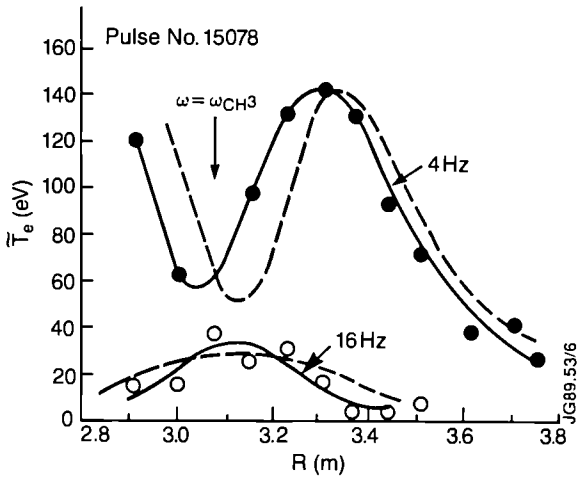

Fig.136: Radial profiles of the modulated temperature in response to 4Hz and 16Hz RF power modulation. Note the central minimum ($R \approx 3.1$m) for the 4Hz case.

Electron heating rates during ICRH have also been measured using the rate of increase of the electron temperature after sawtooth crashes[3]. In particular, measurements made during the RF power ramp-up and ramp-down phases provide a method of distinguishing between direct and indirect heating as the predominant mechanism. An example is shown in Fig.137, where the deduced central power density, P_e, flowing to the electrons is plotted against P_{RF} for both low and high ^{3}He minority ion densities. In the low density case, P_e shows the non-linear behaviour expected of minority species heating due to the long slowing down time (typically 0.2-1 s in JET plasmas). The long collision time is also responsible for the hysteresis effect as the power is reduced from 11 MW to 8 MW. Similar results are found for H minority heating. Theoretical values of P_e are in

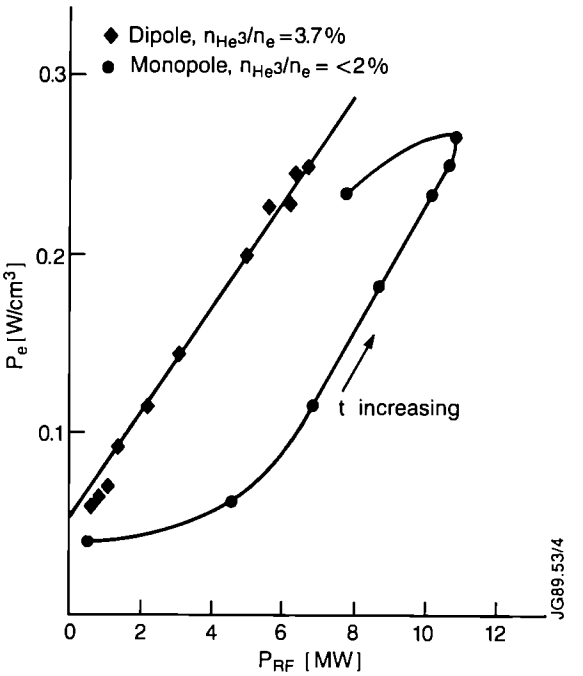

Fig.137: Electron heating power density P_e versus P_{RF} for minority heating (●) and direct heating (♦). In the former case, the long collisional relaxation time for the minority ions causes both a non-linear response during the RF ramp up and a hysteresis effect as the power is switched off.

good agreement with those measured implying that the slowing down is classical and that a large fraction of the fast ions are confined within the plasma centre after each sawtooth crash. At the higher ^{3}He concentrations, the dependence of P_e on P_{RF} is linear suggesting an increased proportion of direct electron heating. This process has the characteristic millisecond time constant of electron-electron collisions, so that P_e is able to follow the RF power ramp proportionally and with negligible delay. At intermediate ^{3}He densities, such cases show power deposition profiles which are considerably broader than those produced in conditions where mode conversion is expected to play a dominant role. Thus, the profile broadening is probably due to TTMP and electron Landau damping (ELD) processes and, indeed, theoretical calculations support this idea.

Evidence for fast wave absorption by TTMP and ELD is encouraging for the planned current drive experiments using the antennae appropriately phased to launch travelling waves. Several possible operating scenarios have been identified. Since the damping rate is proportional to the plasma beta and the current drive efficiency is degraded at high density, high temperature plasmas in low magnetic fields are optimum. The damping is comparatively weak and so competing absorption mechanisms, such as ion damping and mode conversion, need to be minimised. This can be achieved by working at, or below, the fundamental cyclotron frequency of the majority ion species or by operating at the cyclotron frequency of the minority species in the limit of vanishing minority concentration. An example of the latter type

is to use a pure deuterium plasma, an RF frequency of 25 MHz and a toroidal field $B_T \sim 2.4$ T which places the fundamental cyclotron frequency for ^{3}He close to the discharge centre. The fundamental hydrogen and second harmonic deuterium resonances lie outside the vacuum vessel. In the absence of ^{3}He minority, the only competition to TTMP is fundamental damping on the majority deuterium ions close to the inner wall but this resonance is shielded by the polarization effect in a pure plasma.

Current drive by TTMP is expected to produce a centrally peaked current density profile, since the damping will occur mainly in the plasma core. A second method, which should produce an entirely different current density profile, is to asymmetrically heat the minority species. Fokker-Planck studies of this scheme have been carried out for JET and show that the current is highly localised around the flux surface to which the resonant layer is tangential. Moreover, the current flows in opposite directions on opposite sides of this flux surface so that the net current is small but the current density gradient is substantial. For example, the calculations predict that 10 MW of RF power would be sufficient to flatten the current density gradient at the $q=1$ surface in a 2 MA discharge. Therefore, these methods provide two distinct opportunities for current profile control with the aim of stabilising sawteeth and could provide insight as to whether the central safely factor $q(0)$ or the current density profile at $q=1$ are crucial parameters governing the sawtooth relaxation oscillation.

Non-inductive current drive studies have focused principally on the bootstrap current, particularly in H-mode plasmas where the strong pressure gradients have produced up to 0.8 MA in $I_p = 3.5$ MA discharges with a poloidal beta of 0.6. The typical response of the surface voltage, V_{surf}, is illustrated in Fig.138 and is observed to change sign transiently due to the change in the plasma inductance. The experimental time evolution is very well matched by theory based on TRANSP field diffusion calculations [4]. The major part of the bootstrap current is predicted to flow outside 0.7 m minor radius and its broadening effect on the current density profile can be readily observed [5] through the response of the second and third Shafranov current moments Y_2 and Y_3. A plot of the change in Y_2 versus the change in Y_3 between the ohmic L-mode and the additionally heated H-mode is shown in Fig.139. The data all lie in the quadrant corresponding to current profile broadening. In contrast, the results of pellet injection experiments in limiter discharges, also included in Fig.139, show a peaking of the current profile as the central ICRH is applied. The broadening due to the bootstrap current is expected to increase the central safety factor and there is some evidence of this happening both from the equilibrium analysis and from the observed contraction of the sawtooth inversion radius. This latter phenomenon suggests that perhaps some of the H-mode discharges are close to becoming sawtooth-free.

Combined NBI and ICRF heating of H-modes has

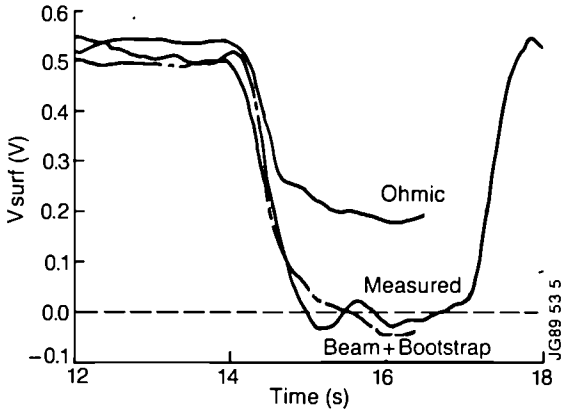

Fig.138: Experimental and theoretical surface voltage traces during a beam heated H-mode. The bootstrap current rises continually during the heating pulse to a level of 0.8 MA. Correspondingly the beam driven current diminishes from 0.1 MA to 0.03 MA due to the density rise.

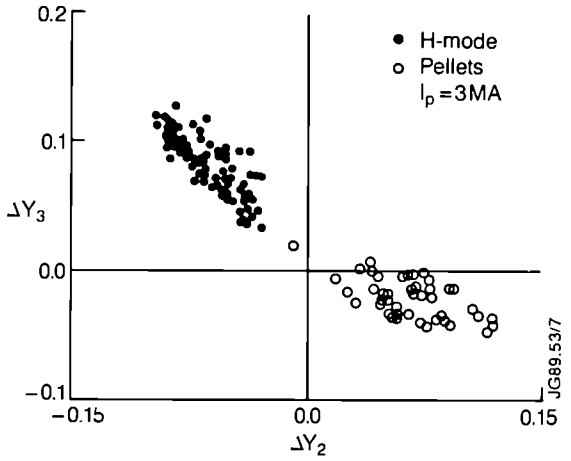

Fig.139: Changes in the second (Y_2) and third (Y_3) Shafranov current moments between ohmic and beam heated H-mode phases showing the broadening of the current density profile due to the bootstrap current. For comparison, data are also shown for discharges that have been fuelled by pellets prior to centrally peaked auxiliary heating. In these cases, the current density profile becomes narrower as the heating produces peaked electron temperature profiles.

been achieved using the double null X-point geometry which provides a good match between the curvature of the antennae and the last closed flux surface [6]. This enables RF power to be coupled at plasma-limiter separations in excess of 3 cm which is the normal requirement for H-mode formation. In most cases, the NBI and RF power levels were in the region of 8 MW and 6 MW, respectively. H-modes with combined heating are generally poorer than with NBI alone. For example, the rate of rise of the radiated power is twice as great leading to shorter H-modes. Also the incremental confinement time is reduced by about 30% in H-modes with combined heating, as shown in Fig.140. Recently, however, an H-mode with a low radiation increase has been produced with 15 MW of NBI and 10 MW of RF with only 1 cm separation between the plasma and the antennae. The stored energy reached 11 MJ, both $T_i(0)$ and $T_e(0)$ exceeded 10 keV and the D-D fusion rate reached 2×10^{16}s^{-1}. So far, no H-mode has been produced by

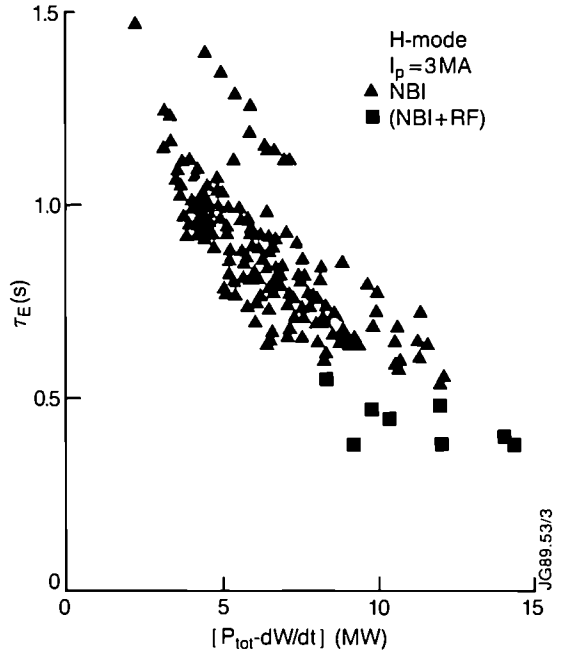

Fig.140: Incremental confinement time τ_{inc} for H-mode discharges versus P_{tot}. The combined (NBI + ICRF) heated plasmas tend to have somewhat lower values of τ_{inc} compared with those produced by NBI alone.

ICRH alone although H-mode signatures, such as short periods of reduced deuterium recycling, have been seen. However, there has been no corresponding improvement in energy confinement. The reason for this is not understood but if nickel impurity release is the problem then the proposed beryllium antennae screens should be greatly beneficial.

According to recent theoretical work, enhanced neutral and impurity influxes could result from parametric decay of the fast magnetosonic wave (FMW). A series of experiments have been carried out to test this idea by studying the RF field near the antennae using both electrostatic and magnetic probes [7]. The fast wave has been seen to decay into two slow waves (SW) and also into an ion Bernstein wave (IBW) and the corresponding quasi-mode (QM). An example of the latter is displayed in Fig.141 which shows frequency spectra recorded at several RF power levels in a 3 MA, 3.15 T discharge containing a mixture of deuterium and ^{3}He plasma with hydrogen as the minority species. The excitation frequency is 48 MHz to give on-axis minority heating. As the RF power is increased, the emerging peaks can be identified as quasi-modes for deuterium (1D) and ^{3}He (1^3He) with their corresponding ion Bernstein waves (2D and 2^3He), respectively. In this case, any decay to two slow waves at 24 MHz is obscured but such decays have been seen when the IBW branch is forbidden. So far, no definite correlation between the amplitude of the decay waves and the impurity release has been identified.

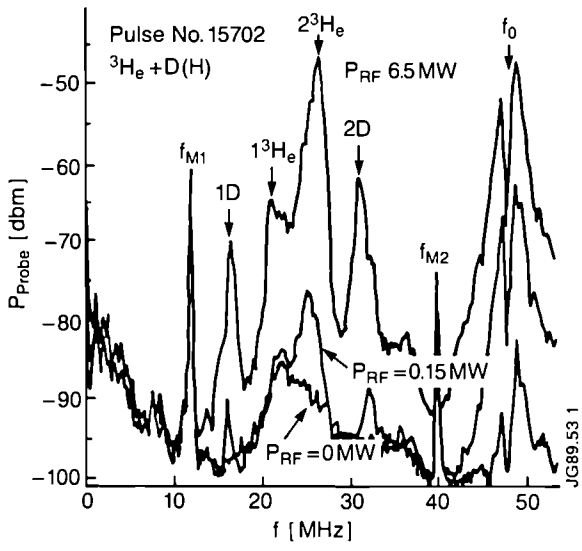

Fig.141: Frequency spectra measured in 3.15 T, 3 MA, ^{3}He+ D(H) discharges at RF power levels of 0, 0.15 and 6.5 MW. The excitation frequency is 48 MHz and f_{M1} and f_{M2} are marker frequencies.

Non-thermal fusion experiments, using ^{3}He minority ICRH in deuterium plasmas have yielded up to 60 kW of fusion power from the ^{3}He-D fusion reactions. The results have been successfully simulated using both a simple Stix model [8] and a more sophisticated, self-consistent full wave/Fokker Planck treatment [9]. These validated models have been used subsequently to study the potential of deuterium minority ICRF in tritium plasma containing deuterium concentrations up to 30%. Initial results for plasma conditions already achieved in JET suggest that fusion Q values ($= P_{fus}/P_{RF}$) in excess of 50% could be achieved provided impurity dilution can be kept to a reasonable level ($Z_{eff} \sim 2$). The calculations predict good absorption on the minority ions even with 30% deuterium. They also rely on some tailoring of the power deposition to achieve the optimum tail temperature over a substantial part of the plasma core. It is planned to test these aspects experimentally in the forthcoming period of operation.

References

[1] Role of Antenna Screen Angle during ICRF Heating Experiments in JET, M.Bures et al, Proc. 15th European Conf. on Contr. Fusion and Plasma Heating Europhysics Conference Abstracts II 713 (Dubrovnik, Yugoslavia 1988).

[2] High Electron and Ion Temperatures Produced in JET by ICRH and Neutral Beam Heating, D.F.H.Start et al, Proc. 15th European Conf. on Contr. Fusion and Plasma Heating Europhysics Conference Abstracts I 354 (Dubrovnik, Yugoslavia 1988).

[3] Electron Heating During ICRH in JET, L.G.Eriksson and T.Hellsten submitted to Nuclear Fusion.

[4] Non Inductive Currents in JET, C.Challis et al, to be published in Nuclear Fusion.

[5] Current Profile Broadening in Plasmas with Enhanced Confinement, J.P.Christiansen and J.B.Cordey, submitted to Nuclear Fusion.

[6] Double Null X-point Operation in JET with NBI and ICRH Heating, B.Tubbing et al, to be presented at the 16th European Conf. on Contr. Fusion and Plasma Physics (Venice, Italy, 1989).

[7] RF Edge Field and Parametric Decay during ICRH Heating on JET, M.Bures et al to be published in Plasma Physics and Controlled Fusion.
[8] ^{3}He-D Fusion Reaction Rate Measurements during ICRH Heating Experiments in JET, D.A.Boyd et al, to be published in Nuclear Fusion.
[9] Calculations of Power Deposition and Velocity Distributions during ICRH; A Comparison with Experimental Results, L.G.Eriksson et al, to be published in Nuclear Fusion.

Theory

Theoretical work at JET concentrates on the prediction of JET performance by computer simulation, the interpretation of JET data and the application of analytic plasma thoery to gain an understanding of plasma behaviour in JET.

Interpretation plays a key role in the assessment of plasma performance and hence in optimisation studies and programme planning. Prediction work continuously checks the measured behaviour against the different computational models and provides a basis for long term programme planning. A major role of analytic theory is to compare the observed behaviour against that expected from existing analysis and to modify the latter when there is divergence. However, traditional analytic theory is carried out only by a small number of staff who continuously review published plasma theory, assess its relevance to JET and, where necessary, adapt it accordingly. Valuable assistance in this area has been provided by a number of Visiting Scientists, extended visits of Associated Staff, Fellowship and Article-14 contracts.

The central task is to construct a quantitative theoretical model of tokamak plasmas which (i) can describe measurements on JET with sufficient accuracy; (ii) can predict future plasma performance in JET and other tokamaks; and (iii) can be used to analyse and understand complex nonlinear mechanisms in the plasma. The model should ultimately reflect all important plasma physics effect in a concise and quantitative manner, (i.e. be a true representation of JET's plasma physics experience).

At present, several major plasma features can be described only by empirical prescriptions. Efforts must be made to replace these by analytically derived (i.e. theoretically understood) formulations, especially when the model is required to make reliable predictions outside the measured plasma paameter range.

The model should be validated continuously by comparison with measured data. This task demands, on the one hand, the identification of sensitive parameters from theory and, on the other hand, building-up the appopiate data banks from measurements. The quantities measured directly on JET often require complex mathematical and computational reduction procedures, and intricate error assessment before being suitable for comparison. The production of such banks of evaluated measured data is strongly coupled with data interpretation and with checks on the consistency of measurements, for which the above-mentioned full plasma model is a useful tool.

The activities of the Division can be subdivided under the following headings:

- Data Banks and Connected Software
- Code Development for Code Library
- Data Interpretation
- Tokamak Plasma Model Development
- Predictive Computations
- Analytic Theory

Only a few, more conspicuous activities and results under these headings are highlighted in the following paragraphs. A detailed account of the 1988 activities is being prepared as a separate JET Report.

The JET SURVEY DATA BANK now contains basic plasma data for all JET discharges with plasma until the end of 1988 (over 12,000 shots; about 320000 time traces; a total of 1 GByte of available data). This data bank will no longer be distributed to the Associations. In the future, a data collection of very similar structure, but only for a selected number of discharges will be distributed. Connected to SURVEY is the JOTTER data base containing technical operating data and pulse reports for over 7200 shots (since June 1986). Both banks are effectively managed and used through the NOMAD2 data management system.

Both for interpretation and design studies, computation of magnetic flux surfaces is of fundamental importance. The carefully checked NOMAD2 data bank of flux patterns has been extended. It has been extensively used by the electron cyclotron emission diagnosticians to unfold the electron temperature profile. The database now contains selected data on the most relevant studies of JET discharges (up to 5MA shots, monster sawteeth, disruptions, H-modes, pellet injection) carefully checked for integrity, monitored by the minimum fitting error on the available signals. Important results of this analysis include the verification of global anisotropic effects in RF heated discharges, and the systematic decrease of the central safety factor, q (0), below unity during monster sawteeth.

A number of codes in the CODE LIBRARY have been upgraded to make them applicable to a wider class of problems, and to be more user-friendly and automatic. This holds especially for the inversion code NEPROF which derives electron density profiles, and for the plasma equilibrium code IDENTC to include measured information on pressure profiles and diamagnetism in addition to the usual magnetic probe signals. A major effort was invested in a complete rewrite of the interpretive transport code JICS to provide reliable data for local transport, i.e. for the electron and ion thermal fluxes and for convection, from evaluating power, momentum, and particle balances.

A new equilibrium code has been developed which self-consistently includes Faraday rotation data in the evaluation of the poloidal magnetic field profile. Another new package (STABM1) evaluates stability criteria for plasma sawtooth activity, and the new PIN code assists the interpretation of boundary plasma measurements. These and other codes have been used extensively for JET DATA INTERPRETATION. Thus, by combining with tomographic and inversion methods, ion temperature profiles have been derived from neutron emission measurements. Two dimensional non-symmetric radiation profiles have been evaluated mainly for X-point configurations. Toroidal rotation, induced by ICRF heating, has been shown to be connected with the creation of fast ions during heating. Analysis of the highest (averaged) plasma-β values reveals that about 70% of the Troyon-Gruber limit is reached, and no sign of β-saturation is observed.

Extensive studies on ideal ballooning stability have been made for two types of JET discharges: high-β shots (produced at low toroidal field) and discharges with large pressure gradients after injection of pellets followed by intense heating. In both groups, locally unstable cases can be found. Flat parts in the electron temperature profile measured with the LIDAR system have been interpreted as caused by helical resistive MHD mode structures close to rational values of the safety factor q. Much effort has been spent in determining the fraction of the ICRF heating power absorbed by the electrons, either directly or indirectly via fast minority ions. High minority concentration favours direct, low concentration indirect heating.

Studies of this type lead directly to improvements in theoretical tokamak plasma models which may then be used for predictive calculations. From a full wave propagation code combined with solving the Fokker-Planck equation for the heated ion species, a simple and routinely applicable model for power deposition profiles during ICRF heating has been extracted. With the present version, all steady-state cases with a single cyclotron resonance can be handled.

Major progress has been achieved also in modelling the boundary plasma. A set of two dimensional two-fluid plasma equations are solved in time, self-consistently with a three dimensional Monte-Carlo calculation for the recycled neutrals. Both limiter and single X-point configurations can be studied. Resistive MHD equations are considered to provide an adequate description for a number of plasma phenomena. In order to elucidate the non-linear features of such equations, they are studied in the 'dynamical system' approach. It has already been shown that simple equilibria are destabilized via symmetry breaking bifurcation into stationary solutions with 'island vortex' structures. Further destabilisation into time dependent regimes via Hopf bifurcation leads to asymmetric oscillations (see Fig.142).

The various plasma models have been used extensively

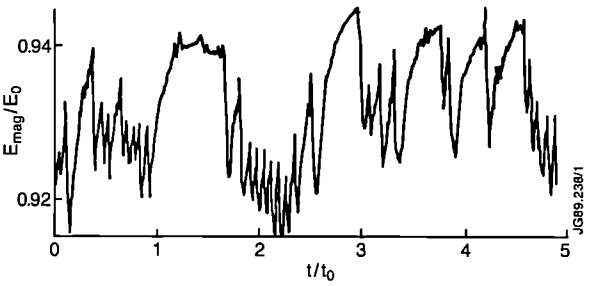

Fig.142: Time behaviour of the normalised magnetic energy, E_{mag}/E_o, (at a Reynolds number R = 6000). Time is measured in units of the Alfvèn time $t_A(t_o \cong 1000\ t_A)$.

for predictive computations for the performance of JET and other tokamaks. Our main plasma model code JETTO has been applied in a predictive (and interpretative) mode to the long standing plasma confinement problem. It is almost certain that the electron and ion thermal conductivities χ_e and χ_i, are both highly anomalous and of comparable magnitude. Both seem to increase separately with their respective input power, i.e. χ_e with P_e, and χ_i with P_i. Non-empirical, theoretical expressions, such as thermal conductivity based on the so-called η_i-instability, have so far not been successful in explaining the observed heat fluxes.

A large number of equilibrium calculations has been made for upgrading the JET poloidal field system, for planning 7MA limiter discharges, for 5MA single X-

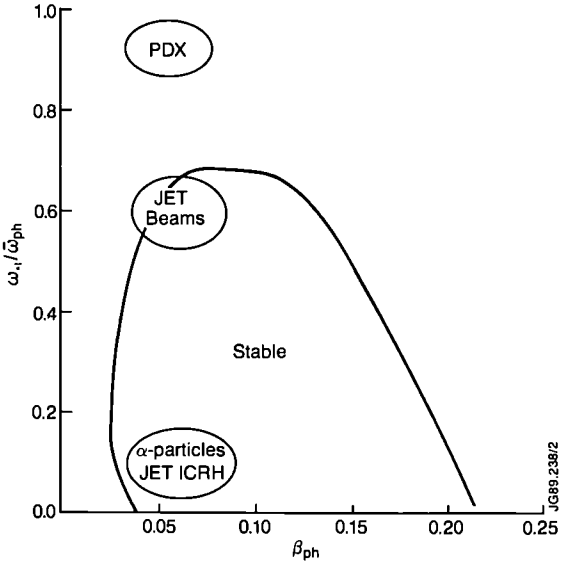

Fig.143: An example of the marginal stability curve for m=1 modes in the plane identified by the parameters $\omega_{*i}/\bar{\omega}_{Dh}$, and β_{ph}, where ω_{Dh} is the core ion diamagnetic frequency at the q=1 surface, ω_{Dh} is a characteristic value of the fast ion magnetic drift frequency, and β_{ph} is the fast ion poloidal beta. The curve is drawn for a value of the core plasma poloidal beta, β_p, in excess of the ideal MHD threshold. Stability is attained in the indicated domain for moderate values of β_{ph}. Outside the stable domain, either fishbones or internal kink modes are predicted to be excited. Also shown in the figure are the relevant values of ω_{*i}/ω_{Dh} for PDX fishbone experiments, for JET auxiliary heated discharges, and for fusion alpha-particles in an ignition experiment.

point operation, and for design studies on Next Step tokamaks. Benchmarks have been provided for the new NET equilibrium code.

To understand the physics underlying the observed plasma behaviour, and thus allow more reliable prediction for new parameter ranges, relevant analytic theory has been developed, both within the project and through Task Agreements and Article 14 Contracts with the Association Laboratories.

A major effort has been devoted to the MHD stability of the m=1 ideal and resistive modes when q_o, the central safety factor, is significantly less than unity. This is relevant to the sawtooth oscillations, which determine confinement near the axis in JET. A possible explanation for these oscillations has been given in terms of a resistive internal kink mode, whose stability depends strongly on the local shear around the q=1 surface. When this instability is included in a transport model, the predicted evolution is consistent with observation. The suppression of the oscillations during 'monster' sawteeth in RF heated plasmas in JET can be explained by the effect of energetic ions. It has been shown that an analogous stabilisation should result from α-particles in an ignited plasma (see Fig.143). The $m=1$ 'fishbone' like oscillations observed in JET can be explained by the same analysis for a plasma with a minority of energetic ions.

Other MHD problems include the interaction of a low-m rotating resistive mode with the multipolar poloidal field system in JET, and the relaxation of the plasma to the minimum permitted energy state. These studies are relevant to feed-back stabilisation of the $m=2$ tearing mode, and the L to H mode transition, respectively.

A possible origin for the anomalously rapid energy loss from tokamaks is electrostatic instabilities. The analysis of the ion temperature gradient instability, performed at ENEA Frascati, Italy, under a Task Agreement, has been extended to include trapped electrons. This changes the threshold gradient above which the instability occurs.

A phenomenon where the particle loss rate was actually less than expected from purely collisional effects is the 'snake', i.e. the filament of increased density sometimes observed after pellet injection. A fuller analysis of the classical processes, including ambipolar electric fields, shows the diffusion to be less than initially estimated, though still rather larger than that observed.

The absorption of ICRF heating power has been found to also produce spatial diffusion of the heated ions. The resulting pump out of resonating ions broadens the heating profile of the main species relative to the absorption profile. Another problem raised by ICRF heating is the absorption of power near the plasma edge, which gives rise to increased impurity influx. One possible mechanism, the parametric decay of the incident fast wave into an ion Bernstein wave and a quasimode, has been shown not to be generally important in JET. Other processes must be considered.

Summary of JET Scientific Progress and Perspective

During 1987, new systems had been added to the machine, as follows:

- assembly and installation of the water-cooled central limiters;
- installation of eight water-cooled ICRF antennae;
- installation of uncooled dump plates near the X-points;
- modification of the central poloidal field coil with 10 sub-coils and other modifications of the sub-coils to increase the potential of the machine for increased current and pulse duration;
- assembly of new vessel supports to withstand vertical instabilities and radial disruptions at higher plasma currents elongations;
- connection of the second Neutral Injector Beam Line;
- installation of the joint US-JET multi-pellet injector (ORNL Launcher).

During 1988, experiments were continued to determine the effects of these new additions. Some of the results have been reported in detail at various International Conferences (see Appendix III).

Introduction

During 1988, JET reached the midpoint of its experimental programme and its achievements can be usefully compared to the Project objectives, which are:

(a) The scaling of plasma behaviour as parameters approach the reactor range;
(b) The plasma wall interactions in these conditions;
(c) The study of plasma heating;
(d) The study of α-particle production, confinement and consequent plasma heating.

At this stage, the first three aspects have been extensively addressed and a general pattern of the plasma behaviour has emerged. Consequently, from these results, it is possible to draw some conclusions relating to the requirements and parameters of a Next Step device.

In the following sections, major results obtained on JET are summarized together with their direct implications for a future thermonuclear reactor. In particular, a distinction is made between the achievements which can safely be regarded as steady-state (i.e. fully reactor relevant), and those corresponding to a more transient state of the plasma.

Parameter Achievements

The new enhancements have extended the operational domain, and in particular, have permitted the following technical and scientific achievements.

In quasi steady-state:

- plasma current, I_p, of 7MA has been obtained for 2s;
- JET has operated routinely with I_p above 5MA, and a current of 6MA has been maintained for 8s;
- ion and electron temperatures, T_i and T_e, in excess of 5keV have been sustained for over 20s at a plasma current of 3MA (see Fig.144);
- additional power up to 32MW has been delivered to a 5MA plasma producing a total stored energy exceeding 10MJ (see Fig. 145);
- both electron and ion temperatures simultaneously in excess of 10keV for 2s were observed at a plasma density of $2\times10^{19}m^{-3}$ (see Fig. 146).
- confinement times in excess of 1s have been observed;
- neutron yields have reached $1.2\times10^{16}n.s^{-1}$ with 20MW D beams at 80kV.

In a more transient situation:

- routine operation with a magnetic separatrix at $I_p=4.5$MA. H-mode plasmas were regularly observed during neutral beam heating;
- A record H-mode plasma at 5MA has been obtained. Transiently, during an H-mode, the fusion product ($n_i\ T_i\ \tau_E$) has reached $3\times10^{20}m^{-3}$.keV.s at temperatures exceeding 5keV;
- the neutron yield has reached 9×10^{15}n/s produced by D-D fusion reactions during an H-mode at 4.5MA; the plasma was heated by 12MW of deuterium beams at an energy of 80keV;
- the total plasma energy content has transiently exceeded 11MJ in X-point operation with 27MW of input power;
- high peaked density plasmas were obtained by using pellet injection ($n_{eo}>10^{20}m^{-3}$). On-axis ICRF heating of such target plasmas produced transiently peak electron pressures in excess of 1 bar.
- 'monster' sawteeth have been observed with ICRF heating during which q_0, the combat safety factor, decreased below unity (0.8).

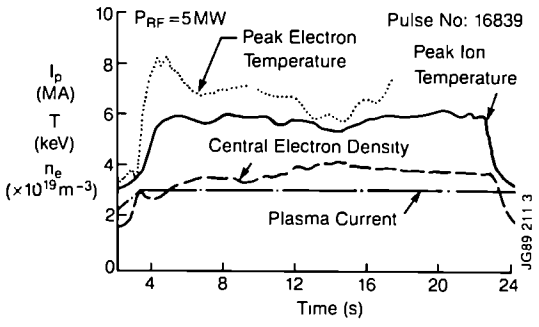

Fig.144: Quasi-stationary plasma exceeding 30s in duration at temperatures in excess of 5keV. The 3MA plasma was heated by 5MW ICRF power.

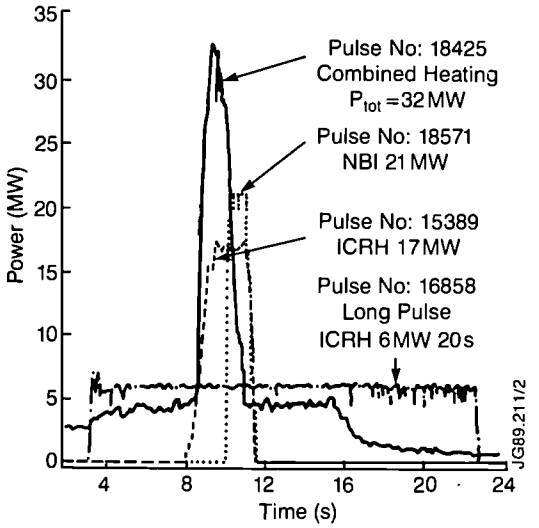

Fig.145: Power delivered to JET plasmas as a function of time. In particular, combined heating power (NB+RF) has exceeded 32MW in the plasma.

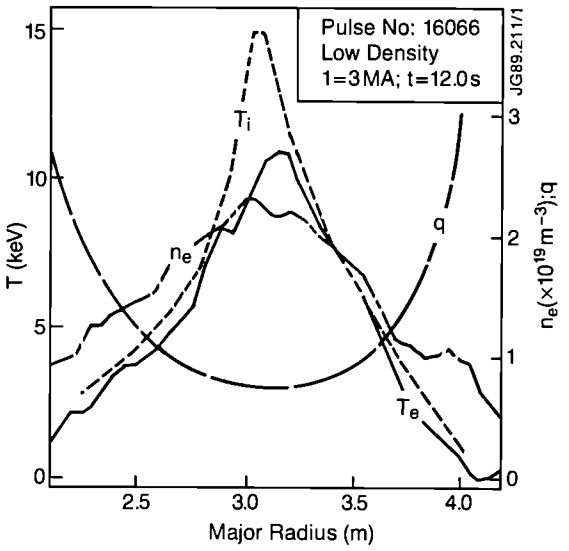

Fig.146: Radial profiles of electron and ion temperatures, electron density and safety factor in a 3MA, low density discharge with B=3.1T, P_{RF}=8MW, P_{TOT}=16.5MW, Z_{eff}=5.2, τ_E=0.4s.

Consequences for a Reactor

Plasmas of thermonuclear quality have been produced in JET and no adverse effects were observed when both electron and ion temperatures reached thermonuclear reactor values. However, record values of neutron yield, pressure and total energy have been obtained when the plasma was in a non-steady-state situation. It seems wise to extrapolate the performance of a future machine by starting from discharges already obtained and truly stationary. Transient improvements may prove to be useful to overcome the ignition pass but should not be relied upon when working quasi-continuously at full fusion power required routinely in a reactor.

Energy Confinement and the Fusion Product

Degradation of energy confinement with additional

power is a well observed phenomenon. Recent experiments on JET have extended such observations to higher input power. Fig.147(a) shows the measured energy confinement time as a function of total power in JET for limiter and L-mode discharges. In this data, the time derivative of the plasma energy content does not exceed 10% of the input power. At higher power, improvement with increased current is observed but detailed examination of individual scans show more complex behaviour. The gain due to increased current saturates in JET as the boundary safety factory, q_a, decreases below 4, since flattening of the pressure profile results from sawtooth relaxations.

For the same input power but with a magnetic separatrix limiting the plasma - X-point operation - confinement is improved in the so-called H-mode. Fig.147(b) shows the energy confinement time for JET H-mode discharges. Again, the time derivative of the plasma energy content is small for these data, but the density is still rising while the temperature is decreasing. No significant difference was observed between single-null and double-null discharges. At low power, τ_E can exceed 1 s (i.e. comparable to ohmic confinement times). In addition, degradation with power is at least as severe as in the L-mode. Similarly, confinement increases with I_p.

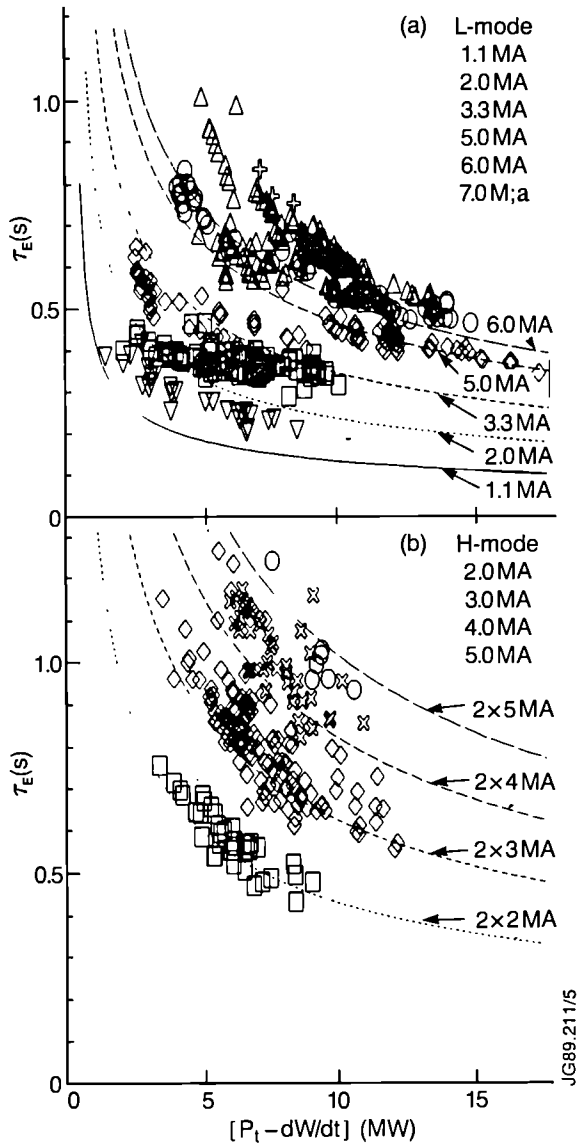

Fig.147(a) L-mode confinement time, τ_E, data versus input power, showing degradation with power. The strong degradation of confinement time and the beneficial effect of plasma current are clearly seen. (b) H-mode confinement time, τ_E, data versus input power showing clear degradation with power. However, confinement is improved by a factor 2 to 3 over the corresponding L-mode case.

Consequences for a Reactor

Degradation of confinement time with the input power is considered a major threat to the success of a future tokamak reactor. The difficulty of improving the fusion parameter ($n_i\, T_i\, \tau_E$) (and thus the ignition margin of a given machine) by additional power alone is illustrated in Fig.148. The major gains observed in JET result either from temporary changes in the confinement or from increasing the magnetic field and/or current. If the scaling laws describing energy confinement in JET continue to apply, then it can be shown that a reactor must be very close to ignition without applying additional heating power. This means that the required temperatures must be obtained in those conditions; in practice, the dependence of radiation and fusion cross-sections impose an average temperature above 7 keV. In addition, density and temperature do not have a symmetric effect on confinement: it is easier to get a improved energy confinement at higher density than at higher temperature.

Particle Transport

Particle and impurity transport in JET have been studied under various operating conditions[1,2]. In most cases, particle confinement, like energy confinement, is anomalous. JET results point strongly towards a common explanation for heat and particle transport. For instance, multi-pellet injection produces peaked high density profiles but flat and low temperature profiles occur in the ohmic regime. Increasing the central electron temperature by on-axis ICRF heating degrades energy confinement and results mostly in a collapse of the central density (i.e. of the particle confinement). In cases where the collapse is delayed, energy confinement in the plasma centre is also better than in usual additionally heated discharges. The particle confinement time is 5-10 times larger than the energy confinement time.

The anomaly in the particle transport prevents impurity accumulation in the discharge centre. Combined with wall-carbonization, this has kept a low metallic impurity content in JET ($\approx 10^{-4} n_e$) and $Z_{eff}=2$ has been achieved with large additional power. However, for most of the discharges the steady state mean value of Z_{eff} ranges between 2 and 4 with a radial profile which tends to peak on axis. Radiation losses in the plasma core are marginal, as long as the dominant impurities are of low

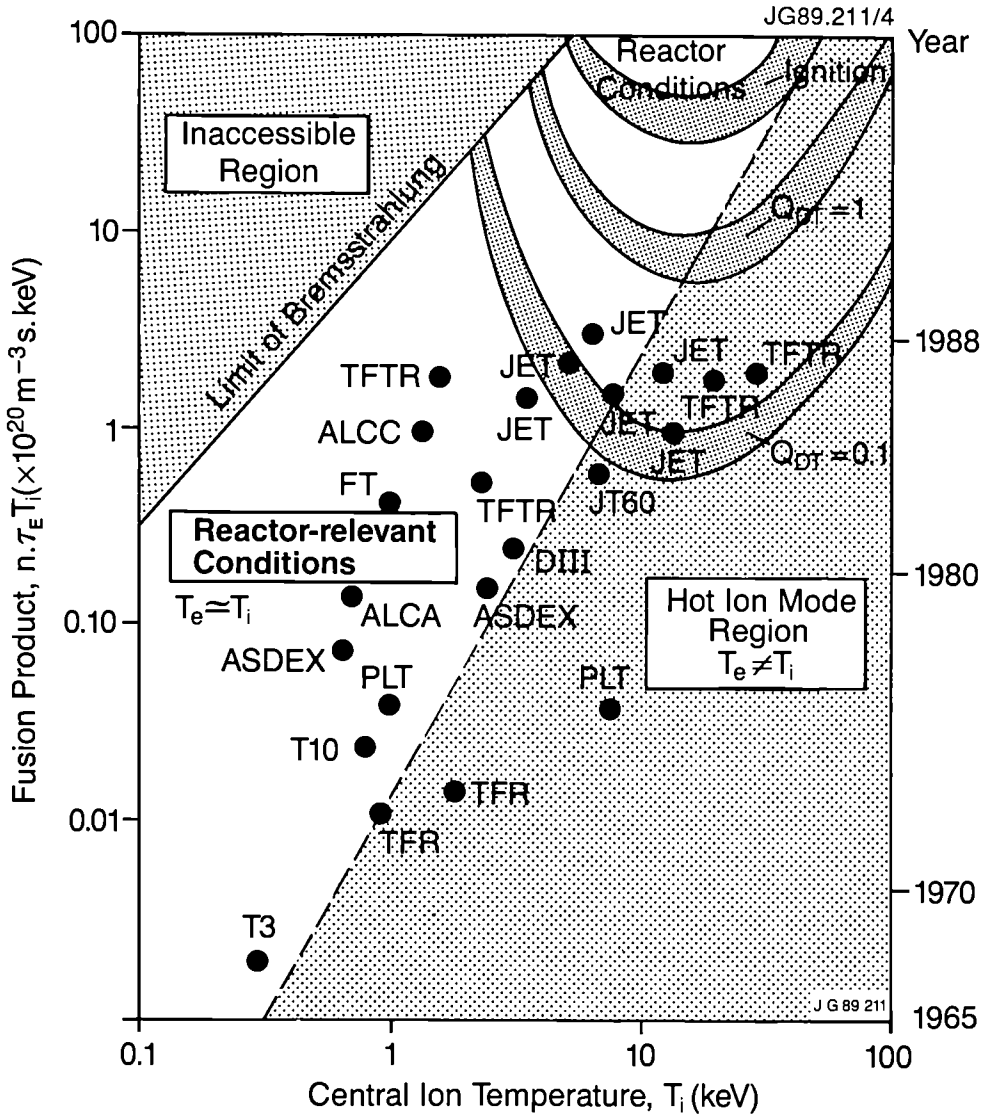

Fig.148: Fusion parameter as a function of central ion temperature for various fusion devices. The mode of operation relevant for a reactor is where the electron and ion temperatures are nearly equal at values between 15 and 50keV. The high density/low temperature region is forbidden due to radiation losses.

atomic number. Under conditions of improved energy confinement, such as H-modes or peak density profiles, impurities are also better confined. Especially in the latter case, the medium- and low-Z impurities seem to accumulate near the plasma axis, showing neo-classical behaviour. This results in an increased deuterium dilution in the plasma centre and increased central radiation losses.

The scrape-off layer of JET plasmas have been studied under various conditions[3,4]. In limiter discharges, the plasma edge temperature ranges from 25 to 100eV, increasing with the input power and decreasing with density. The scrape-off thickness is typically 1cm; this quantity is invariant under most conditions, except that it increases during ICRF heating. In X-point operation, all atoms and molecules recycling from the divertor near the separatrix are ionised locally.

Consequences for a Reactor

The observation that the particle confinement time is several times the energy confinement time has consequences for the reactivity of the core of the plasma: it would result in a relatively high concentration of impurities and helium. For high Z impurities, the radiation losses may prevent attainment of the required reactor temperature. For low Z impurities, in addition to helium produced by nuclear reactions, dilution of reacting ions should reduce the α-particle power.

The small scrape-off layer thickness results in a high power load on any material in contact with the plasma. This prevents the use of pump-limiters in a reactor in favour of an open divertor to take the plasma exhaust, and will require sweeping the separatrix over the divertor plates to reduce the mean peak thermal load.

Plasma-Wall Interactions

A variety of materials have been used for wall protection and high heat flux components[5]. JET initially operated with metallic walls, but the inner surface of the vessel ($\approx 200 m^2$) is now more than 50% covered with fine grained and carbon fibre reinforced graphite tiles. The remaining area is carbonised by performing glow discharges with some methane content. The wall temperature is maintained at ~300°C. If previously conditioned by running discharges in helium, the carbon wall has proved to be a very efficient pump for deuterium during plasma discharges[6]. A variety of models have been proposed but experimental evidence from JET supports the explanation involving co-deposition of hydrogen and carbon in the form of saturated H-C films. Indeed it is observed that more than 10-30% of the deuterium introduced into the vessel remains in the form of a deposited layer of hydrocarbons.

The dominant impurities in JET plasmas are carbon and oxygen. Their total amount is controlled mainly by the interaction of the plasma at the limiter. During a discharge, erosion of the limiter material is observed at the point of contact with the plasma and redeposited slightly further outside. Major plasma disruptions are most efficient in transporting materials from the first wall to the limiter. The ICRF antennae are separated from the plasma by a Faraday shield made of pure nickel. When the ICRF power is turned on metal is released from the screen and can also contaminate the limiters. In absolute terms, the nickel increase is low, especially if the screen has been previously carbonised, but it is planned to use beryllium in the future to take full advantage of this low Z material.

The increase in additional power and therefore of the heat load in JET has necessitated an increase in the material area in contact with the plasma. The belt limiters now in use, handle powers exceeding 40MW for 10s. For X-point operation, eight graphite poloidal rings have been installed to protect the top and the bottom of the vacuum vessel. The surface temperature of the protection tiles has exceeded 1600°C during the heating phase of X-point discharges. This has resulted in unacceptably large carbon influxes. Water cooled dump plates will be installed during the 1989 shutdown to increase the 40MJ-2s present power handling limitation. Protection tiles have been broken during X-point operation. Carbon fibre reinforced graphite has been used in areas where the impact of runaway electrons or neutral beams could occur, as these can withstand $30 MWm^{-2}$ for a few seconds.

Consequences for a Reactor

The use of low-Z material for the plasma facing components still seems to be the best option for a reactor. Graphite, used so far on JET, behaves generally well but problem areas have been identified, such as its role as an impurity source, its high chemical reactivity with hydrogen and its high retention of hydrogen leading to problems with density control and with tritium inventory. Combined use of beryllium carbide and of carbon fibre reinforced graphite is a sensible proposal but this is clearly an area where further research is required. Surface temperatures should be kept below 1000°C.

To avoid fragile cooling systems in the immediate proximity of the plasma, the heat load at the divertor plates should be limited to $2 MWm^{-2}$. To spread the power over a large area and together ease the accuracy required in the shaping of the tiles, an attractive option is to sweep the X-point radially.

Operational Limits

The maximum thermal and mechanical stresses in a tokamak are experienced during plasma major disruptions. The plasma thermal energy is dumped on the limiter and about 50% of the poloidal magnetic energy is dissipated in the vessel walls. The time-scale ranges from 100μs for thermal dump to tens of milliseconds for the dissipation of eddy currents. In addition, runaway electrons are produced in the decaying plasma and can deposit their energy on very small spots (up to $500 MJm^{-2}$). When the elongation becomes too large ($\gtrsim 1.8$), a vertical instability can develop followed by a disruption. In this case, with high currents, vertical forces acting on the vacuum vessel have been measured up to 350tonnes.

Major disruptions occur when the power radiated by the periphery of the plasma, around the $q_\psi = 2$ surface, exceeds the input power in this area or when $q_\psi = 2$ at the plasma boundary. Therefore, these occur preferentially when attempting to increase the plasma density above a limit, which depends on the input power and on the cleanliness of the plasma or when attempting to work at a too low q_a value. These can also occur accidentally when a piece of wall material falls into the plasma or subsequent to the crash of 'monster' sawteeth, where the released energy induces important outgassing from the wall.

Internal disruptions (or sawteeth) present another limitation in performance which can be achieved in JET. The increased volume inside the $q_\psi = 1$ surface is the most likely reason for confinement saturation observed in JET when $q_a < 4$. This is supported by the saturation of the incremental confinement time τ_{inc} $(= \partial W/\partial P)$ when $I_p/B(MA/T)$ exceeds unity in JET (i.e. seen when ≤ 4).

So far, JET performance has not been limited by excessive β values. In experiments performed at 1.4T, and with 10MW ICRF power, the dimensionless factor $g = a.B.\beta/I_p$ has not exceeded 1.6 (i.e. 60% of the Troyon limit).

Consequences for a Reactor

The ignition domain of a reactor must be large enough to avoid operational limits experienced in present days tokamaks. A major disruption at full current cannot be completely excluded and the machine must be able to support the resulting stresses, but repetitive disruptions

must be avoided. This means that the required performance should be achieved at q $\geq$2.5 with a reserve in β and with a low enough heat load on the wall. On the other hand, it can reasonably be expected that the ohmic density limit will be overcome in the presence of strong α-particle heating.

Large internal disruptions must also be avoided to ensure a smooth burn of the plasma. By contrast with the present situation, monster sawteeth could be deleterious in a reactor. This depends upon the steady-state current profile, but operating at a medium value of q_a may be necessary. The size of an ignition device must ensure that the central temperature is large enough even in these conditions to sustain production of fusion power.

Neutron Yield

Neutron yields exceeding 10^{16} n s^{-1} have been observed in JET. Maximum values of Q_{DD} in JET are $\approx 5\times10^{-4}$. In a similar 50% D-T plasma, the maximum corresponding ratio Q_{DT} would be in excess of 0.1. It must be noted that in these conditions, about half of the neutrons result from reactions between the injected beams at 80 keV and the target plasma. The other half are produced by true thermonuclear reactions. At low electron density with neutral beam injection, the ion temperature, T_i, significantly exceeds the electron temperature, T_e. Only a combination of NB and ICRF has produced simultaneous high T_i and T_e.

Neutron fluxes in JET have already been sufficient to induce a non-negligible radioactivity of the inner components of the vacuum vessel. When tritium is introduced in JET in 1991, the total value of the ratio Q_{DT} is expected to exceed 0.5. This corresponds to a total nuclear power of about 15 MW, when beam-plasma reactions are also taken into account. In a D-T plasma at the temperatures already achieved, the percentage of high energy α-particles would be similar to those of a plasma at ignition; it may then be possible to observe the effects of these α-particles in the plasma behaviour and to compare with energetic minority ions created by ICRF heating.

Consequences for a Reactor

Peak Q_{DD} values achieved in present tokamaks are in an operational mode which is not relevant to an energy producing reactor. These so called 'hot-ion' modes cannot be extrapolated towards ignition where the ion temperature should be close to, but lower than, the electron temperature. In a driven system, where the ion temperature could be higher, the recirculating power needed to decouple the ions from the electrons would be prohibitive (see Fig.148).

On the other hand, ICRF heating which produces He^3 minority ions in the 1 MeV range (i.e. close to the α-particle energy) has not shown new deleterious effects. This gives confidence for α-particle heating.

References

[1] Gondhalekar, A, et al, 'Simultaneous Measurements of Electron and Particle Transport in JET'; 15th European Conference on Controlled Fusion and Plasma Heating (Dubrovnik, Yugoslavia, 1988), Europhysics Conference Abstracts, Vol.12B, p151;

[2] Behringer, K., et al, 'Impurity Transport in JET during H-mode, Monster Sawteeth and after Pellet Injection'; 15th European Conference on Controlled Fusion and Plasma Heating (Dubrovnik, Yugoslavia, 1988), Europhysics Conference Abstracts, Vol.12B, p338;

[3] Tagle, J.A., et al, 'The Effect of Edge Temperature on Impurity Production under a Range of Operating Conditions in JET'; 14th European Conference on Controlled Fusion and Plasma Physics (Madrid, Spain, 1987), Europhysics Conference Abstracts, Vol.11D, p662;

[4] Kock, L., et al, Role of the Scrape-off Layer in X-Point Discharges in JET; 15th European Conference on Controlled Fusion and Plasma Heating (Dubrovnik, Yugoslavia, 1988), Europhysics Conference Abstracts, Vol.12B, p655;

[5] Rebut, P.H., Diëtz, K.J. and Lallia, P.P., 'Experience with Wall Materials in JET and Implications for the Future'; 8th International Conference on Plasma Surface Interactions in Controlled Fusion Devices (Jülich, F.R.G., 1988), to be published in J. Nucl. Mater. (see JET Report JET-P(88)21);

[6] Cohen, S.A. and the JET Team, 'Particle Balance and Wall Pumping in Tokamaks', Controlled Fusion and Plasma Physics, **29**, 1205 (1987);

Progress Towards a Reactor

A record value of the fusion product $<n_i(0)\,\tau_E\,T_i(0)>$ of 2.5×10^{20} m^{-3}.s.keV was achieved in 1988, with 15 MW of neutral beam heating during X-point operation in the H-mode. In addition, for limiter discharges, the values of the fusion products obtained for ohmic heating, RF, NB, combinations of these methods and with injection of solid pellets of deuterium have been in the range $1.2\text{-}2.0\times10^{20}$ m^{-3}.s.keV. These similar values result from degradation in confinement time offsetting gains made in the values of the other parameters.

The record fusion parameter value of 2.5×10^{20} m^{-3}.s.keV was achieved in the H-mode of magnetic limiter operation (X-point) with ~15 MW of neutral beam input into a 4 MA plasma, following optimization of the various plasma parameters.

TABLE XII
Maximum values of $\langle n_i(0)\tau_E T_i(0)\rangle$

Experimental Programme	Peak Density $n_i(0)$ ($\times 10^{19} m^{-3}$)	Energy Confinement τ_E (s)	Ion Temperature $T_i(0)$ (keV)	Fusion Product $\langle n_i(0)\tau_E T_i(0)\rangle$ ($\times 10^{19} m^{-3}$.s.keV)	Q_{DT} Equivalent Q_{DT}	Plasma Current I_p (MA)
Ohmic (4.6MW)	4.0	1.0	3.1	12	0.010	5
ICRF (16MW)	3.8	0.4	8.0	12	0.025	3
Pellet +(12MW) ICRF	5.4	0.5	7.2	20	0.10	3
NBI (20MW) low n:	1.5	0.4	20.0	12	0.30*	3
Combined NBI + RF (22MW)	4.5	0.5	8.1	20	0.30*	3.5
X-point (NBI-15MW)	6.0	0.7	6.0	25	0.30*	4

* Beam-Plasma reactions are dominant

However, a significant improvement was made in the fusion product with RF heating of a pellet seeded plasma. A value of $2.0\times10^{20} m^{-3}$.s.keV ($n_i(0)=5.4\times10^{19} m^{-3}$, $T_i(0)=7.2$ keV, and $\tau_E=0.5$ s) was reached using 12 MW RF heating in a 3 MA deuterium plasma. The maximum values of the fusion product and the corresponding values of plasma temperature, density and energy confinement time are given in Table XII for different operating scenarios.

In the RF heated plasma with pellet injection, 12 MW of RF power produced a plasma stored energy in excess of 7 MJ and a D-D fusion rate of $5\times10^{15} s^{-1}$. In this discharge, a significant fraction of the stored energy resulted from the minority ions which are expected to produce high fusion yield in (D)T heating schemes.

The maximum neutron yield obtained so far was $1.2\times10^{16} s^{-1}$ produced with neutral beam heating. This resulted mainly from D-D reactions occurring between the deuterium particles in the heating beams and the plasma. The best ratio of fusion power to input power obtained was $Q_{DD}=5\times10^{-4}$ which is equivalent to $Q_{DT}\sim0.3$, if tritium was introduced into the machine under these conditions. This would correspond to a fusion power production of above 1.5 MW. This enhanced reaction rate is due to interactions between the plasma and neutral heating beams.

Developments and Future Plans

In 1978, the original objectives of JET were set out in the JET Design Proposal, EUR–JET–R5, as follows:

'The essential objective of JET is to obtain and study a plasma in conditions and dimensions approaching those needed in a thermo-nuclear reactor. These studies will be aimed at defining the parameters, the size and the working conditions of a Tokamak reactor. The realisation of this objective involves four main areas of work:

(i) the scaling of plasma behaviour as parameters approach the reactor range;
(ii) the plasma-wall interaction in these conditions;
(iii) the study of plasma heating; and
(iv) the study of α-particle production, confinement and consequent plasma heating.

The problems of plasma-wall interaction and of heating the plasma must, in any case, be solved in order to approach the conditions of interest.

An important part of the experimental programme will be to use JET to extend to a reactor-like plasma, results obtained and innovations made in smaller apparatus as a part of the general tokamak programme. These would include: various additional heating methods, first wall materials, the control of the plasma profiles and plasma formation.'

These objectives still remain valid and continue to provide the focus of the Project's plans. In addition, the JET Project, as a central part of the European Fusion Programme, is directed towards the objectives of that Programme, agreed by the Council of Ministers in the following terms:

'The main objectives of the programme are: to establish the physics and technology basis necessary for the detailed design of NET: in the field of physics and plasma engineering this implies the full exploitation of JET and of several medium-sized specialised tokamaks in existence or in construction ...'

At the end of 1988, the JET Project was about halfway through its existing experimental programme. Two of the main objectives - the study of scaling laws and of additional heating - have, to a large extent, been achieved. The phenomenon of confinement degradation has been confirmed and requires that the physical dimensions of large tokamaks must be a little larger than was thought in the early 1970's. Some aspects of α-particle heating have been studied; further studies in this area will take place with experiments in D-T during the final phase of the programme. Recent experimental results at high power (>30MW) have shown clearly that objective (ii) – the study of plasma wall interactions (including the reduction of impurities to an acceptable level) – becomes the most important area for investigation in the future and will consequently take a substantial amount of the future JET scientific programme. With respect to objective (iv) – study of α-particle production, confinement and consequent plasma heating-scientific and technical plans will focus on the development of α-particle diagnostics and the preparation of the radioactive phase of operation with tritium, this fits within an extension to the life of the JET Joint Undertaking up to December 1992, which was granted in October 1988 by the Council of Ministers.

The JET aims clearly state that JET is an experimental device and that, to achieve is objectives, the latest developments in Tokamak physics must be allowed to influence its programme. The proposed programme includes some new additions and enhancements to overcome confinement degradation to reduce impurity levels, and to push the parameters of the JET plasma even closer to those needed in a thermonuclear reactor. This is in complete agreement with the original objectives laid down for JET.

While present achievements show that the main objectives of JET are being actively addressed and substantial progress is being made, the strategy for JET can be summarised as a strategy 'to optimise the fusion product $< n_i(0)\, \tau_E\, T_i(0) >$'. For the energy confinement time, τ_E, this involves maintaining, with full additional heating, the values that have already been reached with ohmic heating alone. This means overcoming confinement degradation. For the density and ion temperature, it means increasing their central values $n_i(0)$ and $T_i(0)$ to such an extent that D-T operation would produce α-particles in sufficient quantity to be able to analyse their effects on the plasma.

The enhancements to JET aim to build up a high density and high temperature plasma in the centre of the discharge (with minimum impurity levels) where α-particles could be observed, while maintaining an acceptably high global energy confinement time, τ_E. The mechanisms involved are to decouple the temperature

profile from the current density profile through the use of lower hybrid current drive and neutral beam injection to ensure that, at higher central temperatures, the current density in the centre does not reach the critical value that causes sawteeth oscillations.

This will involve the following:

(a) Increase the Central Deuterium Density $n_D(0)$ by:

- using beryllium (Be) evaporators, Be tiles on the belt limiters, Be antennae screens to decrease the impurity content;
- injecting high speed deuterium pellets and higher energy deuterium neutral beams to fuel the plasma centre and dilute impurities;
- injecting pellets to control the influx of edge material;
- stabilising the m=2, n=1 magnetic oscillations present at the onset of a disruption with magnetic perturbation produced from a set of internal saddle coils which will be feedback controlled;

(b) Increase the Central Ion Temperature, $T_i(0)$ by:

- trying to lengthen the sawtooth period;
- controlling the current profile (by lower hybrid current drive in the outer region, and by counter neutral beam injection near the centre) to flatten the profile;
- on-axis heating using the full NB and ICRF additional heating power (30MW, ICRH, and 20MW, NB).

(c) Increase the Energy Confinement Time, τ_E by:

- increasing up to 7MA the plasma current in L-mode operation;
- increasing up to 3MA the plasma current in the full power, long pulse H-mode operation using the cooled separatrix dump plates in the double-null X-point configuration.

In parallel, preparations for D-T operation must proceed at full speed to ensure that the necessary systems for gas processing, remote handling, radiological protection, active handling and operational waste management are fully commissioned and operating satisfactorily in good time before the introduction of tritium into the JET device. In addition, the tritium neutral injection system at 160kV and α-particle diagnostics can be developed for this phase.

The following sections describe various developments which are underway on JET to implement these systems.

High Current Operations

Plasma currents of 7MA have been obtained in JET with a material limiter configuration, and 5.3MA has been obtained with single-null, and 3.5MA has been obtained with double-null magnetic limiter configurations.

The inductive drive (or V-s) available has been increased and more fully utilized by:

- Differential current control of the primary windings, thus increasing by 50% the maximum current in the midplane coil;
- The reduction of stray field at plasma breakdown by adding two coils at primary top/bottom.

The current ramp at constant toroidal field is limited by instability at rational values of q_ψ, which can lead to quasi-stationary modes and subsequent disruption. This limits the area of rise of plasma current to typically 0.25MA/s at 6MA, when $q_\psi = 3$. Despite the low loop voltage (0.5V on-axis), this scenario is expensive in V-s consumption. At constant q_ψ, higher current ramp rates are possible (e.g. 0.75MA/s up to 7MA at $q_\psi = 2.5$). In such a case, sawteeth oscillations are present throughout the current rise and the loop voltage on axis is typically 1V. The saving of resistive V-s with this scenario permitted a flat-top of 2s at 7MA. The ohmic discharges can be made free of disruptions. However, with additional heating power above 20MW at 5 or 6MA, interaction with the limiter is strongly enhanced. This can lead to significant modulation of the total radiated power, carbon influxes, MARFE-like phenomena and disruptions.

Magnetic separatrix configurations can be formed in JET at high plasma currents using the combined fields from primary leakage, shaping coils and, in the case of the single-null configuration, from the radial field produced by unbalanced currents in the main vertical field coils. At 5MA current, the separatrix clears the limiters and the inner wall by 8cm or more and the single null X-point is 10cm in front of the dump plates. When such a configuration is formed, the plasma density pumps out very strongly, at up to 10^{22} particles/s.

Study of X-point Sweeping

Excessive influx of carbon into the plasma during high power operation appears to be related to high surface temperatures of the plasma facing components. This is the so-called carbon catastrophe. In the case of X-point operation, where the power load is strongly localized near the separatrix flux surface, an effective reduction of peak surface temperatures is possible by sweeping the separatrix position in time. The carbon influx is a strongly non-linear function of the surface temperature. Therefore, it is expected that by sweeping the input power, the threshold for the carbon catastrophe can be significantly raised, and possibly eliminated altogether in X-point operation. As an example: in a 3MA plasma, with a projection of about 5cm of the power scrape-off layer on the X-point target tiles, and a sweep amplitude of 0-15cm, a temperature reduction of about 80% would be expected.

Sweeping is performed by modulating currents in the shaping, vertical field and radial field coils. Since radial sweeping is not compatible with high current operation and with coupling ICRF power, the study has concen-

trated on modulating the current in the P3 poloidal shaping coil, connected in series with the P4 imbalance circuit. This should allow sweeping both in single-null and double-null configurations, and maintains the possibility of coupling ICRF heating power.

Study of a Divertor Magnetic Configuration

A divertor mode of operation is being studied which should allow operation with (a) low power loading to control impurities and (b) efficient pumping for plasma density control.

An example of a divertor magnetic configuration at 6MA plasma current is shown in Fig.149. This is achieved by inserting a new inner divertor coil (PD) with a current of 400kA at the bottom of the vacuum vessel. With the PD coil, it should be possible to produce single-null configurations routinely up to plasma currents of 6MA and with a distance between the X-point and the vessel of ~40cm. This distance should be sufficient to accommodate cryogenic pumping systems both on the high and the low field side and to shape target plates in such a way that the heat load is $<700\,Wcm^{-2}$.

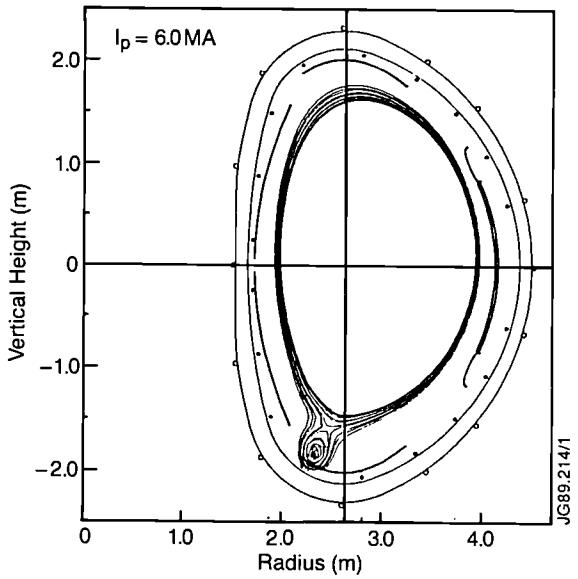

Fig.149: Divertor magnetic configuration at 6MA plasma current.

Stress calculations with localised loads have shown that these values are compatible with the present mechanical structure of the vessel. The forces introduced by the PD coil on the toroidal field (TF) coils will be about 10-20% of those produced by the other poloidal field (PF) coils.

Stabilization of Disruptions

Disruptions have limited the operating range of current and density in all tokamaks and, despite continued efforts, still limit the operation of JET. Due to the large size and D shaped cross-section of JET, high currents up to 7MA have been sustained for seconds, but considerable care is needed to program the rise and decay of the current and density to avoid disruptions at such high values. Since the electromagnetic forces exerted on the vacuum vessel increase in proportion to the square of the plasma current, disruptions at such high currents could present a serious risk to the machine. Furthermore, the design of the next step devices depends very much on the expected severity and frequency of disruptions. Due to the importance of reducing the frequency and severity of disruptions, considerable effort has been devoted to understanding the causes of disruptions and attempting to stabilize them.

One such method to stabilize disruptions, that has been attempted to a limited degree on some smaller tokamaks with partial success, is by magnetic feedback. It has been observed on other tokamaks as well as on JET that disruptions are usually preceded by growing oscillating magnetic field perturbations that have a definite geometrical asymmetry often denoted as m=2, n=1. By utilizing this asymmetry in the magnetic field structure, such growing oscillating modes can be measured when they are still about 0.001% of the equilibrium field of the tokamak. Appropriate placement of diagnostic pick-up coils inside the vacuum vessel are used for this purpose. Combinations of signals from these pick-up coils can then be used as input to a feedback control circuit that will drive a set of well situated large saddle coils also mounted inside the vessel. Through a sophisticated feedback control circuit, the amplitude and phase of the driving magnetic fields produced by the saddle coils will be maintained relative to the measured magnetic field perturbations from within the plasma to cancel out the particular asymmetry of the growing m=2, n=1 instability.

Due to the complexity of disruptions, it is still uncertain whether stabilizing the m=2, n=1 instability will be sufficient to avoid all modes. This method should reduce the total number of disruptions and provide a warning of an impending disruption, so that corrective action can be taken to attempt to reduce its severity. Other asymmetries such as the m=3, n=2 may arise once the m=2, n=1 is stabilized, but the outcome of this experiment will indicate the direction that must be followed to stabilize such disruptions. In addition, theoretical calculations of the growth rate of the instabilities and the poloidal inertia of the m=2, n=1 magnetic structure under the influence of magnetic feedback are being performed to indicate what may be the shortest response time required of the feedback system. Design constraint limits on this response time may also limit the number of disruptions that the feedback system is capable of stabilizing. Questions like these can only be answered conclusively by experiment.

The design of the large saddle coils and their support structures inside the vessel is complete and the compo-

nents are being manufactured. Due to the large size of the saddle coils and their placement inside the vessel optimized to drive maximum power in the m=2, n=1 mode, here have been many constraints on the design. In particular, these coils have been designed around existing structures inside the vessel as well as to avoid interference with diagnostic lines-of-sight. Due to the electromagnetic forces exerted by the strong magnetic fields in the tokamak on the current carrying busbars, the maximum current has been set at 5kA per turn in order to adequately support the busbars within the vessel. It is expected that the saddle coils may be installed during the next major shutdown.

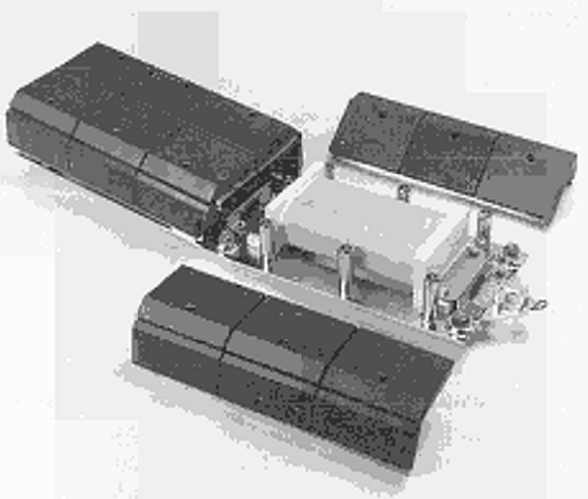

FIG.150: Photograph of one of the JET disruption feedback stabilization poloidal field pick-up coil assemblies. Each assembly contains two 20cm long coils to be mounted vertically in the outer midplane between every two adjacent ICRH antennas.

A set of eight dedicated high sensitivity diagnostic poloidal field pick-up coils has been designed and constructed to measure the perturbations in the magnetic field from the plasma preceding disruptions (Fig.150). The coils will be mounted in pairs inside the vessel between every two adjacent RF antennas with one coil just above and the other coil just below the outboard midplane of the tokamak. These each have a total poloidal surface area of approximately $2.5m^2$ to give high sensitivity to small magnetic field perturbations, particularly at low frequency since the response is proportional to frequency. The coil formers are made of high temperature bonded alumina ceramic to provide a linear frequency response well in excess of the driving saddle coils with little or no phase shift. The ceramic formers are wound with titanium wire with a 1mm pitch spacing to maximise the surface area and yet keep the overall coil dimensions as small as possible. Appropriate combinations of these coils will then be highly sensitive to the m=2, n=1 magnetic field perturbations from the plasma and comparatively insensitive to the driving field of the saddle coils. These combinations of pick-up coils can then be used as input to the feedback circuit to drive the saddle coils to stabilize the modes that arise in the plasma. The precise geometry of the positions of the diagnostic pick-up coils relative to the position of the saddle coils is critical to obtain adequate rejection of the driving fields produced by the saddle coils so that only the field perturbations due to the plasma modes will be picked up. Two pairs of the pick-up coils will be installed in opposite octants during the 1988-89 shutdown to assess the noise levels of the system and determine the measurement capabilities of the diagnostic. The remaining two pairs will be installed during the next major shutdown.

Initial designs for the power amplifiers required to drive the saddle coils have been drawn up and a call for tender has been made. The amplifiers are expected to be installed during the major shutdown in 1990.

In addition to the work on JET, an Article 14 contract has been placed with UKAEA Culham Laboratory, U.K., to perform for JET a mock-up disruption feedback stabilization experiment on the DITE tokamak. The DITE team has attempted as far as possible to emulate the proposed JET experiment on a smaller scale. A set of eight saddle coils have been installed in a similar arrangement to that proposed for JET, except that due to constraints within the DITE vacuum vessel the geometry is asymmetric. The coils have been placed with each pair on opposite sides of the machine, but rather than having 90° toroidal separation between each pair, there are only 67° between two of the pairs of saddle coils. This causes some problems in measuring and producing orthogonal components to the magnetic field perturbations, but may nonetheless answer many of the questions of disruption feedback stabilization that concern the JET experiment. In addition to the saddle coils, the DITE team have borrowed high frequency power amplifiers from the COMPASS experiment to drive the saddle coils at frequencies above 10kHz down to near zero frequency. To pick up the magnetic perturbations inside the plasma, sets of ceramic pick-up coils have been installed near each saddle coil location inside the vacuum vessel. Combinations of the coil signals are then input to a digital feedback circuit that employs a fully programmable microprocessor and look-up table to produce an output waveform with a phase and amplitude that changes depending on the input frequency. In principle, such a feedback circuit can be programmed to take into account any frequency dependent phase shifts that may arise due to eddy currents in the vessel, delays in the electronics, or plasma effects once the open loop characteristics are determined. First results of the plasma response due to the driving saddle coil fields have just been made and are being analyzed. It is expected that the results with feedback will be obtained in the early part of 1989.

Results from the DITE experiment will help to accelerate the JET disruption feedback stabilization programme by answering some of the basic questions concerning feedback stabilization. In particular, the response of the plasma to feedback controlled m=2, n=1 magnetic field perturbations is still not well known.

The design of the JET feedback control circuit is being developed and will be influenced by the results found with the DITE feedback scheme. The required speed of the feedback system and the magnitude of the saddle coil field required for stabilization also still need to be experimentally determined. In addition, the phase error that can be tolerated between the measured plasma field perturbation and the applied saddle coil field can only be found through experiment. Assuming DITE can demonstrate disruption feedback stabilization on a small tokamak, it remains for JET to prove that it can also be done on a large machine in plasmas very near those required in a reactor.

Current Drive and Profile Control

The main objectives of current drive and profile control remain:

- to suppress sawtooth activity and to benefit from higher core reactivity by sustaining peaked profiles of both density and temperature;
- to modify local values of the current gradient and improve energy confinement in the plasma centre;
- to assess the current required for non-inductive operation of large tokamaks.

The tools available on JET, to perform current drive and profile control experiments are:

- neutral beam (NB) current drive;
- self-induced (non-inductive) currents in the plasma, such as the bootstrap current arising from strong local pressure gradients;
- ion cyclotron resonance frequency (ICRF) current drive;
- lower hybrid current drive (LHCD).

High neutron yield and improved energy confinement have been observed when additional heating was applied during the plasma current rise phase, before the onset of sawteeth [1]. These results have further extended those obtained during sawtooth-free periods in the current flat-top ('monster') regime, characterised by a large incremental confinement time and high central ion and electron temperatures.

Neutral beam current drive up to 0.5 MA in low density discharges has been obtained, as reported in the 1987 JET Progress Report. Detailed analysis of such discharges where the bootstrap current is taken into account has allowed simulation models to be assessed. Higher beam energies (up to 140 keV) should increase the operational density for current drive experiments.

An extensive study of bootstrap induced currents [2] has shown that large currents (0.7 MA) have been produced in H-mode plasmas at the plasma periphery, with a significant broadening of the current profile, eventually suppressing sawtooth activity. The estimated bootstrap current in 'monster' discharges is lower (0.1 MA) and closer to the plasma centre. Larger values should be anticipated, if peaked density profiles can be maintained, as obtained in discharges with combined ICRH and pellet injection.

The ICRH system was modified in 1988 to implement proper phase control of the antennae array. The phased array can be operated in the entire frequency bandwidth of the system (23-57 MHz) and at least two promising current drive methods can be evaluated, as follows:

(i) Transit Time Magnetic Pumping (TTMP) and Electron Landau Damping (ELD) of Fast Waves

The intrinsic efficiency of this method is marginally larger than that of LHCD for the same phase velocity. However, the wave absorption is considerably weaker. In JET, suitable conditions exist at 33 MHz, 3.4 T, for a D plasma with no ^{3}He injection or at 25 MHz, 1.5 T for H plasma with the fundamental hydrogen resonance at the plasma centre (25 MHz, 1.5 T). Preliminary experiments in hydrogen at high β showed as much as 40% absorption by TTMP and ELD.

(ii) Minority Ion Current Drive

This scheme relies on asymmetric heating of minority ions and produces highly localized toroidal current:

(a) close to the flux surface tangential to the resonance;

(b) flowing in opposite directions inside and outside this flux surface. Therefore, this method is suitable for local shear control and could be used to flatten the current density profile at $q \sim 1$ which should stabilise sawteeth. Calculations show that the present JET system could lead to sawtooth stabilisation for plasma currents up to 2 MA.

The LHCD programme, described in the 1987 JET Progress Report has been actively developed and the prototype phase was close to completion by the end of 1988. Theoretical work has been devoted to the evaluation of wave absorption and current drive efficiency to be expected in present high performance JET scenarios. Ray-tracing and Fokker-Planck codes have been coupled to JET databases to estimate propagation and absorption in realistic JET scenarios. A variety of high power NBI and ICRH JET plasmas, such as sawteeth stabilised, high current, H-modes and pellet fuelled discharges have been analysed, including fast ion absorption models. The highest wave absorption and current drive efficiency are expected in high temperature plasmas with peaked density profiles.

To assess the validity of these simulations and to evaluate the capability of profile control through lower hybrid waves, possible measurements of the energy distribution and of the radial location of RF induced fast electrons by means of existing diagnostics on JET (ECE emission, fast X-ray emission) are being investigated through Article 14 Contracts with various Associations (CEA Cadarache, France; CNR Milan, Italy; and ENEA Frascati, Italy).

A description of the overall LHCD system and of the

launcher design has been given previously [3,4]. The system design has been completed and manufacture is close to completion. Most of the components have already undergone extensive testing. The JET LHCD system is powered by 24 klystrons operating at 3.7GHz. After extensive testing of seven tubes, the original power rating of 500kW/20s was increased to 650kW/10s, the limiting factor was interception of the electron beam at the lips of the output cavity. The higher power rating leads to lower reflected power requiring a circulator to protect the klystron, which has been successfully developed and tested.

Two klystrons have been operated since July 1988, alternately on a high power test-bed, enabling high power microwave components to be tested prior to installation on JET [1]. Previously, tests were performed at CEA Cadarache, France under an Article 14 contract.

The commissioning of the final high voltage power supply (-65 kV, 100A for four klystrons) began in December 1988. The first module of four klystrons is presently being installed at JET and will be operational during the first half of 1989.

The LHCD launcher will be installed in the equatorial port at Octant No.3 to produce a narrow wave spectrum centred at $n_{\parallel}=1.8$, through an array of 32 waveguides in the horizontal direction. The total number of waveguides in the launcher is 384, obtained from 48 microwave modules using the multijunction technique. Integral phase shifters provide the desired phase distribution at the grill mouth [1].

Following analysis of the disruption forces on the launcher, coated stainless steel waveguides have been selected. Two types of coating will be used: the multijunction will be coated with carbonised copper to minimise waveguide losses at a higher multipactor threshold; and silvercoating will be used for waveguides between the multijunction and vacuum window. Alternative coating techniques are being studied under an Article 14 contract at IPP Garching, F.R.G.

A schematic diagram of the LHCD launcher is shown in Fig.151, which highlights the main Torus Hall components. All the components shown have been tested at high power for their nominal operating conditions, including a prototype multijunction which has been successfully tested under vacuum up to 200kW/20s with short circuit termination. A test launcher ($L\phi$) will be installed on JET in 1989, comprising one third of the final number of waveguides. It consists of 2 parts: a JET-designed launcher ($L\phi P$) and a prototype ($L\phi C$) supplied by the Tore-Supra team from CEA Cadarache,

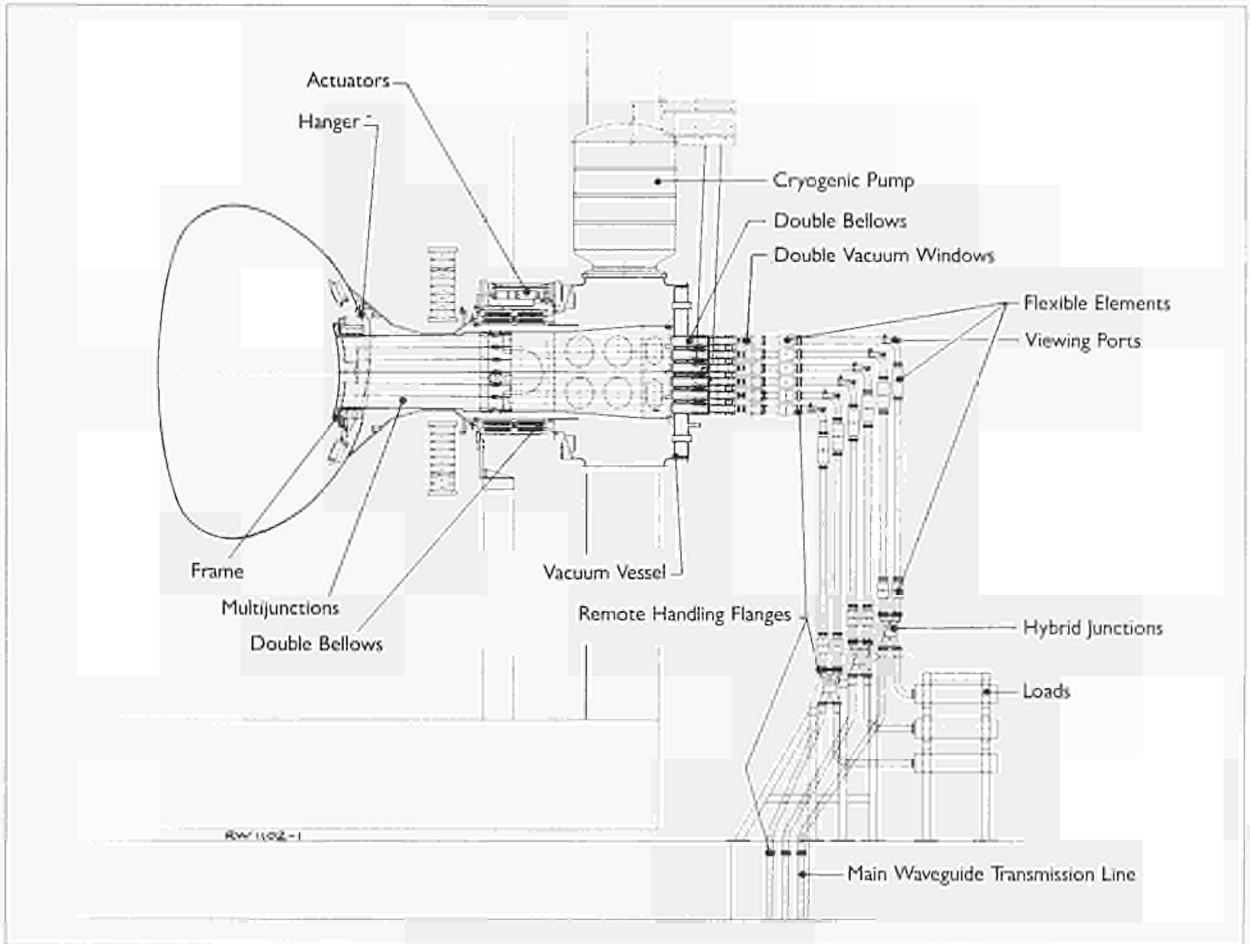

Fig.151: Schematic diagram of LHCD launcher;

France.

The vacuum vessel, which will contain the launcher, is show in Fig.152. The final launcher (L1) will be installed on JET in 1990 and will utilize most of the $L\phi$ hardware, such as vacuum vessel, side protection, and position control system.

Fig.152: The JET LHCD vacuum vessel.

References

[1] D Start, 'Experimental and Theoretical Studies of Ion Cyclotron Heating on JET' IAEA, 12th International Conference, Nice (1988).

[2] J Cordey, C D Challis, P Stubberfield, 'Bootstrap Current Theory and Experimental Evidence', 15th European Conference of EPS, Dubrovnik (1988).

[3] C Gormezano, 'The JET 10MW Lower Hybrid Current Drive System', 12th Symposium on Fusion Engineering, Monterey (1987).

[4] A Kaye, H Brinkschulte, G Evans, C Gormezano, J Jacquinot, S Knomlton, X Litaudon, D Moreau, M Pain, J Plancoulaine, C Walker, G Wilson, 15th Soft Conference, 'The Design of the JET Lower Hybrid Launcher', 15th Symposium on Fusion Technology, Utrecht (1988).

Pellet Injection

The presently installed multiple-pellet injector is capable of delivering pellets with speeds only up to 1500 ms^{-1}. To investigate the velocity dependence of pellet penetration with the aim of more central pellet deposition in heated high-temperature discharges, velocities up to or exceeding 10 kms^{-1} are required.

JET is presently developing a high-speed prototype pellet launcher (i.e. a gun in combination with a pellet-forming and breech-loading cryostat) capable of accelerating pellets of ~5mm diameter with velocities of 3-5 kms^{-1} on the basis of the two-stage light gas gun. To reach higher speeds, hydrogen isotope pellets must be contained in sabots (i.e. cups or cartridges) due to a progressive erosion effect at the barrel wall of the bare pellet when speeds reach ~3 kms^{-1}. After termination of the contract with the Ernst-Mach-Institut, Freiburg, FRG, this work was transferred to the JET Pellet Injection Testbed. A brief description of the Testbed and of the development achieved so far has been reported earlier in this Report. Although the majority of essential problems on the way to the high-speed gun can be regarded as solved, in principle, some extrapolatory development (in particular, in the areas of optimum mechanical strength of the pellet/sabot compound and of optimised gun performance) must still be carried out and a number of technical details also have to be tackled to increase the pellet velocity to 3.8 kms^{-1}. The necessary efforts will keep the Testbed occupied even during the operation of the prototype on the torus in late-1989, and will involve the following areas:

- The useful barrel length is limited due to the fast drop of the driving pressure along the barrel caused by gas expansion, friction and heat loss of the hot gas to the barrel wall. For the necessary speed, this requires accelerations exceeding the present maximum of $6x10^6 ms^{-2}$, which still yields healthy pellets. There is a limitation from shock waves being generated by the rupture disc which sets the break-away pressure, but part of the problem could also be originating from the sabot flight dynamics inside the barrel, particularly for split sabots. The first problem will be tackled in two ways by employing a newly designed fast valve instead of the bursting disc and by integrating a bursting disc into the sabot cartridge; the second method varies the materials, shapes and size (i.e. larger barrel diameter) of the sabot.
- To gain improved understanding of the underlying gas dynamics and to optimise the two-stage gun in the direction of a 'constant (driving) pressure gun', a numerical code (based on the 'Lagrange method') has been devised and experimental results from the testbed guns can now be described quantitatively without the need for free fitting parameters. The only asssumptions implied are that the pressure drop due to friction and the heat loss to the barrel are both characterised by fully developed stationary turbulence. It should be emphasised that the temperature rise of the inner barrel surface due to heat deposition

and its diffusion into the barrel must be taken into account. From experimental results, there is evidence that friction of the sabot in the barrel can be neglected. Similarly, this holds for the piston in the pump tube, probably aided by some gas lubrication opted for in the design to extend the piston lifetime. With high confidence in the computational results, the code is presently being used to extend and optimise the parameters - piston mass, pump tube dimensions, pressures - and to study effects which permit the use of longer barrels, like preheating of driver gas and hot barrels to reduce heat losses (this has experimentally been found to be influenced by the heat conductivity of barrel material, e.g. carbon steel compared to stainless). For instance, calculations have indicated a more constant driving pressure for higher peak pressures in the pump tube in the relevant parameter range; this will now be tested on the second gun system with enhanced pressure capability (up to 4000 bar).

- It is important to maintain the ability of pellet ice formation with changing sabot development. Currently, it is hoped that the pellet cryostat (developed by collaboration with CEN Grenoble, France) can be adapted by relatively small modifications only. This allows insertion of sabots without breaking vacuum, ice formation (cryocondensation as well as injection moulding into the sabot) and its transfer to the breech in a matter of minutes. The conversion of this type of cryostat to work reliably in the Torus Hall under remote control is now one of the major engineering tasks and is on the critical path development.

Preparation for the implementation of the launcher prototype into the torus system was performed under the perspective that the services and the quite demanding mechanical support required for installation and operation must also be compatible with the advanced, remote-handling and tritium compatible, multiple-pellet launcher system contemplated for a later stage. Concerning the support, it does not matter much how many launchers are installed, the single-shot characteristics of a two-stage gun (longitudinal forces of several 100 t and a fraction of this in the transverse direction) already determine gross requirements. Since the prototype launcher is still under development, great care has been taken in planning and in preparations to allow with a minimum of time and effort an easy change-over of a launcher commissioned on the Testbed to the Torus Hall and its immediate operation thereafter. In particular, the control and monitoring is being tailored in an identical manner for both sites, Testbed and torus main control. The prototype implementation is planned for late-1989 and a report on the accomplished part of the preparation can be found in a previous section of the Report.

The CEA Cadarache Laboratory, France has volunteered to carry on the JET prototype development both in design and testing for and to produce the conceptual design of a repeating ($\sim 1\,s^{-1}$) launcher suitable for the advanced system. This more comprehensive activity, employing jointly CEN (Centre d'Études Nuclaires) Grenoble and CEN Saclay, France, in a collaboration with JET under Article 14 Contract, started in mid-1988 to solve the problems of launcher repetitivity and reliability of components to permit the availability of a conceptual design of such a launcher in 1989, ready for a systems procurement decision. So far, the gun parts and a test-stand are under manufacture for test trials at Grenoble in early-1989 and a repetitive cryostat is also under design. The contract continued and expanded the earlier one in which CENG was mainly concerned with the cryogenic development (using for testing more conventional single-stage gas guns) and under which the successful development of the cryostat capable of sabot loading was accomplished in the first half of 1988.

The Article 14 Contract with the Risø National Laboratory, Denmark, was terminated at the end of the year as pursuit of the arc gun work, which so far had not yielded results competitive with those of the two-stage gun, was in JET's view not likely to be successful during the remaining lifetime of the Project at the currently possible level of support. The main problem areas of the arc gas gun lay in low arc heating efficiency, electrode wear and consequent gas contamination by impurities and difficulties with sufficient arc gas fuelling.

Tritium Handling

The JET time schedule requires that the Active Gas Handling System (AGHS) is ready for final commissioning by mid-1990 and is able to commence D-T operation in mid-1991. To achieve this schedule, components must be installed by early 1990. The multi-column cryogenic distillation for isotope separation was identified as the time critical item and a design and procurement contract was placed by the end of 1987.

Further advances on the Active Gas Handling System and progress in Radiological Protection Instrumentation and Safety Analyses are described below.

Active Gas Handling System (AGHS)

During 1988, the design of the major subsystems was completed and procurement contracts were placed. Detailed design work on an analytical laboratory, the gas introduction systems and piping systems is continuing into 1989. An experimental programme running in parallel gave results on crucial components in full agreement with design objectives.

In detail, the status at the end of 1988 was as follows:

a) Cryogenic forevacuum system:

The design was completed and a contract placed;

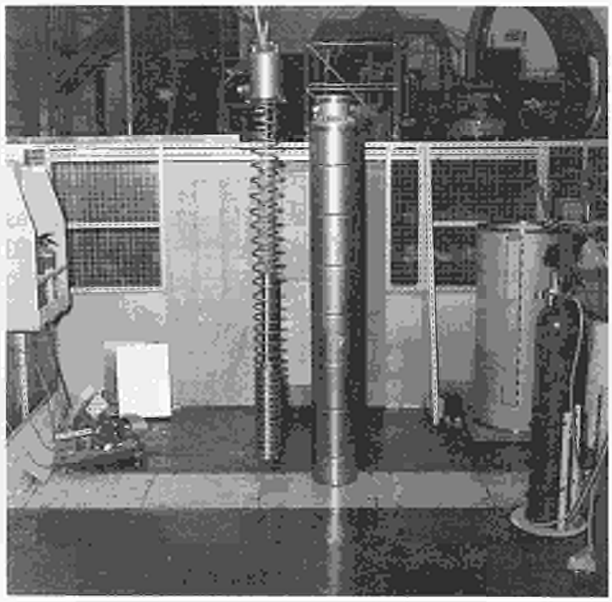

Fig.153: Accumulation Panel (cut-out of centre section only)

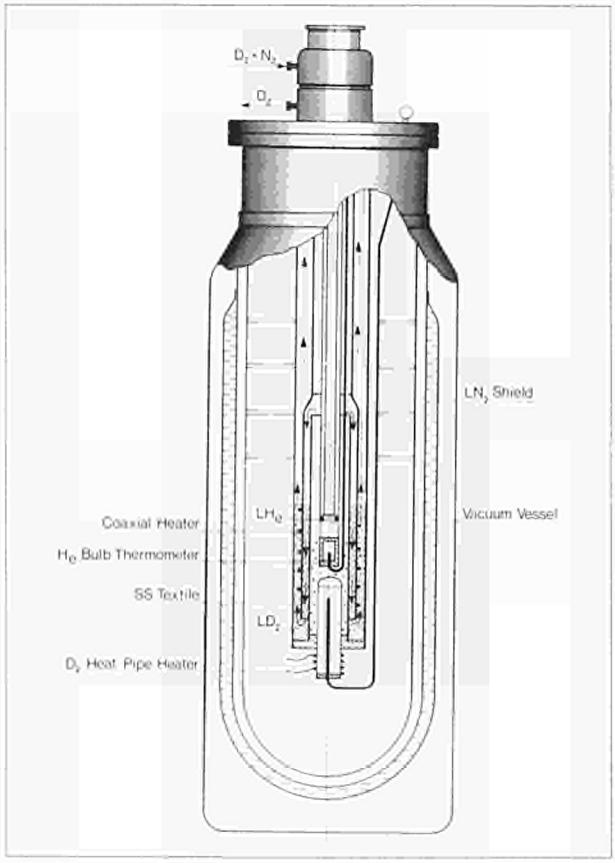

Fig.154: Cryotransfer Pump

detailed drawings were nearing completion and manufacturing should start in early 1989, with delivery expected to be completed at the end of 1989.

The accumulation panel (Fig.153) was tested for pumping speed, resulting in ~12,500 ls-1 at an inlet pressure of 1×10^{-2} mb.

The cryotransfer pump (CTP) (Fig.154) was tested for separation of impurities from hydrogen: an addition of 15 l (STP) of N_2 to a batch of 100 l (STP) D_2 was retained in the CTP during distillation with an N_2 content in the distillate of ~5 ppm.

b) Impurity processing loop:

The design of the main loop was completed and a contract placed; detailed drawings were nearing completion and manufacturing should start in early 1989, with delivery expected to be completed at the end of 1989.

A uranium bed prototype (see Fig.155) was successfully tested for hydrogen storage, charging and discharging dynamics and water decomposition. An identical reaction bed filled with iron powder was tested for water decomposition, showing 80% efficiency in single-pass operation. The design of an auxiliary valve/instrumentation box for this system was completed and a contract placed.

Fig.155: Uranium bed prior to filling (bottom) and fully assembled (top)

c) Mechanical forevacuum system:

The design was completed and a contract for the main vacuum pumps ($1\times600\,m^3\,h^{-1}$, $2\times150\,m^3\,h^{-1}$) as well as for identical pumps for the Impurity Processing Loop ($2\times150\,m^3\,h^{-1}$) were placed.

Six buffer tanks ($10\,m^3$ each) for various purposes (emergency expansion volumes for process gas, cryogenic fluids and for a house vacuum system) were designed and a contract placed, with delivery expected in April 1989.

All-metal vacuum valves for the mechanical forevacuum system and all other auxiliary vacuum systems have been specified and selected from commercial suppliers;

d) Exhaust detritiation

The specification and a layout design was completed. A contract for detail engineering, design and manufacture was placed. The design is nearing completion, and delivery is expected in early 1990.

e) Cryogenic Isotope Separation

The contract placed in 1987 is continuing. New components for this plant were developed and tested at JET including a reboiler with an integral liquid D_2 heat pipe, permitting measurement and control of the reboiler liquid level by vapour pressure sensing. A transpiration pump for the recirculation of hydrogen isotope mixtures, based on the surface tension of the liquid in a porous sinter filter, was also developed.

The system is expected to be installed in two stages: the He-refrigerator will be installed after completion of the Active Gas Handling Building (June 1989). The cryogenic distillation columns and control system will be available at the end of 1989.

f) Gas Chromatography Isotope Separation

The design of a system with four separation columns was completed and agreed with consultants. A contract for the main process box was placed and design of an additional valve/pumping box is nearing completion. Tests on an isotope arrival diagnostics by means of differential thermometry in the column packing were successfully performed at JET. This diagnostic will complement the other instrumentation (catharometer and ionisation chamber).

g) Intermediate Storage, Process Storage

Following the successful test of the uranium beds developed for the Impurity Processing Loop and the strong recommendations of the 1987 Tritium Experts Meeting to use uranium for hydride storage in tritiumpplication, storage and transfer system design was based on the U-bed designed by JET.

A storage module containing four U-beds was designed to be used in intermediate storage, D_2 and T_2 product storage and for He-scrubbing, inter-fraction and eluant receiver in the GC isotope separation system. Tender evaluation is proceeding and a contract should be placed at the end of February 1989.

Related valve/distribution boxes are being designed and tender action will start in early 1989.

h) Gas Introduction

The distribution system for the gases H_2, D_2 and T_2 for the torus and its subsystems is being studied and design should start in early 1989.

i) Control

Significant progress has been made in defining the requirements for the AGHS control system. In particular:

(i) Procurement of a two PLC Simatic system for training and feasibility studies;
(ii) Evaluation of IBM-PC based graphics process control package (FIX);
(iii) Conceptual circuit design for hard-wired interlocks and GC column valve selector unit;
(iv) Setting up of instrumentation data-base for the AGHS;
(v) Selection of design for all-metal pressure instruments.

j) Miscellaneous components

Valves have been tested during 1988 and a contract was placed for supply of approximately 1000 valves ($\sim$ 550 manual, $\sim$ 450 automatic with JET designed actuators) for the various subsystems. These valves will be supplied as free-issue items to all subsystem manufacturers. Pressure transducers for process systems were selected and a contract placed. All metal pressure regulators for tritium service were designed and tested.

k) Analytical equipment

At a Special Expert Meeting, in November 1988, the selection of analytical equipment for process performance monitoring was discussed and a combination of mass spectrometry and gas chromatography was recommended for the main product and impurity analysis laboratory.

l) Design appraisal

A Tritium Experts Meeting, in December 1988, discussed the progress of the JET AGHS, endorsed the approach and expressed satisfaction with progress.

Radiological Protection Instrumentation (RPI)

A contract has been placed to define requirements for additional radiological protection instrumentation for the D-T phase. This includes monitoring of discharge stacks, environmental sampling on site and working area monitoring. Prototype samplers for HT and HTO which use the AECL wet-proofed catalyst are proposed for environmental and stack monitoring.

Safety Analysis

Good progress has been made on the submissions to the UKAEA's Safety and Reliability Directorate (SRD) and UK's Her Majesty's Inspectorate of Pollution (HMIP) which are required to justify the safety of the AGHS. In particular, the Preliminary Safety Analysis Report (PSAR) which sets down the design safety criteria and qualitatively assesses the safety of the overall process concept and building design was endorsed by SRD.

Phase 2 of the SRD approval process is the detailed design safety review of individual AGHS sub-systems. This examines in detail containment systems and protection against overpressurisation. In particular, it is necessary to demonstrate that no single failure can cause a tritium release to the environment which exceeds the personnel exposure limits. It is also necessary to show that for any fault sequence that the product of the frequency and magnitude of tritium release is less than 0.37 TBq per annum. With several hundred components in each sub-system, it is important to analyse potential

faults in a structured way to identify those that are significant and to limit the analysis of faults which are unimportant from the safety point of view. This is carried out in three stages:

(i) by carrying out a Failure Mode and Effect Analysis (FMEA) on every component to identify the consequences of failure;
(ii) using a fault-tree approach to determine the frequency of events which the FMEA shows require safety systems (eg Secondary Containment, over temperature protection, etc.) to be available;
(iii) to use an event-tree analysis of the safety system availability to determine the tritium release and frequency.

Design safety reviews have been completed on Impurity Processing, Cryogenic Forevacuum, and Gas Chromatography Systems and have allowed procurement of these systems to proceed with the knowledge that the basic safety of the design is sound. These Design Safety Reviews and that of the Cryodistillation system have been endorsed by SRD. Analysis of the remaining subsystems is now in progress and the Final Safety Analysis Report, which considers system interfaces and the environmental impact is in course of preparation.

The first stage review of all diagnostics for tritium compatibility has been completed and has shown that the main safety issue is that of vacuum windows. For this reason a double window design is now being considered.

Other torus systems analysed conclude the proposed overpressure protection where advantage can be taken of the exhat detritiation system to provide a route for pressure relief from the torus, thus minimising the discharge of tritium to the environment. Other aspects of torus compatibility with tritium operation considered have been the handling and segregation of tritiated water, so that generation of large volumes of highly contaminated water is avoided. A Preliminary Safety Analysis Report of the torus which sets down the main safety issues for operation of the torus with tritium is now being prepared.

Regular meetings with HMIP and SRD are held to discuss progress on the actions required for JET to receive approval for D-T operation.

Future Plans

The future JET programme has been divided into phases governed by the availability of new equipment and fitting within the accepted lifetime of the Project (up to the end of 1992) (see Fig.156). Taking account of the adjustments to the shutdown schedule and the need to allow for sensible periods of operation to establish high reliability in preparation for the active phase of operation, the D-T phase is now expected to start six months later than previously planned and this will reduce the period for such operation to no more than eight months.

On the JET programme, Phase I, the Ohmic Heating Phase, was completed in September 1984, and Phase II (Additional Heating Studies) was completed in October 1988. The present Phase IIIA (Full Power Optimization Studies) has just started and future phases are as follows.

Phase IIIA (End 1988 – Mid 1990)

The following work is being undertaken in the shutdown at the start of this Phase:

- Vessel reinforcements to strengthen the vacuum vessel;
- Welding of the separatrix dump plate supports;
- Installation of beryllium evaporators and belt limiter tiles;
- Conversion of the first neutral injector to 140kV;

A short opening (2 months) of the vacuum vessel is foreseen in October 1989 to install:

- Be antennae screens;
- prototype Lower Hybrid Current Drive launcher system;
- prototype high speed pellet injector.

The main aim of this phase will be to control the plasma density and improve the plasma purity, by use of beryllium. In addition, work will continue on consolidating the operation of the machine at full additional heating power and to explore further the use of X-point operation as a means of improving confinement. The effect on confinement of the current and density profiles using pellet injection and current drive by ICRH, NBI and LHCD in quasi-stationary states will be established. Emphasis will be given to controlling the plasma density and improving the plasma purity, including, the use of beryllium.

Phase IIIB (Mid 1990 – End 1991)

After the shutdown at the beginning of this phase, the following systems should be operational:

- cooled separatrix dump plates;
- second neutral injector at 140kV;
- final Lower Hybrid Current Drive system for profile control;
- disruption control system using internal saddle coils;
- all remote handling systems required for the active phase;
- diagnostics systems required for the active phase.

The following will also be implemented during Phase IIIB:

- commissioning of the tritium plant;
- installation of the multiple high-speed deuterium pellet injector.

The scientific aims of Phase IIIB will be to reach maximum performance with high reliability in deuterium plasmas and to control the development of disruptions (through feed-back to stabilize magnetic perturbations) and sawteeth (through current-drive effects).

JET PROGRAMME

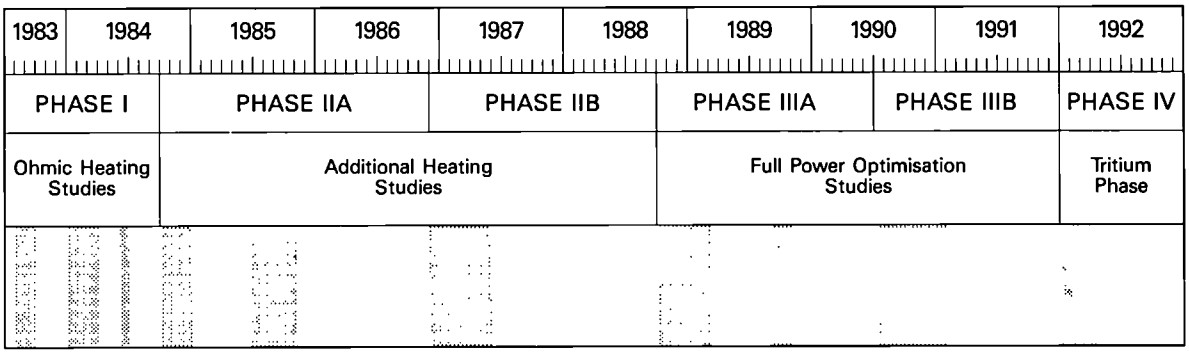

Ohmic Systems	5MA	Vessel restraints and improved volt-seconds for 7MA operation	Vessel reinforcements			
Separatrix		Additional P1 Coils	Separatrix dump plate supports		Cooled separatrix dump plates	
Limiters	Eight carbon mid-plane limiters	Carbon belt limiters	Beryllium belt limiters			
Pellets	Single pellet injector	ORNL multiple pellet injector ($1.5\,km\,s^{-1}$)		Prototype high speed pellet injector ($>3\,km\,s^{-1}$)	Multiple high speed pellet injector	
NBI	First NBI line (80kV)	Second NBI line (2×80kV)	One line modified to 140kV D		Second line modified to 140kV D	One line modified to 160kV T
ICRH	Three A_0 antennae	Eight A_1 antennae		Be antennae Screens		
LHCD			Install Vacuum Chamber	Prototype system	Full system	
Disruption control					Saddle coils	
Tritium and Remote handling					Tritium plant and main RH modifications	Final modifications

Fig.156 The JET Programme.

During this phase, the machine will be upgraded to the status compatible with full radioactive operation (i.e. remote handling systems tested, tritium compatibility of systems completed, shielding requirements implemented, tritium plant commissioned, neutral beam and pellet injectors upgraded for tritium beam and pellet injection).

Phase IV (D-T Phase) (Early 1992–End 1992)

The following work will be undertaken during the shut-down at the beginning of this phase:

- conversion of one neutral injector to operate with tritium at 160kV;
- final modifications for tritium operation including α-particle diagnostics.

D-T operation will begin when the overall reliability of all systems operating simultaneously is acceptable. D-T operation is scheduled to last eight months and should provide essential information on the confinement properties and behaviour of hot plasmas close to those needed in a thermonuclear reactor.

The main aim of this phase is to operate JET with D-T plasmas. In the light of present knowledge, all of the currently planned new equipment will be needed to bring the performance to a level justifying the introduction of tritium in the torus. The phase will develop along two main directions:

(a) Establishment of Tritium Operation

The characteristics of D-T plasmas will be studied, including their confinement properties and impurity content. An important element will be control of the composition of the core plasma using tritium neutral beam injection. New scenarios will be explored leading to the optimisation of ICRH and NBI for D-T plasmas;

(b) High Fusion Yields and the Detection of α-Particle Heating

The study and optimisation of intensely heated D-T plasmas will be required both for the maximisation of the fusion yield and for the database for future devices. It is anticipated that current and density profile control should play important roles.

Appendix I

JET Task Agreements 1988

Title	*Associations (JET Responsible Officer)*	*Duration of Agreement*	*Present Status*
RF HEATING DIVISION			
LOWER HYBRID CURRENT DRIVE ON JET– ● Exchange of knowledge ● Design and construction ofspecial item ● High power tests	EUR-CEA CADARACHE (CEA/TA4) (J. Jaquinot)	January 1987-December 1988	● Work continuing ● High power tests completed ● Construction of prototype launcher close to completion
PHYSICS OF LOWER HYBRID CURRENT DRIVE ON JET ● set-up predictive and interpretive codes ● participation in the LHCD programme at JET	UNIVERSIDAD TECHNICA DI LISBOA (UTL/TA1) (J. Jaquinot)	October 1987-October 1990	● Work continuing ● A prediction code has developed
PREPARATION OF THE LOWER HYBRID CURRENT DRIVE SYSTEM FOR JET ● position control of the launcher ● wave damping by energetic ions ● preparation of profile control experiments	EUR/UKAEA CULHAM LABORATORY (CUL/TA7) (C. Gormezano)	June1987-December 1988	● Work completed
EXPERIMENTAL DIVISION I			
PHYSICS OF SHAPED CROSS-SECTIONS	CULHAM, UK (CUL/TA4) (P. E. Stott)	Being reviewed	● Work continuing
EDGE PLASMAS & PLASMA SURFACE INTERACTIONS	CULHAM, UK (CUL/TA2) (P. E. Stott)	June 1983-June 1989	● Work proceeding
PLASMA WALL INTERACTIONS	GARCHING, FRG (IPP/TA2) (P. E. Stott)	January 1984-June 1989	● Work proceeding
NEUTRON PRODUCTION, RELATED PHYSICS AND ASSOCIATED DIAGNOSTICS	SWEDEN (SERC/TA1) (P. E. Stott)	January 1984-December 1990	● Work proceeding
PLASMA SURFACE INTERACTIONS	SWEDEN (NFR/TA2) (P. E. Stott)	July 1987-July 1990	● Work proceeding
NEUTRON PRODUCTION RELATED PHYSICS	HARWELL, UK (HAR/TA1) (P. E. Stott)	August 1985-December 1992	● Work Proceeding
NEUTRON PRODUCTION RELATED PHYSICS AND ASSOCIATED	FRASCATI, ITALY (ENEA/TA3) (P. E. Stott)	January 1986-January 1989	● Work proceeding
PHYSICS OF TURBULENT AND CONVECTIVE TRANSPORT, MHD AND RELATED DIAGNOSTICS	FOM, NETHERLANDS (FOM/TA2) (P. E. Stott)	November 1987-October 1990	● Work proceeding
EXPERIMENTAL DIVISION II			
BULK IMPURITY PHYSICS AND IMPURITY RELATED DIAGNOSTICS	EUR-IPP FRG (P. R. Thomas)	Started February 1983	● Work proceeding
IMPURITY ANALYSIS	EUR-UKAEA CULHAM LABORATORY (CUL/TA1) (P. R. Thomas)	Started February 1983	● Work proceeding

Title	*Associations (JET Responsible Officer)*	*Duration of Agreement*	*Present Status*
SPECTROSCOPIC MEASUREMENTS: INTERPRETATION AND IMPURITY ANALYSIS	EUR-CEA FAR (P. R. Thomas)	Started July 1984	● Work proceeding
PHYSICS OF ION AND ELECTRON ENERGY TRANSPORT AND RELATED DIAGNOSTICS	EUR-ENEA CREF (P. R. Thomas)	Started October 1983	● Work proceeding
CHARGE EXCHANGE RECOMBINATION SPECTROSCOPY	FOM, NETHERLANDS (M. von Hellerman)	Started June 1983	● Work proceeding
IMPURITY ANALYSIS AND PLASMA DIAGNOSTICS USING SPECTROSCOPIC MEASUREMENTS	EUR-NFR SWEDEN (NFR/TA2) (P. R. Thomas)	Started January 1988	● Work proceeding
THEORY DIVISION			
TESTING THEORETICAL TRANSPORT MODELS AGAINST JET DATA	EUR-UKAEA CULHAM LABORATORY (CUL/TA5) (T. E. Stringer)	Started December 1986	● Work proceeding
THEORY AND MODELS OF ANOMALOUS TRANSPORT	EUR-ENEA FRASCATI, ITALY (D. F. Düchs)	Started January 1988	● Work proceeding

Appendix II

Articles, Reports and Conference Papers Published in 1988

1. Distortion of ion velocity distributions in the presence of ICRH: A semi-analytical analysis.
Anderson D, Core W, Eriksson L G, Hamnen H, Hellsten T, Lisak M.
Chalmers Tekniska Hogskola. Institute for Electromagnetic Field Theory and Plasma Physics, 1986.
Report CTH-IEFT/PP-1986-02, 44p.
2. A semianalytical analysis of ion velocity distributions in the presence of combined neutral-beam and ICRF-heating.
Anderson D, Core W, Eriksson L-G, Hämnen H, Hellsten T, Lisak M.
Physica Scripta, vol.37 no.1 January 1988, pp.83-88.
Report CTH-IEFT/PP-1986-04
3. Singular domains of the low-frequency cold-plasma wave equation.
Appert K, Hellsten T, Vaclavik J, Villard L.
Plasma Physics and Controlled Fusion, vol.30 no.9 August 1988, pp.1195-1199.
4. Operational Regimes for an Ignited Tokamak Plasma
Apruzzese G, Tanga A
Nuclear Fusion
JET-P(88)65
5. The non-linear decay of the fast wave during ICRF heating.
Avinash K, Core W G F, Hellsten T.
Papers presented at Workshop on Plasma Edge Theory in Fusion Devices, Augustusburg, GDR, 26-30 April 1988.
Joint European Torus JET, 1988.
Report JET-P(88)24, pp.10-15.
6. The non-resonant decay of the fast magneto-sonic wave during ICRH of a tokamak plasma
Avinash K, Core W G, Hellsten T, Farrell C M
JET-R(88)11
7. On Internal Kink Instability in Tokamaks with Non-Monotopic q-Profiles
Avinash K
Physics Fluids
JET-P(88)72
8. Feasibility study on a high power (1 MW) millimetre-wave (140 GHz) transmission system for diagnostics of fusion alpha-particles in JET by collective millimetre-wave scattering.
Barkley H J, Muller G A, Schuller P G, Kasparek W, Rebuffi L, Thumm M.
Joint European Torus JET, January 1988.
Report JET-R(88)14, 53p.
9. The JET high resolution bent crystal spectrometer.
Bartiromo R, Bombards F, Giannella R, Mantovani S, Panaccione L, Pizzicaroli G.
Joint European Torus JET, May 1988.
Report JET-P(88)11, 26p.
10. Energy confinement in JET ohmically heated plasmas.
Bartlett D V, Bickerton R J, Brusati M, Campbell D J, Christiansen J P, Cordey J G, Corti S, Costley A E, Edwards A, Fessey J, Gadeberg M, Gibson A, Gill R D, Gottardi N, Gondhalekar A, Gowers C W, Hendriks F, Jarvis O N, Kallne E, Kallne J, Kissel S, De Kock L C J M, Krause H, Lazzaro E, Lomas P J, Mast F K, Morgan P D, Nielsen P, Prentice R, Ross R T, O'Rourke J, Sadler G, Schuller F C, Stamp M F, Stott P E, Summers D R, Tanga A, Taroni A, Thomas P R, Tibone F, Tonetti G, Tubbing B J D, Watkins M L.
Nuclear Fusion, vol.28 no.1 January 1988, pp.73-88.
11. Overview of JET ECE measurements.
Bartlett D V, Campbell D J, Costley A E, Kissel S, Lopes Cardozo N, Gowers C W, Nowak S, Oyevaar Th, Salmon N A, Tubbing B J.
Electron Cyclotron Emission and Electron Cyclotron Resonance Heating. Procs. 6th Joint Workshop, Oxford, 16-17 September 1987. Abingdon, Culham Laboratory, 1987. pp.137-147.
Report JET-P(88)18, pp.1-11.
12. Measurement and interpretation of triton burnup in JET deuterium plasmas.
Batistoni P, Argyle J, Conroy S, Gorini G, Huxtable G, Jarvis O N, Kallne J, Martone M, Pillon M, Podda S, Rapisarda M, Sadler G, Syme D B, van Belle P, Verschuur K
JET contributed papers to the 15th Euro Conf. on controlled fusion and plasma heating, Dubrovnik, Yugoslavia, 16-20 May 1988.
Joint European Torus JET, 1988.
Report JET-P(88)15, pp.165-168.

13. Impurity transport in JET during H-mode, monster sawteeth, and after pellet injection.
Behringer K H, Denne B, Edwards A, Gottardi N, von Hellermann M, Kallne E, Morgan P D.
JET contributed papers to the 15th Euro Conf. on controlled fusion and plasma heating, Dubrovnik, Yugoslavia, 16-20 May 1988.
Joint European Torus JET, 1988.
Report JET-P(88)15, pp.21-24.

14. Status of visible spectroscopy on JET.
Behringer K H, Engelhart W W, Horton L, Morgan P D, Stamp M F, Summers H P, Von Hellermann M, Carolan P G, Forrest M J, Peacock N J.
The Physics of Ionized Gases (SPIG86). 13th Yugoslav Summer School and Int. Symp., Sibenik, 1-5 September 1986.
Singapore, World Scientific, 1986. pp.241-267.

15. XUV spectroscopy in JET.
Behringer K H, Denne B, Magyar G, Mattioli M, Peacock N J, Ramette J, Saoutic B, Schwob J L.
Ultra-violet (UV) and X-ray Spectroscopy of Astrophysical and Laboratory Plasmas. IAU Colloquium No.102, Beaulieu-sur-Mer, 9-11 September 1987.
Journal de Physique, vol.49 Colloque C1, Supplement to no.3 March 1988, pp.C1-387–C1-390.

16. Preparation for D-T operation at JET
Bell A C, Campbell J, Gordon C, Wykes M, Caldwell-Nichols C, Chuilon P, Newbert G.
Invited Paper presented at 15th Symposium on Fusion Technology, Utrecht, The Netherlands, 19th-23rd September 1988
JET-P(88)61

17. JET Project technical development dictated by the recent scientific results and prospects for extensive D-T plasma studies in break-even conditions.
Bertolini E, Huguet M, JET Team
JET papers presented at the 12th Symp. on Fusion Engineering (SOFE), Monterey, USA, 12-16 October 1987.
Joint European Torus JET, 1987.
Report JET-P(87)52, pp.1-8.

18. The JET project: Technical and scientific achievements and development towards deuterium-tritium operation. (Extended abstract).
Bertolini E.
Fusion reactor design and technology 1986. 4th Technical Committee Meeting and Workshop, organised by the IAEA, Yalta, 26 May-6 June 1986.
Vienna, IAEA, 1987. Vol.1, pp.75-76.

19. Effect of sawteeth and safety factor q on confinement during ICRF heating of JET.
Bhatnagar V P, Campbell D, Christiansen J P, Cordey J G, Jacquinot J, Start D F H, Thomas P, Thomsen K.
JET contributed papers to the 15th Euro Conf. on controlled fusion and plasma heating, Dubrovnik, Yugoslavia, 16-20 May 1988.
Joint European Torus JET, 1988.
Report JET-P(88)15, pp.93-96.

20. Effect of Sawteeth, safety factor and current on confinement during ICRF heating of JET
Bhatnagar V P, Cordey J G, Jacquinot J, Start D F H.
Plasma Physics and Controlled Fusion
JET-P(88)51

21. Future for fusion?
Bickerton R J.
Physics Bulletin, vol.39 no.9 September 1988, pp.353-356.

22. Ignition tokamaks.
Bickerton R J, Apruzzese G, Tanga A, Thomas P, Wesson J.
JET contributed papers to the 15th Euro Conf. on controlled fusion and plasma heating, Dubrovnik, Yugoslavia, 16-20 May 1988.
Joint European Torus JET, 1988.
Report JET-P(88)15, pp.37-40.

23. JET and the prospect for nuclear fusion.
Bickerton R J.
Physica Scripta, vol.T23 1988 (Trends in Physics, EPS-7: Procs. 7th General Conf. of the European Physical Society, Helsinki University of Technology, 10-14 August 1987), pp.242-248.

24. JET Results and the Future Prospects for Fusion
Bickerton R J.
Physics Bulletin
JET-P(88)49

25. Results and plans for the Joint European Torus.
Bickerton R J.
Journal of Fusion Energy, vol.7 nos.2/3 September 1988 (Special Issue on Fusion Energy Development: Breakeven and Beyond), pp.115-116.

26. Status of JET. (Abstract).
Bickerton R J.
Plasma Science 1986 IEEE Int. Conf., Saskatoon, 19-21 May 1986. New York, IEEE, 1986. p.2.

27. Status of the JET Project.
Bickerton R J,
Plasma Physics and Controlled Fusion, vol.30 no.14 December 1988 (R.S. Pease and Fusion Research 1950-1987: Symposium at Culham Laboratory, 8 December 1987), pp.2051-2068.

28. A technique for improving the relative accuracy

of JET ECE temperature profiles.
Bindslev H, Bartlett D V.
Electron Cyclotron Emission and Electron Cyclotron Resonance Heating. Procs. 6th Joint Workshop, Oxford, 16-17 September 1987. Abingdon, Culham Laboratory, 1987. pp.309-316.
Report JET-P(88)18, pp.20-27.

29. A technique for improving the relative accuracy of JET ECE temperature profiles.
Bindslev H, Bartlett D V.
Joint European Torus JET, 1988.
Report JET-R(88)04, 78p.

30. Physics of Multiply Charged Ions and Physics of electron Cyclotron Resonance Ion Sources
Bliman S.
Atomic and Molecular Physics
JET-P(88)71

31. Observations and comparisons with theory of the helium-like and hydrogen-like resonance lines and satellites of nickel from the JET tokamak.
Bombarda F, Giannella R, Kallne E, Tallents G J, Bely-Dubau F, Faucher P, Cornille M, Dubau J, Gabriel A H.
Physical Review A. General Physics, vol.37 no.2 15 January 1988, pp.504-522.

32. Ion temperature measurement from doppler broadening of He-like nickel lines.
Bombarda F, Giannella R, Källne E, Tallents G J.
J. Quant. Spectr. Rad. Transf.
JET-P(88)36

33. The additional switching network. A new part of the poloidal field system of JET: Design and early operation.
Bonicelli T, Marchese V, Mondino P L.
JET papers presented at the 12th Symp. on Fusion Engineering (SOFE), Monterey, USA, 12-16 October 1987.
Joint European Torus JET, 1987.
Report JET-P(87)52, pp.17-22.

34. Comparison among different current transparencies used in the JET magnet power supplies in the current range 4-100kA.
Bonicelli T, Eriksson T, Huart M, Moissonnier A, Mondino P L, Raymond C.
JET papers presented at the 12th Symp. on Fusion Engineering (SOFE), Monterey, USA, 12-16 October 1987.
Joint European Torus JET, 1987.
Report JET-P(87)52, pp.27-31.

35. The gas chromatographic isotope separation system for the JET active gas handling plant.
Botter F, Gowman J, Hemmerich J L, Hircq B, Lasser R, Leger D, Tistchenko S, Tschudin M.
Fusion Technology, vol.14 no.2 pt.2A-2B September 1988 (Procs. 3rd Topical Meeting on Tritium Technology in Fission, Fusion and Isotopic Applications, Toronto, Canada, 1-6 May 1988), pp.562-566.

36. ^{3}He-d fusion reaction rate measurements during fast-wave heating experiments in JET
Boyd D A, Campbell D J, Cordey J G, Core W, Christiansen J P, Cottrell G, Hellsten T, Kissel S, Sadler G, van Belle P, Cordey J G, Cottrell G A, Jacquinot J, Lowry C, Start D F H, Wesson J.
Nuclear Fusion
JET-P(88)42

37. Heat shock resistance of graphite determined with a CO_2 laser.
Brinkschulte H, Deksnis E, Bransden A S.
Journal of Nuclear Materials, vol.155-157 pt.A July (II) 1988 (Proc. 3rd Int. Conf. on Fusion Reactor Materials (ICFRM-3), Karlsruhe, 4-8 October 1987), pp.261-266.

38. Plasma edge effects during additional heating in JET with belt limiter configuration.
Brinkschulte H, Clement S, Coad J P, de Kock L, Erents S K, Neill G, Partridge J W, Simpson J C B, Tagle J A.
JET contributed papers to the 15th Euro Conf. on controlled fusion and plasma heating, Dubrovnik, Yugoslavia, 16-20 May 1988.
Joint European Torus JET, 1988.
Report JET-P(88)15, pp.85-88.

39. Particle Diffusion due to Stochastic Fields
Brusati M, Martins A M, Mendonca J T.
The Physics of Fluids
JET-P(88)67

40. Density behaviour and particle influxes during ICRF heating of limiter discharges in JET.
Bures M, Bhatnagar V P, Jacquinot J, Morgan P, Start D F H.
Plasma Physics and Controlled Fusion, vol.30 no.13 December 1988, pp.1833-1844.
Report JET-P(88)03

41. The modification of the plasma edge and impurity production by antenna phasing during ICRF heating on JET.
Bures M, Brinkschulte H, Jacquinot J, Lawson K D, Kaye A, Tagle J A.
Plasma Physics and Controlled Fusion, vol.30 no.2 February 1988, pp.149-167.

42. RF edge field behaviour and the parametric decay during the ICRF heating on JET.
Bures M, Avinash K, Brinkschulte H, Devillers G, Jacquinot J, Knowlton S, Start D, Tagle J.
American Physical Society Bulletin, vol.33 no.9 October 1988 (Program of 30th Annual Meeting of the Division of Plasma Physics, Hollywood, Florida, 31 October-4 November

1988), paper 6U16, p.2032.

43. Role of antenna screen angle during ICRF heating experiments in JET.
Bures M, Bhatnagar V, Corti S, Devillers G, Denne B, Forrest M J, Hellsten T, Jacquinot J, Start D.
JET contributed papers to the 15th Euro Conf. on controlled fusion and plasma heating, Dubrovnik, Yugoslavia, 16-20 May 1988.
Joint European Torus JET, 1988. pp.117-120.
Report JET-P(88)15, pp.117-120.

44. Role of antenna screen angle during ICRF Heating in JET
Bures M, Jacquinot J, Start D, Brambilla M.
Nuclear Fusion
JET-P(88)76

45. Analysis of sawtooth stabilization in JET.
Campbell D J, Baylor L, Bhatnagar V P, Bures M, Cheetham A, Cordey J G, Cottrell G A, de Haas J, Edwards A W, Eriksson L G, Gondhalekar A, Gottardi N, Hastie R J, Hellsten T, Jacquinot J, Lazzaro E, McCarthy L, Morgan P D, O'Rourke J, Pearson D, Pegoraro F, Porcelli F, Schmidt G L, Snipes J A, Start D F H, Stubberfield P, Thomas P R, Thomsen K, Tubbing B J D, Wesson J A.
JET contributed papers to the 15th Euro Conf. on controlled fusion and plasma heating, Dubrovnik, Yugoslavia, 16-20 May 1988.
Joint European Torus JET, 1988.
Report JET-P(88)15, pp.89-92.

46. Plasma resistivity and field penetration in JET.
Campbell D J, Lazzaro E, Nave M F F, Christiansen J P, Cordey J G, Schuller F C, Thomas P R.
Nuclear Fusion, vol.28 no.6 June 1988, pp.981-990.

47. Stabilization of sawteeth with additional heating in the JET tokamak.
Campbell D J, Start D F H, Wesson J A, Bartlett D V, Bhatnagar V P, Bures M, Cordey J G, Cottrell G A, Dupperex P A, Edwards A W, Challis C D, Gormezano C, Gowers C W, Granetz R S, Hamnen J H, Hellsten T, Jacquinot J, Lazzaro E, Lomas P J, Lopes Cardozo N, Mantica P, Snipes J A, Stork D, Stott P E, Thomas P R, Thompson E, Thomsen K, Tonetti G.
Physical Review Letters, vol.60 no.21 23 May 1988, pp.2148-2151.

48. Early operating experience with the JET neutral injector power supplies, reliability and improvements.
Carwardine J A, Claesen R, Christodoulopoulos C, Bertoldi P, Deng J, Rushton R.
JET papers presented at the 12th Symp. on Fusion Engineering (SOFE), Monterey, USA, 12-16 October 1987.
Joint European Torus JET, 1987.
Report JET-P(87)52, pp.13-16.

49. Beam driven and bootstrap currents in JET.
Challis C D, Cordey J G, Hamnen H, Stubberfield P M.
American Physical Society Bulletin, vol.33 no.9 October 1988 (Program of 30th Annual Meeting of the Division of Plasma Physics, Hollywood, Florida, 31 October-4 November 1988), paper 6U17, p.2032.

50. Non-inductively driven currents in JET.
Challis C D, Cordey J G, Hamnen H, Stubberfield P M, Christiansen J P, Lazzaro E, Muir D G, Stork D, Thompson E.
Joint European Torus JET, September 1988.
Report JET-P(88)38, 18p.

51. Simultaneous measurements of electron thermal and particle transport in JET
Gondhalekar A, de Haas J C M, Larsen P D, Watkins M, Cheetham A D, Hubbard A, O'Rourke J.
Plasma Physics and Controlled Fusion
JET-P(88)50

52. Pellet fuelling of tokamaks
Cheetham A.
Europhysics News
JET-P(88)46

53. Analysis of local heat flux in JET.
Christiansen J P, Callen J D, Cordey J G, Thomsen K.
Nuclear Fusion, vol.28 no.5 May 1988, pp.817-826.
Report JET-P(87)48

54. Local transport in JET sawteeth free discharges.
Christiansen J P, Cordey J G, Muir D.
American Physical Society Bulletin, vol.33 no.9 October 1988 (Program of 30th Annual Meeting of the Division of Plasma Physics, Hollywood, Florida, 31 October-4 November 1988), paper 6U6, p.2030.

55. Determination of current distribution in JET from soft X-ray measurements
Christiansen J P, Callen J D, Ellis J J, Granetz R.
Nuclear Fusion
JET-P(88)66

56. Collector probes exposed in JET during the 1987/8 operational campaign.
Coad J P, Bergsaker H, Clement S, Hancock C J, Jakob D, Neill G F, Nicholson C, Partidge J, Simpson J C B, Stevens A, Vince J.
American Physical Society Bulletin, vol.33 no.9 October 1988 (Program of 30th Annual Meeting of the Division of Plasma Physics, Hollywood, Florida, 31 October-4 November 1988), paper 6U5, p.2030.

57. Release of hydrogen isotopes from first-wall surfaces on exposure to air.
Coad J P, Orchard J, Monahan J.
Journal of Nuclear Materials, vol.160 no.1 November 1988, pp.95-97.
Report JET-P(88)28

58. Time-resolved measurements of triton burn-up

in JET plasmas.
Conroy S, Jarvis O N, Sadler G, Huxtable G B.
JET Joint European Torus, May 1988.
Report JET-P(88)16, 17p.

59. The fast beam interlock system for JET neutral injection.
Cooper D, Stork D, Mead M J, Young D.
JET papers presented at the 12th Symp. on Fusion Engineering (SOFE), Monterey, USA, 12-16 October 1987.
Joint European Torus JET, 1987.
Report JET-P(87)52, pp.62-66.

60. The neutral beam protection plate viewing system on JET.
Cooper D, Stabler A, Stork D.
JET papers presented at the 12th Symp. on Fusion Engineering (SOFE), Monterey, USA, 12-16 October 1987.
Joint European Torus JET, 1987.
Report JET-P(87)52, pp.76-80.

61. Suppression of internal plasma oscillations by trapped high energy nuclei.
Coppi B, Hastie R J, Migliuolo S, Pegoraro F, Porcelli F.
Physics Letters A, vol.132 no.5 10 October 1988, pp.267-272.
Report JET-P(88)20

62. Bootstrap current theory and experimental evidence.
Cordey J G, Challis C D, Stubberfield P M.
Plasma Physics and Controlled Fusion, vol.30 no.11 October 1988 (Controlled Fusion and Plasma Heating: 15th EPS Plasma Physics Division Conf., Cavtat, Yugoslavia, 16-20 May 1988. Invited Papers) pp.1625-1635.
Report JET-P(88)29

63. A preliminary analysis of the JET experiments on current drive by neutral beam injection and its future potential.
Cordey J G, Challis C, Hamnen H, Muir D, Stork D, Thompson E.
Non-Inductive Current Drive, report of a Specialists Meeting, held in Garching, 15-17 September 1986.
International Atomic Energy Agency, 1987.
Report IAEA-TECDOC-441, pp.54-55.

64. Transverse magnetic field penetration through the JET toroidal coil and support structure.
Core W G F, Noll P.
Joint European Torus JET, 1988.
Report JET-R(88)03, 39p.

65. Ion temperature profiles and ion energy transport in JET during additional heating and H-modes.
Corti S, Boileau A, Bracco G, Forrest M J, von Hellermann M, Horton L, Larsen P, Sack C, Summers H P, Taroni A, Tibone F.
JET contributed papers to the 15th Euro Conf. on controlled fusion and plasma heating, Dubrovnik, Yugoslavia, 16-20 May 1988.
Joint European Torus JET, 1988.
Report JET-P(88)15, pp.57-60.

66. Diagnostic advances and their impact on our understanding of tokamak relaxation phenomena.
Costley A E.
Plasma Physics and Controlled Fusion, vol.30 no.11 October 1988 (Controlled Fusion and Plasma Heating: 15th EPS Plasma Physics Division Conf., Cavtat, Yugoslavia, 16-20 May 1988. Invited Papers) pp.1455-1466.
JET-P(88)30

67. Integrated electron temperature and density measurements on JET.
Costley A E, Bartlett D V, Campbell D J, Gottardi N, Gowers C W, Hirsch K, Kissel S E, Nielsen P, Nowak S, O'Rourke J, Salzmann H.
JET contributed papers to the 15th Euro Conf. on controlled fusion and plasma heating, Dubrovnik, Yugoslavia, 16-20 May 1988.
Joint European Torus JET, 1988.
Report JET-P(88)15, pp.133-136.

68. Summary remarks: ECE experiments.
Costley A E.
Electron Cyclotron Emission and Electron Cyclotron Resonance Heating. Procs. 6th Joint Workshop, Oxford, 16-17 September 1987.
Abingdon, Culham Laboratory, 1987.
pp.386-387.

69. A Thomson scattering diagnostic to measure fast ion and alpha-particle distributions in JET.
Costley A E, Hoekzema J A, Hughes T P, Stott P E, Watkins M L.
JET Joint European Torus, 1988.
Report JET-R(88)08, 105p.

70. High fusion yield experiments in JET with ICRH.
Cottrell G A, Boyd D, Campbell D J, Christiansen J, Cordey J G, Core W, Edwards A, Eriksson L G, Hellsten T, Jacquinot J, Jarvis O N, Lowry C, Nielsen P, Sadler G, Start D F H, Thomas P R, van Belle P, Wesson J A.
American Physical Society Bulletin, vol.33 no.9 October 1988 (Program of 30th Annual Meeting of the Division of Plasma Physics, Hollywood, Florida, 31 October-4 November 1988), paper 6U15, p.2032.

71. Study of ICRF driven fusion reactivity.
Cottrell G A, Sadler G, van Belle P, Campbell D J, Cordey J G, Core W, Hellsten T, Jacquinot J, Kissel S, Start D F H, Thomas P R, Wesson J A.

JET contributed papers to the 15th Euro Conf. on controlled fusion and plasma heating, Dubrovnik, Yugoslavia, 16-20 May 1988. Joint European Torus JET, 1988. Report JET-P(88)15, pp.125-128.

72. Aspects of combined ICRF and neutral beam heating and current drive.
Cox M, Start D F H.
Plasma Physics Int. Conf. Joint Conf. of 7th Kiev Int. Conf. on Plasma Theory and the 7th Int. Congress on Waves and Instabilities in Plasmas, Kiev, 6-12 April 1987. Procs. of the Invited Papers. Edited by A G Sitenko. 2 volumes.
Singapore, World Scientific, 1987. pp.232-249.

73. χ_e from heat pulse propagation during JET H-mode.
de Haas J C M, Lopes Cardozo N P.
American Physical Society Bulletin, vol.33 no.9 October 1988 (Program of 30th Annual Meeting of the Division of Plasma Physics, Hollywood, Florida, 31 October-4 November 1988), paper 6U4, p.2030.

74. Performance of carbon tiles and in-situ carbon coatings in JET and TEXTOR.
de Kock L.
Joint European Torus JET, June 1988.
Report JET-P(88)22, 24p.

75. The role of the scrape-off plasma in X-point discharges in JET.
de Kock L, Harbour P J, Clement S, Erents S K, Gottardi N, Hubbard A E, Keilhacker M, Lazzaro E, Morgan P D, Stork D, Summers D D R, Tagle J A, Tanga A.
JET contributed papers to the 15th Euro Conf. on controlled fusion and plasma heating, Dubrovnik, Yugoslavia, 16-20 May 1988.
Joint European Torus JET, 1988.
Report JET-P(88)15, pp.73-76.

76. The JET belt limiter
Deksnis E.
JET-R(88)19

77. Comparison of theory with electron cyclotron current drive experiments on WT-2.
Dendy R O, O'Brien M, Cox M, Start D F H.
Electron Cyclotron Emission and Electron Cyclotron Resonance Heating. Procs. 6th Joint Workshop, Oxford, 16-17 September 1987.
Abingdon, Culham Laboratory, 1987. pp.73-80.

78. The role of atomic spectroscopy in fusion research.
Denne B.
Joint European Torus JET, July 1988.
Report JET-P(88)35, 37p.

79. The 3s-3p transitions in neonlike Kr XXVII observed in the JET tokamak.
Denne B, Hinnov E.
Joint European Torus JET, April 1988.
Report JET-P(88)14, 6p.

80. Spectrum lines of KR XXVIII - KR XXIV observed in the JET tokamak
Denne B, Hinnov E, Ramette J, Saoutic B.
Physical Review A
JET-P(88)74

81. Suppression of internal plasma oscillations in the presence of a hot magnetically trapped ion population.
Detragiache P, Coppi B, Hastie R J, Migliuolo S, Porcelli F, Pegoraro F.
American Physical Society Bulletin, vol.33 no.9 October 1988 (Program of 30th Annual Meeting of the Division of Plasma Physics, Hollywood, Florida, 31 October-4 November 1988), paper 3T11, p.1930.

82. Experience with limiter and wall materials in JET.
Dietz K J.
Journal of Nuclear Materials, vol.155-157 pt.A July (II) 1988 (Proc. 3rd Int. Conf. on Fusion Reactor Materials (ICFRM-3), Karlsruhe, 4-8 October 1987), pp.8-14.

83. Modifications to the JET vacuum vessel as a result of plasma operation.
Dietz K J.
Vacuum, vol.38 nos.8-10 1988, (Selected Procs. 1st Euro. Vacuum Conf., Salford, 11-15 April 1988), pp.591-595.

84. Magnetic fluctuations and confinement in JET.
Duperrex P A, Malacarne M.
Procs. Int. Workshop on Small Scale Turbulence and Anomalous Transport in Magnetized Plasmas, Cargese, 6-12 July 1986.
Palaiseau Cedex, Editions de Physique, 1986. pp.197-200.

85. New MHD activity during stable locked-mode in JET.
Duperrex P-A, Pochelon A, Snipes J.
American Physical Society Bulletin, vol.33 no.9 October 1988 (Program of 30th Annual Meeting of the Division of Plasma Physics, Hollywood, Florida, 31 October-4 November 1988), paper 6U21, p.2033.

86. Measurements of 'snakes' following multiple pellet fuelling of JET.
Edwards A, Campbell D, Cheetham A, Gill R D, Gowers C, Hirsch K, Nielsen P, O'Rourke J, Salzmann H, Zasche D.
JET contributed papers to the 15th Euro Conf. on controlled fusion and plasma heating, Dubrovnik, Yugoslavia, 16-20 May 1988.
Joint European Torus JET, 1988.
Report JET-P(88)15, pp.5-8.

87. 'Snakes' in JET and their use as a diagnostic probe of the q=1 surface and sawteeth.
Edwards A W, Campbell D, Cheetham A, Gill R D, Gowers C, Hirsch K, Pasini D, O'Rourke J, Zasche D.
American Physical Society Bulletin, vol.33 no.9 October 1988 (Program of 30th Annual Meeting of the Division of Plasma Physics, Hollywood, Florida, 31 October-4 November 1988), paper 6U10, p.2031.

88. Hydrogen and helium recycling in tokamaks with carbon walls.

Ehrenberg J.
Joint European Torus JET, September 1988.
Report JET-P(88)57, 41p.

89. Dependence of tokamak edge conditions on global plasma parameters in JET.
Erents S K, Tagle J A, McCracken G M, Stangeby P C, De Kock L C J M.
Nuclear Fusion, vol.28 no.7 July 1988, pp.1209-1221.
Report JET-P(87)62

90. Electron heating during ICRH in JET
Eriksson L G, Hellsten T.
Nuclear Fusion
JET-P(88)47

91. ICRF power deposition profile and determination of χ_e by modulation experiments in JET
Gambier D J, Evrard M P, Adam J, Becoulet A, Corti S, Hennequin P, Jacquinot J, Start D F H, Thomsen K, Tubbing B J D, Zanza V.
Nuclear Fusion
JET-P(88)52

92. Calculations of power deposition and velocity distributions during ICRH; a comparison with experimental results
Eriksson L G, Campbell D J, Christiansen J P, Jarvis O N, Nielsen P, Thomas P R, Hellsten T, Cordey J G, Cottrell G A, Kissel S, Sadler G, van Belle P, Boyd D A, Core W, Jacquinot J J, Lowry C, Start D F H, Wesson J A.
Nuclear Fusion
JET-P(88)53

93. Conversion of the JET neutral beam injectors for operation with tritium.
Falter H D, Deschamps G, Hemsworth R S, Massmann P, Grisham L.
American Physical Society Bulletin, vol.33 no.9 October 1988 (Program of 30th Annual Meeting of the Division of Plasma Physics, Hollywood, Florida, 31 October-4 November 1988), paper 6U18, p.2032.

94. Effects on doppler profiles in beam-heated plasmas.
Fussmann G
Joint European Torus JET, 1988.
Report JET-R(87)12, 35p.

95. Control and operation of JET articulated boom.
Galbiati L, Raimondi T.
JET papers presented at the 12th Symp. on Fusion Engineering (SOFE), Monterey, USA, 12-16 October 1987.
Joint European Torus JET, 1987.
Report JET-P(87)52, pp.58-61.

96. An integrated control system for remote handling equipment at JET.
Galetsas A, Rolfe A C, Steed C A.
JET papers presented at the 12th Symp. on Fusion Engineering (SOFE), Monterey, USA, 12-16 October 1987.
Joint European Torus JET, 1987.
Report JET-P(87)52, pp.23-26.

97. High resolution X-ray spectroscopy at JET. (Invited paper).
Giannella R.
Ultra-violet (UV) and X-ray Spectroscopy of Astrophysical and Laboratory Plasmas. IAU Colloquium No.102, Beaulieu-sur-Mer, 9-11 September 1987.
Journal de Physique, vol.49, Colloque C1, Supplement to no.3, March 1988, pp.C1-283-C1-291.
Report JET-P(87)53

98. Neutral particle emission in JET during radiofrequency heating experiments.
Giannella R, Zanza V, Barbato E, Bracco G, Corti S, Gambier D J.
Nuclear Fusion, vol.28 no.2 February 1988, pp.193-206.

99. Fusion research at Harwell in the late 1950s and 1960s.
Gibson A.
Plasma Physics and Controlled Fusion, vol.30 no.14 December 1988 (R.S. Pease and Fusion Research 1950-1987: Symposium at Culham Laboratory, 8 December 1987), pp.2003-2010.

100. Plasma performance in JET: achievements and projections.
Gibson A (presenter) and the JET Team.
Plasma Physics and Controlled Fusion, vol.30 no.11 October 1988 (Controlled Fusion and Plasma Heating: 15th EPS Plasma Physics Division Conf., Cavtat, Yugoslavia, 16-20 May 1988. Invited Papers) pp.1375-1390.
Report JET-P(88)26

101. Recent results from JET and their implications.
Gibson A.
American Physical Society Bulletin, vol.33 no.9 October 1988 (Program of 30th Annual Meeting of the Division of Plasma Physics, Hollywood, Florida, 31 October-4 November 1988), paper 1I2, p.1861.

102. The sawtooth in JET.
Gill R D, Campbell D J, Duperrex P A, Edwards A W, Han W, O'Rourke J, Pegoraro F, Porcelli F, Taroni A, Tibone F.
JET contributed papers to the 15th Euro Conf. on controlled fusion and plasma heating, Dubrovnik, Yugoslavia, 16-20 May 1988.
Joint European Torus JET, 1988.
Report JET-P(88)15, pp.101-104.

103. X-ray emission during pellet injection into JET.
Gill R D.

Joint European Torus JET, September 1988.
Report JET-P(88)39, 17p.

104. Determination of the shear on the q=1 surface of the JET tokamak
Gill R D, Edwards A W, Weller A.
Nuclear Fusion (Letters)
JET-P(88)59

105. Engineering, manufacture and test of the deflection magnets of the JET neutral beam injector.
Goede A P H, Nielsen B R, Shone F, Sonderskov T, Thompson E.
Nuclear Instruments and Methods in Physics Research. Section A: Accelerators, Spectrometers, Detectors, and Associated Equipment, vol.A267 no.1 15 April 1988, pp.203-211.
Report JET-P(87)60

106. Physics design of the deflection magnets of the JET neutral beam injector.
Goede A P H, Nielsen B R, Thompson E.
Nuclear Instruments and Methods in Physics Research. Section A: Accelerators, Spectrometers, Detectors, and Associated Equipment, vol.A267 no.1 15 April 1988, pp.193-202.
Report JET-P(87)63

107. Reionised particles and duct wall protection of the JET neutral beam injection system.
Goede A P H, Papastergiou S, Simkin J, Challis C, Duesing G, Haange R, Jones T T C, Stork D, Thompson E.
JET papers presented at the 12th Symp. on Fusion Engineering (SOFE), Monterey, USA, 12-16 October 1987.
Joint European Torus JET, 1987.
Report JET-P(87)52, pp.38-41.

108. Properties of thermal and particle transport in JET.
Gondhalekar A, Callen J D, Cheetham A D, de Haas J C M, Jarvis O N, Larsen P D, O'Rourke J, Sadler G, Sips G, Watkins M L.
American Physical Society Bulletin, vol.33 no.9 October 1988 (Program of 30th Annual Meeting of the Division of Plasma Physics, Hollywood, Florida, 31 October-4 November 1988), paper 6U12, p.2031.

109. Correlation of heat and particle transport in JET
Gondhalekar A, Cheetham A D, de Haas J C M, Jarvis O N, Morgan P D, O'Rourke J, Sadler G, Watkins M L.

110. Simultaneous measurements of electron thermal and particle transport in JET.
Gondhalekar A, Campbell D, Cheetham A D, Edwards A, de Haas J C M, Hubbard A, Larsen P D, O'Rourke J, Watkins M L.
JET contributed papers to the 15th Euro Conf. on controlled fusion and plasma heating, Dubrovnik, Yugoslavia, 16-20 May 1988.
Joint European Torus JET, 1988.
Report JET-P(88)15, pp.17-20.

111. The tritium safety programme at JET.
Gordon C W.
Fusion Reactor Safety Technical Committee Meeting, organized by the Int. Atomic Energy Agency, held in Culham, 3-7 November 1986.
Vienna, IAEA, 1987. pp.63-72.

112. A comparison study of the 1 MeV triton burn-up in JET using the HECTOR and SOCRATE codes.
Gorini G, Kovanen M A.
Joint European Torus JET, 1988.
Report JET-R(88)09, 13p.

113. The JET 10MW lower hybrid current drive system.
Gormezano C, Bosia G, Brinkschulte H, David C, Dobbing J A, Kaye A S, Jacquinot J, Knowlton S, Moreau D, Pain M, Plancoulaine J, Wade T, Walker C, Lloyd B.
JET papers presented at the 12th Symp. on Fusion Engineering (SOFE), Monterey, USA, 12-16 October 1987.
Joint European Torus JET, 1987.
Report JET-P(87)52, pp.9-12.

114. High rejection ruby filter for laser light scattering experiments.
Gowers C, Hirsch K, Nielsen P, Salzmann H.
Applied Optics, vol.27 no.17 1 September 1988, pp.3625-3629.
Report JET-P(88)04

115. Profile behaviour during L and H phases of JET discharges.
Gowers C W, Bartlett D, Boileau A, Corti S, Edwards A, Gottardi N, Hirsch K, Keilhacker M, Lazzaro E, Morgan P, Nielsen P, O'Rourke J, Salzmann H, Smeulders P, Tanga A, von Hellermann M.
JET contributed papers to the 15th Euro Conf. on controlled fusion and plasma heating, Dubrovnik, Yugoslavia, 16-20 May 1988.
Joint European Torus JET, 1988.
Report JET-P(88)15, pp.33-36.

116. X-ray tomography on JET.
Granetz R S, Smeulders P.
Nuclear Fusion, vol.28 no.3 March 1988, pp.457-476.
Report JET-P(87)49

117. Are the existing measurements and theoretical calculations of the charge transfer correct?
Gryzinski M.
Joint European Torus JET, June 1988.
Report JET-P(88)23, 42p.

118. General overview of the active gas handling system at JET.
Haange R, Bell A, Caldwell-Nichols C, Dombra A, Gordon C, Gowman J,

Groskopfs E, Hemmerich J L Konstantellos A, Kussel E, Tschudin M, Walter K.
Fusion Technology, vol.14 no.2 pt.2A-2B September 1988 (Procs. 3rd Topical Meeting on Tritium Technology in Fission, Fusion and Isotopic Applications, Toronto, Canada, 1-6 May 1988), pp.461-465.

119. Current flow parallel to the field in a scrape-off layer.
Harbour P J.
Papers presented at Workshop on Plasma Edge Theory in Fusion Devices, Augustusburg, GDR, 26-30 April 1988.
Joint European Torus JET, 1988.
Report JET-P(88)24, pp.7-9.

120. Profiles of toroidal plasma rotation.
Hawkes N C, von Hellermann M, Boileau A, Horton L, Kallne E, Peacock N J, Ramette J, Stork D.
JET contributed papers to the 15th Euro Conf. on controlled fusion and plasma heating, Dubrovnik, Yugoslavia, 16-20 May 1988.
Joint European Torus JET, 1988.
Report JET-P(88)15, pp.61-64.

121. Power deposition for ion cyclotron heating in large tokamaks.
Hellsten T, Villard L.
Nuclear Fusion, vol.28 no.2 February 1988, pp.285-295.

122. Resonant ion diffusion in ICRF heated tokamak plasmas.
Hellsten T, Core W.
JET contributed papers to the 15th Euro Conf. on controlled fusion and plasma heating, Dubrovnik, Yugoslavia, 16-20 May 1988.
Joint European Torus JET, 1988.
Report JET-P(88)15, pp.129-132.

123. Resonant ion diffusion in ICRF heated tokamak plasmas
Hellsten T.
Plasma Physics and Controlled Fusion
JET-P(88)41

124. Self-consistent calculations of the power deposition and velocity distribution during ICRH.
Hellsten T, Boyd D, Campbell D, Christiansen J, Cordey J G, Core W, Cottrell G A, Edwards A, Eriksson L, Jacquinot J, Jarvis O N, Lowry C, Nielsen P, Sadler G, Start D, van Belle P, Thomas P R, Wesson J.
American Physical Society Bulletin, vol.33 no.9 October 1988 (Program of 30th Annual Meeting of the Division of Plasma Physics, Hollywood, Florida, 31 October-4 November 1988), paper 6U9, p.2031.

125. The impurity processing loop for the JET active gas handling plant.
Hemmerich J L, Dombra A, Gordon C, Groskopfs E, Konstantellos A.
Fusion Technology, vol.14 no.2 pt.2A-2B September 1988 (Procs. 3rd Topical Meeting on Tritium Technology in Fission, Fusion and Isotopic Applications, Toronto, Canada, 1-6 May 1988), pp.557-561.

126. The JET active gas handling system: Concept and status.
Hemmerich J L, Dombra A, Gordon C, Gowman J, Groskopfs E, Haange R, Huguet M, Konstantellos A, Kuessel E, Tschudin M, Walter K.
JET papers presented at the 12th Symp. on Fusion Engineering (SOFE), Monterey, USA, 12-16 October 1987.
Joint European Torus JET, 1987.
Report JET-P(87)52, pp.85-88.

127. The JET active gas handling system: progress report
Hemmerich J L, Gowman J, Haange R, Küssel E, Milverton P, Walter K, Dombra A, Groskopfs E, Konstantellos A, Lässer R, Walker K.
Invited Paper presented at 15th Symposium on Fusion Technology, Utrecht, the Netherlands, 19th-23rd September 1988
JET-P(88)63

128. Primary vacuum pumps for the fusion reactor fuel cycle.
Hemmerich J L.
Journal of Vacuum Science and Technology A: Vacuum, Surfaces and Films, vol.6 no.1 January/February 1988, pp.144-153.

129. A study of the seizure problem with high current filament feedthroughs in plasma generators
Hemsworth R S, Altmann H, Hurford D.

130. Testing of the upgraded JET neutral injector.
Hemsworth R S, Deschamps G H, Falter H D, Massmann P.
JET papers presented at the 12th Symp. on Fusion Engineering (SOFE), Monterey, USA, 12-16 October 1987.
Joint European Torus JET, 1987.
Report JET-P(87)52, pp.67-71.

131. A Thompson scattering diagnostic to measure fast ion and alpha particle distributions in JET.
Hoekzema J A, Costley A E, Hughes T P, Smith S R P, Boyd D.
American Physical Society Bulletin, vol.33 no.9 October 1988 (Program of 30th Annual Meeting of the Division of Plasma Physics, Hollywood, Florida, 31 October-4 November 1988), paper 6U2, pp.2029-2030.

132. Edge fluctuation measurements during X-point plasmas in JET.
Hubbard A, Bartlett D, Cripwell P, Gill R,

Harbour P J, Malacarne M, Morgan P D, Salmon R, Snipes J.
JET contributed papers to the 15th Euro Conf. on controlled fusion and plasma heating, Dubrovnik, Yugoslavia, 16-20 May 1988.
Joint European Torus JET, 1988.
Report JET-P(88)15, pp.69-72.

133. Papers presented at 8th topical meeting on technology of fusion, Salt Lake City, Utah, 10th-13th October 1989
JET Team (presented by M Huguet).
JET-P(88)43

134. Heat transport in partially stochastic tokamak magnetic fields.
Hugon M, Brusati M, Lallia P P, Rebut P H.
Plasma Physics Int. Conf. Joint Conf. of 7th Kiev Int. Conf. on Plasma Theory and the 7th Int. Congress on Waves and Instabilities in Plasmas, Kiev, 6-12 April 1987. Procs. of the Invited Papers. Edited by A G Sitenko. 2 volumes.
Singapore, World Scientific, 1987. pp.432-440.

135. Heating and confinement in high performance limiter plasmas.
Jacquinot J, Bhatnagar V, Brusati M, Bures M, Corti S, Ehrenberg J, Jones T, Lomas P, Magyar G, Malacarne M, Taroni A, Thompson E, Thomsen K.
American Physical Society Bulletin, vol.33 no.9 October 1988 (Program of 30th Annual Meeting of the Division of Plasma Physics, Hollywood, Florida, 31 October-4 November 1988), paper 6U14, pp.2031-2032.

136. High power ion cyclotron resonance heating in JET.
Jacquinot J (presenter), and the JET Team.
Plasma Physics and Controlled Fusion, vol.30 no.11 October 1988 (Controlled Fusion and Plasma Heating: 15th EPS Plasma Physics Division Conf., Cavtat, Yugoslavia, 16-20 May 1988. Invited Papers), pp.1467-1478.
JET-P(88)40

137. JET Joint Undertaking.
Jacquinot J.
Plasma Physics and Controlled Fusion News Sheet, no.12 September 1988, pp.5-6.

138. Activation of the JET vacuum vessel: a comparison of calculated with measured gamma-radiation fluxes and dose-rates.
Jarvis O N, Sadler G, Avery A, Verschuur K A.
Joint European Torus JET, 1988.
Report JET-R(88)05, 24p.

139. Fusion product measurements at JET.
Jarvis O N.
Joint European Torus JET, 1987.
Report JET-R(87)15, 22p.

140. Study of photoneutron production accompanying plasma disruptions in JET.
Jarvis O N, Sadler G, Thompson J L.
JET contributed papers to the 15th Euro Conf. on controlled fusion and plasma heating, Dubrovnik, Yugoslavia, 16-20 May 1988.
Joint European Torus JET, 1988.
Report JET-P(88)15, pp.77-80.

141. A summary of the Workshop on Alpha-Particle Diagnostics, held at JET on 9-10 December 1986.
Jarvis O N, Costley A E.
Joint European Torus JET, 1987.
Report JET-P(87)05, 8p.

142. X-ray satellite lines of high-n Rydberg transitions in Ar(sup 16+).
Källne E, Källne J, Dubau J, Marmar E S, Rice J E.
Physical Review A. General Physics, vol.38 no.4 15 August 1988, pp.2056-2065.

143. Triton burnup measurements in JET using a neutron activation technique.
Källne J, Batistoni P, Gorini G, Huxtable G B, Pillon M, Podda S, Rapisarda M.
Nuclear Fusion, vol.28 no.7 July 1988, pp.1291-1297.
Report JET-P(88)09

144. NEOTRA: A computer code to calculate the energy deposition of fusion α-particles in Tokamak plasmas; Part 1: theory and code structure
Kamelander G.
Joint European Torus, JET
Report JET-R(88)07

145. Studies of energy transport in JET H-modes.
Keilhacker M, Balet B, Cordey J, Gottardi N, Muir D, Thomsen K, Watkins M.
JET contributed papers to the 15th Euro Conf. on controlled fusion and plasma heating, Dubrovnik, Yugoslavia, 16-20 May 1988.
Joint European Torus JET, 1988.
Report JET-P(88)15, pp.145-148.

146. The curvature of the JET lower hybrid grill face
Knowlton S.
Joint European Torus, 1988.
Report JET-R(88)20

147. Neoclassical current and transport in auxiliary heated tokamaks.
Kim Y B, Callen J D, Hamnen H.
Joint European Torus JET, January 1988.
Report JET-R(88)02, 27p.

148. HECTOR: a code for the study of high energy charged particles in axisymmetric tokamak plasmas.
Kovanen M A, Core W G F.
Joint European Torus JET, 1988.
Report JET-R(88)01, 23p.

149. The JET multi-pellet injector launcher-machine interface.

Kupschus P, Bailey W, Gadeberg M, Hedley L, Twynam P, Szabo T, Evans D.
JET papers presented at the 12th Symp. on Fusion Engineering (SOFE), Monterey, USA, 12-16 October 1987.
Joint European Torus JET, 1987.
Report JET-P(87)52, pp.89-92.

150. JET multi-pellet injection experiments.
Kupschus P.
American Physical Society Bulletin, vol.33 no.9 October 1988 (Program of 30th Annual Meeting of the Division of Plasma Physics, Hollywood, Florida, 31 October-4 November 1988), paper 5I2, pp.1977-1978.

151. JET multi-pellet injection experiments.
Kupschus P (presenter).
American Physical Society Bulletin, vol.33 no.9 October 1988 (Program of 30th Annual Meeting of the Division of Plasma Physics, Hollywood, Florida, 31 October-4 November 1988), paper 6U20, p.2032-2033.

152. Multi-pellet injection on JET.
Kupschus P, Cheetham A, Denne B, Gadeberg M, Gowers C, Gondhalekar A, Tubbing B.
JET contributed papers to the 15th Euro Conf. on controlled fusion and plasma heating, Dubrovnik, Yugoslavia, 16-20 May 1988.
Joint European Torus JET, 1988.
Report JET-P(88)15, pp.157-160.

153. The cryogenic forevacuum system for the JET active gas handling plant.
Kussel E, Gowman J, Hemmerich J L, Walter K.
Fusion Technology, vol.14 no.2 pt.2A-2B September 1988 (Procs. 3rd Topical Meeting on Tritium Technology in Fission, Fusion and Isotopic Applications, Toronto, Canada, 1-6 May 1988), pp.552-556.

154. Tokamak confinement in relation to plateau scaling
Lackner K, Gottardi N.
Nuclear Fusion
JET-P(88)77

155. Chaotic magnetic topology and heat transport in tokamaks.
Lallia P P, Rebut P H, Watkins M L.
Joint European Torus JET, January 1988.
Report JET-P(88)05, 10p.

156. The effect of the instrument function on doppler ion temperature measurements of the JET plasma.
Lawson K, Peacock N.
JET-R(88)12

157. The effect of the instrument function on Doppler ion temperature measurements.
Lawson K D, Peacock N J.
Optics Communications, vol.68 no.2 15 September 1988, pp.121-127.
Report JET-P(88)17

158. Analysis of current and pressure profiles in JET H-mode discharges.
Lazzaro E, Avinash K, Brusati M, Gottardi N, Rimini F, Smeulders P.
JET contributed papers to the 15th Euro Conf. on controlled fusion and plasma heating, Dubrovnik, Yugoslavia, 16-20 May 1988.
Joint European Torus JET, 1988.
Report JET-P(88)15, pp.109-112.

159. Determination of equilibrium global parameters from external magnetic measurements in JET discharges with auxiliary heating.
Lazzaro E, Mantica P.
Nuclear Fusion, vol.28 no.5 May 1988, pp.913-917.

160. Feedback control of rotating resistive modes.
Lazzaro E, Nave M F F.
Physics of Fluids, vol.31 no.6 June 1988, pp.1623-1629.

161. Relaxation model of H-modes in JET.
Lazzaro E, Avinash K, Gottardi N, Smeulders P.
Joint European Torus JET, September 1988.
Report JET-P(88)48, 24p.

162. Relaxation theory of H-modes in JET.
Lazzaro E, Avinash K.
American Physical Society Bulletin, vol.33 no.9 October 1988 (Program of 30th Annual Meeting of the Division of Plasma Physics, Hollywood, Florida, 31 October-4 November 1988), paper 6U8, pp.2030-2031.

163. High current operation in JET.
Lomas P J, Bhatnagar V, Campbell D, Christiansen J P, Chuilon P, Corti S, Green B J, Harbour P, How J, Jacquinot J, Keilhacker M, Jones T T C, de Kock L, Last J, Lazzaro E, Lowry C, Magyar G, Malacarne M, Mondino P L, Morgan P, Noll P, O'Rourke J, Santagiustina A, Schueller F C, Snipes J, Summers D, Tanga A, Thomas P R, Thomsen K, Tubbing B.
JET contributed papers to the 15th Euro Conf. on controlled fusion and plasma heating, Dubrovnik, Yugoslavia, 16-20 May 1988.
Joint European Torus JET, 1988.
Report JET-P(88)15, pp.53-56.

164. Heat pulse propagation in JET.
Lopes Cardozo N J, Tubbing B J D, Huizing G, Brusati M, Campbell D, Cordey J G, Gondhalekar A.
Plasma Physics Int. Conf. Joint Conf. of 7th Kiev Int. Conf. on Plasma Theory and the 7th Int. Congress on Waves and Instabilities in Plasmas, Kiev, 6-12 April 1987. Procs. of the Invited Papers. Edited by A G Sitenko.

2 volumes.
Singapore, World Scientific, 1987. pp.417-431.
165. Heat pulse propagation: Diffusive models checked against full transport calculations.
Lopes Cardozo N J, Tubbing B J D, Tibone F, Taroni A.
Nuclear Fusion, vol.28 no.7 July 1988, pp.1173-1181.
166. Transport coefficients in the JET boundary.
Lowry C G, Harbour P J, Tagle J A.
Papers presented at Workshop on Plasma Edge Theory in Fusion Devices, Augustusburg, GDR, 26-30 April 1988.
Joint European Torus JET, 1988.
Report JET-P(88)24, pp.1-6.
167. The laser blow-off system (KZ3) on JET.
Magyar G, Barnes M R, Cohen S, Edwards A, Hawkes N C, Pasini D, Roberts P J.
JET-R(88)15
168. Observations of turbulence in the JET tokamak.
Malacarne M, Duperrex P A.
Procs. Int. Workshop on Small Scale Turbulence and Anomalous Transport in Magnetized Plasmas, Cargese, 6-12 July 1986.
Palaiseau Cedex, Editions de Physique, 1986. pp.201-204.
169. Plasma diagnostics on large tokamaks
Orlinskij D V, Magyar G.
Nuclear Fusion
JET-P(88)33
170. Impurity ion temperature and toroidal rotation velocity in JET from high-resolution x-ray and XUV spectroscopy.
Mattioli M, Ramette J, Saoutic B, Denne B, Källne E, Bombarda F, Gianella R.
Journal of Applied Physics, vol.64 no.7 1 October 1988, pp.3345-3352.
Report JET-P(88)06
171. Contributions fro ion-atom charge exchange collisions to the CVI lyman intensities in the JET tokamak
Mattioli M, Peacock N J, Summers H P, Denne B, Hawkes N C.
Journale de Physique
JET-P(88)68
172. Identification of radial and toroidal eigenmodes in the coupling of the well defined k-parallel spectrum of the new JET ICRH antennas.
McCarthy A L, Bhatnagar V P, Bures M, Colestock P L, Evrard M P, Gahl J M, Hellsten T, Jacquinot J, Knowlton S, Start D F H.
JET contributed papers to the 15th Euro Conf. on controlled fusion and plasma heating, Dubrovnik, Yugoslavia, 16-20 May 1988.
Joint European Torus JET, 1988.
Report JET-P(88)15, pp.121-124.
173. Power and the power density diagnostics for the JET neutral injection beam lines
Massmann P, Deschamps G H, Falter H D, Hemsworth R S.
Paper presented at 7th International conferfence on High Power Particle Beams (Beams '88), Karlsruhe, FRG, 4th-7th July 1988
JET-P(88)54
174. The thermocouple data acquisition system for JET neutral beam injection.
Mead M J, Browne A, Ewers D, Fullard K, Jones T T C, Stork D.
JET papers presented at the 12th Symp. on Fusion Engineering (SOFE), Monterey, USA, 12-16 October 1987.
Joint European Torus JET, 1987.
Report JET-P(87)52, pp.72-75.
175. Global modes and energetic alpha particles in ignited plasmas.
Migliuolo S, Coppi B, Pegoraro F, Porcelli F.
American Physical Society Bulletin, vol.33 no.9 October 1988 (Program of 30th Annual Meeting of the Division of Plasma Physics, Hollywood, Florida, 31 October-4 November 1988), paper 3T12, p.1930-1931.
176. A practical experience of using special remote handling tools on JET.
Mills S F, Schreibmaier J, Tesini A, Wykes M.
JET papers presented at the 12th Symp. on Fusion Engineering (SOFE), Monterey, USA, 12-16 October 1987.
Joint European Torus JET, 1987.
Report JET-P(87)52, pp.81-84.
177. The JET multipellet launcher and fuelling of JET plasmas by multipellet injection.
Milora S L, Schmidt G L, Jernigan T C, Baylor L R, Combs S K, Houlberg W A, Schissel D, Colestock P, Hammett G, Zarnstorff M, Kupschus P, Cheetham A, Denne B, Gadeberg M, Gowers C, Gondhalekar A, Tubbing B.
JET contributed papers to the 15th Euro Conf. on controlled fusion and plasma heating, Dubrovnik, Yugoslavia, 16-20 May 1988.
Joint European Torus JET, 1988.
Report JET-P(88)15, pp.169-172.
178. The PF system enhancement in JET to produce plasma currents up to 7MA with material limiters and up to 4MA with magnetic separatrix: A report on the electrical study.
Mondino P L, Bonicelli T, Eriksson T, Huart M, Marchese V, Noll P, Petree F, Raymond C, Santagiustina A, Zannelli L.
JET papers presented at the 12th Symp. on Fusion Engineering (SOFE), Monterey, USA, 12-16 October 1987.
Joint European Torus JET, 1987.

Zasche D.
JET contributed papers to the 15th Euro Conf. on controlled fusion and plasma heating, Dubrovnik, Yugosalvia, 16–20 May 1988.
Joint European Torus JET, 1988.
Report JET-P(88)15, pp. 9-12.

195. Experience with graphite in JET.
Pick M A, Celentano G, Deksnis E, Dietz K J, Shaw R, Sonnenberg K, Walravens M
JET papers presented at the 12th Symp. on Fusion Engineering (SOFE), Monterey, USA, 12–16 October 1987.
Joint European Torus JET, 1987.
Report JET-P(87)52, pp.97-100.

196. Calibration of neutron yield activation measurements at JET.
Pillon M, Jarvis O N, Källne J, Martone M.
Joint European Torus JET, March 1988.
Report JET-P(88)10, 22p.

197. Calibration of neutron yield activation measurements at JET using MCNP and FURNACE neutron transport codes.
Pillon M, Verschuur K A, Jarvis O N, Källne J, Martone M.
Joint European Torus JET, February 1988.
Report JET-P(88)08, 12p.

198. Sawtooth oscillations in plasmas with q on axis below unity.
Pocelli F, Han W, Pegoraro F, Taroni A, Tibone F.
American Physical Society Bulletin, vol. 33 no. 9 October 1988 (Program of 30th Annual Meeting of the Division of Plasma Physics, Hollywood, Florida, 31 October–4 November 1988), paper 3T19, pp. 1931-1932.

199. Reflectometry on JET.
Prentice R, Cripwell P, Costley A E, Fessey J A, de Haas J C M, Hubbard A E, Hugenholtz C A J, Oyevaar T, Paume M, Putter A J, Sips A C C, Slavin K.
JET contributed papers to the 15th Euro. Conf. on controlled fusion and plasma heating, Dubrovnik, Yugoslavia, 16–20 May 1988.
Joint European Torus JET, 1988.
Report JET-P(88)15, pp. 81-84.

200. Results from JET reflectometer systems.
Prentice R, Clarke H E, Cripwell P, Costley A E, Fessey J A, Hubbard A E, Hugenholtz C A J, Oyevaar T, Paume M, Putter A J, Sips A C C, Slavin K.
American Physical Society Bulletin, vol. 33 no. 9 October 1988 (Program of 30th Annual Meeting of the Division of Plasma Physics, Hollywood, Florida, 31 October–4 November 1988), paper 6U1, p. 2029.

201. The JET remote maintenace system.
Raimondi T.
Three papers presented at the IAEA Technical Committee Meeting on Robotics and Remote Maintenance, Karlsruhe, 22–24 February 1988.
Joint European Torus JET, April 1988. Report JET-P(88)13, pp. 1–12.

202. Use of teleoperators and transporters in JET.
Raimondi T, Galbiati L, Jones L D P F.
Three papers presented at the IAEA Technical Committee Meeting on Robotics and Remote Maintenance, Karlsruhe, 22–24 February 1988.
Joint European Torus JET, April 1988.
Report JET-P(88)13, pp. 29-41.

203. The JET experience with remote handling equipment and future prospects
Raimondi T
Invited paper presented at the 15th Symposium on Fusion Technology, Utrecht, the Netherlands, 19th–23rd September 1988
JET-P(88)64

204. Current transport in a chaotic magnetic field and self-sustainment of islands.
Rebut P-H
JET contributed papers to the 15th Euro. Conf. on controlled fusion and plasma heating, Dubrovnik, Yugoslavia, 16–20 May 1988.
Joint European Torus JET, 1988.
Report JET-P(88)15, pp. 13–16.

205. Experience with wall materials in JET and implications for the future.
Rebut P-H, Dietz K J, Lallia P P.
Joint European Torus JET, June 1988.
Report JET-P(88)21, 28p.

206. JET latest results and implications for a reactor.
Rebut P-H, Lallia P P.
Plasma Physics Int. Conf. Joint Conf. of 7th Kiev Int. Conf. on Plasma Theory and the 7th Int. Conf. on Plasma Theory and the 7th Int. Congress on Waves and Instabilities in Plasmas, Kiev, 6–12 April 1987. Procs. of the Invited Papers. Edited by A G Sitenko. 2 volumes.
Singapore, World Scientific, 1987, pp. 462-485

207. JET results and the prospects for fusion
Rebut P-H, Lallia P P
Invited Paper presented at the 15th Symposium on Fusion Technology, Utrecht, the Netherlands, 19th–23rd September 1988
JET-P(88)58.

208. The integration, control and operation of JET remote handling equipment.
Rolfe A C
Three papers presented at the IAEA Technical Committee Meeting on Robotics and Remote Maintenance, Karlsruhe, 22–24 February 1988.
Joint European Torus, JET, April 1988.
Report JET-P(88)13, pp. 13-28.

209. Operational aspects of the JET remote handling system.

Report JET-P(87)52, pp.32-37.
179. Fast wave current drive: Experimental regimes and potential for profile control in large tokamaks.
Moreau D, O'Brien M R, Cox M, Start D F H.
Non-Inductive Current Drive, report of a Specialists Meeting, held in Garching, 15-17 September 1986.
International Atomic Energy Agency, 1987.
Report IAEA-TECDOC-441, pp.78-80.
180. Lower hybrid wave stochasticity in tokamaks: A universal mechanism for bridging the N-parallel spectral gap.
Moreau D, Rax J M, Samain A.
JET contributed papers to the 15th Euro Conf. on controlled fusion and plasma heating, Dubrovnik, Yugoslavia, 16-20 May 1988.
Joint European Torus JET 1988.
Report JET-P(88)15, pp.113-116.
181. The evolution of Z_{eff}(r) profiles in JET plasmas.
Morgan P D.
JET contributed papers to the 15th Euro Conf. on controlled fusion and plasma heating, Dubrovnik, Yugoslavia, 16-20 May 1988.
Joint European Torus JET, 1988.
Report JET-P(88)15, pp.153-156.
182. Global impurity behaviour in JET plasmas during additional heating and fuelling.
Morgan P D.
American Physical Society Bulletin, vol.33 no.9 October 1988 (Program of 30th Annual Meeting of the Division of Plasma Physics, Hollywood, Florida, 31 October-4 November 1988), paper 6U13, p.2031.
183. Results on JET plasma and impurity behaviour based on measurements of radial profiles in the soft X-ray region.
Morsi H W, Behringer K, Denne B, Källne E, Rupprecht G, Schumacher U.
JET contributed papers to the 15th Euro Conf. on controlled fusion and plasma heating, Dubrovnik, Yugoslavia, 16-20 May 1988.
Joint European Torus JET, 1988.
Report JET-P(88)15, pp.25-28.
184. Stability of the ideal m=1 mode in a tokamak.
Nave M F F, Wesson J.
Nuclear Fusion, vol.28 no.2 February 1988, pp.297-301.
185. Calibration of the fast 12-channel ECE spectrometer at JET.
Niestadt R M, Tubbing B J D , Oyevaar Th.
Euratom FOM-Instituut voor Plasmafysica, Rijnhuizen, July 1986.
Report Rijnhuizen 86-168, 35p.
186. Measurement of two-dimensional temperature profiles in JET and simulation of the spectra.
Nowak S, Bartlett D V, Campbell D J, Costley A E, Kissel S.
Electron Cyclotron Emission and Electron Cyclotron Resonance Heating. Procs. 6th Joint Workshop, Oxford, 16-17 September 1987.
Abingdon, Culham Laboratory, 1987.
pp.149-156.
Report JET-P(88)18
187. Cryogenics of the Joint European Torus (JET) and the Next European Torus (NET).
Obert W.
Joint European Torus JET, July 1988.
Report JET-P(88)32, 11p.
188. Plasma diagnostics on large tokamaks: Review paper.
Orlinskij D V, Magyar G.
Nuclear Fusion, vol.28 no.4 April 1988, pp.611-697.
Report JET-P(88)33
189. Plasma conductivity and current penetration in JET.
O'Rourke J, Galvao T, Lazzaro E, Morgan P D, Schmidt G.
American Physical Society Bulletin, vol.33 no.9 October 1988 (Program of 30th Annual Meeting of the Division of Plasma Physics, Hollywood, Florida, 31 October–4 November 1988), paper 6U11, p.2031.
190. Polarimetric measurements of the Q-profile.
O'Rourke J, Blum J, Cordey J G, Edwards A, Gottardi N, Keegan B, Lazzaro E, Magyar G, Stephen Y, Stufferfield P, Veron D, Zasche D.
JET contributed papers to the 15th Euro. Conf. on controlled fusion and plasma heating, Dubrovnik, Yugoslavia, 16–20 May 1988.
Joint European Torus JET, 1988.
Report JET-P(88)15, pp.29-32.
191. Q-profiles. (Report on 6th European Tokamak Programme Workshop, Varenna, December 1987.)
O'Rourke J.
Plasma Physics and Controlled Fusion, vol.30 no.10 September 1988, pp.1369-1371.
192. Q-profiles.
O'Rourke J.
JET papers presented at 6th Euro. Tokamak Programme Workshop, Varenna, Italy, 2–4 December 1987.
Joint European Torus JET, 1988.
Report JET-P(88)19, pp.15-18.
193. JET X-ray pulse-height analysis system.
Pasini D, Gill R D, Holm J, van der Goot E, Weller A.
Review of Scientific Instruments, vol.59 no.5 May 1988, pp.693-699.
194. Simulation of soft X-ray emissivity during pellet-injection and H-mode in JET.
Pasini D, Edwards A, Gill R, Weller A,

Rolfe A C.
Joint European Torus JET, April 1988.
Report JET-P(88)12, 11p.

210. Ion temperature gradient driven modes and anomalous ion transport in tokamaks.
Romanelli F
Joint European Torus JET, 1988.
Report JET-P(88)07, 26p.

211. Toroidal semicollisional microinstabilities and anomalous electron and ion transport.
Romanelli F, Briguglio S.
JET Joint European Torus, July 1988.
Report JET-P(88)31, 34p.

212. Soft X-ray detectors for the spectral and spatial scanning double crystal monochromators KS1 and KS2 at JET
Rupprecht G
JET-R(88)13

213. Diagnosing RF driven high energy minority tails with gamma-ray and neutral spectroscopy.
Sadler G, Jarvis O N, van Belle P,
Adams J M.
JET contributed papers to the 15th Euro. Conf. on controlled fusion and plasma heating, Dubrovnik, Yugoslavia, 16–20 May 1988.
Joint European Torus JET, 1988.
Report JET-P(88)15, pp. 65-68

214. Fusion product measurements on JET during combined heating.
Sadler G, Adams J M, van Belle P, Elevant T, Jarvis O N.
Amercian Physical Society Bulletin, vol. 33 no. 9 October 1988 (Program of 30th Annual Meeting of the Divison of Plasma Physics, Hollywood, Florida, 31 October–4 November 1988), paper 6U3, p.2030.

215. High spatial resolution temperature measurements in JET using a multichannel heterodyne radiometer.
Salmon N A, Bartlett D V, Costley A E.
Electron Cyclotron Emission and Electron Cyclotron Resonance Heating. Procs. 6th Joint Workshop, Oxford, 16–17 September 1987.
Abingdon, Culham Laboratory, 1987.
pp. 157-164.
Report JET-P(88)18.

216. LIDAR Thomson scattering. (Report on 6th European Tokamak Programme Workshop, Varenna, December 1987.)
Salzmann H.
Plasma Physics and Controlled Fusion, vol. 30 no. 10 September 1988, p. 1368.

217. LIDAR Thomson scattering.
Salzmann H.
JET papers presented at 6th Euro. Tokamak Programme Workshop, Varenna, Italy, 2–4 December 1987.
Joint European Torus JET, 1988.
Report JET-P(88)19, pp. 13-14

218. XUV spectroscopy in JET during the second semester 1986.
Saoutic B, Mattioli M, Behringer K,
Peacock N J, Schwob J L, Talbot A,
Ramette J, Denne B, Magyar G, Ravestein A,
Sieweke F.
Joint European Torus JET, 1987.
Report JET-R(87)14, 84p.

219. Sawtooth oscillations in ion cyclotron emission from JET
Schild P, Cottrell G, Dendy R O.
Nuclear Fusion Letters
JET-P(88)62

220. Ion cyclotron emission measurements on JET.
Schild P, Cottrell G A
JET contributed papers to the 15th Eur. Conf. on controlled fusion and plasma heating, Dubrovnik, Yugoslavia, 16–20 May 1988.
Joint European Torus JET, 1988.
Report JET-P(88)15, pp. 137-140.

221. The design of an isotope separation system for JET.
Sherman R H
JET papers presented at the 12th Symp. on Fusion Engineering (SOFE), Monterey, USA, 12–16th October 1987.
Joint European Torus JET, 1987.
Report JET-P(87)52, pp. 42-45.

222. Ion beam analysis of surface probes used to study plasma boundary phenomena and first-wall interactions in JET
Simpson J C B, Bergsaker H, Clement S,
Coad J P, de Kock L, Ehrenberg J,
Hancock C J, Neill G F, Partridge J,
Vince J E.
Nuclear Instruments and Methods B
JET-P(88)75

223. Use of Balmer radiation from injected neutral beams for measurement of beam deposition and plasma density profiles.
Sleaford B W, Cottrell G A, Jinchoon Kim.
Nuclear Fusion, vol. 28 no. 3 March 1988, pp. 523-527.

224. Effects of large amplitude MHD activity on confinement in JET.
Snipes J A, Campbell D J, Hugon M,
Morgan P, Stork D, Summers D, Thomsen K,
Tubbing B.
JET contributed papers to the 15th Euro. Conf. on controlled fusion and plasma heating, Dubrovnik, Yugoslavia, 16–20 May 1988.
Joint European Torus JET, 1988.
Report JET-P(88)15, pp. 41-44.

225. Large amplitude quasi-stationary MHD modes in JET.
Snipes J A, Campbell D J, Haynes P S,

Hender T C, Hugon M, Lomas P J, Lopes Cardozo N J, Nave M F F, Schüller F C
Nuclear Fusion, vol. 28 no. 6 June 1988, pp. 1085-1097.
Report JET-P(88)01

226. High speed pellet development.
Sonnenberg K, Kupschus P, Bailey W, Helm J, Krehl P, Claudet G, Disdier F, Lafferranderie J.
JET papers presented at the 12th Symp. on Fusion Engineering (SOFE), Monterey, USA, 12–16 October 1987.
Joint European Torus JET, 1987.
Report JET-P(87)52, pp. 93-96.

227. JET pump limiter.
Sonnenberg K, Shaw R, Croessmann D, Koski J, Deksnis E, Watson R, Watkins J, Reiter D.
Joint European Torus JET, 1988.
Report JET-R(88)10, 16p.

228. Measurements of the cross-field diffusion coefficient $D_{\parallel}$ in the edge plasma of JET.
Stangeby P C, Tagle J A, Erents S K, Lowry C.
Plasma Physics and Controlled Fusion, vol. 30 no. 12 November 1988, pp. 1787-1803.

229. Additional papers presented at the workshop on plasma edge theory in fusion devices, Augustusburg, GDR, 26th–30th April 1988
Stangeby P C, Farrell C, Wood L, Simonini R, Spence J.
JET-P(88)55

230. RF heating.
Start D
JET papers presented at 6th Euro. Tokamak Programme Workshop, Varenna, Italy, 2–4 December 1987.
Joint European Torus JET, 1988.
Report JET-P(88)19, pp. 19-20.

231. High electron and ion temperatures produced in JET by ICRH and neutral beam heating.
Start D F H, Bhatnagar V, Bures M, Campbell D J, Challis C, Cottrell G A, Eriksson L G, Hellsten T, Jacquinot J, Jones T T C, McCarthy A L, Stork D, Thomas P R, Thompson E, Thomsen K.
JET contributed papers to the 15th Euro Conf. on controlled fusion and plasma heating, Dubrovnik, Yugoslavia, 16–20 May 1988.
Joint European Torus JET, 1988.
Report JET-P(88)15, pp. 97-100.

232. RF heating. (Report on 6th European Tokamak Programme Workshop, Varenna, December 1987.)
Start D F.
Plasma Physics and Controlled Fusion, vol. 30 no. 10 September 1988, pp. 1371-1372.

233. Front end embedded microprocessors in the JET computer-based control system past, present and future.
Steed C A, van der Beken H, Browne M L, Fullard K, Reed K, Tilley M, Schmidt V.
JET papers presented at the 12th Symp. on Fusion Engineering (SOFE), Monterey, USA, 12–16 October 1987.
Joint European Torus JET, 1987.
Report JET-P(87)52, pp. 46-49.

234. Incremental confinement analysis of transient phases during neutral beam heating on JET.
Stork D, Kaneko O, Morgan P D, von Hellermann M.
American Physical Society Bulletin, vol. 33 no. 9 October 1988 (Program of 30th Annual Meeting of the Division of Plasma Physics, Hollywood, Florida, 31 October–4 November 1988), paper 6U19, p. 2032.

235. Density limits and disruptions in plasmas (Report on the IAEA Technical Committee Meeting, JET Joint Undertaking, Abingdon, 26–28 January 1988).
Stott P E
Nuclear Fusion, vol. 28 no. 8 August 1988, pp. 1469-1473.

236. Disruptions and density limits.
Stott P E
Joint European Torus JET, July 1988.
Report JET-P(88)27, 10p.

237. The JET plasma boundary with limiter and X-point discharges.
Stott P E (presenter), and the JET Team
Joint European Torus JET, July 1988.
Report JET-P(88)34, 22p.

238. Plasma-surface interactions in controlled fusion devices (Report on the 8th Int. Conf., Julich, 2–6 May 1988).
Stott P E
Nuclear Fusion, vol. 28 no. 9 September 1988, pp. 1695-1702 and JET-P(88)45

239. Book Review: Plasma physics and controlled nuclear fusion research, 11th Conf., Kyoto, 1986.
Stringer T E (reviewer)
Plasma Physics and Controlled Fusion, vol. 30 no. 8 July 1988, p. 1099.

240. Atomic collisions in fusion: Conference Report–Oxford, 30 July–1 August 1987.
Summers H P
Comments on Atomic and Molecular Physics, vol. 21 no. 5 1988, pp. 277-293.

241. Ionization, recombination and radiation of impurities in plasmas. An interactive atomic data and applications structure.
Summers H P, Wood L
Joint European Torus JET, April 1988.
Report JET-R(88)06, 91 p.

242. The JET H-mode.
Tanga A, Bartlett D, Bures M, Gibson A, Gottardi N, Gowers C, Harbour P J, Hubbard A, Keilhacker M, Lazzaro E, Morgan P D, Noll P, Rebut P-H, Salmon N, Stork D, Summers D D R, Tagle A J, Thomas P R, Thomsen K, von Hellermann M, Watkins M L.
JET contributed papers to the 15th Euro Conf. on controlled fusion and plasma heating, Dubrovnik, Yugoslavia, 16–20 May 1988.
Joint European Torus JET, 1988.
Report JET-P(88)15, pp. 149-152.

243. Experimental contamination and decontamination studies on JET remote handling tools and materials when exposed to tritium.
Tesini A, Jalbert R A.
Joint European Torus JET, 1988.
Report JET-R(88)18, 84p.

244. Local heat transport models in JET plasmas.
Thomas P R, Christiansen J P, Connor J W, Cordey J G, Lauro-taroni L, Muir D, Sack H C, Tarton A, Tibone F, Turner M F.
JET contributed papers to the 15th Euro. Conf. on controlled fusion and plasma heating, Dubrovnik, Yugoslavia, 16–20 May 1988.
Joint European Torus JET, 1988.
Report JET-P(88)15, pp. 45-48.

245. Overview of 1987 JET results.
Thomas P R (presenter), and the JET Team
JET papers presented at 6th Euro. Tokamak Programme Workshop, Varenna, Italy, 2–4 December 1987.
Joint European Torus JET, 1988.
Report JET-P(88)19, pp. 1-12.

246. Overview on 1987 JET results. (Report on 6th European Tokamak Programme Workshop, Varenna, December 1987.)
Thomas P R (presenter), and the JET Team.
Plasma Physics and Controlled Fusion, vol. 30 no. 10 September 1988, pp. 1359-1368.

247. Plasmas set to ignite? Report from the 12th IAEA Conf. on Plasma Physics and Controlled Thermonuclear Fusion, Nice, France, 12–19 October 1988.
Thomas P R, Key M.
Physics World, December 1988, pp. 20-21.

248. Global confinement characteristics of JET limiter plasmas.
Thomsen K, Campbell D J, Christiansen J P, Cordey J G, Thomas P R.
JET contributed papers to the 15th Euro. Conf. on controlled fusion and plasma heating, Dubrovnik, Yugoslavia, 16–20 May 1988.
Joint European Torus JET, 1988.
Report JET-P(88)15, pp. 49-52.

249. Predictions for ICRF power deposition in JET and modulation experiment during sawtooth-free periods.
Tibone F, Evrard M P, Bhatnagar V, Campbell D J, Cordey J G, Core W, Eriksson L-G, de Haas J C M, Hamnen H, Hellsten T, Jacquinot J, Knowlton S, Koch R, Lean H, Rimini F, Roberts D, Start D F H, Thomas P R, Thomsen K, Van Eester D.
JET contributed papers to the 15th Euro. Conf. on controlled fusion and plasma heating, Dubrovnik, Yugoslavia, 16–20 May 1988.
Joint European Torus JET, 1988.
Report JET-P(88)15, pp. 105-108.

250. Testing of beam stopping element using hypervapotron cooling.
Tivey R B, Falter H D, Haange R, Hemsworth T S, Massmann P, Stabler A.
JET papers presented at the 12th Symp. on Fusion Engineering (SOFE), Monterey, USA, 12–16 October 1987.
Joint European Torus JET, 1987.
Report JET-P(87)52, pp. 50-53.

251. A feasibility study of microwave methods for the calibration of ECE spectrometers.
Tubbing B J D, Kissel S E.
Electron Cyclotron Emission and Electron Cyclotron Resonance Heating. Procs. 6th Joint Workshop, Oxford, 16–17 September 1987.
Abingdon, Culham Laboratory, 1987.
pp. 317-323.
Report JET-P(88)18

252. MHD phenomena related to pellet injection in JET.
Tubbing B J D, Baylor L, Edwards A, Kupschus P, Oomens A, Schissel D, Schmidt G, Snipes J.
American Physical Society Bulletin, vol. 33 no. 9 October 1988 (Program of 30th Annual Meeting of the Division of Plasma Physics, Hollywood, Florida, 31 October–4 November 1988), paper 6U7, p. 2030.

253. Investigation of slowing-down and thermalized alpha particles by charge exchange recomination spectroscopy–a feasibility study.
von Hellermann M, Summers H, Boileau A.
JET contributed papers to the 15th Euro. Conf. on controlled fusion and plasma heating, Dubrovnik, Yugoslavia, 16–20 May 1988.
Joint European Torus JET, 1988.
Report JET-P(88)15, pp. 141-144.

254. Automatic ICRH power coupling to any plasma in JET.
Wade T J, Bosia G, Schmid M, Sibley A.
JET papers presented at the 12th Symp. on Fusion Engineering (SOFE), Monterey, USA, 12–16 October 1987.
Joint European Torus JET, 1987.
Report JET-P(87)523, pp. 54-57.

255. The final phase of JET disruptions.

Ward D J, Gill R D, Morgan P D, Wesson J A
JET contributed papers to the 15th Euro. Conf. on controlled fusion and plasma heating, Dubrovnik, Yugoslavia, 16–20 May 1988.
Joint European Torus JET, 1988.
Report JET-P(88)15, pp. 1-4.

256. Sawtooth relaxations.
Ward D J.
Theory of fusion plasmas. Procs. Int. School of Plasma Physics 'Pier Caldirola' Workshop, Villa Cipressi, Varenna, 24–28 August 1987.
Bologna, Editrice Compositori for Societa Italiana di Fisica, 1988. pp. 295-302.

257. Spontaneous transitions in the temperature of a tokamak plasma with separatrix.
Watkins M L, Rebut P-H, Lallia P P.
JET contributed papers to the 15th Euro Conf. on controlled fusion and plasma heating, Dubrovnik, Yugoslavia, 16–20 May 1988.
Joint European Torus JET, 1988.
Report JET-P(88)15, pp. 161-164.

258. Disruptions in JET.
Wesson J A, Gill R D, Hugon M, Schuller F C, Snipes J A, Ward D J, Bartlett D, Campbell D J, Duperrex P A, Edwards A W, Granetz R S, Gottardi N A O, Hender T C, Lazzaro E, Lomas P J, Lopes-Cardozo N, Mast F K, Nave M F F, Salmon N A, Smeulders P, Thomas P, Tubbing B, Turner M F, Weller A.
Joint European Torus JET, September 1988.
Report JET-P(88)44, 83p.

259. Magnetic reconnection in tokamaks.
Wesson J A.
Trends in Physics 1984. Procs. 6th General Conf. of the European Physical Society, Prague, 27–31 August 1984.
Prague, Union of Czechoslovak Mathematicians and Physicists, 1985. Vol. 1, pp. 144-149.

260. Snakes and monsters. (Report on 6th European Tokamak Programme Workshop, Varenna, December 1987).
Wesson J A.
Plasma Physics and Controlled Fusion, vol. 30 no. 10 September 1988, pp. 1372-1374.

261. Snakes and monsters.
Wesson J A.
JET papers presented at 6th Euro. Tokamak Programme Workshop, Varenna, Italy, 2–4 December 1987.
Joint European Torus JET, 1988.
Report JET-P(88)19, pp.21-23.

262. Theory of sawtooth oscillations.
Wesson J A.
Theory of fusion plasmas. Procs. Int. School of Plasma Physics 'Piero Calidrola' Workshop, Villa Cipressi, Varenna, 24-28 August 1987.
Bologna, Editrice Compositori for Societa Italian di Fisica, 1988. pp.253-282.

263. Observations of sawtooth postcursor oscillations in JET and their bearing on the nature of the sawtooth collapse
Westerhof E, Smeulders P, Lopes-Cardozo N.
Nuclear Fusion Letters
JET-P(88)73

264. Safety analysis of torus vacuum breach.
Wykes M E P.
Joint European Torus JET, 1988.
Report JET-P(88)37, 9p.

265. Plasma equilibria and stationary flows in axisymmetric systems Part I
Zelazny R, Stankiewicz R, Potempski S.
JET-R(88)16

266. Plasma equilibria and stationary flows in axisymmetric systems Part II
Zelazny R, Stankiewicz R, Potempski S.
JET-R(88)17

267. JET papers presented at the 12th symp. on Fusion Engineering, (SOFE), Monterey, USA, 12–16 October 1987.
Joint European Torus JET, 1987.
Report JET-P(87)52, 100p.

268. JET contributed papers to the 15th Euro. Conf. on Controlled Fusion and Plasma Heating, Dubrovnik, 16–20 May 1988.
Report JET-P(88)15, 172p.

269. Papers presented to 3rd topical meeting on tritium technology, Toronto, Canada, 1st–6th May 1988.
Haange R F, Küssel E, Hemmerich J L.
Conference Proceedings
JET-P(88)56

270. Contributed papers presented at 12th International Conference on Plasma Physics and Controlled Nuclear Fusion Research, Nice, France, 12th–19th October 1988 JET Team
Conference Proceedings
JET-P(88)78

271. Papers presented at the 8th International conference on Plasma Surface Interactions in Controlled Fusion Devices, Jülich, FRG, 2nd–6th May 1988
Goodall D H J et al
JET-P(88)70

272. Contributed papers presented at the 15th Symposium on Fusion Technology (SOFT), Utrecht, the Netherlands, 19th–23rd September 1988
Kaye A S et al
Conference Proceedings
JET-P(88)69

273. Papers presented at the Workshop on plasma edge theory in fusion devices, Augustusburg, GDR, 26th–30th April 1988
Lowry C G, Harbour P J, Avinash K, Tagle J A, Hellsten T, Core W.

Conference Proceedings
JET-P(88)24

274. JET Annual Report 1987.
Abingdon, JET Joint Undertaking, July 1988.
Edited by B E Keen, G W O'Hara and
I E Pollard.
57p.

275. JET Progress Report 1987.
Abingdon, JET Joint Undertaking, March
1988.
Edited and compiled by B E Keen.
566p.

Appendix III

Reprints of JET Papers

(a) JET-P(88)15 JET Contributed Papers presented at the 15th European Conference on Controlled Fusion and Plasma Heating (Dubrovnik, Yugoslavia, 16th-20th May 1988) - Many Authors;

(b) JET-P(88)21 Experience with Wall Materials in JET and Implications for the Future - Invited paper presented at the 8th International Conference on Plasma Surface Interactions, Jülich, F.R.G., 2nd-6th May 1988) - P.H.Rebut, K.J. Dietz and P.P. Lallia

(c) JET-P(88)26 Plasma Performance in JET: Achievements and Projections - A. Gibson (for JET Team) - Invited Paper presented at 15th European Conference on Controlled Fusion and Plasma Heating (Dubrovnik, Yugoslavia, 16th-20th May 1988);

(d) JET-P(88)40 High Power Ion Cyclotron Resonance Heating in JET - J.Jacquinot (for JET Team) - Invited Paper presented at 15th European Conference on Controlled Fusion and Plasma Heating (Dubrovnik, Yugoslavia, 16th-20th May 1988);

(e) JET-P(88)44 The JET Plasma Boundary with Limiter and X-Point Discharges - P. Stott (for JET Team) - Invited Paper presented at 8th International Conference on Plasma Surface Interactions (PSI) (Jülich, FRG, 2nd-6th May 1988);

(f) JET-P(88)69 Contributed Papers to 15th Symposium on Fusion Technology, (SOFT), (Utrecht, The Netherlands, 19th-23rd September 1988) - Many Authors;

(g) JET-P(88)58 JET Results and the Prospects for Fusion - P.H.Rebut and P.P. Lallia - Invited Paper presented at 15th Symposium on Fusion Technology (SOFT), (Utrecht, The Netherlands, 19th-23rd September 1988);

(h) JET-P(88)61 Preparation for D-T Operation at JET - A.C. Bell et al - Invited Paper presented at 15th Symposium on Fusion Technology (SOFT), (Utrecht, The Netherlands, 19th-23rd September 1988);

(i) JET-P(88)63 Key Components of the JET Active Gas Handling System - Experimental Programme and Results - J.L. Hemmerich et al - Invited Paper presented at 15th Symposium on Fusion Technology (SOFT), (Utrecht, The Netherlands, 19th-23rd September 1988);

(j) JET-P(88)64 The JET Experience with Remote Handling Equipment and Future Prospects - T. Raimondi - Invited Paper presented at 15th Symposium on Fusion Technology (SOFT), (Utrecht, The Netherlands, 19th-23rd September 1988);

(k) JET-P(88)78 Contributed Papers Presented at 12th IAEA Conf. on Plasma Physics and Controlled Nuclear Fusion Research, (Nice, France, 12th-19th October 1988) - Many Authors;

(l) JET-P(88)43 JET Progress Towards D-T Operation - M. Huguet et al - Invited paper presented at 8th Topical Meeting on Technology of Fusion, (Salt Lake City, Utah, USA, 10th-14th October 1988).